Charles University in Prague

Faculty of Science

Department of Inorganic Chemistry

Inorganic chemistry

RNDr. Jaroslav Žádný

Příprava a využití komplexů přechodných kovů s helikálními ligandy

Synthesis and Use of Transition Metal Complexes with Helical Ligands

Ph.D. Thesis

Supervisors:

Doc. RNDr. Pavel Vojtíšek, CSc.

RNDr. Ivo Starý, CSc.

Prague, 2015

Prohlášení:

Prohlašuji, že jsem závěrečnou práci zpracoval samostatně a že jsem uvedl všechny použité informační zdroje a literaturu. Tato práce ani její podstatná část nebyla předložena k získání jiného nebo stejného akademického titulu.

V Praze, 3. 2. 2015

Podpis

Acknowledgement

At first my greatest thanks belong to my supervisors Doc. RNDr. Pavel Vojtíšek, CSc. (CU Prague) and particularly to RNDr. Ivo Starý, CSc. and his wife RNDr. Irena G. Stará, CSc., who are one of the most inspiring people that I have ever met, distinguished researchers and great visionaries. I am grateful to them for everything what they taught me and for their patience and optimism. I would like to thank to my colleagues from the Chemistry of Functional Molecules group, namely to Ing. Jiří Rybáček, PhD., Ing. Michal Šámal, PhD., Mgr. Jiří Klívar and Mgr. Andrej Jančařík, PhD. for their help, an everlasting good mood and their friendship. My thanks also belong to my ex-colleagues Mgr. Angelina A. Andronova, PhD., Mgr. Zuzana Krausová, PhD., Dr. Nathan C. Clemence and Mgr. Jiří Míšek, PhD. for their initial experiments on helicene-like compounds or providing me some of a starting material for my experiments.

I would like to thank to Ing. David Šaman, CSc., Ing. Radek Pohl, PhD. and Ing. Jan Sýkora, PhD. (ICPF AS CR) for measuring NMR spectra, Ing. Pavel Fiedler and Ing. Beata Seidlerová for measuring IR spectra, Mgr. Lucie Bednárová, PhD. for measuring CD spectra, RNDr. Anna Březinová and Ing. Petra Cuřínová, PhD. (ICPF AS CR) for measuring mass spectra and Ing. Lucie Holasová for measuring optical rotations. I am also grateful to RNDr. Jaroslav Vacek, PhD. and RNDr. Jana Vacek Chocholoušová, PhD. for DFT studies and computational chemistry, to RNDr. Ivana Císařová, CSc. (CU Prague) for performing X-ray structure analysis and to Ing. Romana Hadravová for TEM analysis.

My special thanks belong to Mgr. Petr Žáček, PhD. and Mrs. Anna Nekolová for helping me with analysis of hydrogenation experiments, Raffael C. Wende, MSc. (Justus-Liebig University Giessen, Germany) for performing the organocatalytic experiments, Mgr. Martin Dračínský, PhD. for through-space coupling (TSC) NMR measurements and RNDr. Václav Kašička, CSc. for acidity constants determination.

Last but not least I am grateful to my parents for their never-ending support. The greatest thank belongs to my wife, Katka, and my wonderful son, Vítek, for their huge patience and love.

Abstract

The Thesis describes our successful endeavour to develop asymmetric synthesis of functionalized 2*H*-pyran or 2,7-dihydrooxepine helicene-like compounds in an optically pure form. These helicene surrogates were fully characterized and their use in enantioselective catalysis as chiral ligands, organocatalysts or chiral modifiers was explored. A general method for the preparation of optically pure [5]- and [6]heterohelicenes by asymmetric synthesis is based on highly diastereoselective [2+2+2] cycloisomerization of centrally chiral triynes mediated/catalyzed by transition metal complexes. Stereochemical outcome of the cyclization process is controlled by 1,3-allylic-type strain. This new methodology is highly versatile providing an easy access to chiral ligands, organocatalysts or modifiers in a nonracemic form. Optically pure 2,7-dihydrooxepine [5]helicene-like phosphite ligands were explored in enantioselective allylic amination under catalysis by iridium(I) complexes to reach up to 82% *ee*. An organocatalysts represented by the optically pure 2*H*-pyran [5]helicene-like DMAP analogue was synthesized and applied to kinetic resolution of racemic sulfoximines. Finally, various functionalized derivatives of helicenes and helicene-like compounds (azahelicenes, DMAP analogues, (thio)urea derivatives) were prepared and their possible role as new chiral modifiers in asymmetric heterogeneous reduction of ethyl pyruvate to ethyl lactate was studied.

Table of Contents

Abbreviations and signs

%cat.	percent of catalyst
(=)	ethylene
Ac	acetyl
acac	acetylacetonate
acc. to	according to
acc. to lit.	according to literature
Ad	1-adamantyl
AFM	atomic force microscopy
AS CR	Academy of Sciences of the Czech Republic
atm	atmosphere (unit)
BHc	benzohelicenocyanines
BINOL	1,1'-bi-2-naphthol
Boc	*tert*-butyl carbamate
ca	approximately (*circa*)
cat.	catalyst *or* catalytically
CCDC	Cambridge Crystallographic Data Centre
CD	circular dichroism *or* cinchonidine
cf.	compare (*confer*)
CN	cinchonine
cod	1,5-cyclooctadiene
coll.	collective
COSY	correlation spectroscopy
Cp	cyclopentadienyl
Cp*	1,2,3,4,5-pentamethylcyclopentadienyl
cryst.	crystalisation
CU	Charles University
Cy	cyclohexyl
d	doublet (NMR)
dba	dibenzylideneacetone
DBU	1,8-diazabicyclo[5.4.0]undec-7-ene
DCE	1,2-dichloroethane
DCM	dichloromethane
de	diastereomeric excess
decomp.	decomposition
DFT	density functional theory
DIAD	diisopropyl azodicarboxylate
DIPEA	*N*,*N*-diisopropylethylamine
DMA	*N*,*N*-dimethylacetamide
DMAP	4-dimethylaminopyridine *or* 2-(4-dimethylaminopyridyl)
DMF	*N*,*N*-dimethylformamide
DMSO	dimethyl sulfoxide
DPFGSE	double pulse field gradient spin echo
dppe	1,2-bis(diphenylphosphino)ethane
d.r.	diastereomeric ratio
e.g.	for example (*exampli gratia*)
ECD	electronic circular dichroism
ee	enantiomeric excess
EI	electron ionization
eq	equivalent
ESI	electrospray ionization
Et	ethyl
et al.	and others (*et alii*)
etc.	and other things, and so forth (*et cetera*)
FID	flame ionization detector
fum	dimethyl fumarate
GC	gas chromatography
GIAO-DFT	gauge-including atomic orbitals DFT
GPC	gel permeation chromatography
Hc	helicenocyanines
heat.	heating
HELOL	4,4',5,5'-tetramethoxy-2,2'-bipentahelicene-1,1'-diol
HMBC	heteronuclear multiple-bond correlation spectroscopy
HMDS	hexamethyldisilazane *or* bis(trimethylsilyl)amide
HPFC	high-performance flash chromatography
HPLC	high-performance liquid chromatography
HR	high resolution
HSQC	heteronuclear single quantum coherence
hv	quantum of energy *or* irradiation
ICPF	Institute of Chemical Process Fundamentals, v.v.i.
IOCB	Institute of Organic Chemistry and Biochemistry, v.v.i.
ion. liq.	ionic liquid
*i*Pr	*iso*-propyl
IR	infrared spectroscopy
J	indirect dipole-dipole coupling constant

LDA	lithium diisopropylamide
m	mobility *or* middle (IR)
MAE	mean absolute errors
*m*CPBA	*meta*-chloroperoxybenzoic acid
Me	methyl
mid	middle
Mp	melting point
MW	microwave irradiation
MS	mass spectroscopy
NBS	*N*-bromosuccinimide
*n*Bu *or* Bu	*normal* butyl
NC-AFM	non-contact atomic force microscopy
NEXAFS	near-edge X-ray absorption fine structure
Nf	perfluorobutanesulfonyl
NLO	non-linear optics
NMR	nuclear magnetic resonance
NOE	nuclear Overhauser effect
NPs	nanoparticles
PAA	polyacrylic acid
PFG	pulsed field gradient
pH	negative log of the hydrogen ions activity
Ph	phenyl
pK_a	negative log of acidity constant
PNEA	pantoylnaphtylethylamine
ppm	parts per million
Pr	*normal* propyl
PVD	physical vapor deposition
PVP	poly(*N*-vinyl-2-pyrolidone)
py	pyridine *or* 2-pyridyl
q	quartet (NMR)
QD	quinidine
QN	quinine
rac	racemate
ref.	reference
R_f	retention factor
rpm	rotations per minute
rt	room temperature
s	singlet (NMR) *or* strong (IR)
sh	shoulder (IR)
solv.	solvent
STM	scanning tunneling microscopy
t	triplet (NMR)
TA	tartaric acid
*t*Am	*tert*-amyl
TBAF	tetra-*n*-butylammonium fluoride
*t*Bu	*tert*-butyl
TD-DFT	time-dependent density functional theory
TEM	transmission electron microscopy
temp.	temperature
Tf	trifluoromethanesulfonyl
TFA	trifluoroacetic acid
TFPB	tetrakis[3,5-bis(trifluoromethyl)phenyl]borate
THF	tetrahydrofuran
TIPS	triisopropylsilyl
TLC	thin layer chromatography
TMEDA	tetramethylethylenediamine
TMS	trimethylsilyl *or* tetramethylsilane
Tol	*para*-tolyl
TR	time of retention
TS	transition state
TSC	through-space coupling
UHV	ultra high vacuum
UV	ultra violet light
vol.	volumetric(al)
vs	very strong (IR)
vs.	versus
vw	very weak (IR)
wt%	weight percent
w	weak (IR)
XPD	X-ray photoelectron diffraction

“Si, avons nous beau monter sur des échasses, car sur des échasses encore faut-il marcher de nos jambes. Et au plus élevé trône du monde, si ne sommes assis que sur notre cul.”

“No matter that we may mount on stilts, we still must walk on our own legs. And on the highest throne in the world, we still sit only on our own bottom.”

Michel de Montaigne,

Essais, Book III, ch. 13

1. Introduction

1.1 Helicenes, heterohelicenes and helicene-like structures

Helicenes are polycyclic aromatic non-planar compounds consisting of *ortho*-fused benzene rings[1]. The defining properties of helicenes comes from their structure. Due to the steric hindrance of the terminal benzene rings helicenes become screw-shaped holding a non-planar arrangement with the C_2-symmetric axis perpendicular to the helix axis. This makes them chiral even though they have no center of chirality. The left-handed helix is designated by "minus" and denoted by *M* descriptor whereas the right-handed helix is designated by "plus" and *P*.[2] Helicenes can be divided into three main groups according to the structure which they possess. When the helical backbone is consisting solely of *ortho*-fused benzene rings we are speaking about *carbohelicenes*, whereas *heterohelicenes* contain one or more heteroatoms in their structure. *Helicene-like* molecules are not fully aromatic but helicene-shaped compounds (Figure 1.1).

Figure 1.1

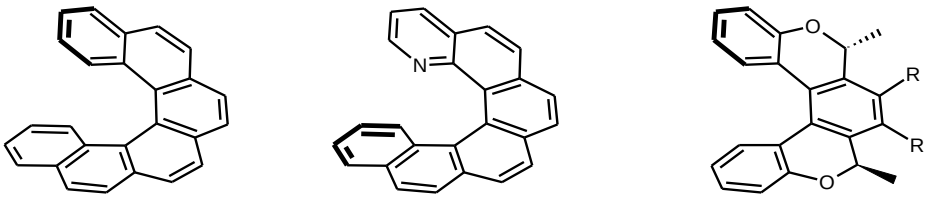

1 (*P*)-carbo[6]helicene

2 (*M*)-1-aza[6]helicene

3 (*P*)-[5]helicene-like

The highly delocalized large π-electron system of fully aromatic helicenes along with the previously mentioned inherent chirality predetermines the unique properties of such molecules and their use in many fields of research from optoelectronics to nanotechnology, whereas helicene-like compounds, due to their easy synthetic accessibility, represent a promising class of candidates for asymmetric organo- or transition metal catalysis.

Although the attempts to resolve racemic mixtures of helicenes or to affect their asymmetric synthesis dates back to the 20th century, the general synthetic approach to fully aromatic optically pure carbohelicenes has not yet been developed. Their utilization in diastereoselective reactions as chiral inducers in mid-1980´s was limited to stoichiometric amounts. The recent interest in helicenes as chiral ligands dates back to the late 1990´s. As complementary ligands to biaryl-type ligands of C_2 symmetry they bring some advantages as a higher rigidity, higher thermal stability to racemization, larger volume in space and better donor-acceptor properties for charge-transfer complexation. Those attributes play an

important role in further development of non-racemic helicene chemistry in the sense of their utilization as chiral ligands, chiral additives or chiral auxiliaries in asymmetric synthesis.

1.2 Homogenous catalysis with helical systems

One of the earliest reports on the ability of carbohelicenes to control absolute configuration at a newly formed stereogenic center was published in 1985[3]. Although the diastereoselective reduction of α-ketoester **4** with $NaBH_4$ (Scheme 1.2) was in fact a stoichiometric reaction where the carbohelicene was connected directly to the α-ketoester as a chiral auxiliary, it demonstrated that helicenes can control absolute stereochemistry of the produced secondary alcohol function (such as **5**, Scheme 1.2).

Scheme 1.2

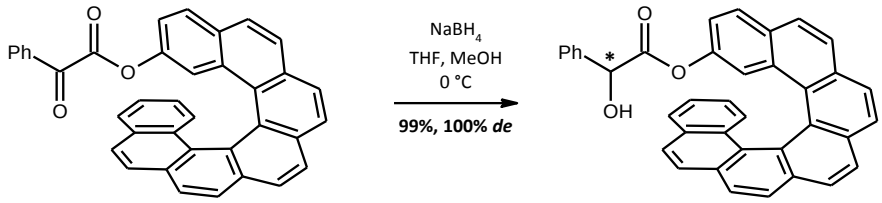

rac-**4** **5**

The high stereocontrol of the reaction came from the fact that the helical backbone discriminated the attack of the carbonyl group from one face. Similar results (86%, 100% *de*) were achieved in the ene reaction with cyclohexene at 0 °C in the presence of $SnCl_4$ as a catalyst (there was no precomplexiation of cyclohexene to the metal center) with (*E*)-crotonate ester of the racemic 2-hydroxy[7]helicene[4]. These results were indicative of specific attributes of helicenes as chiral auxiliaries for promoting asymmetric synthesis. Martin and co-workers used the [7]helicene derivatives in the same manner also in hydroxyamination[5] and epoxidation[6] of olefins and in the synthesis of atrolactic ester[7].

Among the first reactions involving helicenes as chiral reagents was the enantioselective epoxidation (Scheme 1.3).[6,7]

Scheme 1.3

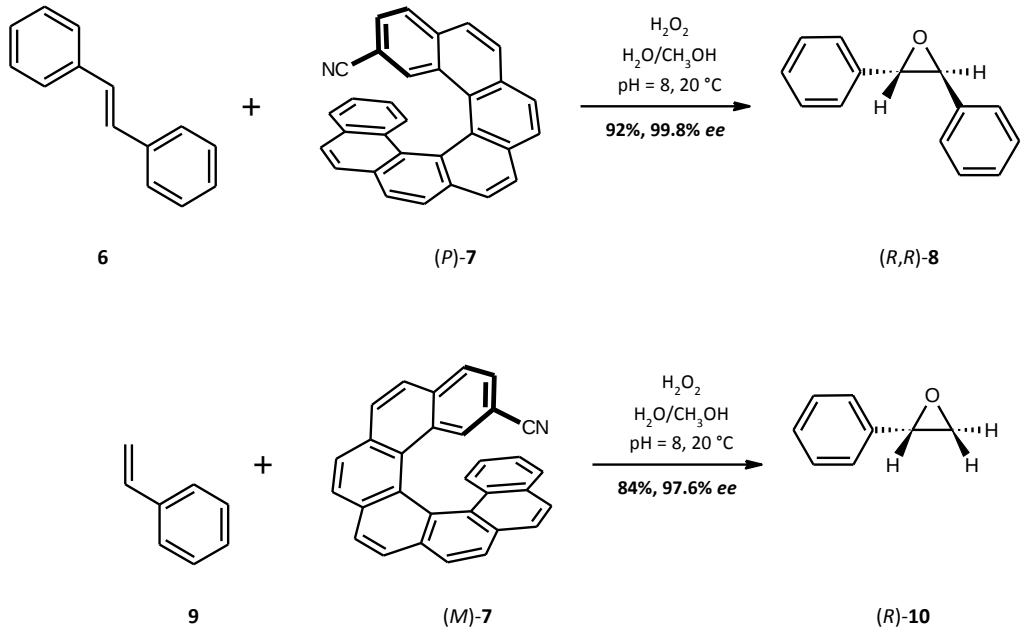

6 (*P*)-**7** (*R*,*R*)-**8**

9 (*M*)-**7** (*R*)-**10**

Helicenes acted here as effective chiral stereodiscriminating reagents. 2-cyano-[7]helicene as an additive generated *in situ* a chiral hydroperoxyimine as a reactive oxidative reagent[8]. Other use of helicenes in organocatalysis will be discussed later on.

Surprisingly, no ligands with helical chirality were employed in asymmetric transition metal catalysis until 1997 despite the fact that a plenty of chiral catalysts and ligands were developed so far. A brief summary of transition metal catalyzed reactions and the synthesis of active helical ligands will be given in next.

1.2.1 Helicenes in transition metal catalysis

1.2.1.1 Asymmetric hydrogenation

Reetz and co-workers reported the first catalyst based on a helically chiral ligand[9]. It was a rhodium catalyzed hydrogenation of methyl itaconate **11** (Scheme 1.4). The catalytic species was formed *in situ* from an equimolar mixture of $[Rh(cod)_2]BF_4$ and (*M*)-PHelix **12** (2,15-bis(diphenylphosphino)-[6]helicene, [6]heliphos).

Scheme 1.4

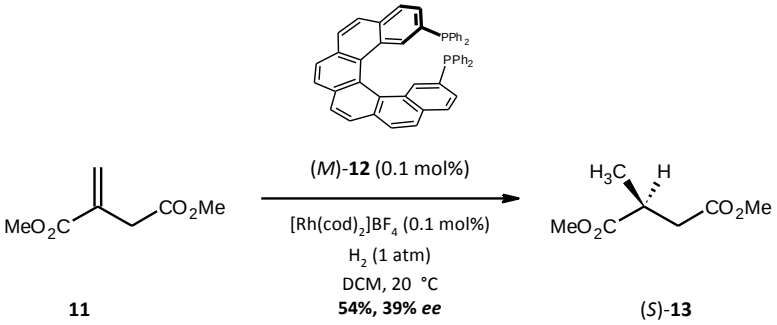

The reaction afforded (*S*)-**13** under mild conditions in 54% yield and 39% *ee*.

The synthesis of **12** started from 2,7-dibromomethylnaphtalene **14** (Scheme 1.5) and the key intermediate in the synthesis was 2,15-dibromo[6]helicene **18** first published by Yamamoto et al[10]. The generated double ylide from **15** underwent the Wittig reaction with corresponding aldehyde **16** giving stilbene **17**, which was photocyclized and oxidized to form racemic **18** (Scheme 1.5).

Scheme 1.5

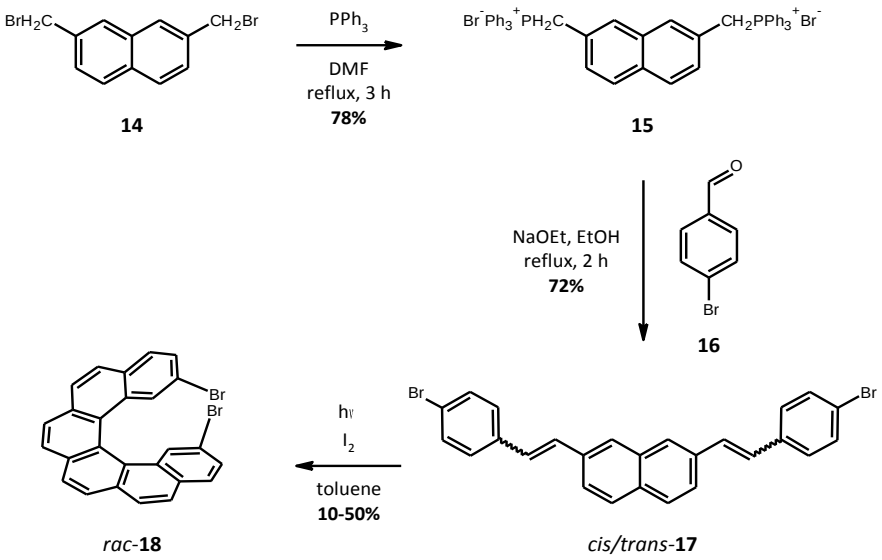

The antipode separation of racemic **18** was achieved on a preparative scale by using HPLC with a chiral stationary phase (Chiralcel) to receive both enantiomers of **18** in >96% optical purity. Consequently, the (*M*)-**18** was subjected to lithiation/phosphinylation yielding (*M*)-**12** in an essentially optically pure form (>98% *ee*) (Scheme 1.6).

Scheme 1.6

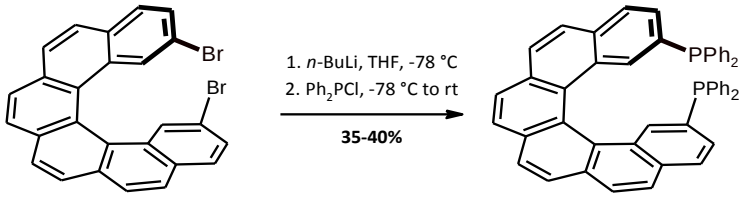

(*M*)-**18** (*M*)-**12**

Brunner published practically the same synthesis of racemic **12** ([6]Heliphos, Scheme 1.6) together with its smaller [5]helicene analogue called [5]Heliphos at the same time[11].

The hydrogenation of methyl itaconate **11** was reexamined by Yamaguchi and Nakano in 2003 using the bihelicenol phosphite **19**[12] (Scheme 1.7). The ligand bearing helical (*M*) and axial (*S*) chirality together with stereogenic center of (*l*)-menthyl gave the best results (100%, 96% *ee*), whereas the phosphite **20** gave only 49% *ee* with the same yield (Scheme 1.7).

Scheme 1.7

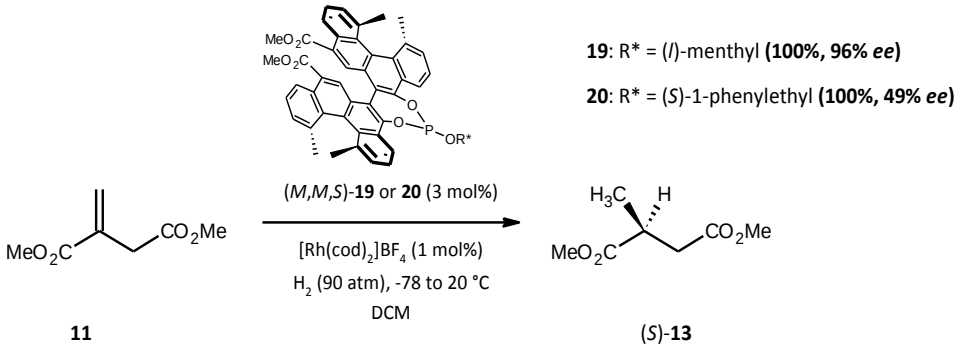

11 (*S*)-**13**

The configurational stability of the [4]helicene at 20 °C comes from the steric repulsion of the inner methyl groups so it can be applied as the smallest helicene for further use in asymmetric catalysis. The synthesis of the phosphite ligand used in previous started with the corresponding bihelicenols **25**[13] prepared from (*M*)-**21**[14] by the same authors (Scheme 1.8).

Scheme 1.8

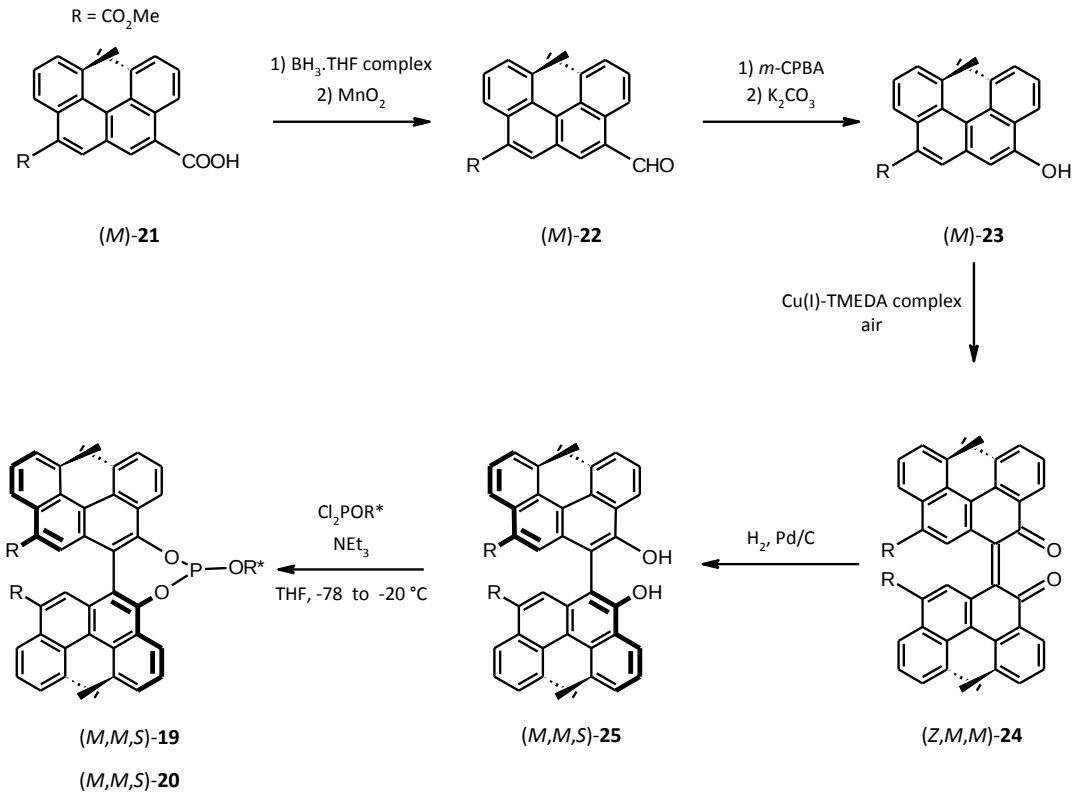

Aldehyde (*M*)-**22** (Scheme 1.8) obtained from (*M*)-**21** was converted to the helicenol (*M*)-**23** by Baeyer–Villiger oxidation with *m*-chloroperbenzoic acid followed by hydrolysis of the resulted formate. Treatment of (*M*)-**23** with a Cu(I)-TMEDA complex under air gave a dimeric quinone (*Z*,*M*,*M*)-**24**, where (*Z*)-isomer was obtained exclusively without any trace of the (*E*)-isomer. Bihelicenol (*M*,*M*,*S*)-**25** is available upon stereoselective hydrogenation of (*Z*,*M*,*M*)-**24**. No traces of (*M*,*M*,*R*)-**25** were detected and it seems that the stereoselectivity of the reduction is under the kinetic control. The (*M*,*M*,*R*)-**25** isomer is formed under reflux in toluene from (*M*,*M*,*S*)-**25**. The diastereomers can be isolated by column chromatography.

1.2.1.2 Kinetic resolution in Pd-catalyzed allylic substitution

Another utilization of (+)-PHelix (+)-**12** in catalysis came from Reetz in 2000[15]. Kinetic resolution in Pd-catalyzed allylic substitution of 1,3-diphenyl-propenylacetate **26** (Scheme 1.9) with dimethyl malonate **27** was disclosed. Using the (+)-**12** antipode, a mixture of the substitution product (*R*)-**28** and unreacted allylic acetate (*R*)-**26** was formed at *ca* 50% conversion providing them in 82.7% *ee* and 99% *ee*, respectively (Scheme 1.9).

Scheme 1.9

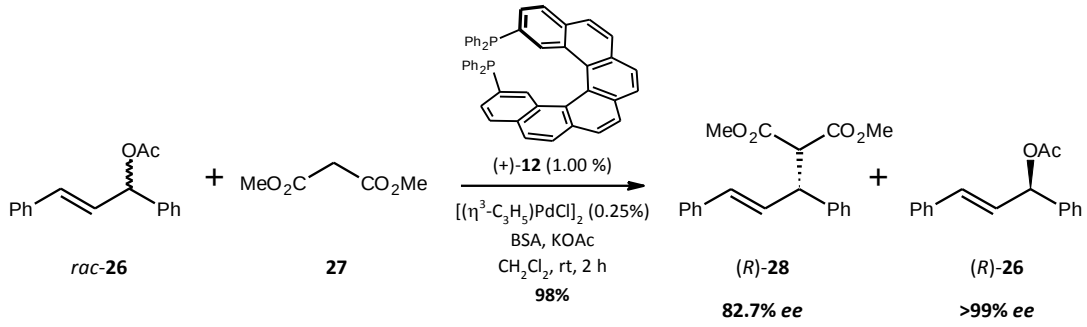

The (+)-**12** was behaving as a monodentate ligand in the reaction as showed by the NMR studies and also the X-ray analysis of the ligand displaying the large distance 6.481(1) Å of the two phosphorus atoms. Other substrates were studied with respect to the possible influence of the leaving group. A similar trend was observed in the case of benzoate. Although no significant difference in the substitution process was observed, in the step of kinetic resolution the acetate was a more efficient leaving group.

1.2.1.3 Enantioselective addition of organozinc reagents to aldehydes

Yamaguchi et al. published a synthesis of the optically pure cycloamide (*P*,*P*)-**30** (Scheme 1.10) consisting from two [4]helicene subunits[16]. The asymmetric addition reaction of diethylzinc to aldehydes was catalyzed by chiral amino alcohols, binaphthols, sulfonamides, etc.[17]. A brief catalytic study employing the (*P*,*P*)-**30** in the same reaction was done. The best results were achieved using β-naphthaldehyde **29** as a substrate (59%, 50% *ee*, Scheme 1.10).

Scheme 1.10

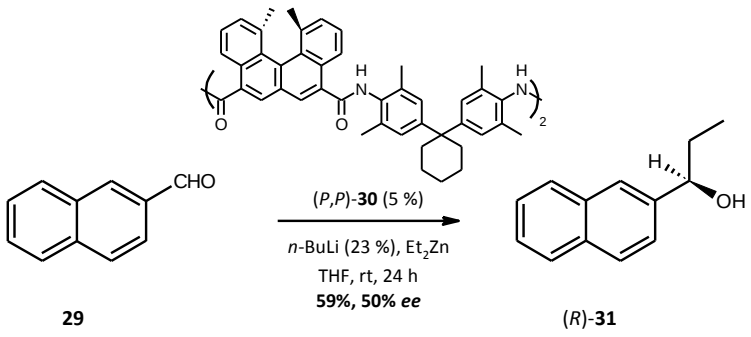

The lithiation of (*P*,*P*)-**30** and use of THF solvent were essential. Macrocycles with less and more helical subunits (such **37**, **38**, Scheme 1.12) gave racemic alcohols. Although the asymmetric induction was moderate the use of the macrocyclic ligand was novel and potentially interesting.

The synthesis of the macrocyclic amide (*P*,*P*)-**30** started from the resolved dicarboxylic acid (*P*)-**34** (Scheme 1.11).

Scheme 1.11

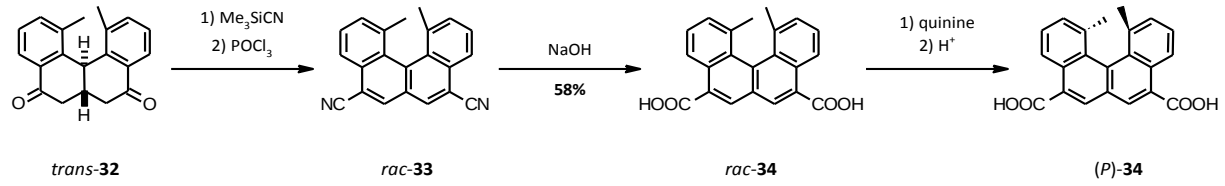

A known diketone **32** (Scheme 1.11) prepared by Newman[18] possessing *trans* configuration as proved by the X-ray analysis[19] was converted to dinitrile **33** by cyanation[20] and dehydration with concomitant dehydrogenation. Then, **33** was hydrolyzed to dicarboxylic acid **34** in 58% yield from **33**. Optical resolution was pursued by forming diastereomeric salts with 2 eq of quinine. It was found that recrystallization of the quinine salt from a chloroform-methanol mixture gave one diastereomer, which was converted to (*P*)-**34** on acidification (98% *ee* by HPLC analysis). The chiral acid (*P*)-**34** was transformed to corresponding chloride (*P*)-**35** (Scheme 1.12) and treated with diamine bridge **36** to form the macrocyclic ligands (*P*,*P*)-**30**, (*P*,*P*,*P*)-**37** and (*P*,*P*,*P*,*P*)-**38** (Scheme 1.12) that were separated by GPC in 24%, 23% and 19% yield, respectively.

Scheme 1.12

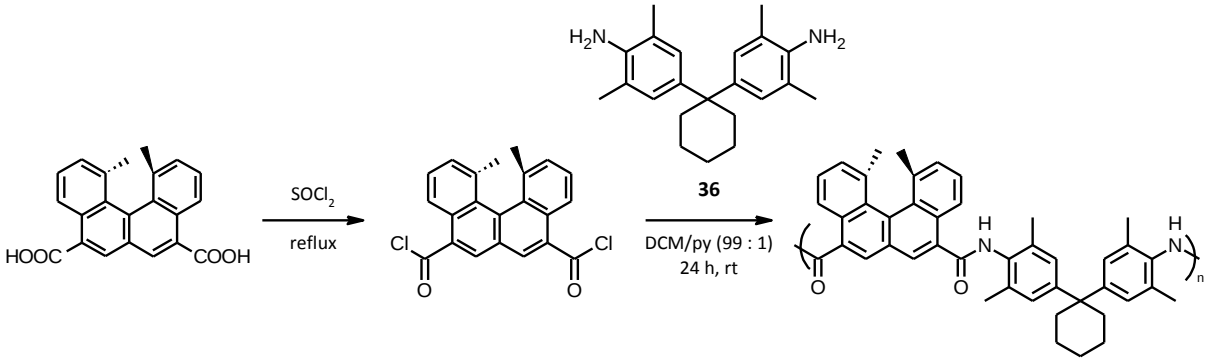

In 2000, Katz and co-workers reported the same catalytic reaction utilizing another helical ligand (*P*,*P*,*S*)-[5]HELOL[21] **40** (Scheme 1.13). The optimized reaction of benzaldehyde **39** with Et_2Zn furnished the product (*S*)-1-phenylpropanol **41** in 93% yield with 81% *ee* (Scheme 1.13).

Scheme 1.13

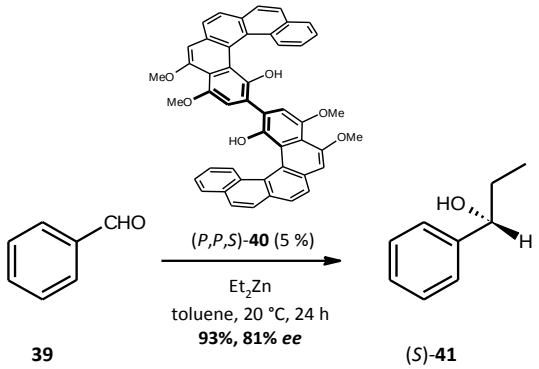

The [5]HELOL **40** was studied in comparison to BINOL and other simple diols (without additional heteroatoms at the active site) that are not usually very effective in this reaction (e.g. (*R*)-BINOL gave *ceteris paribus* 56% yield, 34% *ee*).

Starting from the commercially available 3-acetylphenanthrene **42** (Scheme 1.14), the key intermediate [5]helicenequinone **45** was obtained in overall 81% yield within three steps (Scheme 1.14). The starting material **42** contained up to 10% of hardly separable 2-acetylphenanthrene. Therefore there were no separation steps during the synthesis of **45**. The quinone **44** was alkylated in the last step, whereas the planar molecule coming originally from 2-acetylphenantrene was not reacting so fast and the racemic helical quinone **45** was precipitated by pouring the reaction mixture into water. All side products coming from 2-acetylphenantrene are not depicted for simplicity in Scheme 1.14.

Scheme 1.14

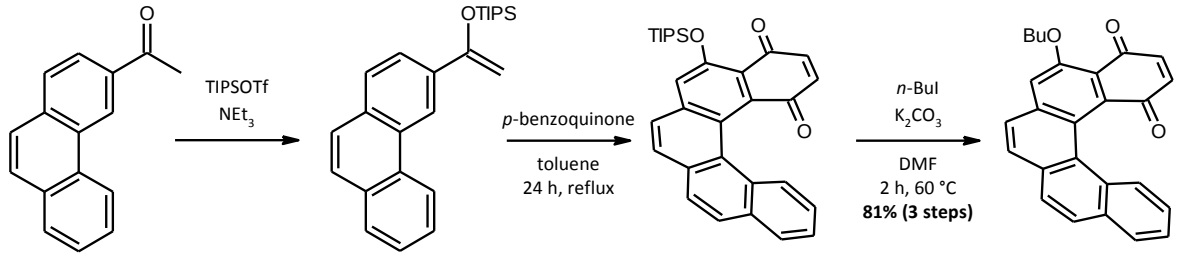

Then the quinone **45** was transformed into the monoalkylated ether **46** (Scheme 1.15) by the Russig[22] and Laatsch[23] methodology using reduction by sodium dithionite followed by the reaction with an alcohol saturated with HCl. Ether **46** was then treated with (*S*)-(-)-camphanoyl chloride **47** to afford the resolved (*P*)-[5]helicene camphanate (*P*)-**48** precipitating after trituration with diethyl ether in 80% yield and >98% *ee*. (*P*)-**46** obtained after hydrolysis of (*P*)-**48** dimerized to the stereochemically pure dimer (*P*,*P*)-**49**. Finally,

(*P*,*P*)-**49** was reduced by zinc in acetic acid to form (*P*,*P*,*S*)-**40** in 98% enantiopurity and quantitative yield (Scheme 1.15).

Scheme 1.15

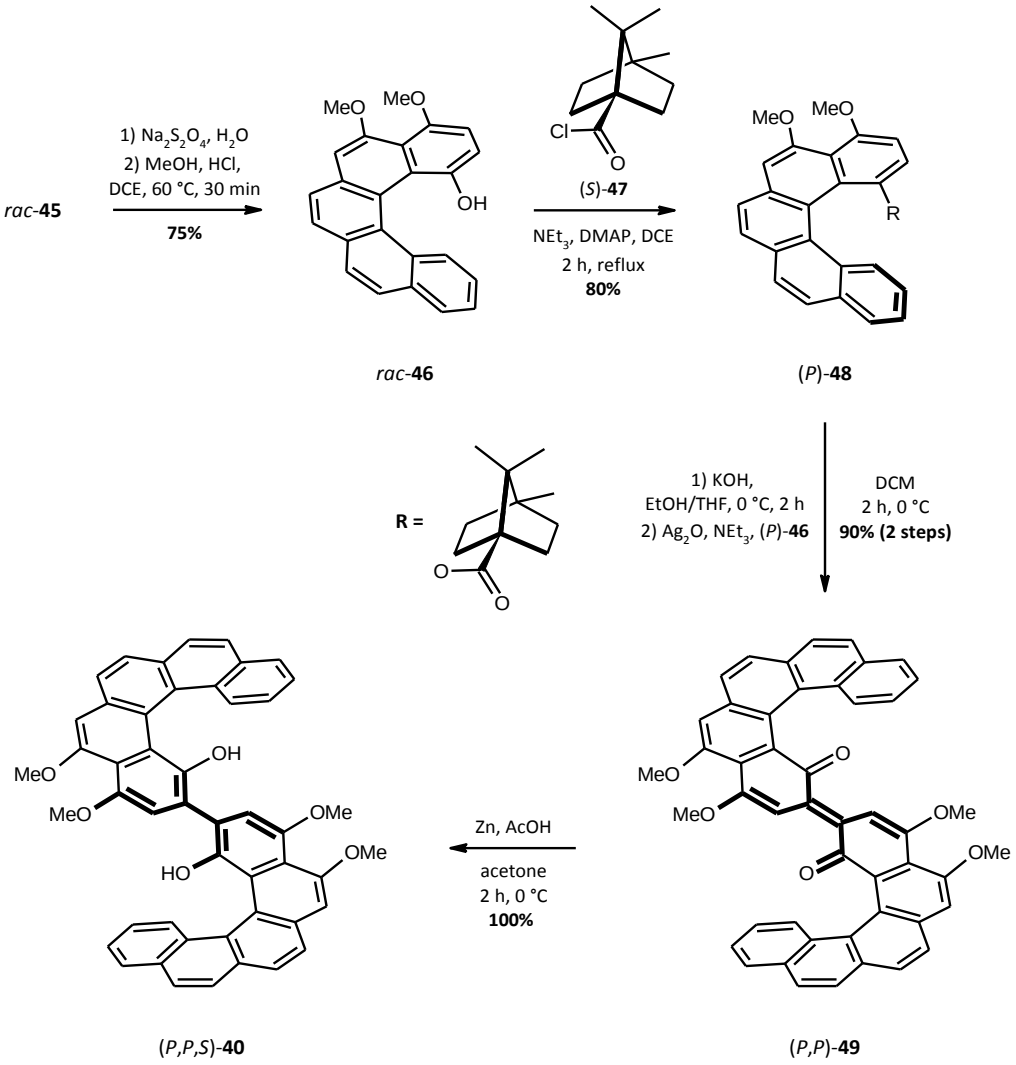

The asymmetric amplification in the catalytic asymmetric synthesis is of a great interest. Soai and co-workers published the autocatalytic enantioselective addition of dialkylzinc to aldehydes[17b]. Later on in 2001 they found that [6]helicene (*P*)-**1** (Figure 1.1), can serve as an asymmetric trigger in such a reaction[24] (Scheme 1.16).

Scheme 1.16

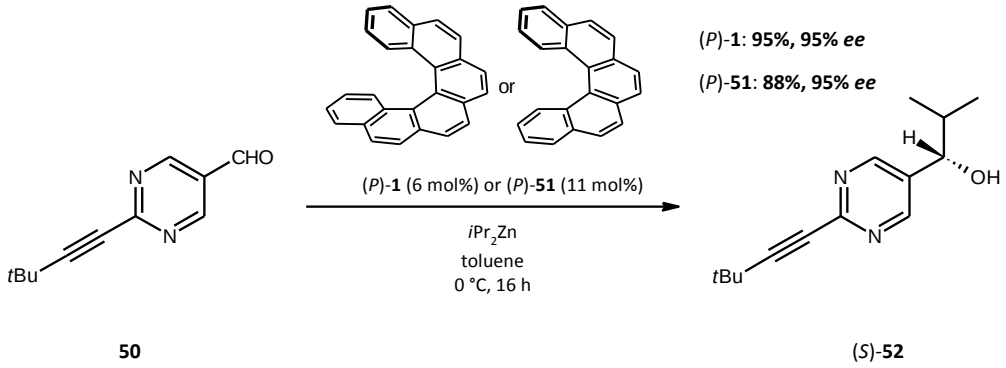

50 (*S*)-**52**

The high *ee* values and the absolute configuration was explained as follows: [6]- and [5]helicenes without any heteroatoms induced asymmetry in the initially formed zinc alkoxide of **52** (Scheme 1.16), with the absolute configuration regulated by the (*P*) (giving rise to (*S*) configuration of **52**) or (*M*) (giving rise to (*R*) configuration of **52**) helicity of helicenes. Asymmetric autocatalysis of the zinc alkoxide of **52** with an amplification of *ee* afforded alcohol **52** with very high *ee*. The optically pure (*P*)-**1** afforded (*S*)-**52** in 95% yield with 95% *ee*. The consecutive asymmetric catalysis was more evident when only enantiomerically enriched helicenes were used. Using (*P*)-**51** of 67% optical purity gave the product **52** in 95% *ee*. Even if the optical purity of helicene **1** was very low ((*P*)-**1**: 0.13% *ee*; (*M*)-**1**: 0.56% *ee*), the resulted product **52** was obtained with 56% and 62% *ee*, respectively.

The synthesis of **1** (Figure 1.1) and **51** (Scheme 1.16) will not be discussed in detail. There is a range of synthetic methodologies for construction of racemic carbohelicenes involving photocyclization, Diels-Alder reactions, Friedel-Crafts type reactions, Pd catalyzed coupling reactions, ring closing metathesis, metal catalyzed [2+2+2] cyclization and radical cyclizations, all followed by optical resolution or there are many of mentioned methods used in the asymmetric way.[25,26]

Similarly, the tetrathia[7]helicenes **53** and **54** (Scheme 1.17) were found to affect the asymmetric autocatalytic reaction too[27]. All the conclusions said before hold true for this case. The helicene of (*P*) configuration gave rise to the (*S*)-pyrimidyl alcohol **52**, (*M*) helicity led to the (*R*) configuration of **52**. The reaction was promoted by autocatalytic influence of the zinc alkoxide of **52** as was proved by using poorly enantiomerically enriched helicenes. Both tetrathia[7]helicenes were found to be very potent in furnishing the desired product in high yield and excellent *ee* values (Scheme 1.17).

Scheme 1.17

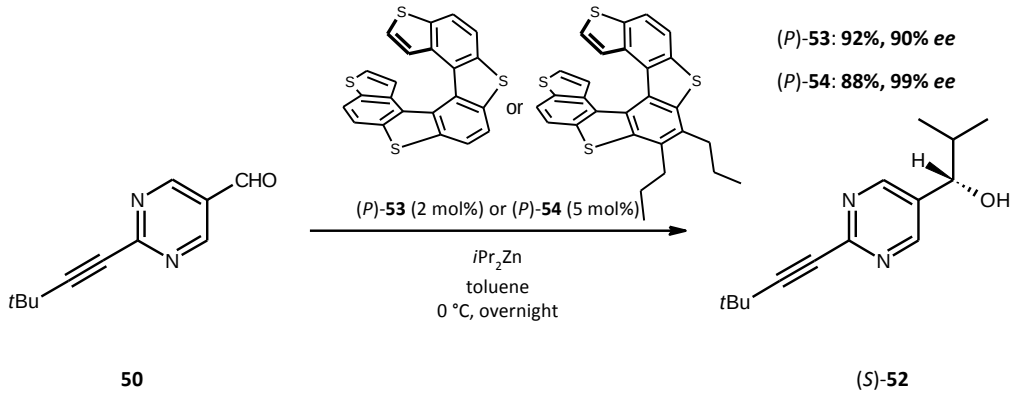

50 (*S*)-**52**

The helicene (*P*)-**53** with 98% optical purity gave (*S*)-**52** in 92% yield with 90% *ee*. On the other hand, when using (*M*)-**53** with 90% *ee*, (*R*)-**53** was obtained in 91% yield with 89% *ee*. When thiahelicene **53** with low *ee* (10% *ee* for (*P*), 12% *ee* for (*M*)) was used as a chiral inducer, **52** was obtained with high *ee* (75% *ee* and 88% *ee*, respectively) in yields over 90%. Even using the (*P*)-**53** with 2% *ee* (or (*M*)-**53** with 3% *ee*)**,** (*S*)- and (*R*)-**52** in reproducible yield higher than 80% with 83% *ee* and 85% *ee*, respectively were obtained. Similarly, (*P*)-**54** with 99% *ee* optical purity gave (*S*)-**52** in 88% yield with 99% *ee* and (*M*)-**54** with 95% *ee* produced (*R*)-**52** in 88% yield with 95% *ee*. When thiahelicene **54** with low *ee* (2% *ee* for (*P*), 3% *ee* for (*M*)) was used as a chiral inducer, **52** was obtained with 83% *ee* and 48% *ee*, respectively, in the same 88% yield. The enantioselectivity observed in this asymmetric reaction was explained as follows: *i*Pr_2Zn was coordinated to sulfur atoms of the chiral thiahelicene to form an active chiral zinc species. Since these chiral species reacted with pyrimidine-5-carbaldehyde **50** in the initial stage of the reaction, a small enantiomeric excess was induced. Then, a subsequent asymmetric autocatalysis with an amplification of *ee* afforded alkanol **52** (as zinc alkoxide) with a high *ee*, which showed the corresponding absolute configuration.

The synthetic route to tetrathia[7]helicenes comprised double photocyclization reactions of an appropriate precursor first published in 1971[28]. A simplified method reported in 2003 by Maiorana et al.[29] is described (Scheme 1.18).

Scheme 1.18

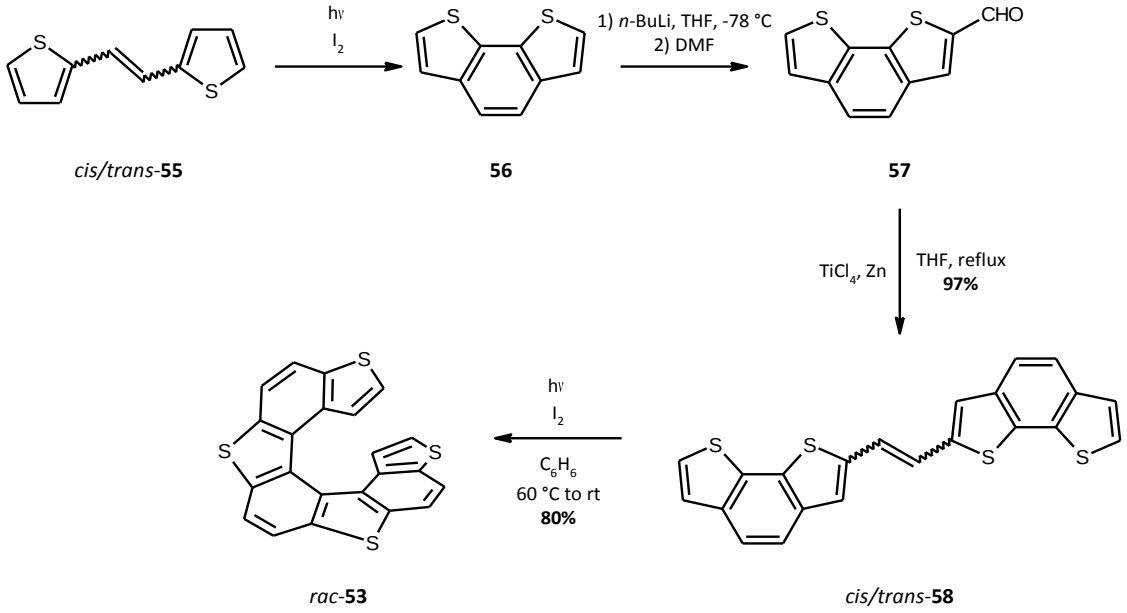

In general, benzodithiophene **56** (Scheme 1.18) synthetized photochemically[28] from **55** was transformed into aldehyde **57**. The McMurry coupling reaction under standard conditions provided the alkene **58** in high yield (97%). Photocyclization of **58** formed the racemic **53** in 80% yield (overall yield was 48%, Scheme 1.18). Its enantiomeric forms were available after the racemate resolution using a chiral HPLC stationary phase (Chiralpak IA)[27]. The dipropyl analogue **54** was prepared in a similar way[30] (Scheme 1.19).

Scheme 1.19

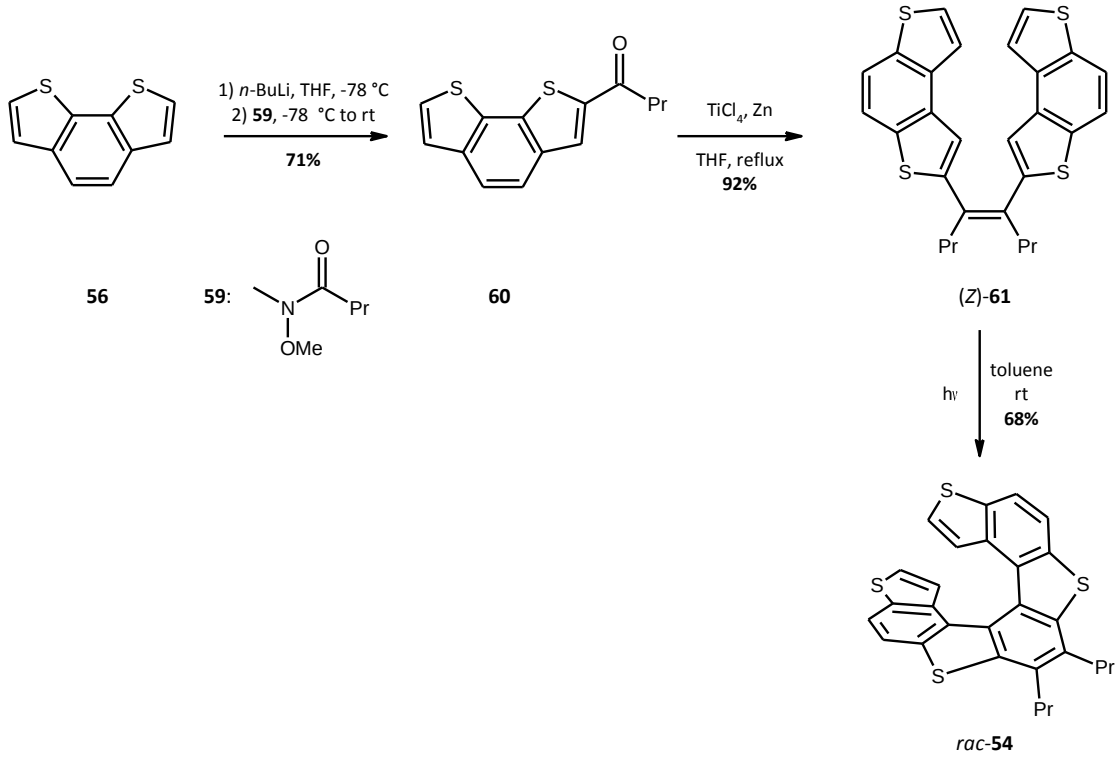

Starting from **56**, ketone **60** was synthetized by lithiation followed by treatment with the Weinreb amide **59**[31]. Using the previously mentioned strategy, the McMurry coupling reaction was applied to form the alkene species (*Z*)-**61** which upon photocyclization gave racemic **54**. It was resolved on a chiral HPLC stationary phase (Chiralpak IA)[27,32] giving optically pure (*P*)- and (*M*)-**54** enantiomers.

1.2.1.4 Asymmetric hydroformylation

Eilbracht, Starý, Stará and co-workers reported on Rh-catalyzed hydroformylation utilizing helical phosphites[33]. Phosphine/phosphite ligands are the most frequently employed ligands along with rhodium catalysts in the asymmetric hydroformylation of terminal alkenes[34,35]. The branched product **63** (Scheme 1.20) was obtained regioselectively by using the ligand (*P*,*S*)-**62** bearing a *biphenyldiol* moiety even though the *ee* value was only moderate (up to 32% *ee*, Scheme 1.20).

Scheme 1.20

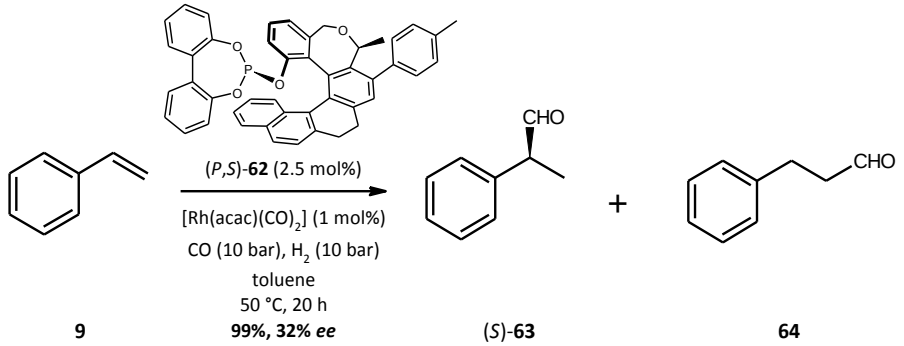

9 **99%, 32% *ee*** (*S*)-**63** **64**

Styrene **9** (Scheme 1.20) and its derivatives were examined in this reaction together with the helical ligands **62** and **65** – **67** differing from **62** in the connected phophite part (Figure 1.21).

Figure 1.21

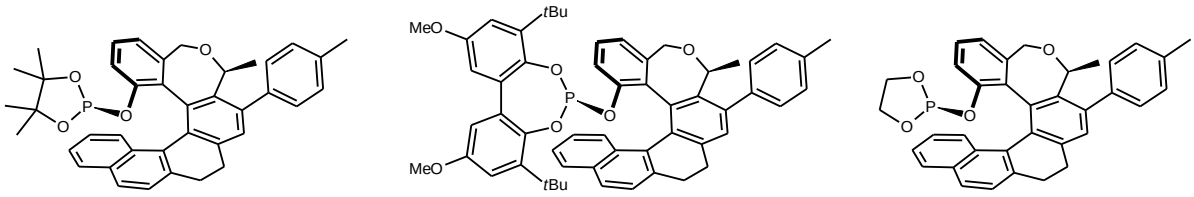

(*P*,*S*)-**65** (*P*,*S*)-**66** (*P*,*S*)-**67**

Nevertheless, there were common features of all examined reactions: the conversions were higher than 90% except for the two cases were only about the 70% conversion was achieved. The branched product **63** was favored in all cases; regioselectivity was usually higher than 91% except for the two cases where **64** was obtained in 14% and 33% yield. The (*P*,*S*) configuration of phosphites **62**, **65**, **66** and **67** gave rise to the enantiomerically enriched product (*S*)-**63**. Only (*P*,*S*)-**66** gave the racemic **63** in two cases during the testing.

The phosphites (*P*,*S*)-**62**, (*P*,*S*)-**65**, (*P*,*S*)-**66**, (*P*,*S*)-**67** were prepared from the corresponding helical alcohol **68**[36] (Scheme 1.22) by its deprotonation and subsequent treatment with commercially available chlorophosphites (**69** – **72**) (Scheme 1.22).

Scheme 1.22

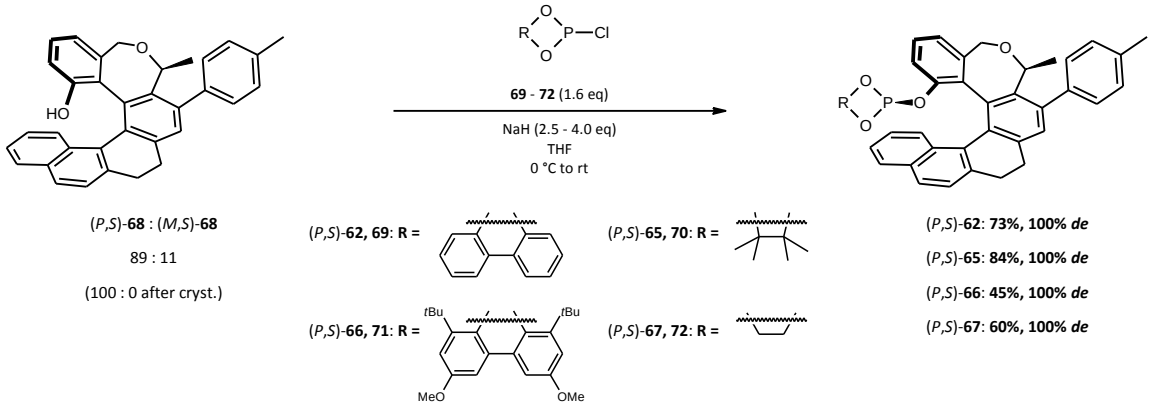

The multistep synthesis of the optically pure alcohol (*P*,*S*)-**68**, starting from *o*-vanillin **73** (Scheme 1.23), was based on [2+2+2] diastereoselective cyclotrimerization mediated by Co(I) catalysts. A synthetic route to the triyne **80** involved the incorporation of the chiral building block (*S*)-**75**[37], coming from the commercially available (*S*)-butynol, into its structure (Scheme 1.23).

Scheme 1.23

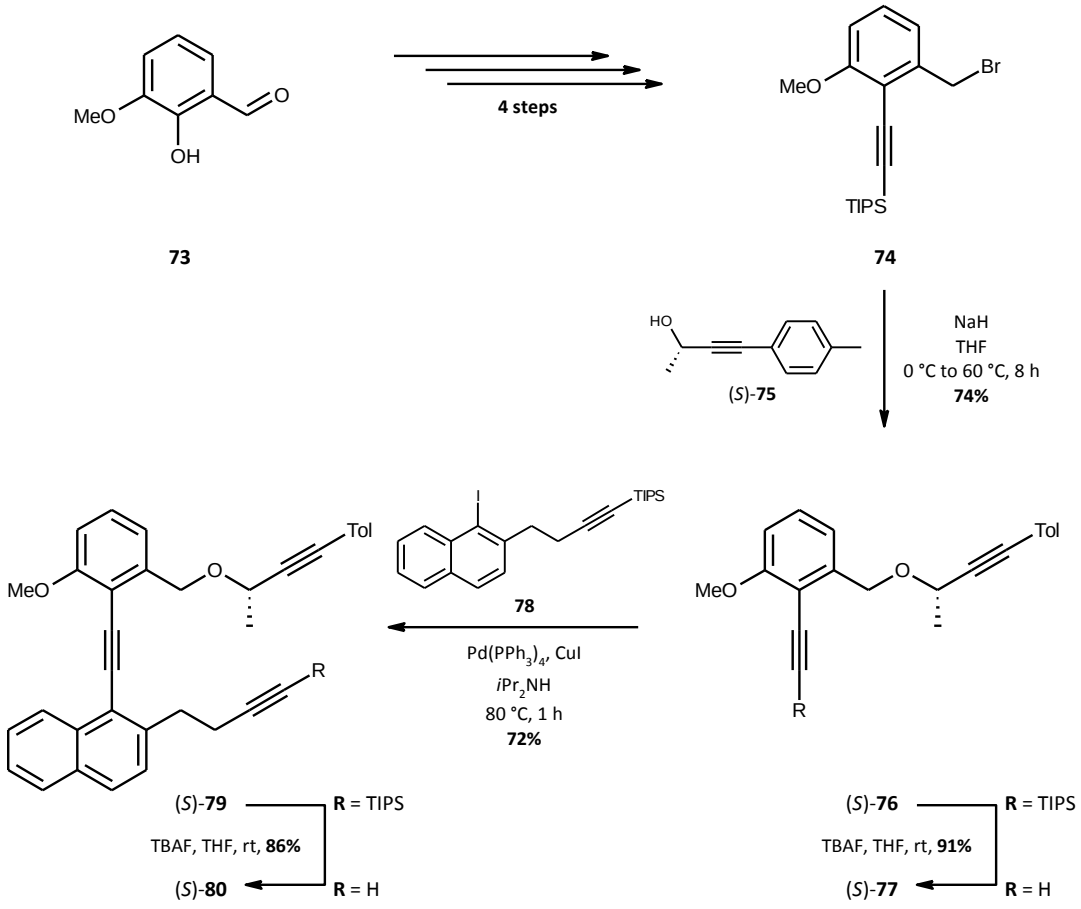

The absolute configuration of the chiral center presented in the molecule of triyne (*S*)-**80**, constructed via Sonogashira coupling reaction with **78**[38], is proposed to control the stereochemical outcome of the cyclization giving rise to the (*P*) or (*M*) helicity predominantly[39] (Scheme 1.24).

Scheme 1.24

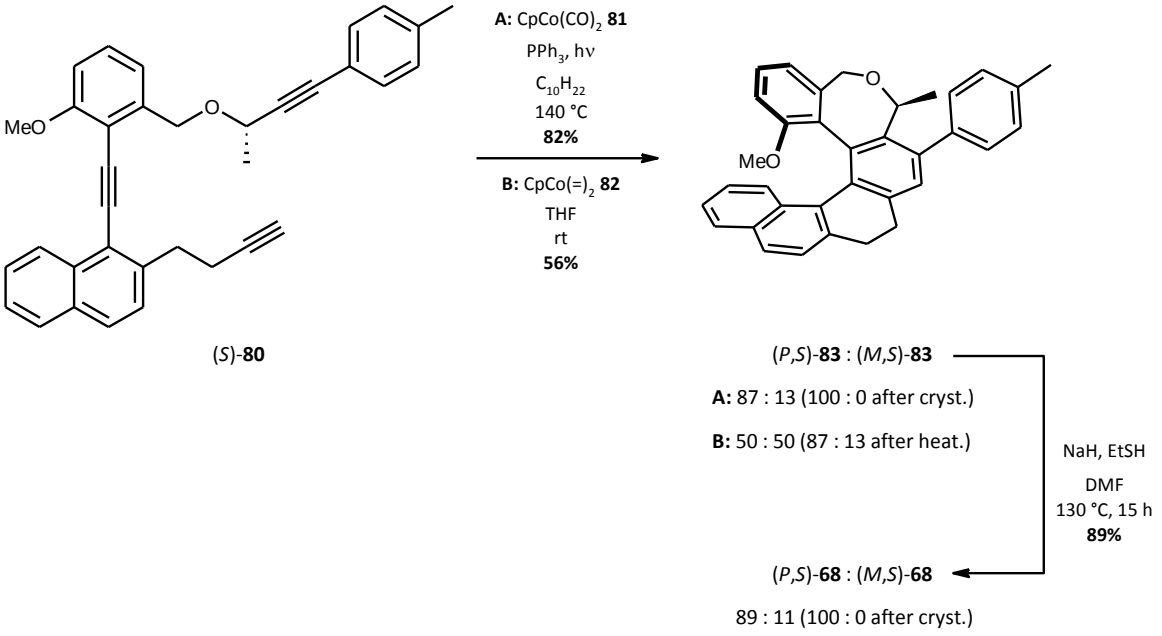

The (*S*) configuration at the asymmetric center of triyne **80** induced predominantly (*P*) helicity of the product. Performing $CpCo(=)_2$ **82** (Jonas catalyst[40]) mediated [2 + 2 + 2] cycloisomerization (**B**) of the chiral triyne (*S*)-**80** at room temperature, no diastereoselectivity of cyclization was observed. Kinetic studies revealed that (*M*,*S*) and (*P*,*S*) diastereomers of the helicene-like compounds (such as **83**) with a hexacyclic backbone underwent thermal equilibration, which led finally to the same ratios of (*M*,*S*) and (*P*,*S*) diastereomers as those monitored in the corresponding [2 + 2 + 2] cycloisomerizations at elevated temperature (**A**). Barriers to epimerization were found to be lower than those for the parent [6]helicene **1** due to a higher flexibility of the not fully aromatic helicene-like skeleton. It clearly indicated that diastereoselectivity of [2 + 2 + 2] cycloisomerization of the chiral triyne (*S*)-**80** at 140 °C was controlled by thermodynamic factors whereas kinetic factors operated at room temperature. Stemming from these findings, the preparation of the optically pure helicene-like alcohol (*P*,*S*)-**68** was accomplished on a multigram scale by removal of the methyl group from **83** (see Scheme 1.24).

1.2.1.5 Asymmetric allylic amination

This type of a reaction will be described herein more detailed in relation to the Results and Disccusion part of this Thesis. Allylamines (such as **86**, **87**, **89**, Scheme 1.25) are fundamental building blocks in organic chemistry representing a frequent structural motif encountered in many natural products. Moreover, the presence of the double bond in their structure enables further transformations. The synthesis of allylamines can be formally divided into three subgroups of reactions (two of them in Scheme 1.25).

Scheme 1.25

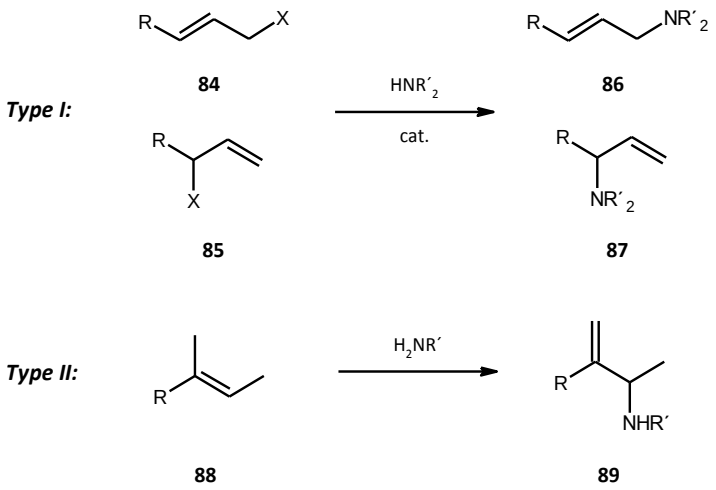

The *type I* of allylamines can be synthesized by nucleophilic allylic substitution and the *type II* represents a direct allylic amination of simple alkenes. The third type of the synthesis relates to indirect approaches leading to allylamines. Regarding the results achieved in the field of homogenous asymmetric catalysis using the helical ligands, the *type I* synthetic way to nonracemic allylic amines using the transition metal catalysis will be discussed in next. For the *type II* and *III* approach see the literature[41].

The nucleophilic allylic substitution of alkenes (such as **84** or **85**) was for decades a domain of palladium-catalyzed reactions[41e,42]. The scope of nucleophiles in these reactions is broad and many of ligands were found to create catalysts exhibiting high stereoselectivities. However, reactions catalyzed by complexes of other metals may differ in stereoselectivity and regioselectivity achieved. In particular, the palladium-catalyzed reactions usually form the linear products (**86**) from electrophiles that are substituted at only one terminus (**84**), whereas catalysis based on other transition metals leads to typically branched product **87** (see Scheme 1.25).

Branched isomers coming from substitution at the more hindered position of various allylic electrophiles can be obtained with high enantioselectivity using different, often readily accessible, catalysts. Such

complexes include certain palladium[43], molybdenum[44,45] and tungsten[46] systems. Unfortunately, the last two types of metal complexes disallow the use of heteroatom nucleophiles.

Recently, there were several important achievements in allylic amination (and its asymmetric version) employing rhodium and iridium complexes. Evans and coworkers published reactions of optically enriched, branched allylic carbonates that underwent nucleophilic substitution (with C-nucleophiles) with a high degree of retention of configuration in the presence of rhodium catalyst and achiral phosphite ligand.[47] In addition, Takeuchi et al. showed that iridium/achiral phosphite ligand systems catalyze the allylic amination of linear allylic carbonates (such **84**, see Scheme 1.25) and generate branched substitutions products **87**[48] (see Scheme 1.25). An early study of Helmchen and Janssen using the iridium/chiral phosphine-oxazoline ligand catalytic system afforded excellent regioselectivity and high *ee* values with soft carbon nucleophiles[49]. Further studies done namely by Hartwig showed that a catalyst generated from $[Ir(cod)Cl]_2$ **91** and a chiral monodentate phosphoramidite ligand (such as **90**, Figure 1.26) is very efficient in allylic aminations yielding high branch-to-linear ratios and excellent enantioselectivities[50,51] allowing to employ a broad range of nucleophiles of primary benzylic, allylic, and saturated aliphatic amines as well as cyclic and acyclic secondary amines and a series of allylic carbonates.

Figure 1.26

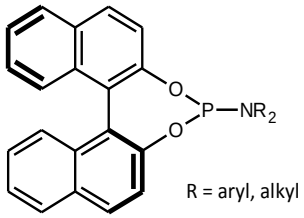

(*R*)-**90**

Phosphoramidites showed to be versatile ligands in this reaction owing to their chirality induction efficiency, facile availability, and possibility to apply new combinatorial approaches to asymmetric allylic amination and catalysis in general. A catalytically active species **95** (see Scheme 1.28) is formed after coordination of phosphoramidite to low-valent iridium and subsequent base-mediated C-H activation[52] (Scheme 1.27).

Scheme 1.27

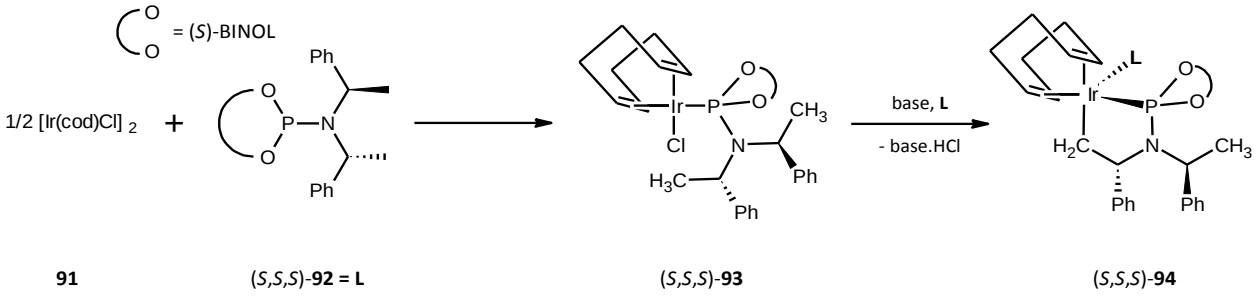

91 (*S*,*S*,*S*)-**92 = L** (*S*,*S*,*S*)-**93** (*S*,*S*,*S*)-**94**

The proposed catalytic system is shown (Scheme 1.28). For more detailed mechanistic study on Ir catalyzed allylic amination see ref.[41g]

Scheme 1.28

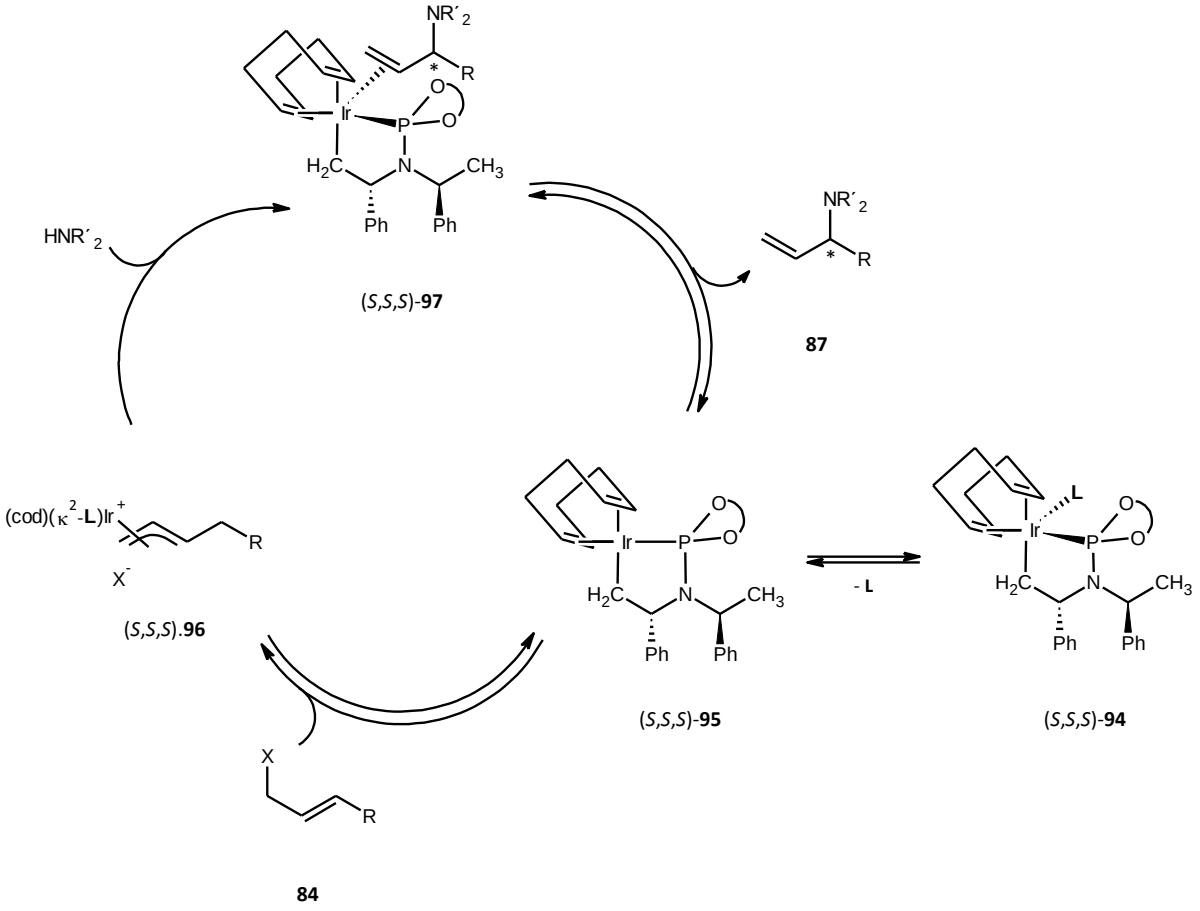

Next to ligands possessing central, axial or planar chirality, helically chiral ligands can serve as effective chiral inducers in asymmetric allylic aminations as demonstrated by Eilbracht, Starý, Stará and co-workers[33]. They studied the catalytic system consisting from the Ir(I) complex **91** and chiral phosphite

ligands (*P*,*S*)-**62**, (*P*,*S*)-**65**, (*P*,*S*)-**66** and (*P*,*S*)-**67** (see Scheme 1.20 and Figure 1.21) with the cinnamyl carbonate **102** or (pyridinyl)allyl carbonate **103** as electrophiles and different primary and secondary amines **99** – **102** as nucleophiles (Figure 1.29).

Figure 1.29

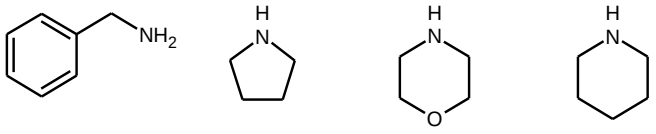

98 **99** **100** **101**

The best results were achieved with (*P*,*S*)-**65** for both the substrates providing the branched products (such as **87**) with 95% and higher branch-to-linear selectivity (the linear products are not depicted for simplicity, Scheme 1.30).

Scheme 1.30

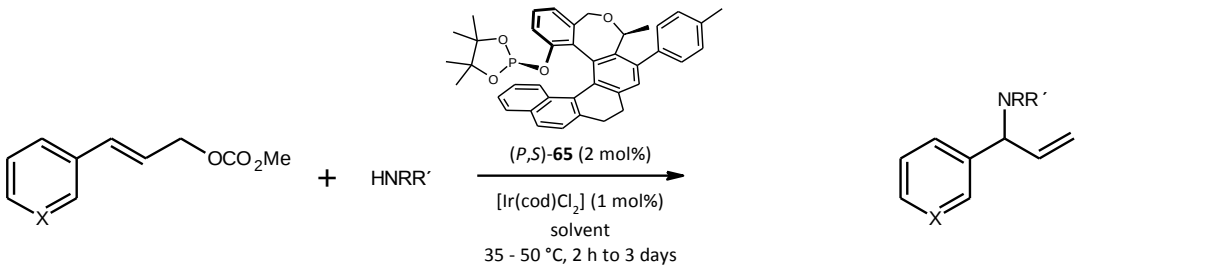

102: X = CH

103: X = N

98 - **101**

(*S*)-**104:** X = CH, R = H, R´ = CH_2Ph, **25%, 93% *ee***

(+)-**105:** X = CH, R = R´ = -$(CH_2)_4$-, **60%, 92% *ee***

(+)-**106:** X = CH, R = R´ = -$(CH_2)_2O(CH_2)_2$-, **69%, 91% *ee***

(+)-**107:** X = N, R = R´ = -$(CH_2)_5$-, **70%, 94% *ee***

The previously examined phosphite ligand (*P*,*S*)-**62** in hydroformylation (see Scheme 1.20, Chapter 1.2.1.4) provided only moderate enantioselectivity, whereas (*P*,*S*)-**66** and (*P*,*S*)-**67** were in the allylic amination inactive. The originally low yield of (*S*)-**104** dramatically increased with the change of a solvent (from THF to DCM) maintaining the comparable enantiomeric excess (95%, 90% *ee*), so all other reactions were performed in DCM. The efficiency of phosphite (*P*,*S*)-**65** within the series (**62**, **65** – **67**) leading to the best enantioselectivities along with predominantly highest reactivities regardless of the substrate and *N*-nucleophile used might be related to its proposed C–H activation to generate a catalytically active P–C-chelated iridium species[52] (owing to the presence of the CH_3 groups in the dioxaphospholanyl moiety).

1.2.2 Helicenes in organocatalysis

The advantages of organocatalysts (small organic molecules) include the lack of sensitivity to moisture and oxygen, their availability, low cost, and low toxicity, which confers a huge direct benefit in the production of pharmaceutical intermediates when compared with (transition) metal catalysts. An achiral organocatalysis have a long history but current interest in organocatalysis is focused on asymmetric catalysis[53]. Similarly to transition metal catalysis, there are only scattered examples of utilizing helically chiral organocatalysts.

Going back to the results reached by Martin and coll. in mid-80´s, helicenes were used in fact as organoreagents with no assistnace of a metal center. In fact all reported results utilized the helical scaffold connected directly to the vicinity of the reaction center as a chiral inducer or they were used in an equimolar amount as mentioned above (see Chapter 1.2)[3-7].

1.2.2.1 Ring opening of meso-epoxides

Takenaka et al.[54] published in 2008 the first study of a catalytic effect of *N*-oxide derived from 1-aza[6]helicene **2** (Figure 1.1) that it is known in literature since 1975[55]. They decided to examine the effectiveness of helical organocatalysts in desymmetrization of *meso*-epoxides in the presence of chlorosilanes originally studied by Denmark and co-workers[56]. The best results were achieved with *N*-oxide **111** in opening *meso*-epoxides **8**, **108**-**110** bearing aromatic groups (Scheme 1.31):

Scheme 1.31

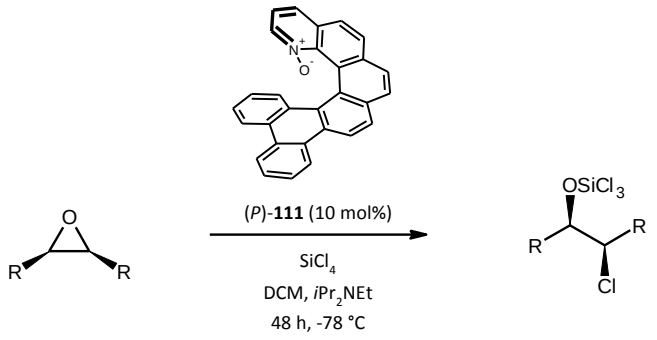

8: R = Ph

108: R = 2-dinaphtyl

109: R = 4-ClC_6H_4

110: R = 4-$CF_3C_6H_4$

112: R = Ph, **77%, 93% *ee***

113: R = 2-dinaphtyl, **76%, 92% *ee***

114: R = 4-ClC_6H_4, **84%, 94% *ee***

115: R = 4-$CF_3C_6H_4$, **83%, 92% *ee***

Other structurally similar catalysts were proved to catalyze this reaction too (Figure 1.32).

Figure 1.32

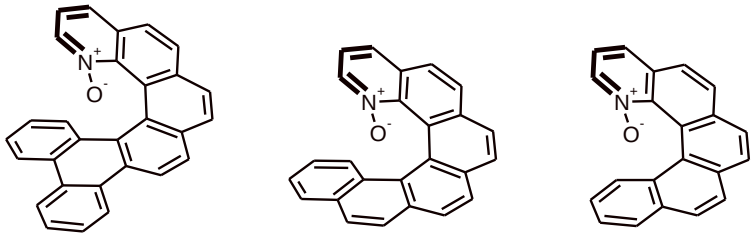

(*P*)-**111** (*P*)-**116** (*P*)-**117**

Using *N*-oxide **116** (derived from **2,** Figure 1.1) led to worse enantioselectivity (the product **113** was obtained in 77% yield with 73% *ee*). Although the reactivity of **116** and **117** was almost the same, the shorter analogue **117** was inactive in opening cyclic substrate. In the course of this study, they provided the first demonstration that the appropriate structural modification of the helical backbone beneath the plane of the pyridine *N*-oxide (a catalytic centre) can serve as a powerful means for tuning the catalyst enantioselectivity anticipating that this strategy would be general for the tuning of the catalyst for this class of chiraphores. The *N*-oxide **111** was found to be comparable with the best catalyst in the literature[56,57].

The preparation of the key unit started from the commercially available pyridine **118** (Scheme 1.33) and the phosphonium salt **119** (prepared from 2-bromo-1-(bromomethyl)-4-methylbenzene[58]) connected via *Z*-selective Wittig olefination[59] and followed by Stille-Kelly reaction[60] to form benzoquinoline **120**. It was converted to **121** via C-H activation by Sanford[61] and the methyl derivative was turned to aldehyde **122**. Repeating the Wittig and Stille-Kelly sequence with **123** – **125**, the corresponding 1-aza-[5]helicene **126**, 1-aza-[6]helicene **2** and 11,12-benzo-1-aza[6]helicene **127** were synthesized. The azahelicenes were oxidized to appropriate *N*-oxides **111**, **116**, **117** by *m*CPBA and they were finally resolved to their enantiomers by chiral HPLC (Daicel CHIRALCEL OD-H, Scheme 1.33)[54,62].

Scheme 1.33

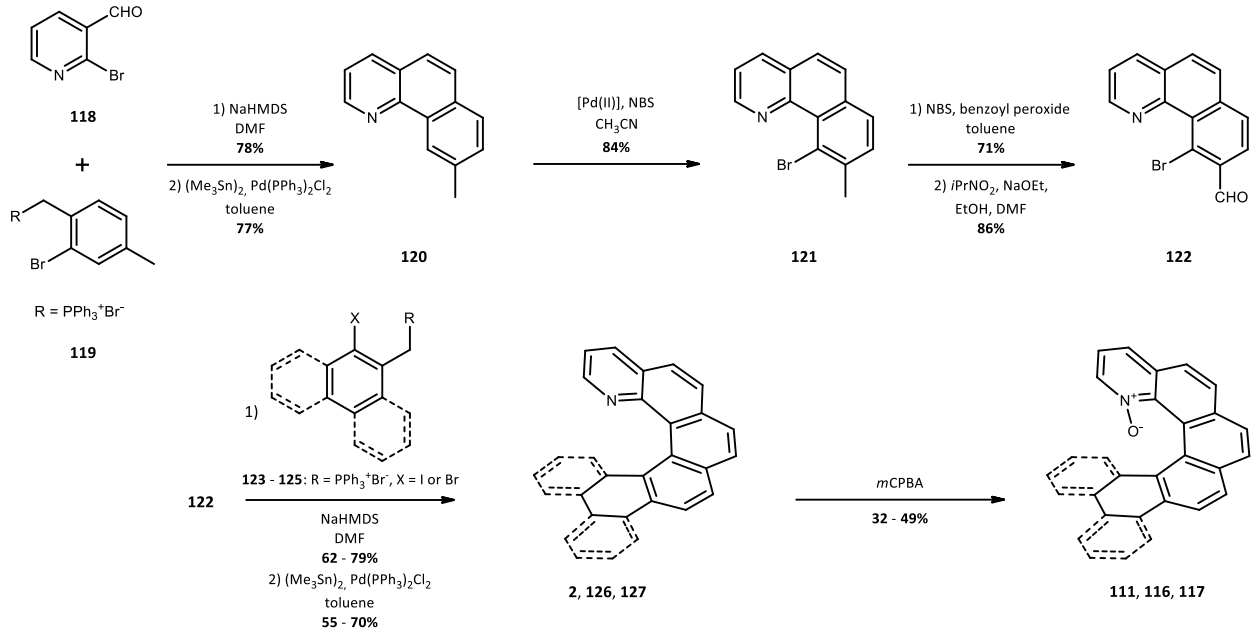

1.2.2.2 Asymmetric addition of electrophiles to dihydroindole (using H-bond donor catalysts)

Two years later, in 2010, the same author developed a new class of hydrogen-bonding donor catalysts derived from azahelicenes **2** (Figure 1.1) and **127**[63] (Scheme 1.33). Chiral (thio)ureas belong to the most used class of H-bonding catalysts. On the other hand, there are other motives related to the capability of forming two H-bonds and therefore activating the substrate. Furthermore, they can orient it into a well-defined position necessary for the asymmetric induction. The report aimed at studying dual H-bonding catalysts involving the 2-aminopyridinium ion[64] moiety in their structure. The most efficient catalyst in asymmetric addition of 4,7-dihydroindole **128** (Scheme 1.34) to nitroalkenes (such as **129**) was (*P*)-**130** structurally related to **127** (Scheme 1.34).

Scheme 1.34

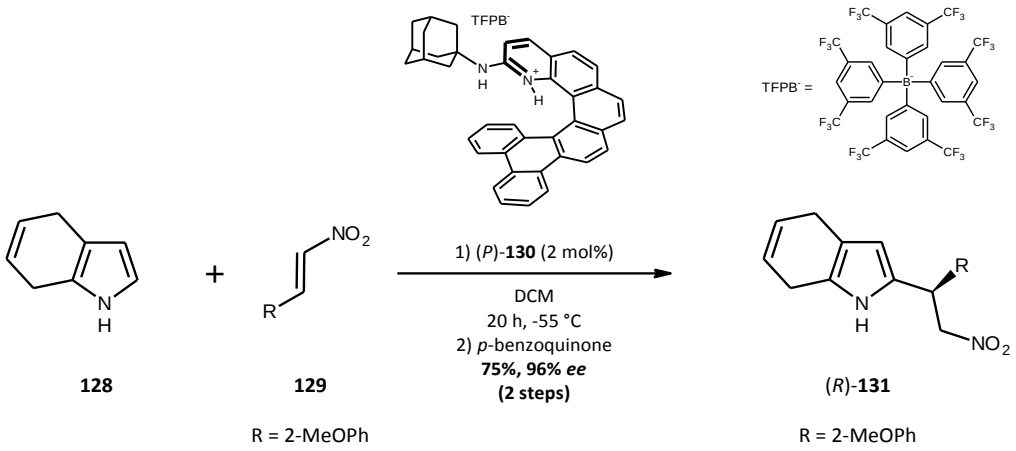

Various aromatic nitroalkenes (such as **129**: R = 2-MeOPh) were found to be tolerated by **130** giving *ee* values higher than 90% in the most cases. Aliphatic nitroalkenes (**129**: R = Me) also provided good enantioselectivity. It was possible to successfully recover corresponding aminopyridines (such as **130**) after finishing the reaction. The study showed that 1-azahelicenes are effective chiral scaffolds for construction of catalysts with aminopyridinium motif enabling H-bonding.

The aminopyridine (*P*)-**132** was easily available from a one pot reaction of the appropriate *N*-oxide (*P*)-**111** by the Yin and co-workers methodology[65]. Thereafter (*P*)-**132** was transformed to (*P*)-**130** (Scheme 1.35).

Scheme 1.35

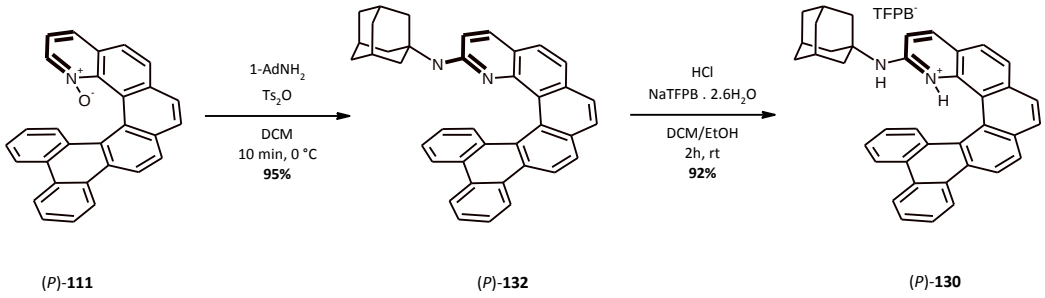

Other aminopyridines can be prepared in the same way.

1.2.2.3 Asymmetric acylative kinetic resolution of racemic secondary alcohols (acyl transfer)

In 2009 Starý, Stará and coll. investigated azahelicenes as organocatalysts in acyl transfer reaction[66] leading to kinetic resolution of racemic secondary alcohols. They successfully demonstrated that the helically chiral species can promote this type of reaction with an enantiodiscrimination. Employing (*P*)-**2** (Figure

1.1) led to a negligible amount of the acylated product **135** (Scheme 1.36). The catalytic inefficiency of (*P*)-**2** was ascribed to a limited accessibility of the nitrogen atom in the most sterically congested position 1 rather than to its low nucleophilicity. This hypothesis was confirmed by utilizing the isomeric (*M*)-2-aza[6]helicene **134** that gave rise to the optically pure (*R*)-1-phenylethanol (*R*)-**133**. The optimized reaction is shown below (Scheme 1.36).

Scheme 1.36

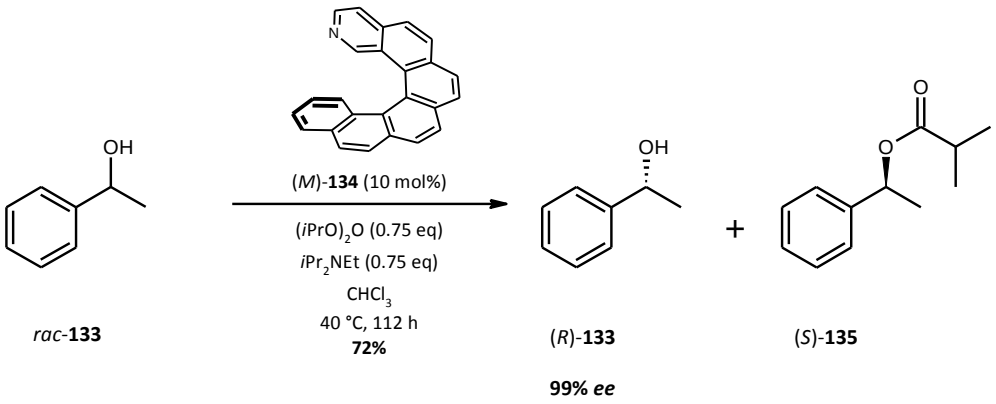

The synthetic approach to azahelicenes developed by Starý and Stará[67] is considerably different from the Takenaka's one mentioned in previous. It was based on [2+2+2] cyclotrimerization of alkynes catalyzed by $CpCo(CO)_2$ **81**. Alkyne **139** (Scheme 1.37) was formed in two steps from a commercially available bromopyridine **136**. Sonogashira coupling of **139** with acetylene **140** (prepared from **78**, Scheme 1.23) afforded the triyne **142** after deprotection of terminal alkyne units. The subsequent cyclization followed by oxidation with MnO_2 under microwave irradiation furnished the desired 2-aza[6]helicene **134** (Scheme 1.37).

Scheme 1.37

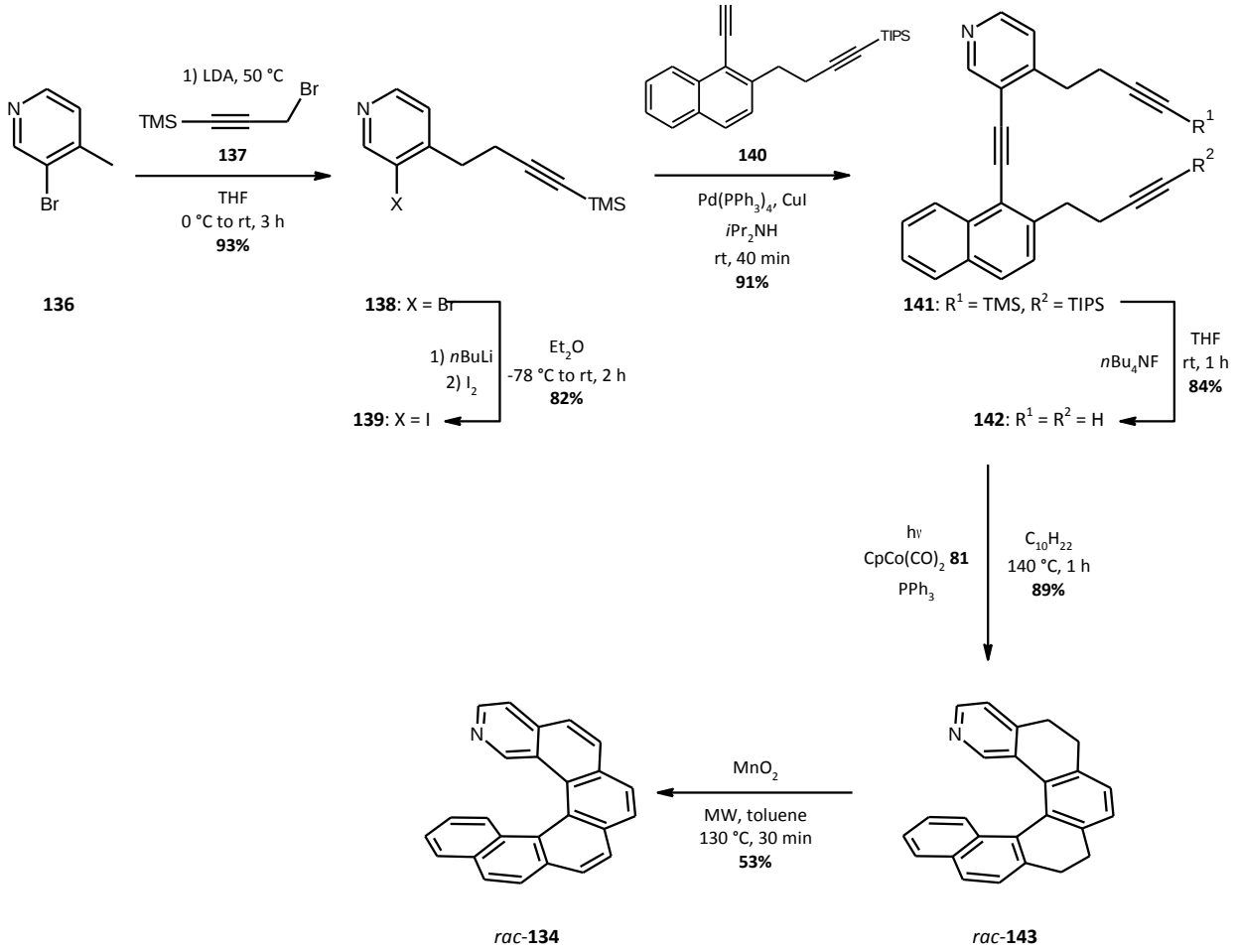

The racemic mixture of **134** was easily resolved into its enantiomers by HPLC on a Chiralcel OD-H column. This separation and a subsequent crystallization afforded (*M*)-**134** in an optically pure form.

Having in mind that 4-(dimethylamino)pyridine (DMAP) is a powerful catalyst in acyl transfer reactions[68] due to the presence of the electron donating dimethylamino group increasing nucleophilicity of the pyridine nitrogen atom, Carbery reported on a helical Lewis base, a DMAP subunit incorporated into the helical backbone[69]. Examining the catalytic ability of (*P*)-**145**, he succeeded in kinetic resolution of the racemic 1-anthracenylethanol **144** (Scheme 1.38).

Scheme 1.38

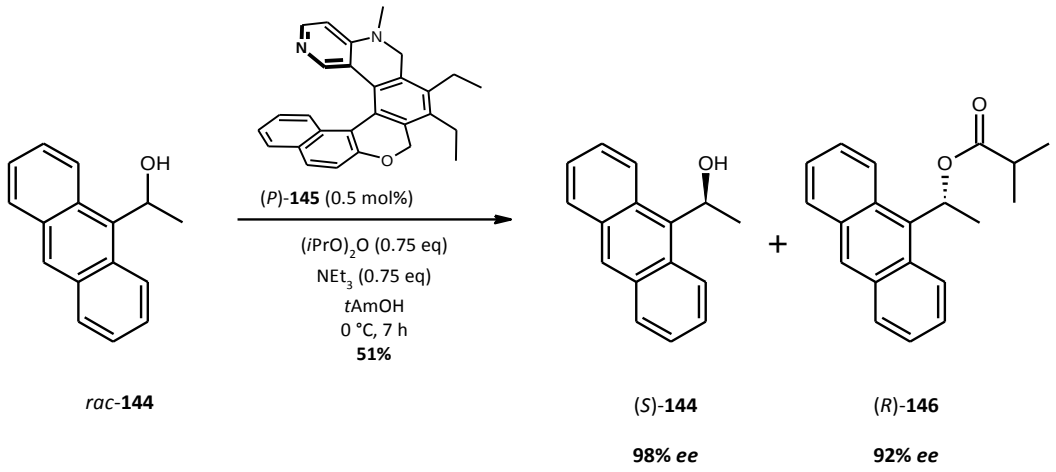

rac-**144**

(*S*)-**144**

98% *ee*

(*R*)-**146**

92% *ee*

Employing the racemic 1-phenylethanol **133** (examined previously by Starý *et al.*[66]), under the same conditions described above, Carbery achieved much lower enantiomeric excess of (*S*)-**133** (46% yield with 65% *ee*) and comparable selectivity (*s* = 16 vs. *s* = 9[66]).

The preparation of (*P*)-**145** began with 1-iodo-2-hydroxynaphtalene **147** which was turned to the appropriate ether **148** in two steps. It was coupled with the protected aminopyridine **149** to form diyne **150** and, after following transformations, triyne **151**, which underwent Rh(I) mediated [2+2+2] cyclotrimerization to build the helical skeleton with an incorporated DMAP moiety **145** (Scheme 1.39).

Scheme 1.39

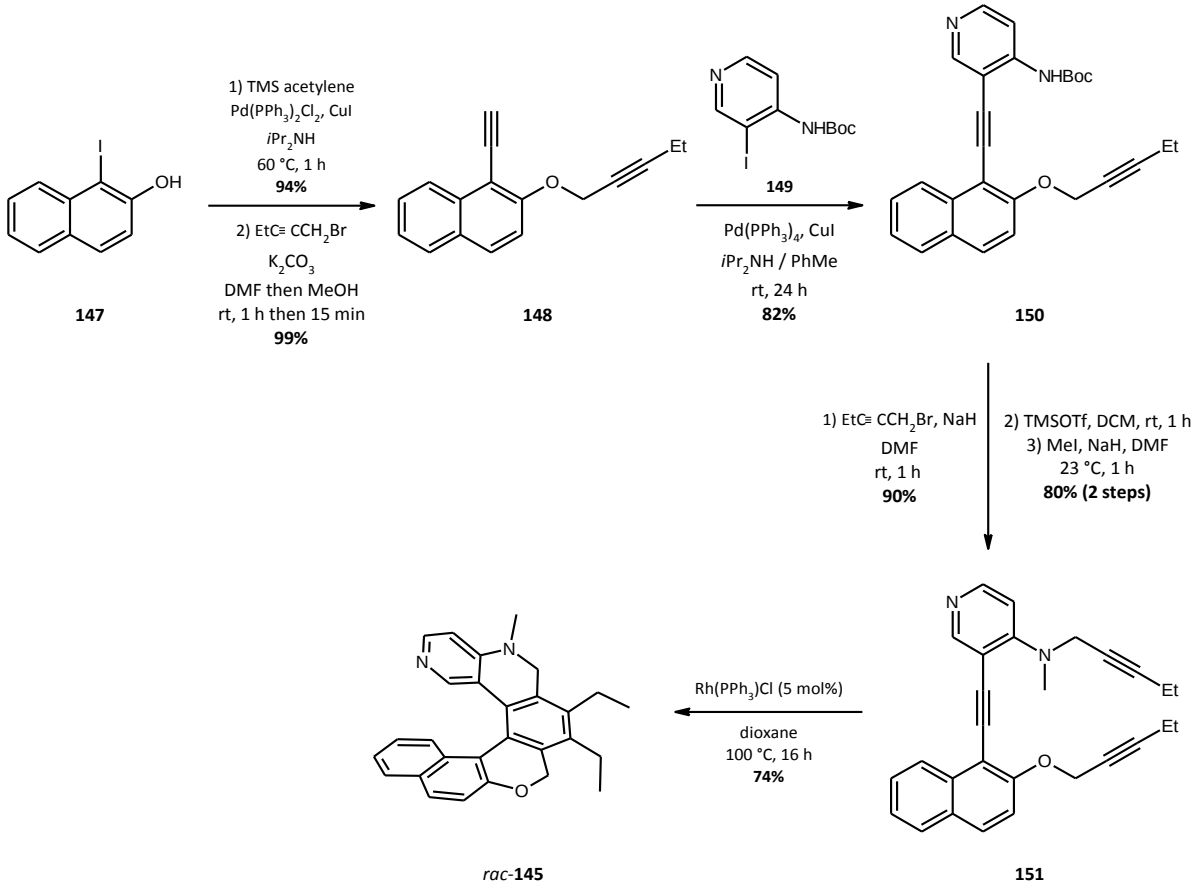

The both enantiomers (*M*)-**145** and (*P*)-**145** were available in >99% *ee* upon resolution on a chiral preparative HPLC (Chiralpak IC).

1.3 Heterogeneous catalysis with helical systems

Optically pure compounds become increasingly important in many fields such as pharmaceuticals, fine chemicals, agro and food industry, flavor and fragrance industry. Such materials can only be prepared either by a separation of their racemic mixtures, which is intrinsically wasteful, or by asymmetric synthesis. The second and more preferable approach applies conditions of organocatalysis or catalysis controlled by transition metal complexes in their homogeneous or heterogenized form. With the respect to the practical implementations, enantioselective synthesis remains a domain of homogeneous catalysis. The higher selectivity as a consequence of the presence of one active side and therefore a better understanding of the mechanism can enable a rational catalyst design. This fact seems to be limiting for heterogeneous catalysts that typically show a range of adsorption sites and prevents their wider use despite the well-

known advantages. With regard to selectivity, the enantioselectivity represents a true challenge, especially in the area of heterogeneous catalysis. Effective heterogeneously-catalyzed reactions are still rarities, despite the enormous effort which has been made. In a variety of approaches the main method usually involves immobilization of known homogenous catalyst on the surface of either organic or inorganic solids, including mesoporous materials[70], polymers[71,72] and dendritic systems[73]. The other approach can be represented by metal-catalyzed heterogeneous catalysis[74], such an asymmetric hydrogenation of C=O or C=C bonds which seems to be of a great importance as explained above.

In order to achieve a chiral induction during the surface-catalyzed reaction, nanoparticles are used in the practical catalysis because of their large surface. In the particular case of nanocrystals also their well-defined surface can significantly influenced results of the catalysis[75]. Moreover, during the last decade a significant progress in the development of new synthetic methods for the preparation of metal nanoparticles and, especially, single-crystalline nanocrystals has been done and so a large number of nanoparticles, which differs in their size, shape and surface facets, can be prepared according to known protocols (as shows the example of Pd nanocrystals[76]). The application of functionalized nanoparticles in the catalysis attracted a considerable attention nowadays. A small number of atoms in the outer shell of nanoparticles should lead to catalytic activities similar to homogenous catalysis. In connection to highly developed separation methods of nanoparticles, such as centrifugation, precipitation, nanofiltration or (magnetic) decantation, nanoparticles might be superior or homogeneous catalysts from an environmental point of view. It has to be distinguished between the two cases of chirality origin. Either the surface itself is endowed by chiral adsorption sides[77] or an achiral (or racemic) surface is modified by an adsorption of one enantiomer of a chiral selector.[78] Such systems can be used in two different ways. In the first case the metal surface of a nanoparticle serves as a structural element for an assembly of chiral ligands with an additional function different from the chelating groups, which then defines the catalytic center. Enantioselectivity then arises from the metal center binding chiral ligands and such systems are similar to those used in classical heterogeneous catalysis. An enhanced enantiocontrol caused by the accumulation of active centers on the periphery in combination with an easy separation and recycling from the reaction mixture makes such systems very powerful. In the second alternative approach, the metal of a nanoparticle is also responsible for catalytic activity (as mentioned above) and the ligands are coordinatively bound to the metal surface through some of the chelating atoms presented in their structure. The enantiocontrol depends on how the ligands are able to transmit their chiral influence to the substrates coordinated to the particles in their vicinity. Helicenes seems to be promising in this regard as chiral selectors (or modifiers) on the metal surface.

To the best of our knowledge, helicene-based modifiers have never been used in heterogeneous catalysis. The only case of utilizing helicenes in a sense of heterogeneous catalyst is related to the purification of water from the calmagite (azoic dye) in the presence of hydrogen peroxide and Pd(II) **154** (Scheme 1.40) and Ru(II) **156** complexes bearing racemic helical phosphines[79] (Scheme 1.40). Although the ruthenium complex **156** exhibited an excellent catalytic activity along with easy separation from the aqueous media, this methodology seemed to be rather expensive. The author curiously did not test such complexes (**154**, **156**) as a part of a homogenous catalytic system.

Scheme 1.40

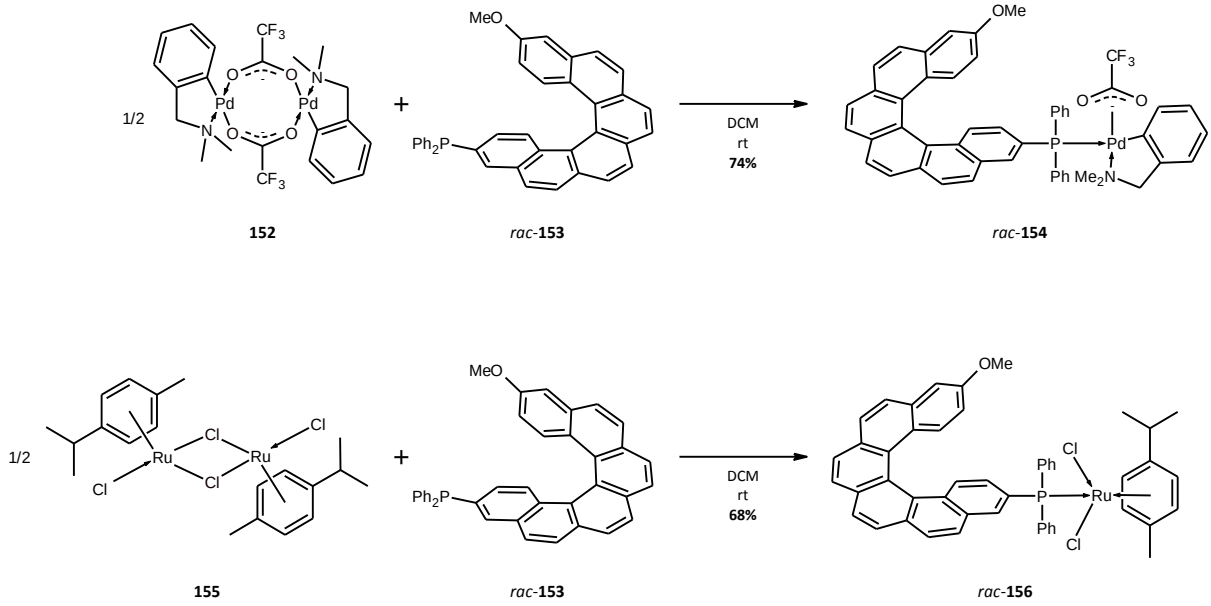

The synthesis of **153** was published by the same author few years earlier[80] and it is based on the photochemical approach (Scheme 1.41).

Scheme 1.41

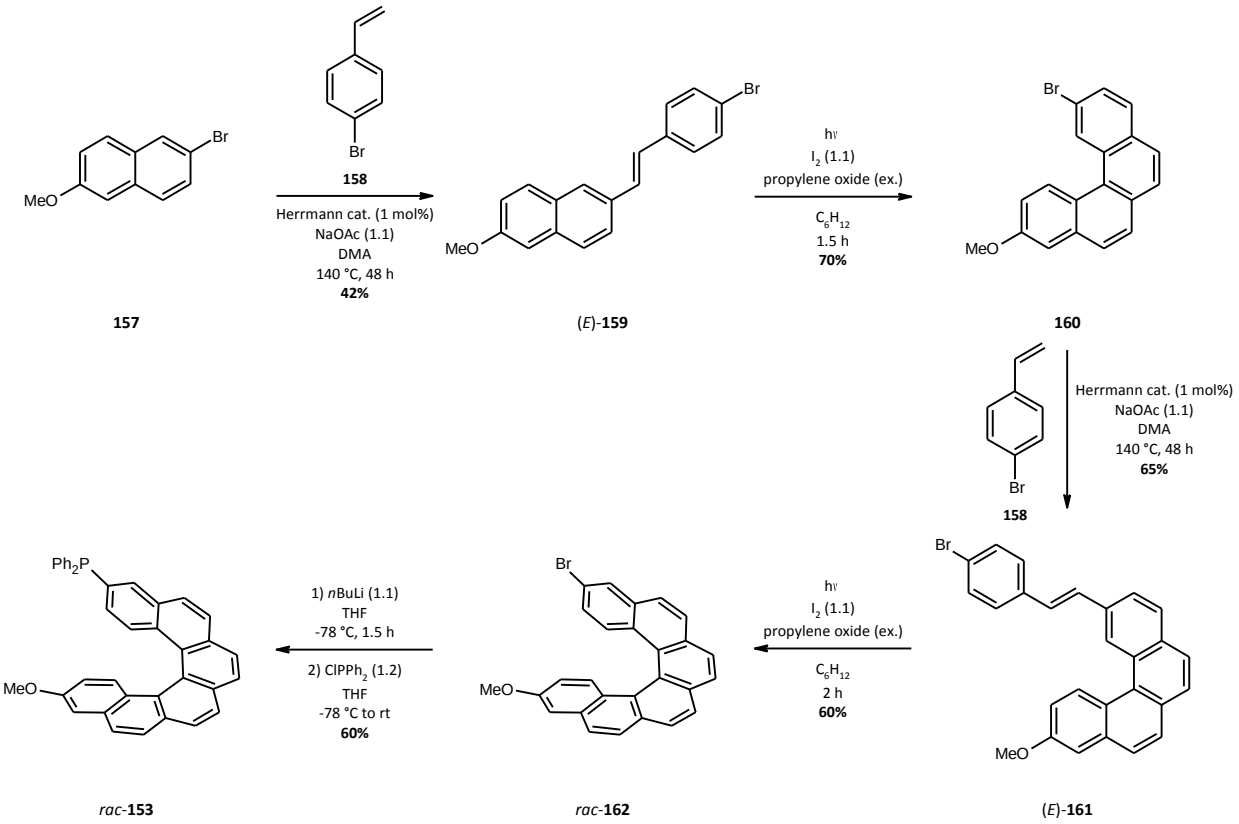

The naphthalene derivative **157** underwent the Heck reaction with styrene **158** to form **159** possessing (*E*) conformation of the double bond. Consequently, **159** was photochemically cyclized to furnish **160** in good yield. Repeating the reaction sequence gave rise to the racemic 3-bromo-14-methoxy[6]helicene **162** which upon lithiation and phospholation formed the desired racemic phosphine ligand **153**.

1.3.1 Self-assembly on metal surfaces

Self-assembly properties of helicenes are known either in solutions, crystals or on metal surfaces. For the first mentioned kind of self-assembly see the literature[25,26]. The secondly mentioned ability of helicenes will be briefly discussed in later with regard to endowing the metal surface by helicenes as chiral modifiers in heterogeneous catalysis. However, no direct connection between self-assembly and catalytic activity was ever reported.

Taniguchi studied self-assembly of thiahetero[11]helicene **163** (Figure 1.42) on different gold surfaces by STM under ultrahigh vacuum (UHV) conditions.[81]

Figure 1.42

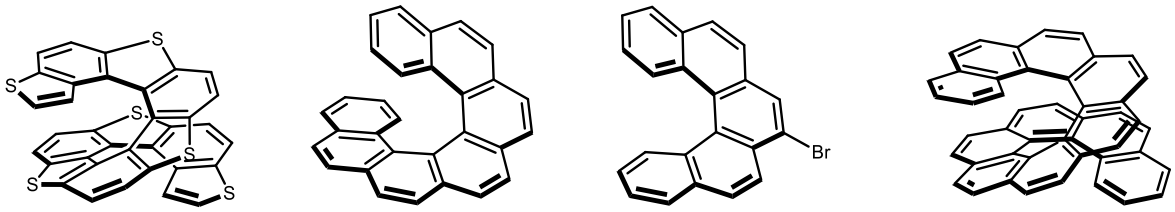

rac-**163** **164** *rac*-**165** **166**

On Au(111), the two-dimensional layer of **163** on wide terraces exhibited a hexagonal lattice in which helicenes were randomly arranged without any chiral discrimination in their interactions, while on narrow steps gave enantiomeric arrays of (*P*)- or (*M*)-isomers were formed.[81a] In contrast, [11]helicene **163** was aligned into chirality-sensitive chains on Au (110).[81b] Moreover, **163** self-assembled on a gold film on mica with the higher index surface, affording homochiral arrays.[81b] Thus, the structure of the substrate plays an important role in self-assembly of **163**.

Ernst and co-workers investigated self-assembly of [7]helicene **164** (Figure 1.42) on different metal surfaces.[82,83] They found that optically pure **164** formed a closely packed adsorbed layer on Ni(111), in which the distance between the helicenes was 1 nm. Subsequent physical vapor deposition (PVD) afforded a chiral organic film.[83a] The orientations of the helicenes were determined by near-edge X-ray absorption fine structure (NEXAFS) and X-ray photoelectron diffraction (XPD) studies, which showed that the molecules were bound to the surfaces via π-orbitals and spiraled away from the substrates.[83b,c] On Ni(100), for a saturated monolayer of (*P*)-**164**, the tilt angle between the helical axis and the substrate surface was ca. 43°.[83b] Other arrangements on metal surfaces are shown below (Figure 1.43).

Figure 1.43

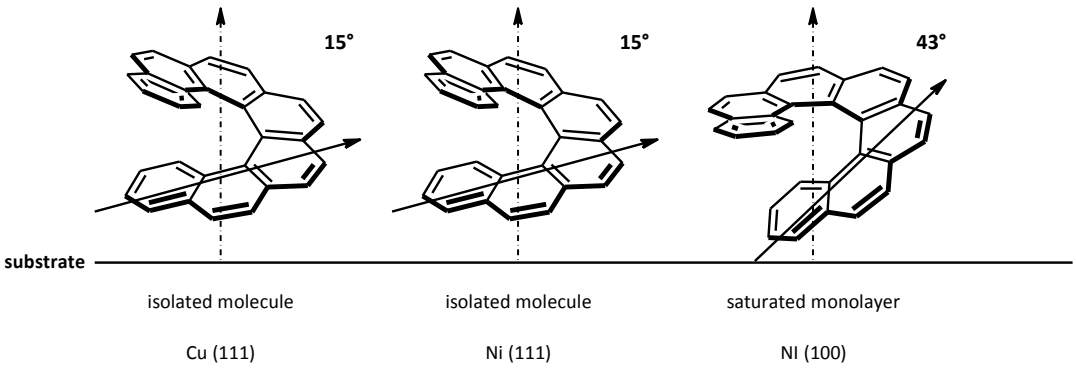

(*M*)-**164** adsorbed on Cu(111) and Cu(332) with different azimuthal arrangements, in both of which three terminal benzene rings of the helicenes were found to be parallel to the (111) terrace planes. In particular, the step-molecule interaction rendered the surface chiral in the Cu(332) system.[83c] Moreover, chirality directed by the intermolecular steric repulsive forces was transferred from the single molecule to the two-dimensional homochiral layer on Cu(111).[82b] The same authors observed a unique phenomenon of the amplification of chirality.[83e-g] Self-assembly of racemic **164** on Cu(111) did not lead to the expected resolution[82a] but instead formed two enantiomorphous closely packed domains with different supramolecular handedness (left-handed, λ and right-handed, ρ) in equal probability.[83e-g] If the helicene was enantiomerically enriched, the domain sizes changed dramatically. The λ-(*M*) and ρ-(*P*) interfaces are energetically favored.[83e] According to calculations, neither of the domains can incorporate the excessive enantiomers, which are expelled to the edges or residual areas, keeping the main terrace homochiral.

Gringas et al. reported[84] the non-contact AFM (NC-AFM) study on 7-bromo[5]helicene **165** (Figure 1.42). Helicene **165** was evaporated onto the Ag(001) surface in the UHV chamber. NC-AFM image obtained in situ exhibited a granular structure on the surface which corresponded to a monolayer of **165**. An additional annealing of the sample at 130 °C for an hour did not allow a sufficient molecular mobility on the surface for self-assembly. It might be caused by a strong molecular interaction with Ag. Heating at 250 °C finally led to a complete removal of the molecular layer.

Another STM study was done on the non-functionalized [11]helicene **166**[85] (Figure 1.42). With the aim of developing molecular wires transversal to the (semi)conducting layer, Szymonski, Starý, Stará and coworkers attempted the deposition and characterization of [11]helicene **166** on InSb (001). The sample was prepared at room temperature and subsequently measured at 77 K. The molecules do not appear to be present at the flat terrace areas but to be preferentially arranged along the substrate atomic step edges forming molecular chains. This indicates that the helicene diffusion length at room temperature is larger than the flat terrace lateral dimensions and that the InSb step edges act as the adsorption traps. The study revealed that racemic [11]helicene **166** and enantiopure (-)-**166** are organized differently at step edges of the substrate.

1.3.2 Coordination chemistry of helicenes

In catalysis, biding (helical) ligand to the catalyst's metal center is essential. In almost all of the previously mentioned examples of catalysis, the catalytically active species are formed *in situ* without any further knowledge of real bonding relations between the ligand(s) and the transition metal center. On the other hand, the separately prepared complexes may serve as active catalysts or pre-catalysts. Despite the fact

of so far rather limited helicene chemistry regarding the transition metal catalysis, there has been synthetized a number of organometallic compounds bearing either a directly bound helical ligand (via donor atom(s)) or a ligand where the helical moiety presents an attached subunit as a part of the more complex ligand system. A specific group is represented by ligands where the transition metal center is directly incorporated into the helical backbone (metallahelicenes). Some of such complexes already found their application in catalysis, non-linear optics and polymer chemistry or as dye materials, but others were prepared just to show possible coordination assemblies of helical ligands. Illustrative examples will be presented in next.

1.3.2.1 Phosphinohelicene resolution

Phosphinohelicenes are potentially applicable ligands for asymmetric catalysis. Next to the previously mentioned PHelix **12** (Scheme 1.6) prepared by Brunner[11] and resolved by Reetz[9], a series of helical phosphines have been prepared in their racemic or non-racemic forms (more in lit.[25,26]). Ben Hassine[86] and coworkers developed not only the synthesis of 2-(diphenylphosphino)[7]helicene **167** (Scheme 1.44) but also its resolution based on the use of chiral cyclopalladated amine complexes[87]. Their reactions with racemic phosphines afforded diastereoisomers which could be separated either by crystallization or by chromatography. Following this approach, enantiomeric resolution of **167** was conveniently performed through the *ortho*-palladated (*R*)-1-(naphthyl)ethylamine complex **168**[88], which reacted with the helical phosphine **167** to afford the diastereomeric adducts **169a**, **b**. The diastereomers **169** could be satisfactorily separated by column chromatography on silica gel. Removal of the enantiomerically enriched phosphines **167** from their palladium complexes was completed by the reaction with bis(diphenylphosphino)ethane (dppe) at room temperature (Scheme 1.44).

Scheme 1.44

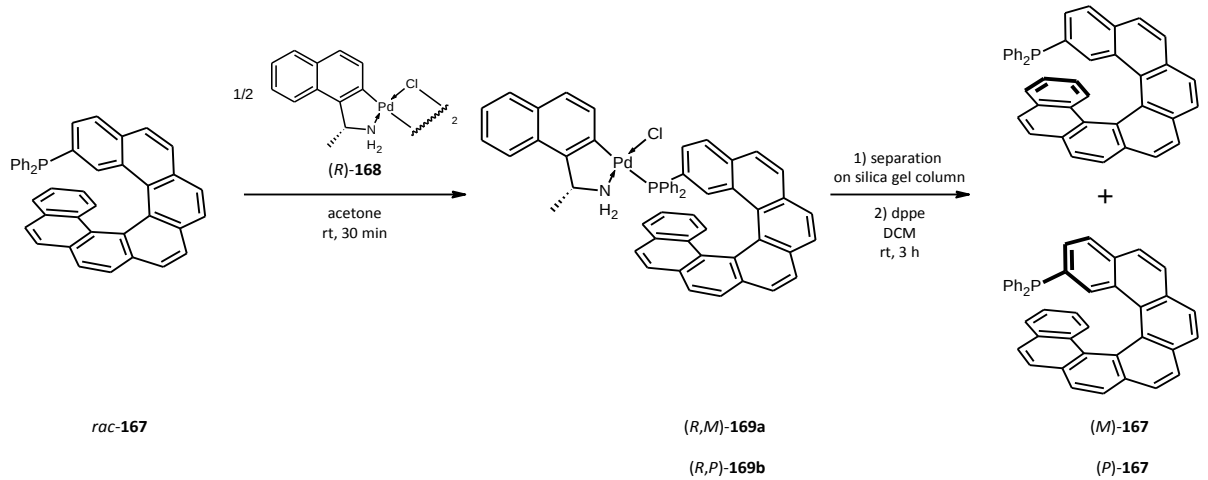

rac-**167** (*R*,*M*)-**169a** (*M*)-**167**

(*R*,*P*)-**169b** (*P*)-**167**

1.3.2.2 Organometallic compounds for NLO

Garcia *et al.*[89] published in 2009 coordination properties of three newly synthetized tetrathia[7]helicene ligands **170** – **172** (Figure 1.45). The thiahelicenes **170** and **172** bearing cyano group(s) were synthetized from the corresponding (di)aldehyde following the photodehydrocyclization approach (*cf*. Scheme 1.18). The ligand **171** was prepared from **170** by nitration.

Figure 1.45

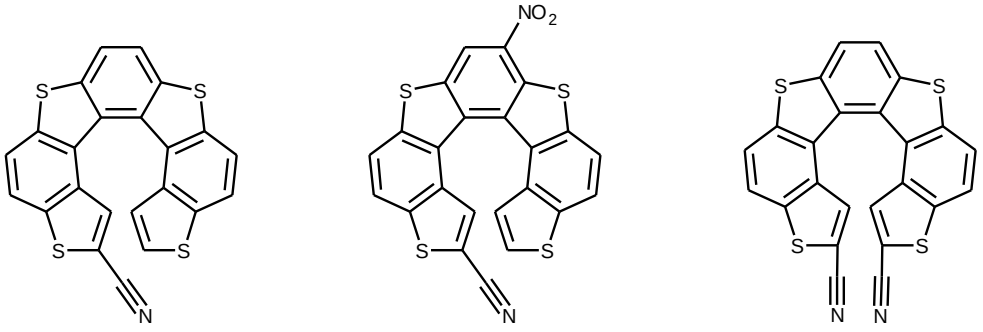

rac-**170** *rac*-**171** *rac*-**172**

These ligands were subsequently reacted with cyclopentadienyl complexes of Fe(II) or Ru(II) to form the appropriate cationic complexes (Scheme 1.46).

Scheme 1.46

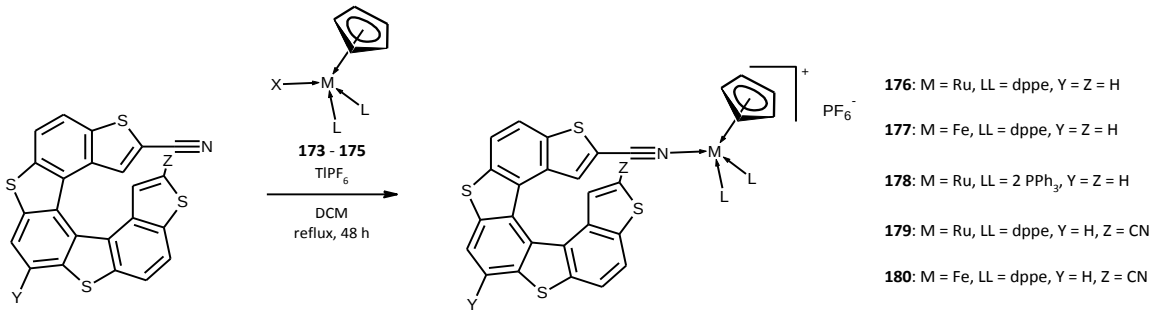

rac-**170** - **172**

173: M = Ru, LL = dppe, X = Cl

174: M = Ru, LL = 2 PPh_3, X = Cl

175: M = Fe, LL = dppe, X = I

rac-**176** - **182**

176: M = Ru, LL = dppe, Y = Z = H

177: M = Fe, LL = dppe, Y = Z = H

178: M = Ru, LL = 2 PPh_3, Y = Z = H

179: M = Ru, LL = dppe, Y = H, Z = CN

180: M = Fe, LL = dppe, Y = H, Z = CN

181: M = Ru, LL = dppe, Y = NO_2, Z = H

182: M = Fe, LL = dppe, Y = NO_2, Z = H

The substituted tetrathia[7]helicene derivatives used as ligands in the presented organometallic complexes **176** - **182**, may also be interesting as NLO organic materials as their significant β values were predicted by theoretical studies for other tetrathia[7]helicene derivatives[90]. The major interest in this family of NLO compounds is their intrinsic chirality but they have not yet been exploited, since the ligands **170** - **172** were prepared as a racemic mixture. Nevertheless, the developed synthetic procedure is useful for the synthesis of pure isomeric complexes, starting from the respective enantiomerically pure helicenes **170** - **172**, bearing in mind that an interconversion of enantiomers is not possible.

1.3.2.3 Coordination assemblies of some heterohelicenes

The heterohelicenes (such as **2** (Figure 1.1), **126**, **127** (Scheme 1.33), **134** (Scheme 1.37) or **145** (Scheme 1.39)) derived from pyridines can profit from the presence of an electron pair of the nitrogen atom in the helical backbone. If more Lewis base sites are embedded into the helical skeleton or connected to that, the molecule can act as a multidentate ligand. The coordination chemistry is in general significantly underdeveloped even in the case of the simplest azahelicenes. Next to the elegant synthesis of azahelicenes, Starý, Stará and coworkers reported on Ag(I) complexes **183** and **184** (Figure 1.47) of racemic 1-aza[6]helicene **2** (Figure 1.1) and racemic 2-aza[6]helicene **134**, respectively[67].

Figure 1.47

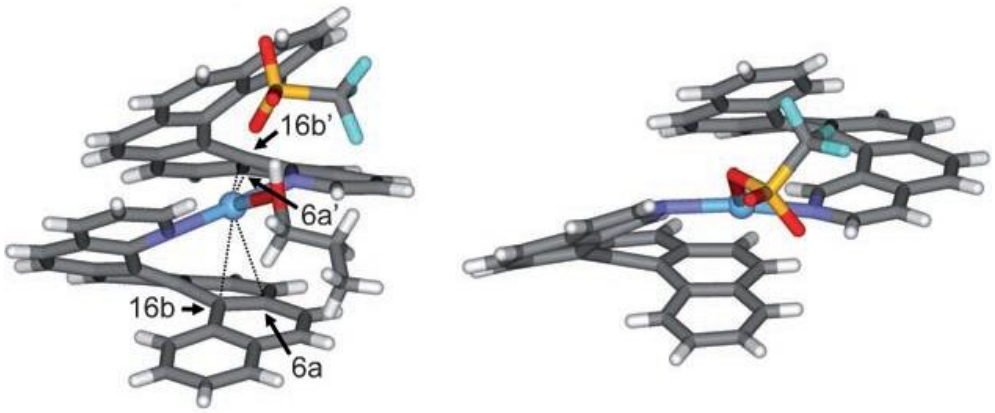

(*P*,*P*)-**183** (*P*,*P*)-**184**

Mixing silver triflate with racemic **2** (Figure 1.1) or **134** (Scheme 1.37) afforded T-shaped complexes with an anticipated 1 : 2 Ag : helicene stoichiometry and homochiral helicene subunits were coordinated to the silver atom. The performed X-ray analysis of **183** showed a trigonal bipyramidal geometry of the coordination environment, in which each 1-aza[6]helicene **2** acts as an N,C-bidentate ligand, with the nitrogen atom and C=C bond occupying axial and equatorial positions, respectively (the C-Ag biding interaction is obvious from the interatomic distance between the central metal and 6a, 16b or 6a', 16b' carbons, Figure 1.47).

Bidentate P,N-azahelicene complexes with palladium and copper (e.g. **185**, **186**, Figure 1.48) were prepared by Crassous et al.[91] The resolved 4-aza[6]helicene phosphole derivatives contained stereogenic center also on phosphorus atom, but the inversion barrier was rather low and the (*P*) helicene ligand afforded therefore a diastereomeric mixture of (*P*,R_P) and (*P*,S_P) and similarly (*M*) ligand afforded (*M*,R_P) and (*M*,S_P) diastereomers respectively. Some of these complexes are depicted in the picture below (Figure 1.48).

Figure 1.48

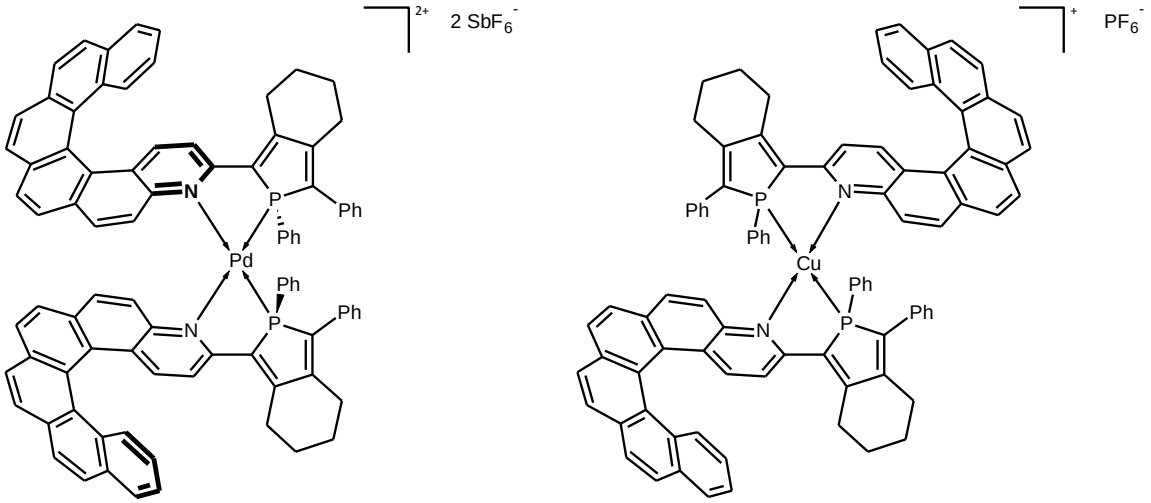

(*P*,*S*$_P$)-**185** **186**

The stereogenic center on the phosphorus atom was key for a stereoselective coordination of aza[6]helicene phospholes to Pd(II). The multinuclear NMR data corresponded well with those of related dicationic Pd(II)-(2-pyridylphosphole)$_2$ complexes[92] having a distorted square-planar coordination sphere, in which the P atoms had a mutual *syn* arrangement in accordance with the *trans* effect. The mirror image of **185** were obtained from a (*M*,*R*$_P$)/(*M*,*S*$_P$) diastereomeric mixture of corresponding ligands. Using the same synthetic approach the cationic tetrahedral Cu(I) complexe **186** was prepared.

1.3.2.4 Coordination polymers (cyclopentadienyl containing helicenes)

Having the delocalized electron system, helicenes can be employed in construction of π-complexes with transition metals. Some metallocene-based complexes (**187**, **188**, Figure 1.49) of helicenes with terminal cyclopentadienyl rings were published by Katz and coworkers in 80's[93]. Later on in 1993, they succeeded in the synthesis of various helical metallocene oligomers and other sandwich complexes[94] (e.g. **189**, **190**, Figure 1.49).

Figure 1.49

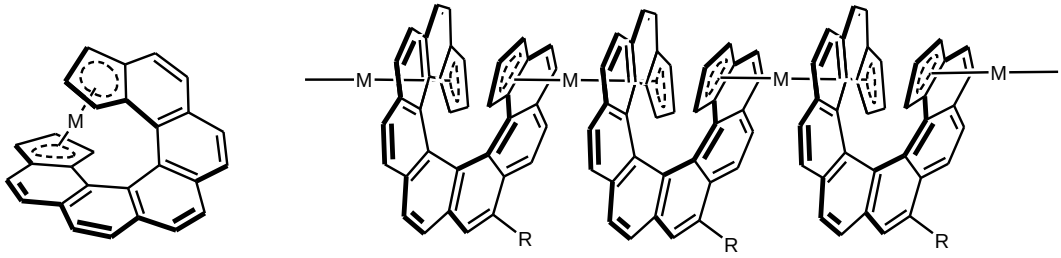

187 (M = Fe)

188 (M = $Co^{+}PF_6^{-}$)

189 (M = $Co^{+}PF_6^{-}$, R = TMS)

190 (M = $Co^{+}PF_6^{-}$, R = H)

Such oligomers were studied in context of the charge transport[94a]. The study did by cyclic voltammetry showed, unfortunately, that the interactions between two helicene subunits are weak and electronic communication is not efficient enough. Other organometallic ladder polymers based on helical structures containing salicylaldimine subunits coordinated to Ni(II) were prepared and studied by Katz and coworkers[95].

1.3.2.5 Helicenocyanines

Mandal and coworkers succeeded in the synthesis of fused [5]helicene moieties surrounding the phtalocyanine core so called *helicenocyanines*[96]. The [5]helicenocyanines (Hc) **192**, **193** (Scheme 1.50) and their extended forms benzo[5]helicenocyanines (BHc) **195** and **196** can be prepared by tetramerization of appropriate cyanoderivatives of [5]helicenes. If a metal salt was presented during this process, metal complexes were formed (Scheme 1.50).

Scheme 1.50

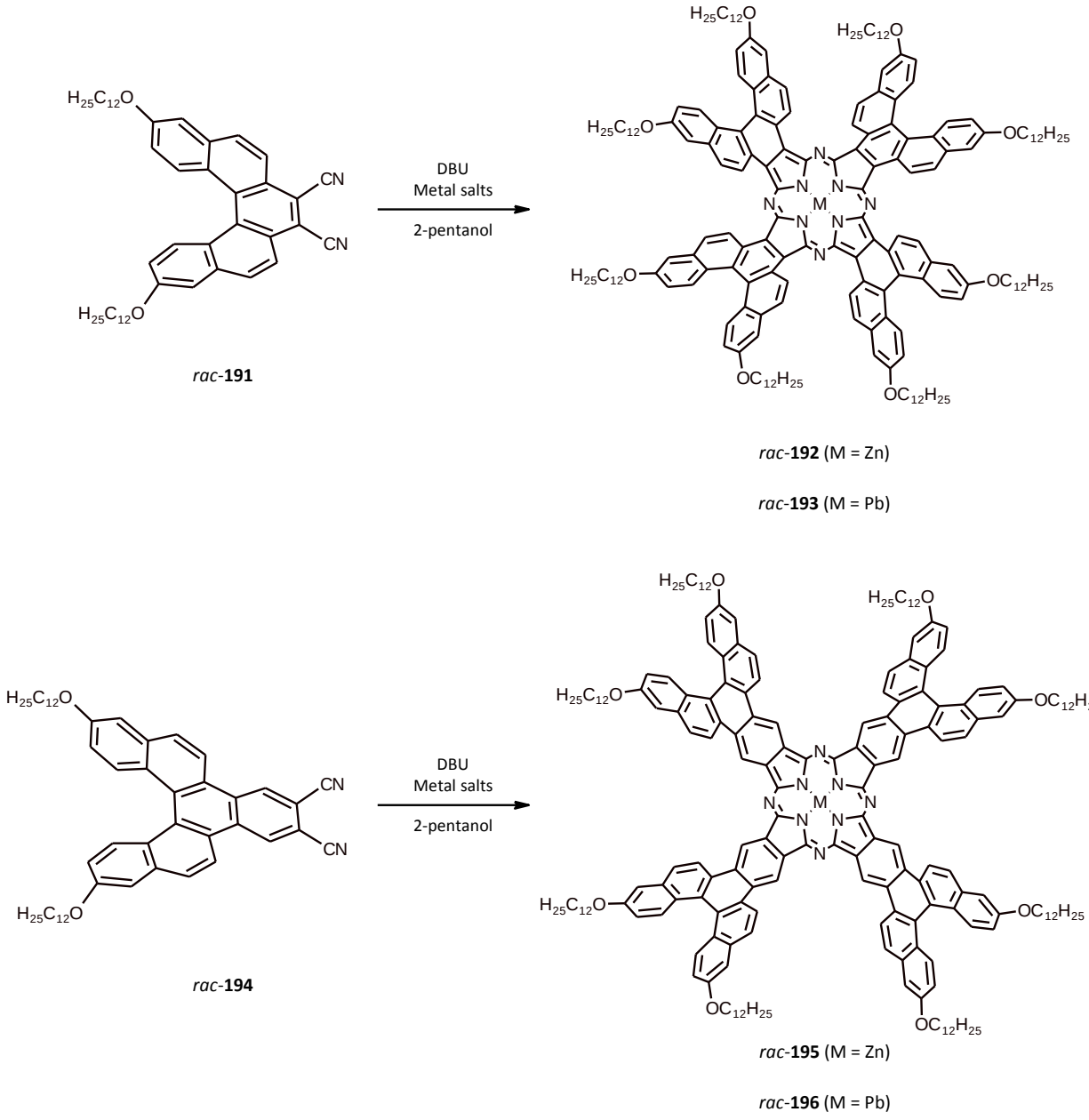

rac-**191**

rac-**192** (M = Zn)

rac-**193** (M = Pb)

rac-**194**

rac-**195** (M = Zn)

rac-**196** (M = Pb)

Helicenocyanines containing the nonracemic [7]helicene moiety were prepared by Katz et al.[97] in 1999 from the optically pure (*M*)-[7]helicenebisquinone (*M*)-**197** which was reacted with **198** and so turned into dicyano[7]helicene (*M*)-**199** giving corresponding phtalocyanines **200**, **201** with Ni(II) or Cu(II) metal core upon tetramerization with metal acetates (Scheme 1.51).

Scheme 1.51

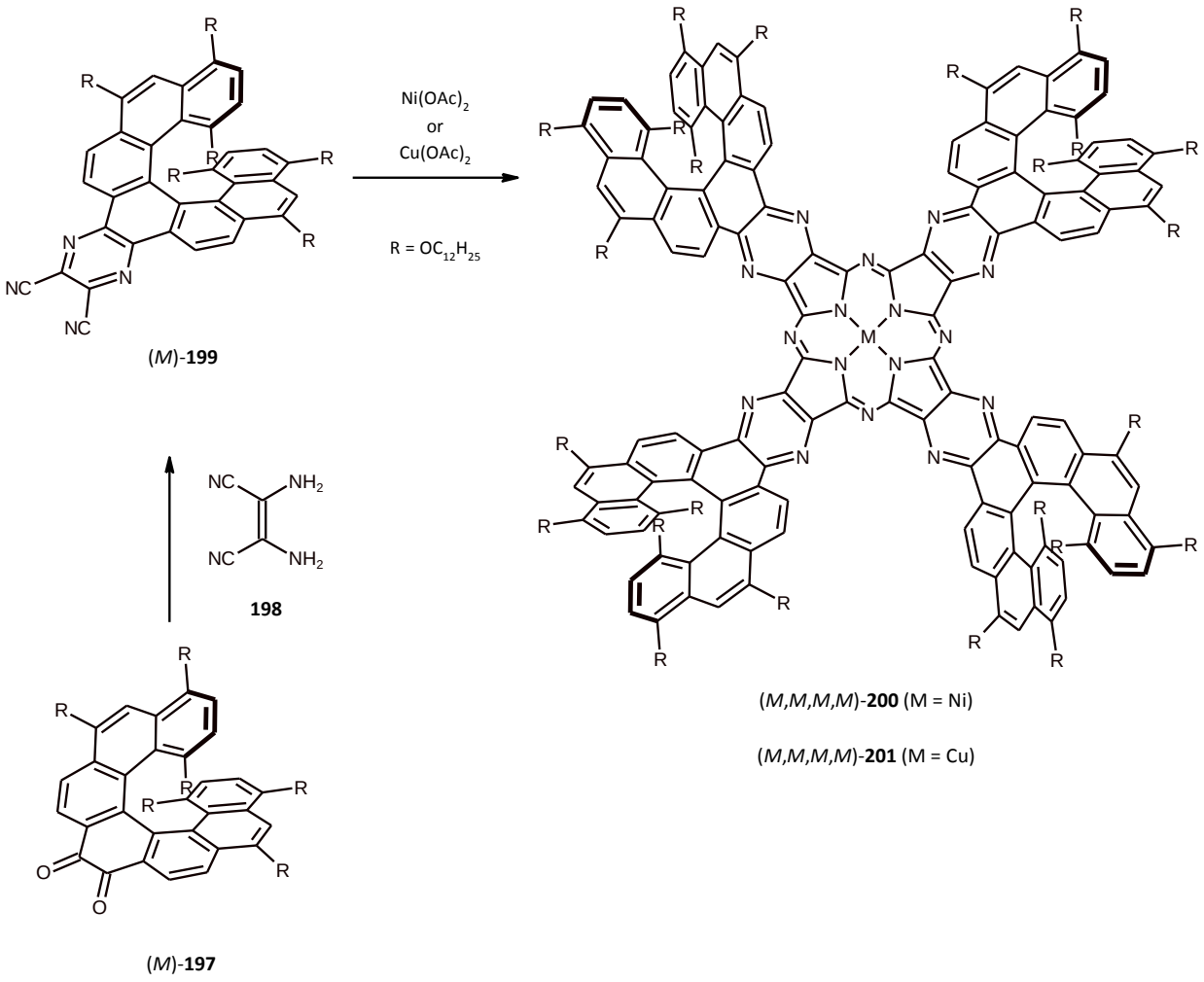

Materials based on Hc and BHc underwent self-assembly and the last mentioned enantiomerically pure phtalocyanines opened up a new direction towards conductive and semi-conductive films and materials with large second-order nonlinear optical properties.

1.3.2.6 Metallahelicenes

Metal based π-conjugated materials represent multifunctional organometallic compounds with intimate electronic interactions between metallic ions and π-ligands that give rise to a great diversity of properties which can be further tuned by using the metal reactivity (like redox behavior, ligand exchange, metal – metal interactions etc.). The potential applicability of helicenes depends greatly on the facility of generating different frameworks to modulate and optimize their electronic and optical properties[98]. Réau, Crassous, Autschbach and collective started to investigate a special class of helicenes containing platinum

incorporated directly into the helical scaffold[99]. The metallahelicenes consist of platinum coordinated to 2-phenylpyridine based ligands. In their work a number of hetero- and homochiral platinahelicenes were synthetized via the cyclometalation reaction of 4-(2-pyridyl)benzo[g]phenanthrene derivatives (such as **202**). An illustrative example is given below (Scheme 1.52).

Scheme 1.52

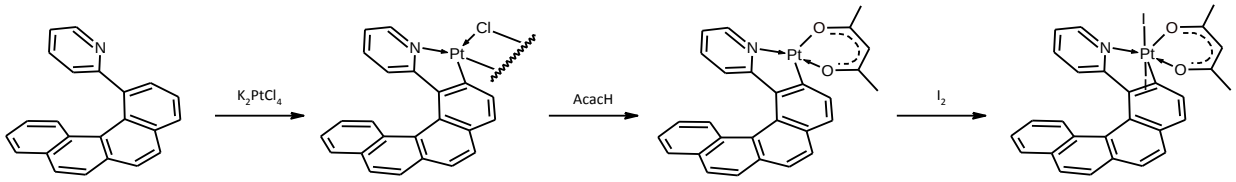

202 *rac*-**203** *rac*-**204** *rac*-**205**

Variously functionalized [6]platina- and [7]platinahelicenes were prepared in the same manner and their properties were studied[99]. Ir(III)-containing structures bearing two methoxy-functionalized **202** units[99a] belong to other. The first d^4-metallahelicenes containing osmium were currently reported[100]. Not only due to the efficient phosphorescence and tunable chiroptical properties, metallahelicenes represent a new promising and perspective class of helicenes.

Despite the underdeveloped chemistry of helicenes in the field of catalysis and organometallic chemistry, they represent compounds with high potential for application that is obvious from the achieved results mentioned in the previous (Introduction part). Besides this, helicenes belong to the fascinating group of molecules which already found (or still waiting for) their utilization as molecular machines, dye materials, polymers, liquid crystals, systems for molecular recognition, or they were successfully applied to biology, electronics or optics. Helicenes witness a gradually increasing attention from the side of scientific community.

2. Goals

The main goals of the Thesis are following:

2.1 The development of a general synthetic route to optically pure helicene-like compounds

The main goal is to prepare the novel helicene-like compounds containing either two (2*S*)-2-methyl-2,7-dihydrooxepine rings, *dihydrooxepine-type compounds*, or two (2*R*)-2-methyl-2*H*-pyran rings, 2*H-pyran-type compounds*, (Figure 2.1) using the diastereoselective synthesis.

Figure 2.1

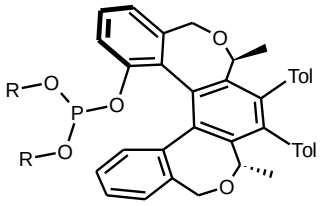

(*P*,*S*,*S*)-**206**

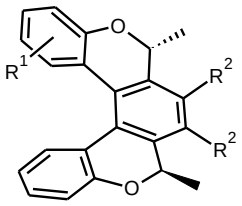

(*P*,*R*,*R*) / (*M*,*R*,*R*)-**207**

2.2 The functionalization of enantiopure helicene-like compounds enabling coordination of transition metals

Aiming at the use of helicenes in transition-metal catalysis it is necessary to functionalize the optically pure helical structures with groups enabling coordination to the metal center. Hence, we propose to prepare helical precursors that could be easily transformed to different phosphite ligands (Scheme 2.2).

Scheme 2.2

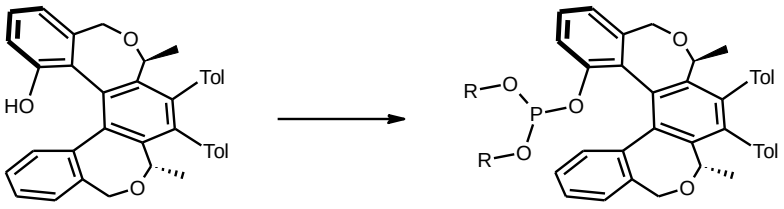

(*P*,*S*,*S*)-**208** (*P*,*S*,*S*)-**206**

2.3 The use of optically pure helical phosphites (and other helical ligands) in homogeneous transition metal catalysis

In connection with the results achieved in the field of transition-metal catalysis with helicenes, the proposed helical phosphites are to be applied to asymmetric allylic aminations (Scheme 2.3).

Scheme 2.3

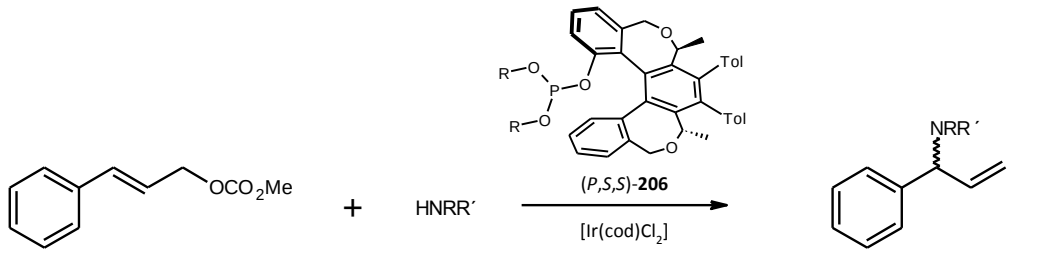

102 **99 - 101**

105: R = R´= -$(CH_2)_4$-

106: R = R´= -$(CH_2)_2O(CH_2)_2$-

209: R = R´= -$(CH_2)_5$-

2.4 Exploring the use of the helicene-like ligands in heterogeneous catalysis and organocatalysis

The proposed synthetic approach to optically pure helicene-like compounds is intended to be utilized in preparation of potentially interesting compounds, which can be employed in heterogeneous transition metal catalysis and/or organocatalysis (Figure 2.4).

Figure 2.4

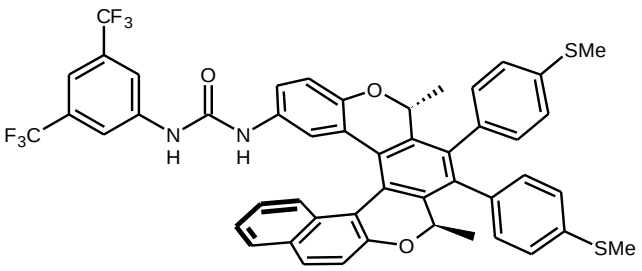

(*M*,*R*,*R*)-**210**

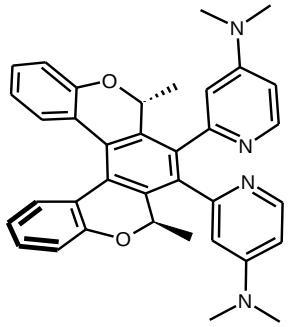

(*M*,*R*,*R*)-**211**

2.5 The preparation of new transition metal complexes with helical ligands and their structure characterization

We propose to prepare novel transition metal complexes bearing various helicene or helicene-like ligands and characterize them. The attention will be paid mainly to *N*-donating optically pure ligands (Figure 2.5).

Figure 2.5

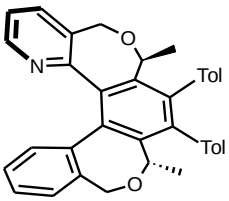

(*P*,*S*,*S*)-**212**

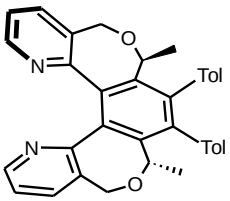

(*P*,*S*,*S*)-**213**

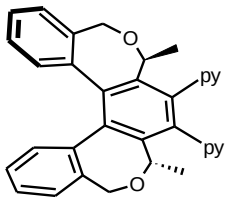

(*P*,*S*,*S*)-**214**

3. Results and discussion

3.1 Diastereoselective synthesis of helicene-like compounds

The concept of the diastereoselective synthesis of helicene-like compounds containing one (*S*)-methyl-2,7-dihydrooxepine ring was introduced by Starý and coworkers[36]. It was found, that thermodynamic factors play an important role in the cobalt mediated [2+2+2] cyclotrimerizations of a chiral triyne at elevated temperatures and are manifested by the difference in energy between both diastereomeric forms. This fact was confirmed by performing the reaction (see Scheme 1.24) at room temperature resulting in an equimolar mixture of diastereomers differing in helicity (kinetically driven reaction). The steric repulsion of the methyl and tolyl substituents gave rise predominantly to the (*P*,*S*)-**83** diastereomer as described in Chapter *1.2.1.4*. The phenomena of this diastereoselective cyclization was later elaborated on helicene-like compounds containing two (*S*)-methyl-2,7-dihydrooxepine rings in the helical backbone. Based on the DFT study (B3LYP/TZV+P, made by Dr. Vacek and Dr. Vacek Chocholoušová), a further increase in the energy difference between the (*M*) and (*P*) helices caused by the structural change can be observed[101] (Figure 3.1).

Figure 3.1

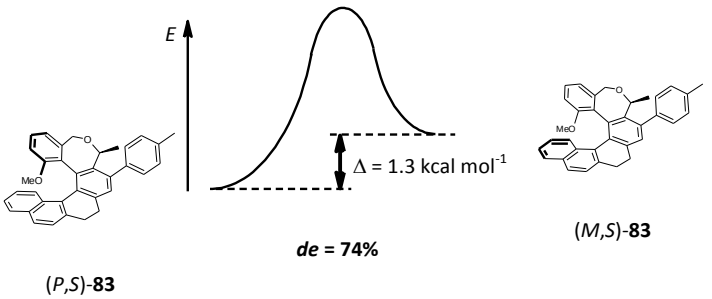

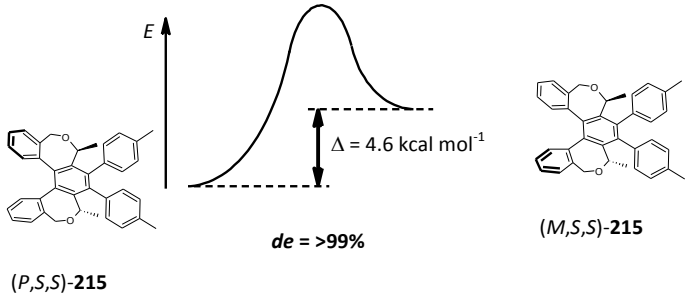

Although the barrier to the helix inversion in **215** is rather lower than in the case of the parent [5]helicene (this fact is caused by the presence of two seven-membered rings in the structure), the energy difference of 4.6 kcal mol^{-1} between the (*P*,*S*,*S*) and (*M*,*S*,*S*) diastereomers of **215** would result in a 99.96 to 0.04 ratio. In other words, if the energy difference between the two diastereomers of opposite helicity is significantly high (> 2.7 kcal mol^{-1}) and they are stereolabile at a given temperature, asymmetric transformation of the first kind[102] might control the stereochemical outcome of the entire cyclization process to reach up the > 99 : < 1 diastereomeric ratio.

A key factor affecting the stereochemical outcome of the [2+2+2] cyclotrimerization reaction is the *allylic-like 1,3-strain* which will be discussed in detail below. To explain the essence of this important factor influencing the stereocontrol of the reaction, a concept of allylic 1,3-strain[103] can be used. Information on relative energies of preferred conformations of the allylic stereocenter and prochiral double bond is crucial for mechanistic understanding[104]. An *ab initio* calculation (MP2/6-31G*//3-21G) of relative energies of conformers of *cis*-4-methylpent-2-ene **216**, where a substituent is attached to the terminus of the *cis* double bond, was done[105] (Figure 3.2).

Figure 3.2

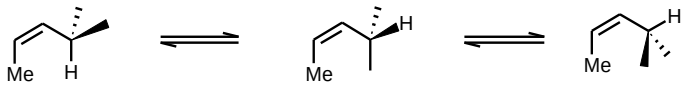

	216a	**216b**	**216c**
Relative energy [kcal mol^{-1}]	0	+ 4.86	+ 3.44

The eclipsed conformer **216b** is strongly disfavored by the steric repulsion between two methyl groups and represents an energy maximum. This spatial interference is called allylic 1,3-strain. The conformers **216a** and **216c** represent the energy minima, but double-*skew* conformer (**216a**) is more stable than the double-*gauche* (**216c**) one (ΔE = 3.4 kcal mol^{-1}), so it prevails in equilibrium (although changes in dihedral angle ±30° are possible with a gain of energy). If one of the methyl substituents is replaced with another one (stereocenter formation), the dissimilarity of substituents may optimally induce the facial selectivity for reactions at the olefin moiety.

3.1.1 The synthesis of oxepine containing helicene-like compounds

The helicene-based ligands have been shown to be promising candidates for utilizing them in homogenous catalysis with transition metals as mentioned in the Introduction part. Among others, the P-donating

ligands have reached the privileged position in homogeneous catalysis due to their easy steric and electronic tuning affording versatile and robust catalytic systems with transition metals and catalyzing an immense number of synthetically important reactions. The phosphites represent a class of P-donating ligands where the carbon-centered substituents are replaced by oxygen substituents. If nitrogen is used as a connecting atom together with oxygen then we are speaking about amidites (such as **95**, Scheme 1.28) already described in Chapter *1.2.1.5*. In contrast to phosphine ligands, phosphites and phosphoramidites are usually more easy to make, they allow more variable structural changes and variation of properties. They are less sensitive towards oxidation, but they are often more prone to hydrolysis (depending on the structure). Ligands of the type **90** (Figure 1.26) have become of great importance in recent years. Although the chiral phosphite and phosphoramidite ligands are known, they mostly exhibit another type of chirality (often axial chirality) than a helical one. Starý et al. were first who employed the helically chiral phosphites in a rhodium-catalyzed hydroformylation and iridium-catalyzed allylic amination[33]. Based on these results, the aim was to develop the synthetic approach to the novel phosphite ligands containing two oxepine rings incorporated to a helical scaffold (type of **215**, see Figure 3.1).

The synthesis of various phosphite ligands obviously stems from a corresponding helical alcohol with the hydroxy group placed in a proper position (see Scheme 2.2). The position 1 (as in **208**, Scheme 2.2), the inner most closed position of the chiral helical backbone seemed to be the position of choice for connecting the donor function. From the stereochemical point of view this placement of the OH group would mostly affect the arrangement of ligands and substrate bound to the metal center during the catalytic cycle and so influencing the resulting stereochemistry of products. Phosphites **62** (Scheme 1.20), **65**, **66** and **67** (Figure 1.21) consequently confirmed this hypotesis[33]. The modular synthesis of **208** reflecting previously published results[36,106] involves the preparation of the chiral triyne and its subsequent [2+2+2] diastereoselective cyclisation.

The already published synthesis of the first chiral block (*S*)-**77**[36] starts from the commercially available *o*-vanillin **73** (see Scheme 1.23, 3.3), that was, upon transformation to nonaflate **218**, ethynylated with (triisopropylsilyl)acetylene **220** under Pd(II) catalysis. The presence of two *ortho* substituents did not hamper the coupling reaction, which led smoothly to **221**. The triisopropylsilyl protecting group was chosen to survive basic conditions in the following steps. To attach a chiral moiety, the aldehyde group in **222** was reduced with diisobutylaluminum hydride to afford the benzylic alcohol **222**, which was further reacted with phosphorus tribromide providing the benzylic bromide **74**. Afterward, **74** was treated with a sodium salt of (*S*)-**75** (chiral alcohol (*S*)-**75** was synthetized according to the ref.[37] see Scheme 3.3) to

accomplish the synthesis of ether (*S*)-**76**, leaving the triisopropylsilyl group untouched. (*S*)-**76** was desilylated with tetrabutylammonium fluoride to the resulting terminal alkyne (*S*)-**77** (Scheme 3.4).

Scheme 3.3

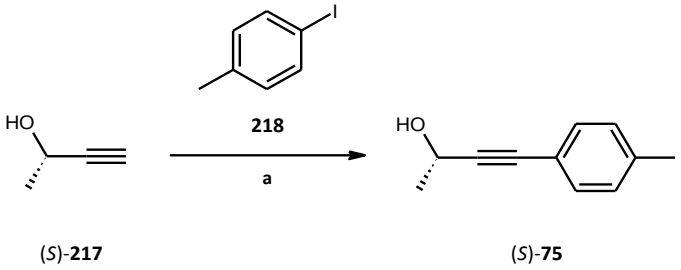

(a) **218** (1.0 eq), $Pd(PPh_3)_2Cl_2$ (0.3 mol%), CuI (1.5 mol%), PPh_3 (1.5 mol%), *i*Pr_2NH (1.0 eq), toluene, rt, overnight, **96 %**

Scheme 3.4

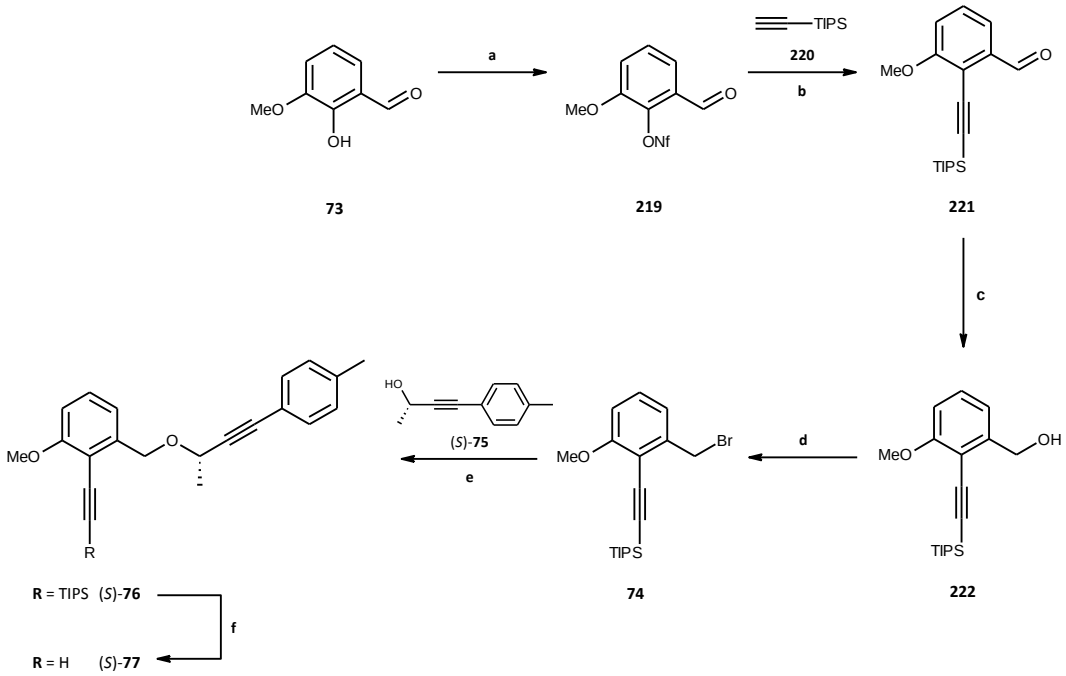

(a) NaH (1.3 eq), NfF (1.2 eq), DMF, 0 °C to rt, 20 h, **65%**

(b) **220** (1.5 eq), $Pd(PPh_3)_2Cl_2$ (5.0 mol%), NEt_3 (6.0 eq), DMF, 90 °C, 1.5 h, **85%**

(c) DIBAH (1.6 eq), toluene, -78 °C, 4 h, **88%**

(d) CBr_4 (2.4 eq), PPh_3 (2.4 eq), MeCN, rt, 3 h, **88%**

(e) KH (4.3 eq), (*S*)-**75** (1.0 eq), THF, 0 °C to rt, 3 h, **88%**

(f) *n*Bu_4NF (2.4 eq), THF, rt, 1.5 h, **94%**

The second building block (*S*)-**224** (Scheme 3.5) was completed in a one-step reaction of the commercially available 1-(bromomethyl)-2-iodobenzene **223** with the sodium salt of the chiral alcohol (*S*)-**75**. To assemble triyne (*S*,*S*)-**225**, (*S*)-**77** was coupled with iodide (*S*)-**224** under Pd(0)/Cu(I) catalysis to provide (*S*,*S*)-**225** (Scheme 3.5).

Scheme 3.5

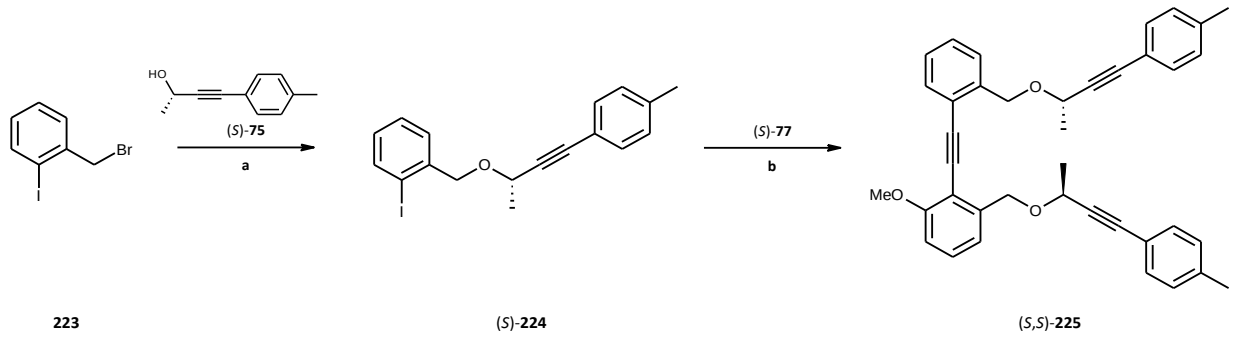

223 (*S*)-**224** (*S*,*S*)-**225**

(a) KH (1.2 eq), (*S*)-**75** (1.0 eq), THF, 0 °C to rt, 2 h, **82%**

(b) (*S*)-**77** (1.0 eq), $Pd(PPh_3)_4$ (5.0 mol%), CuI (9.0 mol%), *i*Pr_2NH, 80 °C, 3 h, **72%**

Before the final [2+2+2] cyclotrimerization step was made to provide the corresponding 1-methoxyhelicene-like compound (*P*,*S*,*S*)-**233** (see Scheme 3.9), a brief screening of various catalysts potentially applicable to diastereoselective cyclotrimerization using substrates structurally similar to (*S*,*S*)-**225** was made. Both substrates and catalysts used are depicted in the picture below (Figure 3.6). The substrates (*S*,*S*)-**229** and (*S*,*S*)-**230** were prepared by Dr. A. A. Andronova in our research group.

Figure 3.6

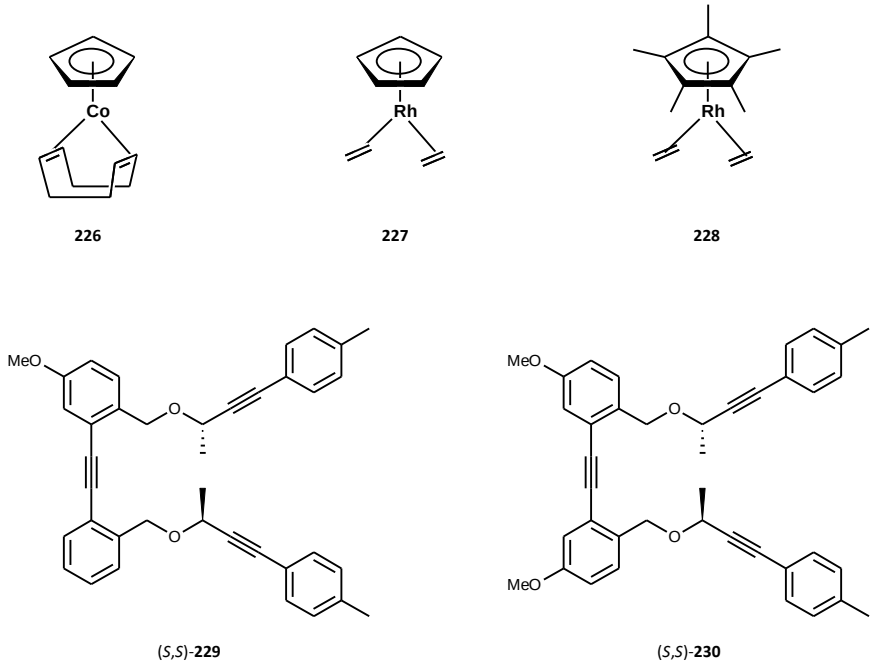

226 **227** **228**

(*S*,*S*)-**229** (*S*,*S*)-**230**

The choice of catalysts was inspired by the structure of Jonas catalyst **82**[40], which is very effective in [2+2+2] cyclotrimerization even at room temperature[36].However, it is a labile organometallic compound requiring storage under the ethylene atmosphere at low temperatures and therefore it is hard to handle. Whereas **226** (Figure 3.6) represents another Co(I) species (like frequently used **81** or **82**, see Scheme 1.24) exhibiting a better tolerance towards oxidation, **227** and **228** bear easy-to-remove ethylene ligands in the coordination sphere. Comparing Co(I) and Rh(I), the later is much more stable towards oxidation, therefore the handling in air is possible and they can be stored over a long period of time. On the other hand, Rh(I) species **227** and **228** are more expensive. The catalysts were prepared according to the literature with specific changes in protocols described in Experimental part (**226**[107], **227**[108], **228**[109]). The results from cyclotrimerizations of the substrates (*S*,*S*)-**229** and (*S*,*S*)-**230** (Scheme 3.7) are summarized in the table below (Table 3.8).

Scheme 3.7

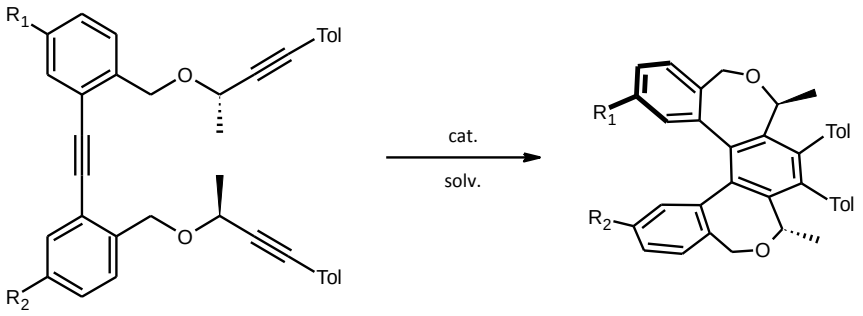

(*S*,*S*)-**229:** R_1 = MeO, R_2 = H

(*S*,*S*)-**230:** R_1 = MeO, R_2 = MeO

(*P*,*S*,*S*)-**231:** R_1 = MeO, R_2 = H

(*P*,*S*,*S*)-**232:** R_1 = MeO, R_2 = MeO

Table 3.8

	substrate	cat.	%cat. [%]	solv.	temp. [°C]	time [min]	other conditions	yield [%]
1	**229**	CpCo(cod) **226**	100	THF	50	45	-	0
2	**229**	CpCo(cod) **226**	100	$C_{10}H_{22}$	140	120	hν / PPh_3	0
3	**229**	CpCo(cod) **226**	100	THF	140	20	MW	0
4	**229**	$CpRh(ethylene)_2$ **227**	100	THF	50	45	-	0
5	**229**	$CpRh(ethylene)_2$ **227**	100	toluene	110	60	-	0
6	**229**	$CpRh(ethylene)_2$ **227**	100	$C_{10}H_{22}$	140	35	hν	75
7	**229**	$CpRh(ethylene)_2$ **227**	10	$C_{10}H_{22}$	130	60	hν	25
8	**229**	$CpRh(ethylene)_2$ **227**	5	THF	50	40	hν	0
9	**229**	$Cp^*Rh(ethylene)_2$ **228**	100	THF	140	20	MW	61
10	**230**	$CpRh(ethylene)_2$ **227**	100	$C_{10}H_{22}$	130	60	hν	63

Based on our experience with similar substrates, a halogen lamp (hν) or microwave (MW) irradiation along with an equimolar amount of catalyst was used in cyclisation experiments in most cases. Examining the reactivity of the substrate (*S*,*S*)-**229**, the catalyst **226** was ineffective at low temperature (Table 3.8, entry 1) as well as at high temperature using visible light or microwave irradiation (Table 3.8, entries 2, 3). This fact was quite surprising regarding the results achieved with other Co(I) catalysts (**81**, **82**, Scheme 1.24)[36] and it was caused probably by a higher stability of **226** and its lower reactivity. The catalytic activity of the "rhodium analog of Jonas catalyst" **227** was first examined without any hν or MW assistance at low temperature (Table 3.8, entry 4), but no conversion to the corresponding product (*P*,*S*,*S*)-**231** was observed. Even at the elevated temperature (Table 3.8, entry 5), the catalyst **227** was totally ineffective. When a visible light irradiation along with high temperature was applied, the situation dramatically

changed and a full conversion was achieved in a short period of time (35 min). The desired product (*P*,*S*,*S*)-**231** was isolated in good yield (75%, 100% *de*) (Table 3.8, entry 6). Applying these conditions to the other substrate (*S*,*S*)-**230** bearing two methoxy groups, the product (*P*,*S*,*S*)-**232** was isolated in 63% with 100% *de* (Table 3.8, entry 10). Being encouraged by these results, we decided to decrease the catalyst loading in the reaction with the substrate (*S*,*S*)-**229**. The experiments showed that the catalyst **227** is efficient only at the elevated temperature (Table 3.8, entry 7, 8), but using 10 mol% of **227** the isolated yield of (*P*,*S*,*S*)-**231** was below-average (25%, 100% *de*). Avoiding the use of high-boiling solvents, the substrate (*S*,*S*)-**229** was cyclized to the product (*P*,*S*,*S*)-**231** (61%, 100% *de*) in the presence of an equimolar amount of **228** at high temperature in THF using microwave irradiation (Table 3.8, entry 9).

These methodologies were later successfully applied to [2+2+2] cyclotrimerization of (*S*,*S*)-**225** (Scheme 3.9) and are summed up in the following table (Table 3.10).

Scheme 3.9

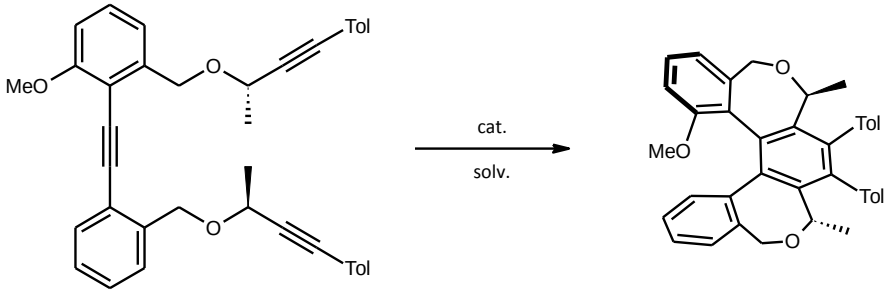

(*S*,*S*)-**225** (*P*,*S*,*S*)-**233**

Table 3.10

	cat.	%cat. [%]	solv.	temp. [°C]	time [min]	other conditions	yield[a] [%]
1[b]	$CpRh(ethylene)_2$ **227**	100	$C_{10}H_{22}$	140	60	hν	76
2	$CpRh(ethylene)_2$ **227**	50	THF	140	40	MW, ion. liq.[c]	84
3	$CpCo(CO)_2$ **81**/ PPh_3	100 / 200	THF	200	20	MW, ion. liq.[c]	84
4	$CpCo(CO)_2$ **81**/ PPh_3	50 / 100	THF	200	60	MW, ion. liq.[c]	62
5	$CpCo(CO)_2$ **81**	100	THF	200	20	MW, ion. liq.[c]	50
6	$Cp^*Rh(ethylene)_2$ **228**	100	THF	140	20	MW, ion. liq.[c]	55

[a]) isolated yield

[b]) an experiment done by Dr. Nathan C. Clemence

[c]) ion. liq. = 1-butyl-2,3-dimethylimidazolinium tetrafluoroborate

Applying the conditions from previous (Table 3.8, entry 6), Dr. Nathan C. Clemence from our group found out that the complex **227** is efficient also in a cyclisation of (*S*,*S*)-**225** giving the product (*P*,*S*,*S*)-**233** in good yield (76%, 100% *de*) (Table 3.10, entry 1). The experiment made under the microwave irradiation led to a better result with a lower amount of the catalyst **227** (84%, 100% *de*) (Table 3.10, entry 2): The reaction period was shorter (40 min) and a cleaner product was obtained in comparison with the halogen lamp irradiation. To compare the catalytic activity of the rhodium complex **227** with that of a cheaper but more unstable $CpCo(CO)_2$ **81** under the microwave irradiation conditions, a series of experiments were made. Although the result achieved with the $CpCo(CO)_2/PPh_3$ system were comparable with the use of the Rh(I) complex (84%, 100% *de*) (Table 3.10, entry 3), the amount of the Co(I) complex was two time higher than the Rh(I) one and harsher conditions were necessary (200 °C vs. 140 °C). When decreasing the amount of the Co(I) catalyst (to 50 mol. %), the yield decreased to 62% (Table 3.10, entry 4). Interestingly, the added triphenylphosphine ligand plays an important role. Using the catalyst **81** without any PPh_3 addition, the yield decreased further to 50% (Table 3.10, entry 5). From the catalytic activity point of view, the rhodium complex **227** gave the best results. To examine the catalytic activity of the structurally similar $Cp^*Rh(ethylene)_2$ **228** in comparison with **227**, an experiment under the same conditions was done (Table 3.10, entry 2). Although a full conversion of the starting material was achieved in a shorter time, the isolated yield was much worse reaching only 55% (Table 3.10, entry 6).

The assignment of helicity of all products relied on DFT calculations.[101] The formation of a single diastereomer (predicted by DFT calculations) was confirmed by NMR spectra of the products where only one set of signals was observed.

Subsequently, the 1-methoxy substituted helicene (*P*,*S*,*S*)-**233** was transformed into the corresponding alcohol (*P*,*S*,*S*)-**208** (Scheme 3.11).

Scheme 3.11

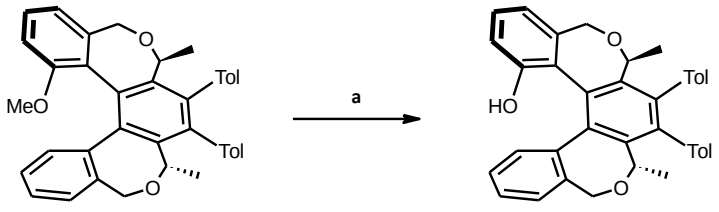

(*P*,*S*,*S*)-**233** (*P*,*S*,*S*)-**208**

(a) EtSH (20.0 eq), NaH (20.0 eq), DMF, 130 °C, overnight, **79%**

The compound **208** served as starting material for the synthesis of helical phosphites. The choice of a P-donor moiety, which can be connected to the helical backbone of (*P*,*S*,*S*)-**208** via P–O bond, was inspired by achievements in the field of homogenous catalysis with structurally relative phosphites[33]. With respect to the chosen catalytic reaction (asymmetric allylic amination), three helical phosphites (*P*,*S*,*S*)-**234**, (*P*,*S*,*S*)-**235** and (*P*,*S*,*S*)-**236** were proposed and their synthesis was attempted (Figure 3.12).

Figure 3.12

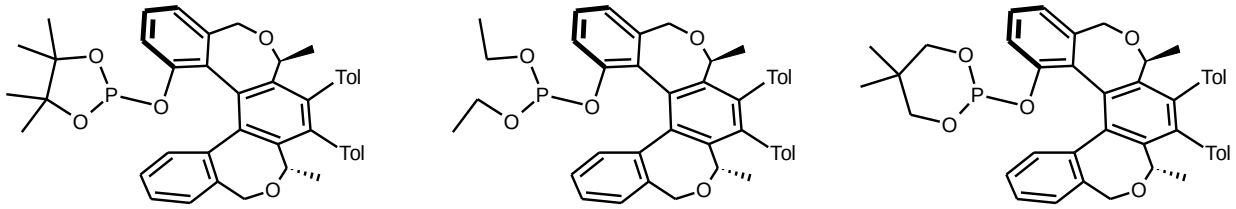

(*P*,*S*,*S*)-**234** (*P*,*S*,*S*)-**235** (*P*,*S*,*S*)-**236**

The depicted ligands (*P*,*S*,*S*)-**234**, (*P*,*S*,*S*)-**235** and (*P*,*S*,*S*)-**236** could be synthesized within a single-step from alcohol (*P*,*S*,*S*)-**208** upon its deprotonation with a strong base and treatment with the corresponding chlorophosphite (Scheme 3.13).

Scheme 3.13

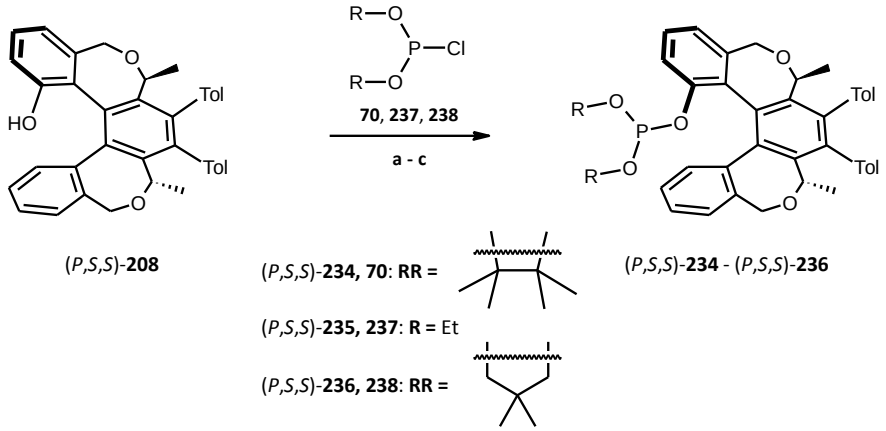

(*P*,*S*,*S*)-**208** (*P*,*S*,*S*)-**234** - (*P*,*S*,*S*)-**236**

(*P*,*S*,*S*)-**234, 70**: **RR =**

(*P*,*S*,*S*)-**235, 237**: **R =** Et

(*P*,*S*,*S*)-**236, 238**: **RR =**

(a) NaH (4.0 eq), **70** (1.1 eq), THF, 0 °C to rt, 2 h, **75%**

(b) NaH (4.0 eq), **237** (2.2 eq), THF, 0 °C to rt, 2 h, **29%**

(c) NaH (4.0 eq), **238** (2.2 eq), THF, 0 °C to rt, 2 h, **61%**

All the prepared phosphites (*P*,*S*,*S*)-**234** – **236** showed a low tolerance towards oxygen as they spontaneously underwent partial oxidation to respective phosphoric esters, whose presence was indicated by ^{31}P-NMR measurements.

3.1.2 The synthesis of 2*H*-pyran containing helicene-like compounds

A concept of [2+2+2] diastereoselective cyclotrimerization of centrally chiral triynes was proved to enable the synthesis of nonracemic helicene-like compounds containing dihydrooxepine and dihydroazapine ring(s)[36,39,85]. This promising approach, however, has not yet reached the merit of being general in the sense of the synthesis of optically pure helicenes with a wide structural diversity. To make the method more general, the synthesis of optically pure [5]- and [6]heterohelicenes **207**, **210**, **211** (see Figures 2.1, 2.4) was proposed. The scope and limitations of such a methodology were studied utilising triynes as substrates for cyclization to receive a novel type of helical scaffolds with two six-membered (*R*)-methyl-2*H*-pyran rings. The presence of these heterocyclic units in the structure kept the molecular shape of the corresponding helicene-like compounds as close as possible to the parent carbohelicenes and made the target molecules structurally as well as synthetically attractive.

3.1.2.1 [5]helicene-like compounds

The synthesis of pyridohelicenes **211** (see Figure 2.4), **239** (see Figure 3.14), **256** (see Scheme 3.27), **260** (see Scheme 3.35), **263**, **264** (see Figure 3.42) is based on [2+2+2] diastereoselective cyclotrimerization of corresponding centrally chiral triynes. As the first model system was chosen the 2*H*-pyran [5]helicene-like compound (*M*,*R*,*R*)-**239** containing two tolyl groups at the central benzene ring in the position 7 and 8 (Figure 3.14).

Figure 3.14

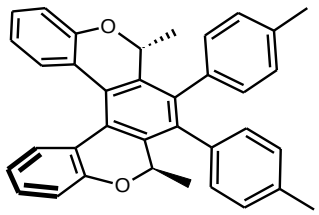

(*M*,*R*,*R*)-**239**

The preparation of the first building block (*R*)-**241** started with the attachment of chiral units via Mitsunobu reaction. The chiral alcohol (*S*)-**75** was connected to 2-iodophenol **240** (Scheme 3.15).

Scheme 3.15

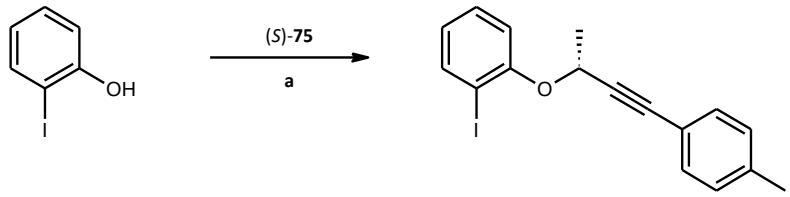

240 (*R*)-**241**

(a) (*S*)-**75** (1.05 eq), PPh_3 (1.2 eq), DIAD (1.1 eq), DCM, rt, 3 h, **71%**

Although the original idea was to construct the triyne (*R*,*R*)-**242** through a double Sonogashira reaction of **241** with a gaseous acetylene, it was found that this reaction (Scheme 3.16) did not work.

Scheme 3.16

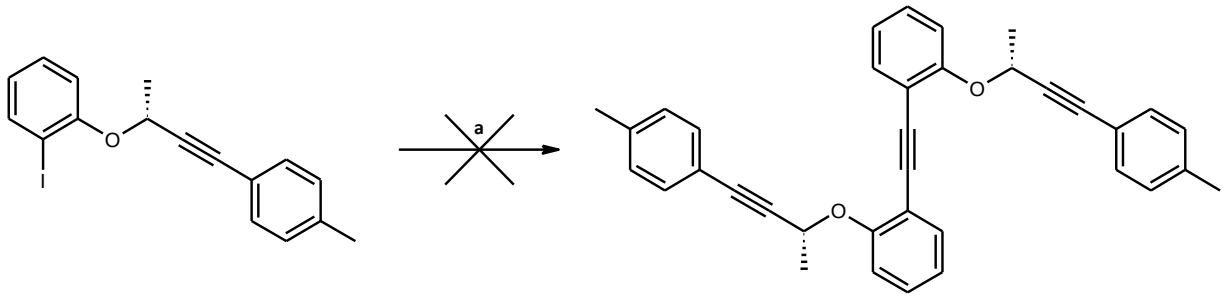

(*R*)-**241** (*R*,*R*)-**242**

(a) Acetylene (g) (0.5 eq), $Pd(PPh_3)_4$ (5 mol%), CuI (9 mol%), *i*Pr_2NH, rt, 6 h, **0%** (according to GS-MS detection)

To construct (*R*,*R*)-**242** stepwise, aryl iodide **241** was reacted first with trimethylsilyl acetylene **243** under the conditions of Sonogashira coupling. However, an inseparable mixture of the desired diyne (*R*)-**244** accompanied by the side product **245** was formed (detected by NMR, Scheme 3.17).

Scheme 3.17

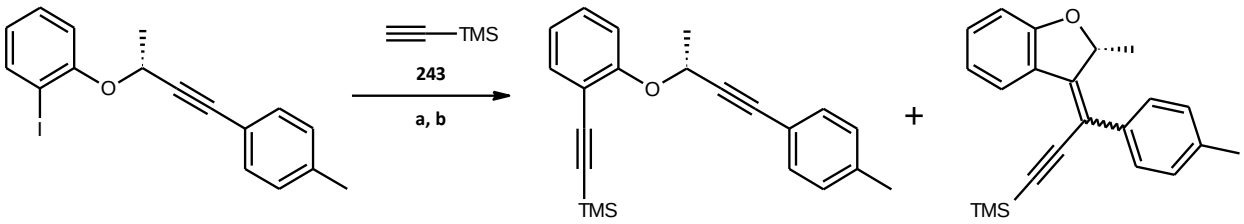

(*R*)-**241** (*R*)-**244** (*R*)-**245**

(a) **243** (4.0 eq), $Pd(PPh_3)_4$ (5 mol%), CuI (9 mol%), *i*Pr_2NH, rt, overnight, **244** : **245** = 81 : 19

(b) **243** (4.0 eq) + $Pd(PPh_3)_4$ (5 mol%), CuI (9 mol%), *i*Pr_2NH, rt, overnight, **59%**, **244** : **245** = 100 : 0

Obviously **245** is a product of a competitive alkyne insertion (formed probably also in the reaction of (*R*)-**241** with gaseous acetylene, see Scheme 3.16) and can be eliminate by using conditions **b** (see Scheme 3.17) when **243** is added to the reaction mixture along with the Pd complex. The triyne (*R*,*R*)-**242** can be obtained by deprotection of the terminal alkyne unit in (*R*)-**244** followed by cross-coupling of alkyne (*R*)-**246** with iodide (*R*)-**241** under Sonogashira conditions (Scheme 3.18).

Scheme 3.18

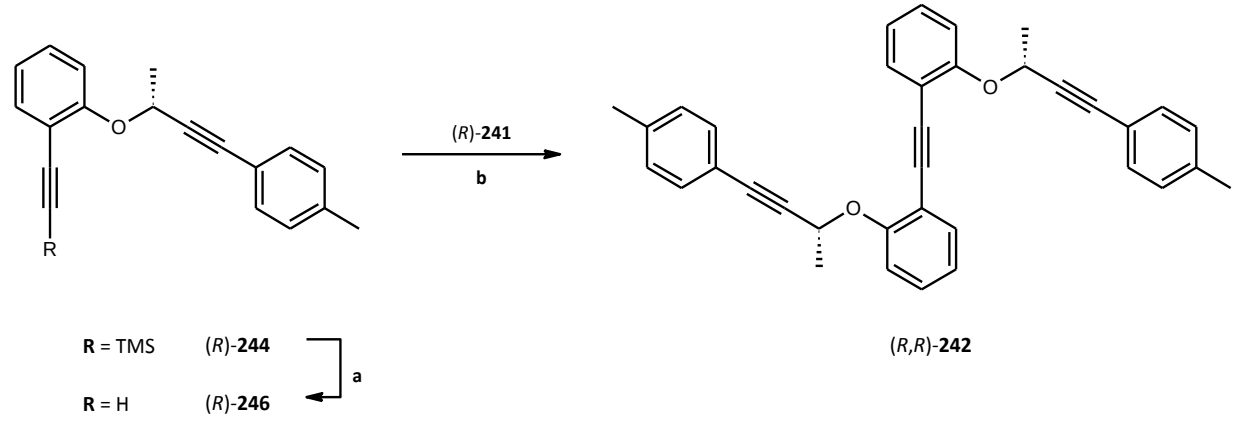

(a) K_2CO_3 (5.0 eq), MeOH, rt, 3 h, **85%**

(b) (*R*)-**241** (1.0 eq), $Pd(PPh_3)_4$ (5 mol%), CuI (9 mol%), *i*Pr_2NH, rt, overnight, **89%**

A more elegant way to triyne (*R*,*R*)-**242**[110] led through a protected triyne (*R*,*R*)-**252**. The synthetic route was developed for the preparation of differently substituted heterohelicenes on the central ring in the positions 7 and 8. Moreover, this method completely eliminated the competitive alkyne insertion described above (see Scheme 3.17) by introducing the sterically demanding triisopropyl moiety as a

protecting group of terminal ethyne units. The synthesis starts with the reaction between **240** and the commercially available (*S*)-(-)-3-butyn-2-ol (*S*)-**217**, following the Mitsunobu protocol as in previous. The terminal ethyne unit is then modified by introducing the protective group (Scheme 3.19).

Scheme 3.19

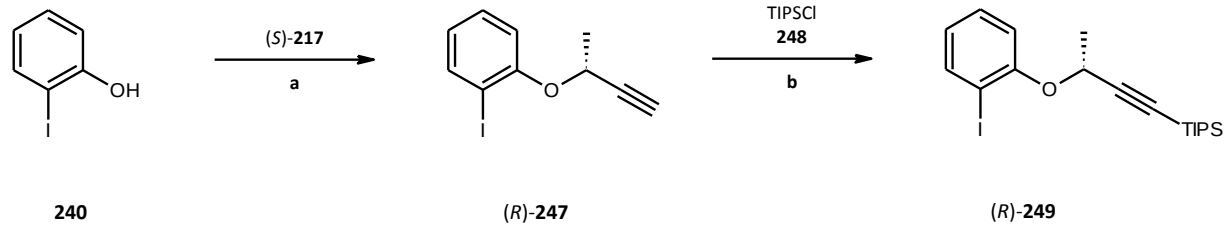

240 (*R*)-**247** (*R*)-**249**

(a) (*S*)-**217** (1.05 eq), PPh_3 (1.0 eq), DIAD (1.0 eq), C_6H_6, rt, overnight, **82%**

(b) LDA (1.0 eq), THF, -78 °C, 1.5 h, **248** (1.1 eq), THF, -78 °C to rt, 3 h, **89%**

The iodide (*R*)-**249** was then turned into the protected diyne (*R*)-**250** with no side-reaction. After desilylation, the unprotected diyne (*R*)-**251** was coupled with (*R*)-**249** under Pd catalysis to form the symmetrical triyne (*R*,*R*)-**252** (Scheme 3.20).

Scheme 3.20

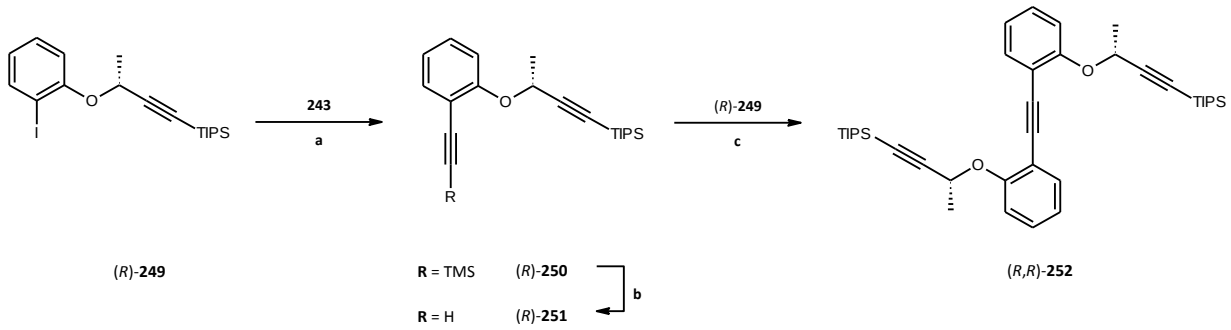

(*R*)-**249** (*R*,*R*)-**252**

(a) **243** (2.0 eq), $Pd(PPh_3)_4$ (5 mol%), CuI (9 mol%), *i*Pr_2NH, rt, 1 h, **89%**

(b) K_2CO_3 (5.0 eq), MeOH, rt, 2 h, **93%**

(c) (*R*)-**249** (1.0 eq), $Pd(PPh_3)_4$ (5 mol%), CuI (9 mol%), *i*Pr_2NH, rt, overnight, **96%**

The triyne (*R*,*R*)-**252** was desilylated to give (*R*,*R*)-**253** enabling further functionalization leading to various symmetrical [5]heterohelicenes as will be mentioned in following. The synthesis of (*R*,*R*)-**242** is presented below (Scheme 3.21).

Scheme 3.21

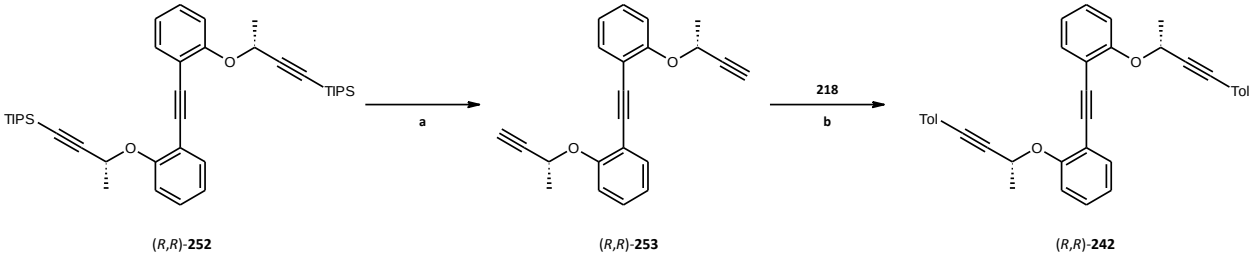

(*R*,*R*)-**252** (*R*,*R*)-**253** (*R*,*R*)-**242**

(a) NBu_4F (4.8), THF, rt, 2 h, **95%**

(b) **218** (2.1 eq), $Pd(PPh_3)_4$ (10 mol%), CuI (18 mol%), *i*Pr_2NH, rt, 2 h, **93%**

Two examples of the consequent cyclisation (Scheme 3.22) are discussed in detail from the stereochemical point of view. The results of diastereoselective cyclotrimerization of (*R*,*R*)-**242** and (*R*,*R*)-**253** are summarized in tables (Table 3.23 and 3.28) placed under the reaction schemes (Scheme 3.22 and 3.27).

Scheme 3.22

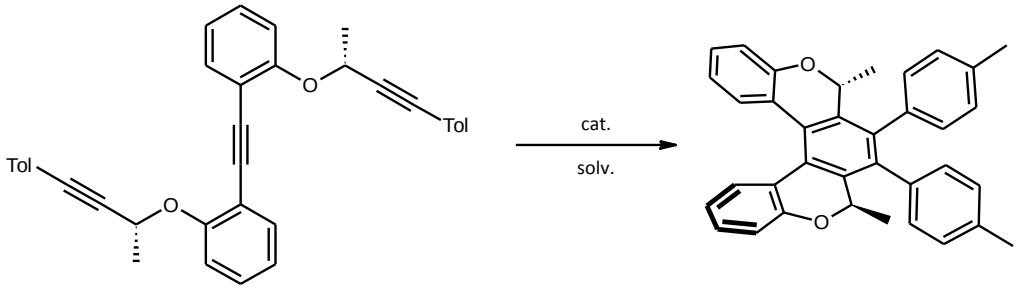

(*R*,*R*)-**242** (*M*,*R*,*R*)-**239**

Table 3.23

	cat.	%cat. [%]	solv.	temp. [°C]	time [min]	other conditions	yield[a] [%]
1	$CpCo(CO)_2$ **81**/ PPh_3	20 / 40	$C_{10}H_{22}$	140	60	hν	81
2	$Ni(cod)_2$ **254**/ PPh_3	20 / 40	THF	rt	30	-	91
3	CpCo(CO)(fum) **255**	100	THF	200	30	MW, ion. liq.[b]	70
4	CpCo(CO)(fum) **255**	20	THF	180	20	MW, ion. liq.[b]	89
5	$Rh(cod)_2BF_4$ **257**/ PPh_3	10 / 20	CH_2Cl_2	rt	48 h	H_2[c]	20[d]

[a]) isolated yield

[b]) ion. liq. = 1-butyl-2,3-dimethylimidazolium tetrafluoroborate

[c]) for creation of catalytically active species

[d]) full conversion was not achieved, stopped after 48 h

In all cases the reaction delivered (*M*,*R*,*R*)-**239** in good yields (from 70 to 91%) except for the cyclisation mediated by a cationic Rh(I) species **257** when the full conversion was not reached and the product (*M*,*R*,*R*)-**239** was isolated from the reaction mixture in 20% yield. On the other hand, the catalytic systems of CpCo(CO)(fum) **255** and $Ni(cod)_2$ **254** provided the best results with comparable isolated yields. The measured ^1H NMR spectra showed the presence of a sole diastereomer (*M*,*R*,*R*)-**239** in the reaction mixture. The absolute configuration of the product **239** was assigned by several methods. To verify the assumption about the stereochemistry of helicene-like compounds mentioned above (see Chapter 3.1), the diastereomeric pair of the simple pentacyclic model (*M*,*R*,*R*)-**239**/(*P*,*R*,*R*)-**239** was first investigated computationally (Figure 3.24, Appendix A, Dr. J. Vacek; Dr. J. Vacek Chocholoušová).

Figure 3.24

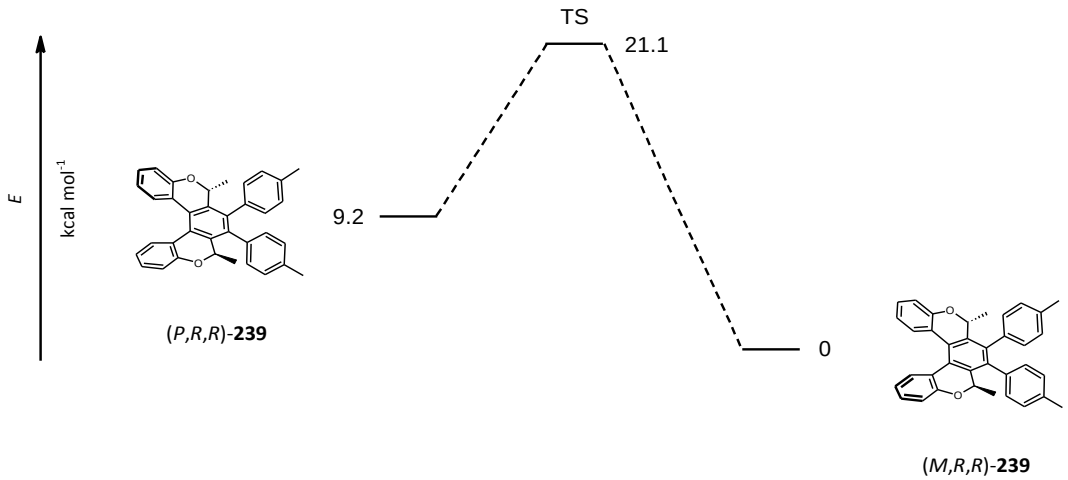

The relative free energies and barriers of epimerization of (*M*,*R*,*R*)-**239**/(*P*,*R*,*R*)-**239** were calculated by DFT (B3LYP/cc-pVTZ), and the transition states (TS) were localized by the QST3 method (Gaussian 09). The energy difference between the tolyl-substituted diastereomers was remarkable: 9.2 kcal mol^{-1} in favor of the diastereomer with the (*M*) helicity. The system obviously adopts a deep-minimum conformation with the CH_3 groups at the stereogenic centers in the pseudo axial position (moving out of the plane of the central benzene ring). Such an arrangement evidently prevents an unfavorable allylic-like 1,3-strain arising otherwise from the interaction between the CH_3 groups at the stereogenic centers occupying the pseudo equatorial position and the tolyl groups at the central benzene ring (both lying in the same plane) of the diastereomeric (*P*,*R*,*R*)-**239**. Accordingly, (*M*,*R*,*R*)-**239** should exist as a sole diastereomer (detectable within the HPLC or NMR limits) in the thermodynamic equilibrium regardless of the barrier to helicity inversion, which was calculated to be 11.9 or 21.1 kcal mol^{-1} respectively.

It was indispensable to confirm the results obtained above experimentally. Unfortunately the absolute configuration of **239** could not be assigned equivocally by NOE NMR measurements and so further computations were necessary to do (Dr. R. Pohl). The experimentally observed ^{1}H and ^{13}C NMR chemical shifts were compared with calculated ones for (*M*,*R*,*R*)-**239** and juxtaposed with synthetically inaccessible (*P*,*R*,*R*)-**239**. ^{1}H and ^{13}C chemical shifts of the saturated part of helicene (CH_3, CH) were calculated by GIAO DFT OPBE/6-31G* method using geometries optimized by B3LYP/6-31G*. The calculated nuclear shielding constants were referenced to TMS calculated at the same level of theory. The results are summarized in the next table (Table 3.25); mean absolute errors (MAE) are given.

Table 3.25

		Experimental	Calculated	
		(*M*,*R*,*R*)-**239**	(*M*,*R*,*R*)-**239**	(*P*,*R*,*R*)-**239**
^{1}H NMR [ppm]	CH_3	0.93	0.76	1.18
	CH	5.26	5.17	5.36
^{13}C NMR [ppm]	CH_3	18.30	19.02	24.77
	CH	72.92	73.20	71.35
MAE			0.32	2.10

The results shown in the table (Table 3.25) indicate that the isolated helicene **239** possesses the (*M*) helicity.

Another confirmation of helicity of **239** came from comparison of measured and calculated electronic circular dichroism spectra. The structure of (*M*,*R*,*R*)-**239** was first optimized using the DFT method with the B3LYP functional and cc-pVTZ basis set. The electronic CD spectra were calculated for this optimized structure using TD-DFT with B2PLYP functional and cc-pVDZ or cc-pVTZ basis sets (both approaches provided similar outputs). The influence of solvent effects (acetonitrile) was also examined at the B2PLYP/cc-pVDZ/CPCM level of theory to see only negligible changes in the ECD spectra. The comparison of the experimental (blue) and calculated (red) electronic CD spectra of (*M*,*R*,*R*)-**239** featured a strong band associated with a positive dichroism (Figure 3.26, Appendix B, Dr. J. Vacek; Dr. J. Vacek Chocholoušová).

Figure 3.26

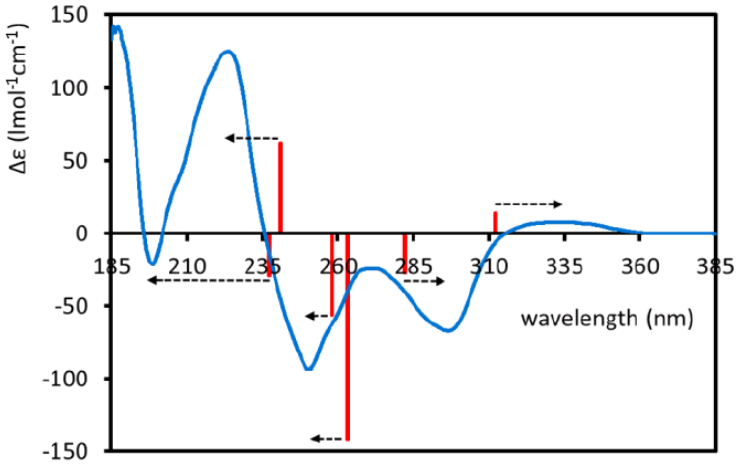

Good agreement of a theory and an experiment in the helicity correlation by CD supported fully the assignment of the helicity obtained by previous method (calculations of chemical shifts).

A completely different stereochemical outcome of [2+2+2] cyclotrimerization of (*R*,*R*)-**253** with terminal alkyne units was observed, as a 34 : 66 mixture of (*M*,*R*,*R*)- and (*P*,*R*,*R*)-**256** was formed (Scheme 3.27) regardless of the reaction conditions used (Table 3.28).

Scheme 3.27

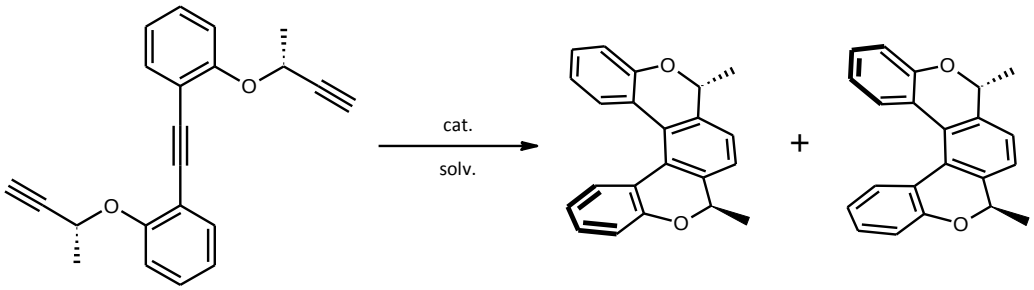

(*R*,*R*)-**253** (*M*,*R*,*R*)-**256** (*P*,*R*,*R*)-**256**

Table 3.28

	cat.	%cat. [%]	solv.	temp. [°C]	time [min]	other conditions	yield[a] [%]
1	$CpCo(CO)_2$ **81**/ PPh_3	20 / 40	$C_{10}H_{22}$	140	60	hν	77
2	$Ni(cod)_2$ **254**/ PPh_3	20 / 40	THF	rt	30	-	71
3	CpCo(CO)(fum) **255**	100	THF	200	30	MW, ion. liq.[b]	74
4	CpCo(CO)(fum) **255**	20	THF	180	20	MW, ion. liq.[b]	96

[a]) isolated yield

[b]) ion. liq. = 1-butyl-2,3-dimethylimidazolium tetrafluoroborate

As in the previous case of the tolyl-substituted analog **239** all cyclizations proceeded in good to excellent yields (from 71 to 96%). The best result (96% yield) was achieved with a catalytic amount of CpCo(CO)(fum) **255**. To assign the absolute configuration of the products **256**, DFT calculations for the (*M*,*R*,*R*)-**256**/(*P*,*R*,*R*)-**256** diastereomeric pair were done as in the previous case (Figure 3.29, Appendix A, Dr. J. Vacek; Dr. J. Vacek Chocholoušová).

Figure 3.29

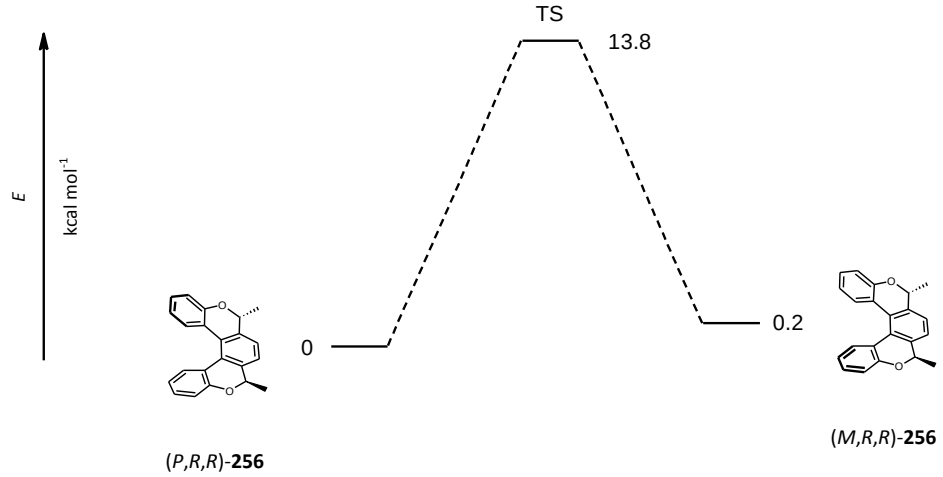

The relative free energies and barriers of epimerization of (*M*,*R*,*R*)-**256**/(*P*,*R*,*R*)-**256** were calculated by DFT (B3LYP/cc-pVTZ), and the transition states (TS) were localized by the QST3 method (Gaussian 09). (*P*,*R*,*R*)-**256** was found to be only about 0.2 kcal mol^{-1} more stable than (*M*,*R*,*R*)-**256**. The methyl groups at the stereogenic centers in the non-tolylated **256** can occupy either the pseudo equatorial position as in (*P*,*R*,*R*)-**256** or *pseudo* axial position as in (*M*,*R*,*R*)-**256** (not encompassing any 1,3-diaxial interaction). There is a small preference for (*P*,*R*,*R*)-**256** over (*M*,*R*,*R*)-**256** (66:34 as found experimentally). The dynamic equilibrium between (*M*,*R*,*R*)-**256** ↔ (*P*,*R*,*R*)-**256** allowed to determine the barrier of interconversion by temperature dependent ^{1}H NMR (Figure 3.30, experiment in blue, theory in red, Dr. R. Pohl).

Figure 3.30

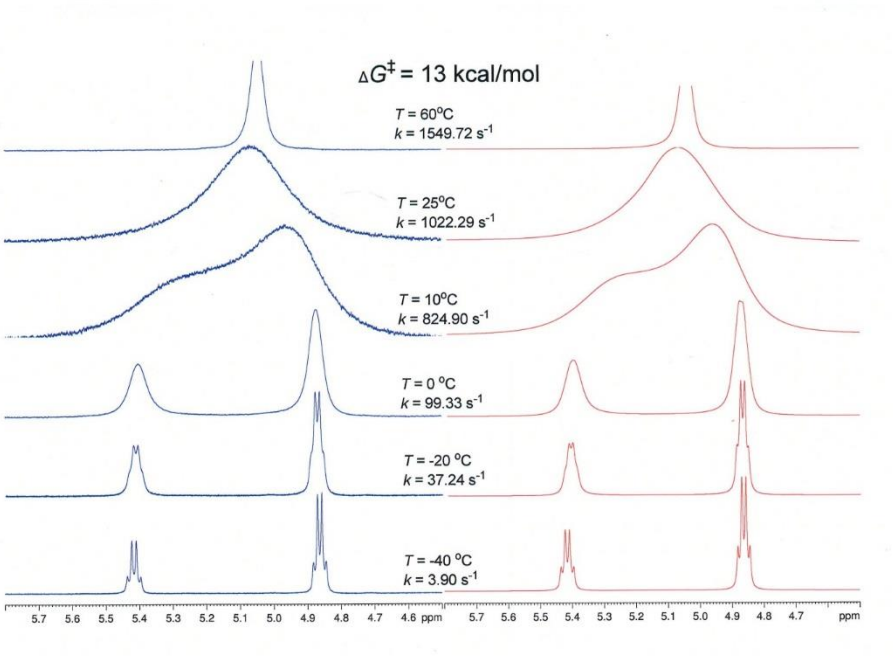

The ^{1}H NMR at the room temperature showed broad signals, especially from CH_3 and CH saturated part of the helicene **256**. When cooled down to -40 °C, two distinctive epimers can be observed in ratio ca 2 : 1. When heated up to +60 °C, an average spectrum of both diastereomers of **256** can be observed. The barrier of epimerization was estimated from the Eyring equation using dynamic NMR ($\Delta G^{\ddagger}$ = 13.0 kcal mol^{-1}) and it is fully in accord with the value obtained from previously performed DFT calculations, where the TS of interconversion was found to be located 13.8 kcal mol^{-1} (or 13.6 kcal mol^{-1}) above the ground state of (*P*,*R*,*R*)-**256** (or (*M*,*R*,*R*)-**256**).

The helicity of (*P*,*R*,*R*)/(*M*,*R*,*R*)-**256** was assigned by measuring the NOE in ^{1}H NMR spectra at low temperature (Dr. R. Pohl). Even at the low temperature, there was still an exchange between the exchangeable nuclei ($t_{1/2}$ = 0.22 s at -40 °C; $t_{1/2}$ = 3.40 s at -60 °C) and therefore the mixing time in the DPFGSE NOE experiment had to be shortened to 100 ms. Using these optimized conditions the NOE between CH_3 or CH and protons from the central phenyl ring was observed (Figure 3.31).

Figure 3.31

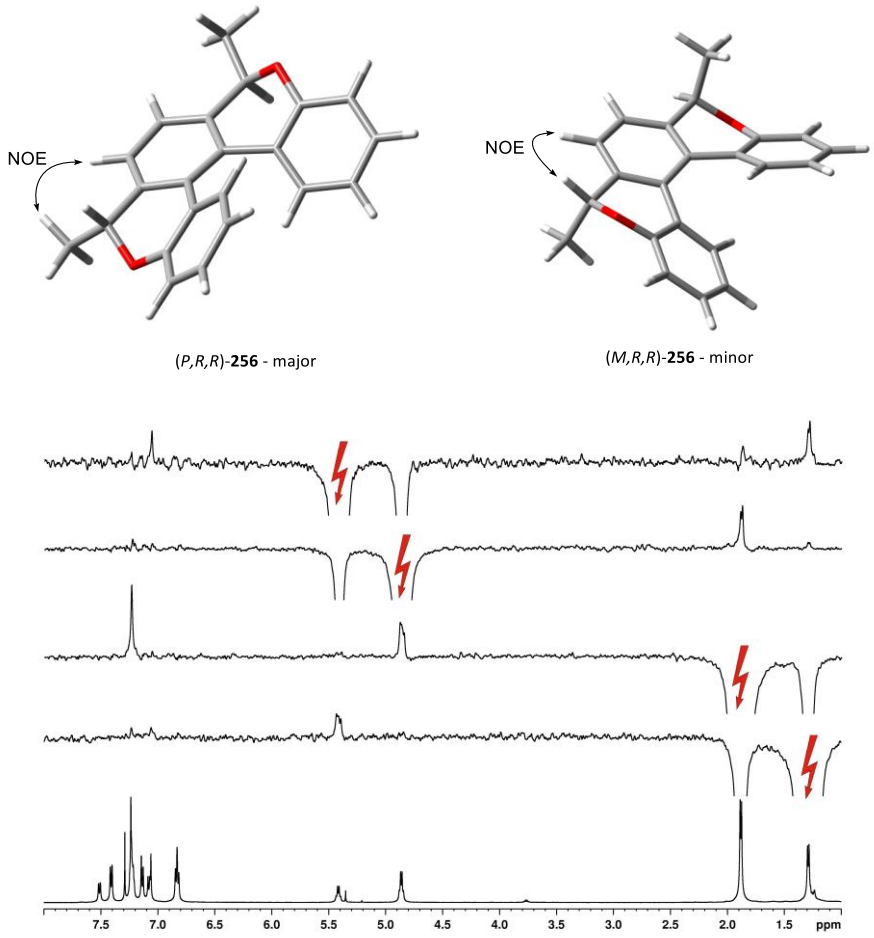

Furthermore, a good agreement was found between observed and calculated ^{1}H and ^{13}C NMR shifts between the distinguishable diastereomers of (*P*,*R*,*R*)/(*M*,*R*,*R*)-**256**. Theoretical and experimental values are summarized in table below (Table 3.32). The results (Table 3.32) are consistent with the previously done measurement.

Table 3.32

		Experimental		Calculated	
		(*M*,*R*,*R*)-**256**	(*P*,*R*,*R*)-**256**	(*M*,*R*,*R*)-**256**	(*P*,*R*,*R*)-**256**
^{1}H NMR [ppm]	CH_3	1.29	1.88	1.17	1.65
	CH	5.41	4.86	5.27	4.92
^{13}C NMR [ppm]	CH_3	20.4	18.3	21.8	19.1
	CH	74.7	74.2	75.6	74.1

Crystallization was performed to get the suitable single-crystal for an X-ray diffraction experiment (Dr. I. Císařová). The minor epimer (*M*,*R*,*R*)-**256** crystalized preferentially from the 34 : 66 diastereomeric mixture and its structure is displayed in the figure (Figure 3.33, Appendix C).

Figure 3.33

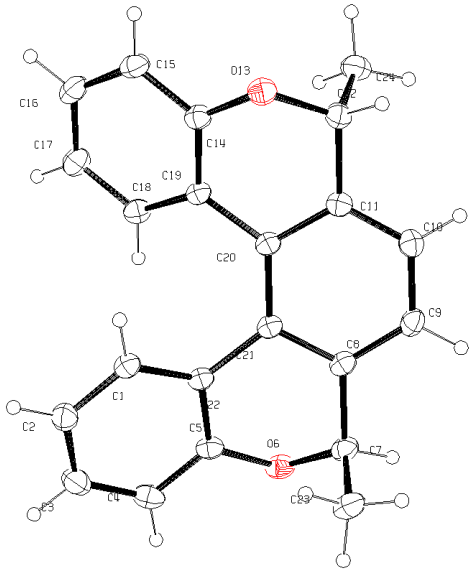

The ORTEP drawing of the X-ray structure (CCDC 851844) of (*M*,*R*,*R*)-**256** with 30% probability atomic displacement ellipsoids is displayed.

The synthetic strategy described in previous was adopted to the preparation of other helicene-like derivatives containing two 2*H*-pyran units. Relying on highly diastereoselective [2+2+2] cyclotrimerization controlled by the predictable 1,3-allylic-type strain, the synthesis of other helicene-like molecules in an optically pure form could be performed. The synthetic route to the potentially interesting ligand (*M*,*R*,*R*)-**260** bearing two pyridine rings in the position 7, 8 (see Scheme 3.35) started from the chiral triyne (*R*,*R*)-**253** with two terminal acetylene units that enabled double Sonogashira coupling (Scheme 3.34).

Scheme 3.34

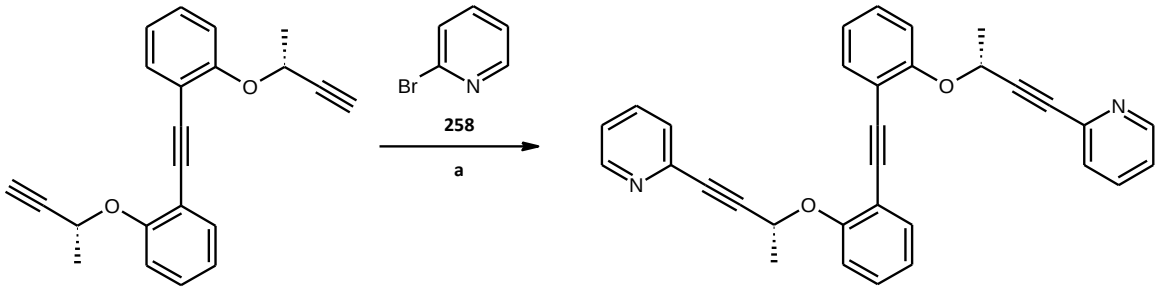

(*R*,*R*)-**253** (*R*,*R*)-**259**

(a) **258** (2.1 eq), $Pd(PPh_3)_4$ (10 mol%), CuI (18 mol%), *i*Pr_2NH, rt, overnight, **83%**

The final product (*M*,*R*,*R*)-**260** was obtained after cyclization (Scheme 3.35). Results are summarized in the following table (Table 3.36).

Scheme 3.35

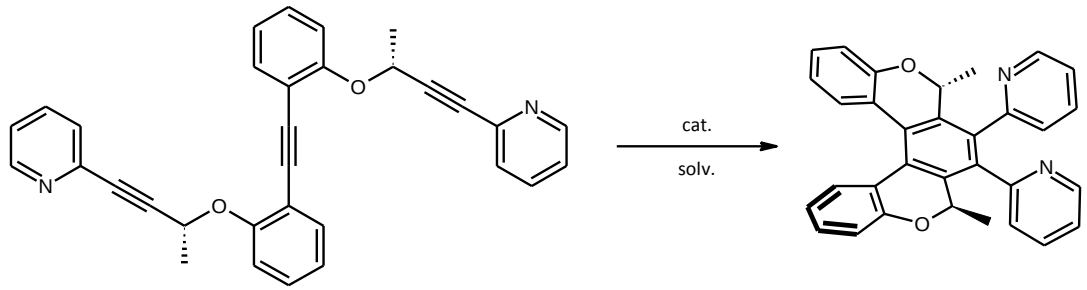

(*R*,*R*)-**259** (*M*,*R*,*R*)-**260**

Table 3.36

	cat.	%cat. [%]	solv.	temp. [°C]	time [min]	other conditions	yield[a] [%]
1	$CpCo(CO)_2$ **81**/ PPh_3	20 / 40	$C_{10}H_{22}$	140	60	hν	49
2	$Ni(cod)_2$ **254**/ PPh_3	20 / 40	THF	rt	6 h	-	42[b]
3	CpCo(CO)(fum) **255**	100	THF	180	20	MW, ion. liq.[c]	72
4	CpCo(CO)(fum) **255**	20	THF	180	20	MW, ion. liq.[c]	79

[a]) isolated yield
[b]) full conversion was not achieved according to TLC
[c]) ion. liq. = 1-butyl-2,3-dimethylimidazolium tetrafluoroborate

The cyclisations of (*R*,*R*)-**259** to (*M*,*R*,*R*)-**260** proceeded in fair to good yields. The best results were achieved by using **255** in both the equimolar and catalytical amounts (72% and 79% respectively). Full conversion of the starting material was not observed in an experiment using the Ni(0) catalyst **254**, which

explains the moderate yield of (*M*,*R*,*R*)-**260** (42%). The observed diastereoselective formation of (*M*,*R*,*R*)-**260** is apparently controlled by the post-cyclization equilibration between the (*M*,*R*,*R*) and (*P*,*R*,*R*) epimers (under thermodynamic stereocontrol) owing to the expected low barrier to epimerization of the both diastereomers **260** similarly to **239**. Based on the previous assignments of helicity to helicene-like products (such as **239**) utilizing helicity correlation by CD spectra, chemical shifts of methyl groups indicative for helicity and quantum mechanical calculations, it was possible to assign (*M*) helicity also to (*M*,*R*,*R*)-**260** and all other [5]- and [6]helicene 2*H*-pyran analogs bearing *p*-tolyl, *m*-(4-(dimethylamino)pyridyl) or *p*-(4-(methylthio)phenyl) substituents in the positions 7 and 8 of the helical backbones (their synthesis will be discussed in the following text). Surprisingly, a dynamical behavior on the NMR time scale at room temperature can be observed for (*M*,*R*,*R*)-**260**. The rotational barrier of the pyridyl units was found to be 12.3 kcal mol^{-1} (calculated by the semi-empirical method PM3 by Dr. R. Pohl)[111]. The observed behavior and calculated barrier to rotation are in accord with that of other helicene-like molecules bearing pyridyl rings at the central benzene ring of the helical backbone[112].

As (*M*,*R*,*R*)-**260** contains two adjacent pyridyl units, its basicity was determined by capillary electrophoreses (Dr. V. Kašička). Measurements were performed in a bare fused silica capillary with outer polyimide coating (total/effective length 305/195 mm, id/od 50/375 μm) in the home-made capillary electrophoresis device equipped with UV-photometric absorption detector operating at 206 nm[113]. The separation voltage was +12 kV (anode at the injection end) and electric current was in the range 11.7-14.5 μA. First, the effective electrophoretic mobilities of (*M*,*R*,*R*)-**260** were measured in nonaqueous methanol as a solvent for the background electrolytes within a pH range (pH_{MeOH} = 1.6 – 12.0) and at ambient temperature (22-26°C). Second, the effective mobilities were corrected to reference temperature (25°C) and constant ionic strength (25 mM)[114]. From the obtained pH dependence of effective mobilities (see Figure 3.37), the so-called mixed acidity constant, $pK_{a,mix}$, of ionogenic group(s) of (*M*,*R*,*R*)-**263** was calculated by a non-linear regression analysis[114]. Then, the mixed acidity constant $pK_{a,mix}$ was recalculated to thermodynamic acidity constant pK_a by the Debye-Hückel theory of non-ideality of electrolyte solutions. Finally, from the thermodynamic $pK_{a,MeOH}$ value in methanol, the aqueous thermodynamic constant $pK_{a,H2O}$ was estimated using the empirical relations between methanolic and aqueous pK_a values derived for structurally related pyridines.[114,115,116] Using this procedure, the following acidity constants of (*M*,*R*,*R*)-**260** were obtained:

$pK_{a,MeOH}$ = 4.66 , $pK_{a,H2O}$ = 4.27

Figure 3.37

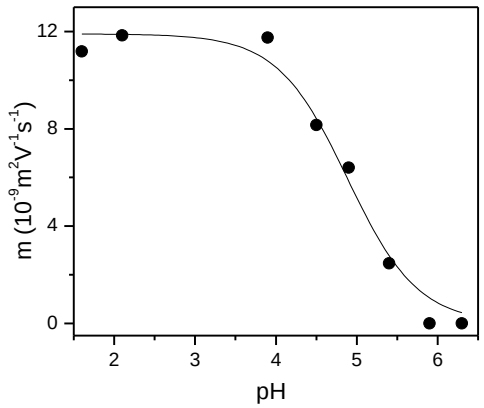

Surprisingly, only one of the two nitrogen atoms of (*M*,*R*,*R*)-**260** was found to be protonated. Similar effect was observed in related structures, such as (*M*,*R*,*R*)-**263** (see below), diazahelicenes and 1,8-bis(dimethylamino)naphthalene[117]. The possible theoretical explanation of this unexpected behavior is given in discussion of (*M*,*R*,*R*)-**263** (see below).

Another potentially interesting molecule accessible through a simple functionalization proceeding the final cyclization step is a derivative containing 4-(*N*,*N*-dimethylaminopyridine) units. Helically chiral compounds bearing such structural moiety were already successfully examined in acyl transfer reactions[68,69] (as noted in Chapter *1.2.2.3*). The use of (*M*,*R*,*R*)-**263** in the same way will be discussed in the following part. The centrally chiral triyne (*R*,*R*)-**262** was synthetized similarly to (*R*,*R*)-**259** by employing Sonogashira coupling of (*R*,*R*)-**253** with **261** (Scheme 3.37) prepared according to the literature procedure[118] by A. Andronova in our group.

Scheme 3.38

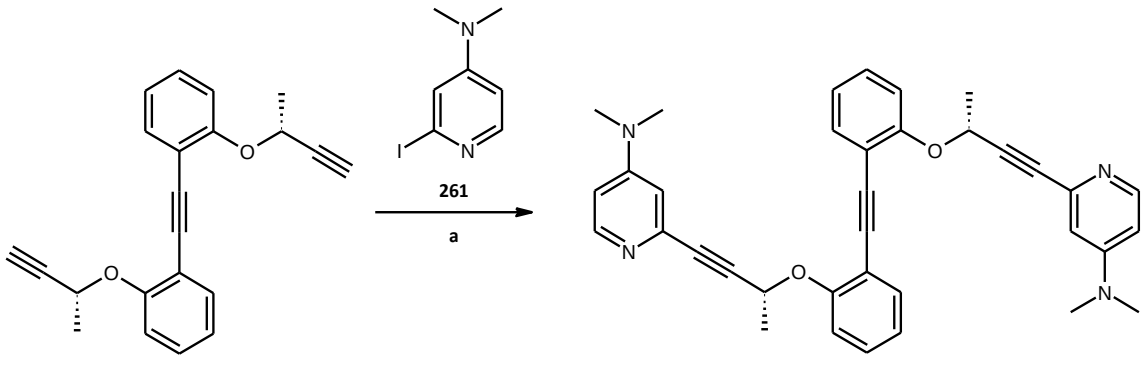

(*R*,*R*)-**253** (*R*,*R*)-**262**

(a) **261** (2.1 eq), $Pd(PPh_3)_4$ (10 mol%), CuI (18 mol%), *i*Pr_2NH (5.0 eq), DMF, 90 °C, overnight, **61%**

On a small scale (ca 50 mg of the starting material), the cyclization product (*M*,*R*,*R*)-**211** (see Scheme 3.39) can be furnished using both Co(I) **255** and Ni(0) **254** catalytic systems in satisfactory yield (Table 3.40, entries 1, 2 and 3), whereas on a larger scale (over 100 mg of the starting material) only the Ni(0) catalyst **254** at higher temperature (50 °C) is efficient enough to form the desired product in good yields (Table 3.40, entries 4, 5 vs. 6, 7). Experiments using an equimolar amount of Ni(0) **254**/PPh_3 led to product contaminated by traces (up to 2%) of triphenylphosphine oxide (as observed by ^1H NMR) inseparable from each other even after repeated chromatographic purifications (Table 3.40, entry 6). This problem is caused by the similar polarity of these two compounds and can be eliminated by using smaller catalyst loading *ceteris paribus* (Table 3.40, entries 3, 7).

Scheme 3.39

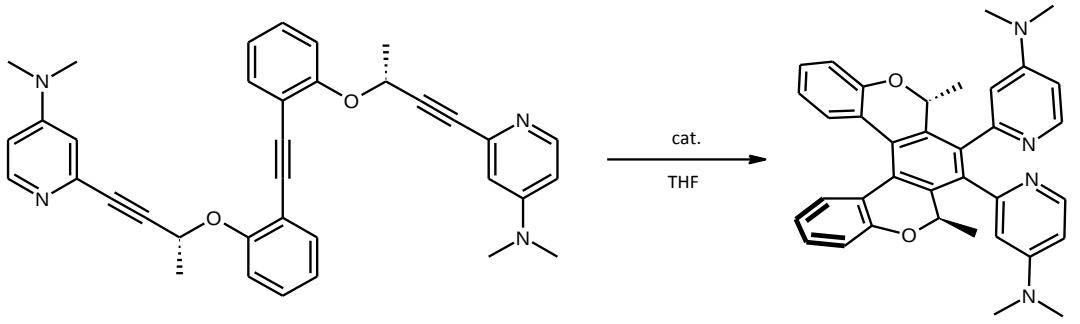

(*R*,*R*)-**262** (*M*,*R*,*R*)-**211**

Table 3.40

	cat.	reaction scale[a] [mg]	%cat. [%]	temp. [°C]	time [min]	other conditions	yield[b] [%]
1	CpCo(CO)(fum) **255**	49.5	100	180	20	MW, ion. liq.[c]	61
2	CpCo(CO)(fum) **255**	20.5	20	180	20	MW, ion. liq.[c]	51
3	$Ni(cod)_2$ **254**/ PPh_3	21.2	20 / 40	rt	210	-	50
4	CpCo(CO)(fum) **255**	98.0	100	180	20	MW, ion. liq.[c]	16
5	CpCo(CO)(fum) **255**	200.0	20	180	20	MW, ion. liq.[c]	27
6	$Ni(cod)_2$ **254**/ PPh_3	183.0	100 / 200	50	overnight	-	88[d]
7	$Ni(cod)_2$ **254**/ PPh_3	83.7	5 / 10	50	overnight	-	78

[a]) mg of used starting material (*R*,*R*)-**262**

[b]) isolated yield

[c]) ion. liq. = 1-butyl-2,3-dimethylimidazolium tetrafluoroborate

[d]) contains up to 2 mol% of $O{=}PPh_3$

A sole diastereomer (*M*,*R*,*R*)-**211** is formed, whose (*M*) helicity is assigned similarly as discussed above. In contrast to the previous pyridine analog (*M*,*R*,*R*)-**260**, no dynamic behavior can be seen on the NMR time scale at room temperature. This fact is caused by the presence of *N*,*N*-dimethylamino groups at the pyridine rings making their rotation along the aryl-aryl axis more difficult.

Acidobazic properties of (*M*,*R*,*R*)-**211** were investigated employing capillary electrophoreses as described for (*M*,*R*,*R*)-**260** before (Dr. V. Kašička). Accordingly, the following acidity constants of (*M*,*R*,*R*)-**211** were obtained:

$pK_{a,MeOH}$ = 8.60 ± 0.06, $pK_{a,H2O}$ = 8.31 ± 0.23.

The pH-dependent effective mobilities (see Figure 3.41) read out the mixed acidity constant, $pK_{a,mix}$ from the non-linear regression analysis[114]. Thermodynamic acidity constant pK_a was calculated using the Debye-Hückel theory of non-ideality of electrolyte solutions.

Figure 3.41

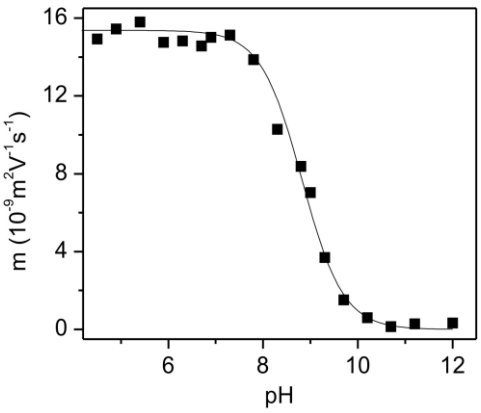

The estimated pK_a indicates single protonation although four basic centers are present in the molecule. This is in an agreement with the previously observed behavior of (*M*,*R*,*R*)-**260** and other structures[117].

To use the robust [2+2+2] diastereoselective cyclotrimerization methodology for the preparation of unsymmetrically substituted [5]helicenes or higher [6]helicenes, a slightly different synthetic approach has to be used. The basic concept of connecting two chiral building blocks to form an optically pure triyne is maintained, but both differently substituted aryl subunits have to be synthetized independently. This approach was used in the preparation of the methoxy-substituted derivatives (*M*,*R*,*R*)-**263** and (*M*,*R*,*R*)-**264** (Figure 3.42).

Figure 3.42

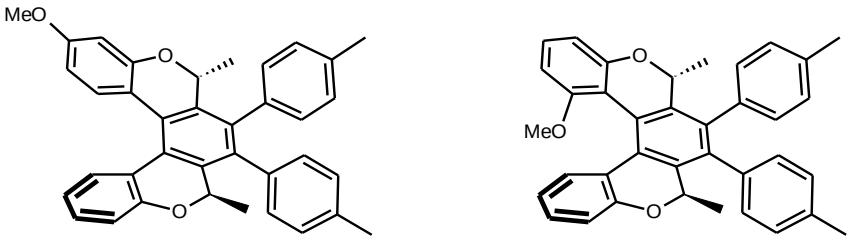

(*M*,*R*,*R*)-**263** (*M*,*R*,*R*)-**264**

The synthesis of (*M*,*R*,*R*)-**263** begins with the preparation of the suitably substituted phenol **266** (according to the literature procedure[119]) from the commercially available 3-methoxyphenol **265**. Then, **266** reacts further under the Mitsunobu reaction conditions with (*S*)-(-)-3-butyn-2-ol (*S*)-**217** to provide the terminal alkyne (*R*)-**267** (Scheme 3.43).

Scheme 3.43

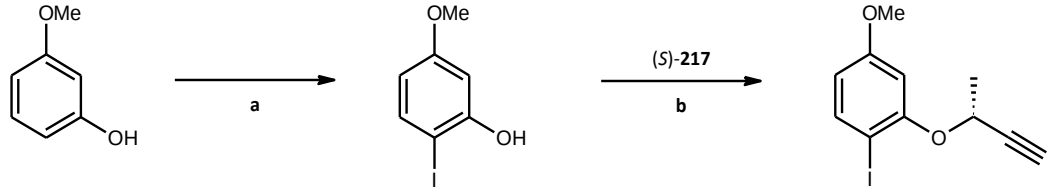

265 **266** (*R*)-**267**

I_2 (1.05 eq), $NaHCO_3$ (1.10 eq), H_2O, 0 °C to rt, 15 min, **50%**

(a) (*S*)-**217** (1.05 eq), PPh_3 (1.0 eq), DIAD (1.0 eq), C_6H_6, rt, overnight, **77%**

(*R*)-**267** is necessary to be protected by silylation with **248** to prevent its participation in the next step of the synthesis. The building block (*R*)-**268** then undergoes the Pd/catalyzed Sonogashira coupling reaction with the already prepared chiral diyne (*R*)-**251** to complete the synthesis of the protected triyne (*R*,*R*)-**269** that can be easily desilylated to (*R*,*R*)-**270.** To avoid the formation of a diastereomeric mixture after the final cyclization step, triyne (*R*,*R*)-**270** was modified at both terminal acetylene units by Sonogashira reaction with 4-iodotoluene **218** to form the tolyl-substituted (*R*,*R*)-**271** suitable for the following [2+2+2] cyclotrimerization step (Scheme 3.44).

Scheme 3.44

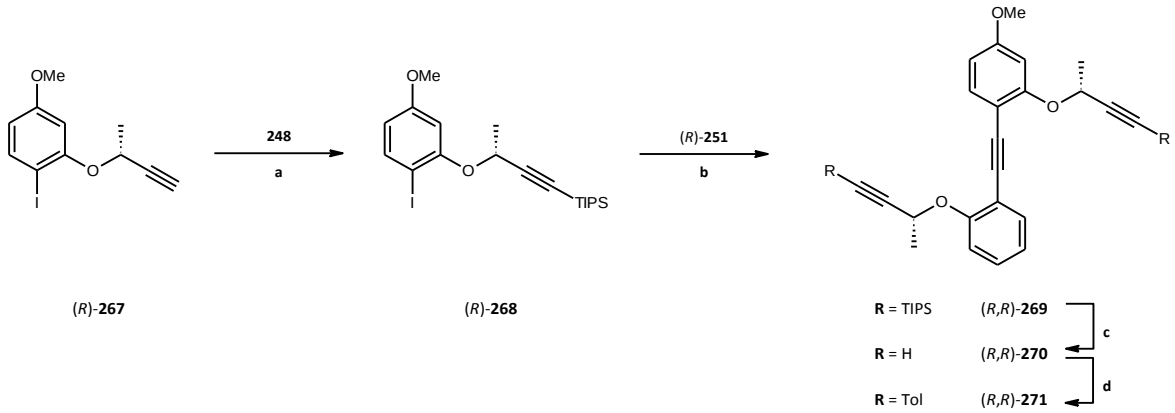

(a) LDA (1.0 eq), THF, -78 °C, 2 h, **248** (1.1 eq), THF, -78 °C to rt, 2 h, **83%**

(b) (*R*)-**251** (1.0 eq), $Pd(PPh_3)_4$ (5 mol%), CuI (9 mol%), *i*Pr_2NH, rt, overnight, **94%**

(c) NBu_4F (5.0), THF, rt, 2 h, **78%**

(d) **218** (2.1 eq), $Pd(PPh_3)_4$ (10 mol%), CuI (18 mol%), *i*Pr_2NH, rt, 1.5 h, **92%**

The final cyclization afforded (*M*,*R*,*R*)-**263** as a sole diastereomer possessing (*M*) helicity (Scheme 3.45). The results from this particular cyclizations are summarized in the following table (Table 3.46).

Scheme 3.45

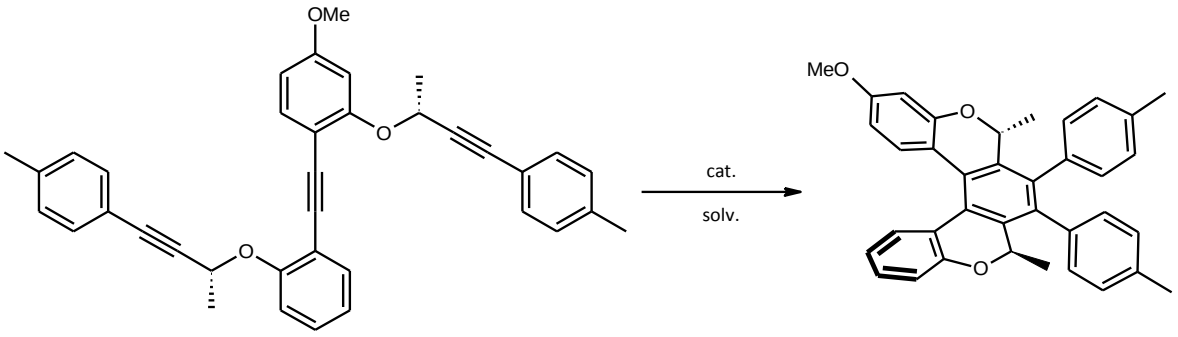

(*R*,*R*)-**271** (*M*,*R*,*R*)-**263**

Table 3.46

	cat.	%cat. [%]	solv.	temp. [°C]	time [min]	other conditions	yield[a] [%]
1	$CpCo(CO)_2$ **81**/ PPh_3	20 / 40	$C_{10}H_{22}$	140	60	hν	88
2	$Ni(cod)_2$ **254**/ PPh_3	20 / 40	THF	rt	120	-	78
3	CpCo(CO)(fum) **255**	100	THF	180	20	MW, ion. liq.[b]	83
4	CpCo(CO)(fum) **255**	20	THF	180	20	MW, ion. liq.[b]	57

[a]) isolated yield

[b]) ion. liq. = 1-butyl-2,3-dimethylimidazolium tetrafluoroborate

Whereas cyclization under the catalytic amount of $CpCo(CO)_2$ **81** proceeded smoothly in high yield (88%) and with a comparable outcome as the reaction catalyzed by Ni(0) **254** (78%), it was astonishing to find out that an equimolar amount of CpCo(CO)(fum) **255** is needed to reach the similar result (83%).

For a series of model systems, Dračínský et al. reported the experimental evidence of through-space NMR spectroscopic *J* coupling between hydrogen nuclei[120]. *J* coupling in NMR spectroscopy is conventionally associated with covalent bonds. A noncovalent contribution often called through-space coupling (TSC) has been known for heavy atoms. In this study, the TSC was detected and analyzed for the more common ^1H–^1H coupling as well. There is a strong distance and conformational TSC dependence that can be potentially used in structural studies of molecules and their complexes. It was found that aromatic systems can strongly participate in the noncovalent contribution to the coupling. The compound (*M*,*R*,*R*)-**263** served as a model compound for such kind of study[121]. An intramolecular TSC was measured between spatially proximate H1 and H14 nuclei, which are separated by seven bonds, using a long-range COSY experiment. The aromatic region of the spectrum is depicted in Figure 3.47 with highlighted cross-peaks of the TSC interaction.

Figure 3.47

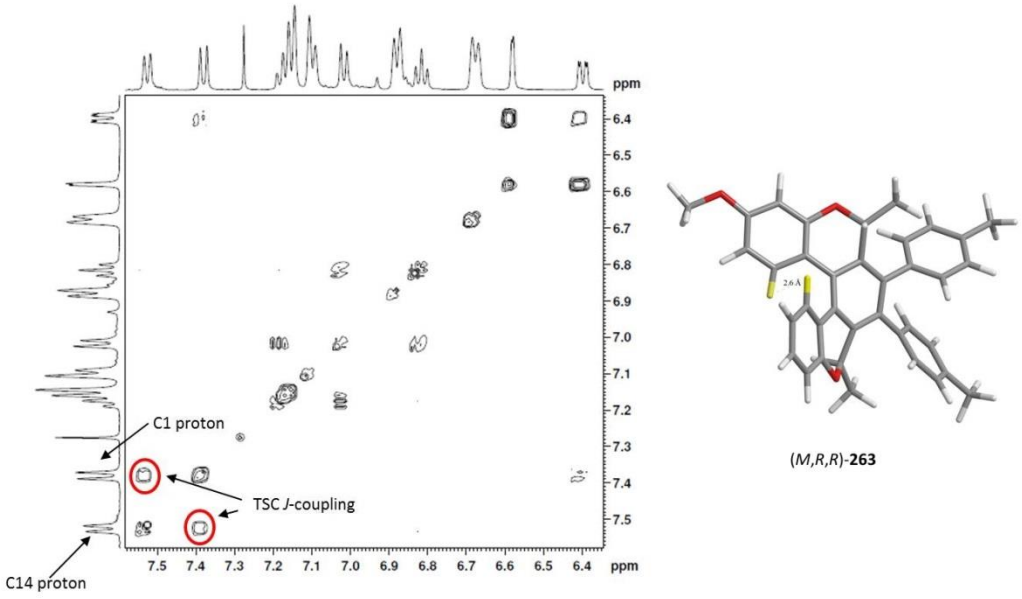

The 1-methoxy substituted helicene-like target molecule (*M*,*R*,*R*)-**264** was prepared in a similar way from two different building blocks. At the early stage of the synthesis, problems with the preparation of the building block **272** were encountered (see Scheme 3.48). The first attempt (**a**) at obtaining the substituted 2-iodo-3-methoxyphenol **272** relied on the demethylation reaction of the commercially available 2,6-dimethoxyiodobenzene **273** with $NbCl_5$ (analogously to lit.[122]). It completely failed probably due to the presence of iodine at the aromatic core. Next idea was to deprotect one methoxy group at the same substrate **273** under different conditions, but both alternative methodologies using BBr_3 (**b**) or EtSNa (**c**) did not work. The substrate **275** suitable for Mitsunobu reaction with MeOH (**e**) was synthetized from the commercially available resorcinol **274** (acc. to the lit.[123]). Although the reaction proceeded, its yield was moderate (30%). The direct methylation of one hydroxyl group of **275** by using MeI (**f**) led to a mixture of the mono- and bis-methylated products **272** and **273**, respectively, in low yield (the isolated yield of **272** was only 5%). Iodination of the commercially available **276** through double deprotonation with *n*BuLi (**g**) failed due to the formation of an unreactive phenoxide anion, which did not undergo a further deprotonation. To avoid this, phenol **276** was converted to carbamate **278** using isopropylisocyanate **277** (prepared acc. to lit. [124]), that underwent a multistep one-pot reaction (**i**) (acc. to lit.[124]) to form the desired product **272** in satisfactory 56% yield. It was found that only *t*BuLi is reactive enough as a deprotonating agent and it is needed to be used in this reaction instead of *n*BuLi.

Scheme 3.48

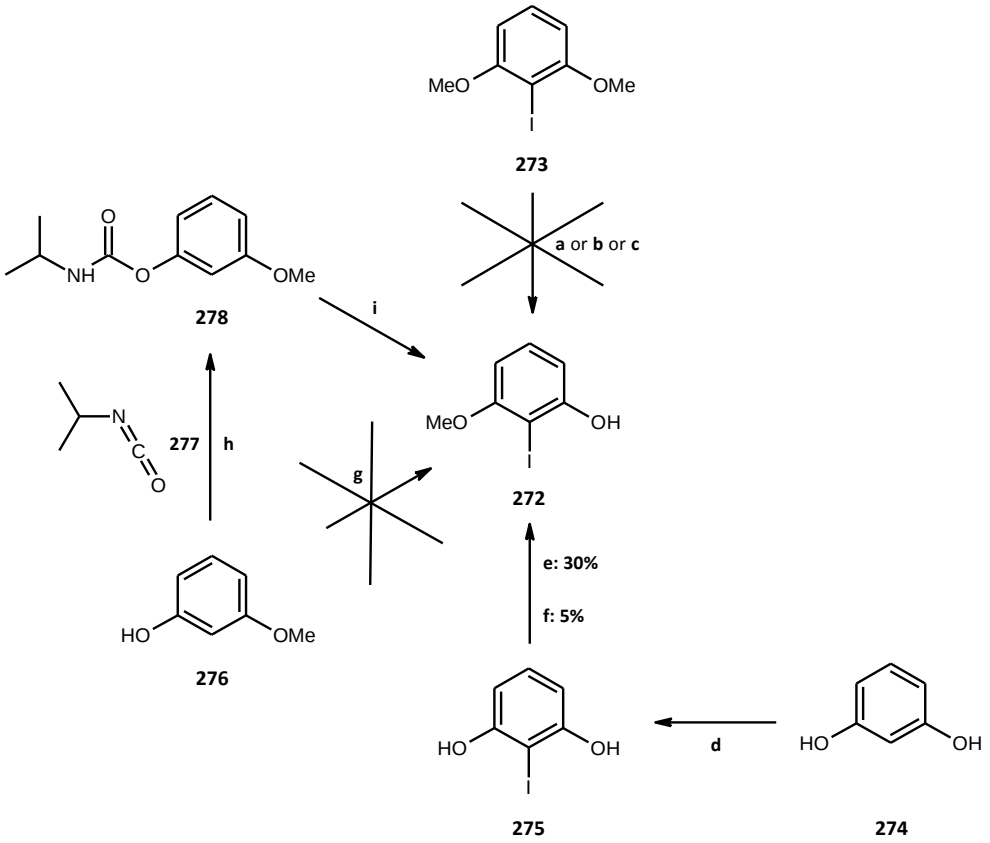

(a) $NbCl_5$ (1.1 eq), toluene, reflux, 1 h, **0%** (decomp.)

(b) BBr_3 (1.05 eq), DCM, rt, 2 h, **0%**

(c) NaH (10.0 eq), EtSH (10.0 eq), DMF, 130 °C, overnight, **0%**

(d) I_2 (1.07 eq), $NaHCO_3$ (1.10 eq), H_2O, 0 °C to rt, 10 min, **40%**

(e) DIAD (1.0 eq), PPh_3 (1.0 eq), MeOH (ex.), DCM or THF, rt, 25 to 130 min, **30%**

(f) NaH (1.1 eq), THF, 0 °C, 20 min, MeI (1.2 eq), THF, 75 °C, 48 h, **5%**

(g) *n*BuLi (2.25 eq), THF, -78 °C, TMEDA (1.0 eq), THF, 0 °C, 60 min, I_2 (1.0 eq), THF, -78 °C, 120 min and -78 °C to rt, overnight, **0%**

(h) **277** (1.1 eq), DMAP (0.1 eq), THF, 60 °C, 48 h, **95%**

(i) TMEDA (1.1 eq), TMSOTf (1.1 eq), Et_2O, rt, 30 min, TMEDA (2.0 eq), *t*BuLi (2.5 eq), Et_2O, -78 °C, 60 min, I_2 (1.0), THF, -78 °C to rt, 120 min + 30 min, NaOH aq. (4.0 eq), EtOH, 120 min, **56%**

Once the initial problems were overcame, the synthesis followed the well-known scenario. Phenol **272** was converted to the terminal alkyne (*R*)-**279** using Mitsunobu reaction. Its lithiation and a consequent treatment with TIPSCl **248** led to the protected alkyne (*R*)-**280** (Scheme 3.49).

Scheme 3.49

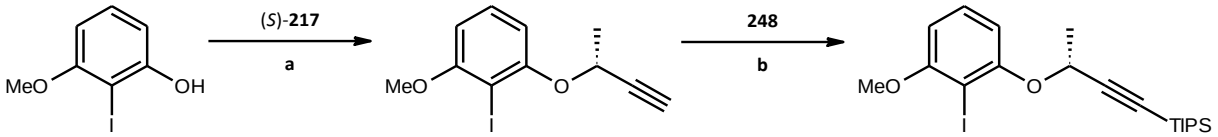

272 (*R*)-**279** (*R*)-**280**

(a) (*S*)-**217** (1.05 eq), PPh_3 (1.0 eq), DIAD (1.0 eq), C_6H_6, rt, overnight, **81%**

(b) LDA (1.0 eq), THF, -78 °C, 2 h, **248** (1.1 eq), THF, -78 °C to rt, 1.5 h, **91%**

The Pd(II) catalyzed coupling reaction gave rise to the chiral triyne (*R*,*R*)-**281** that was desilylated to (*R*,*R*)-**282** and consequently reacted with **218** to afford the suitably substituted triyne (*R*,*R*)-**283** (Scheme 3.50).

Scheme 3.50

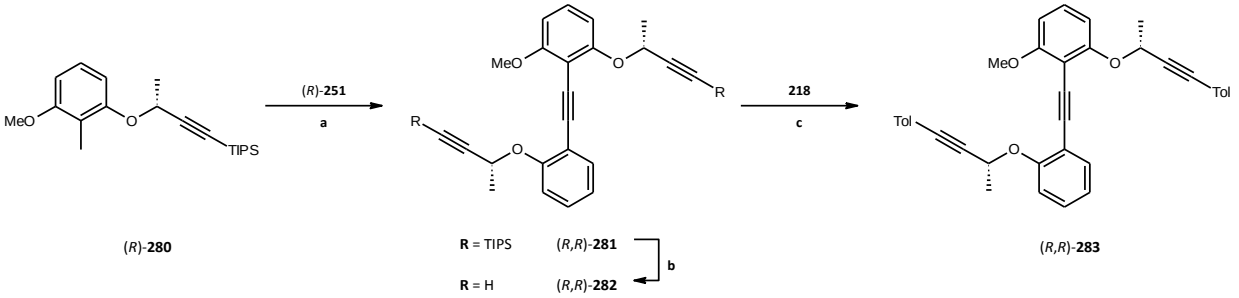

(*R*)-**280** (*R*,*R*)-**283**

(a) (*R*)-**251** (1.0 eq), $Pd(PPh_3)_4$ (5 mol%), CuI (9 mol%), *i*Pr_2NH, rt, overnight, **48%**

(b) NBu_4F (4.8), THF, rt, 2 h, **99%**

(c) **218** (2.1 eq), $Pd(PPh_3)_4$ (10 mol%), CuI (18 mol%), *i*Pr_2NH, rt, 1.5 h, **86%**

The reaction sequence was completed by the diastereoselective cyclotrimerization reaction (Scheme 3.51). (*M*,*R*,*R*)-**264** was found to be a sole diastereomer in the reaction mixture. The cyclization results are summarized in the following table (Table 3.52).

Scheme 3.51

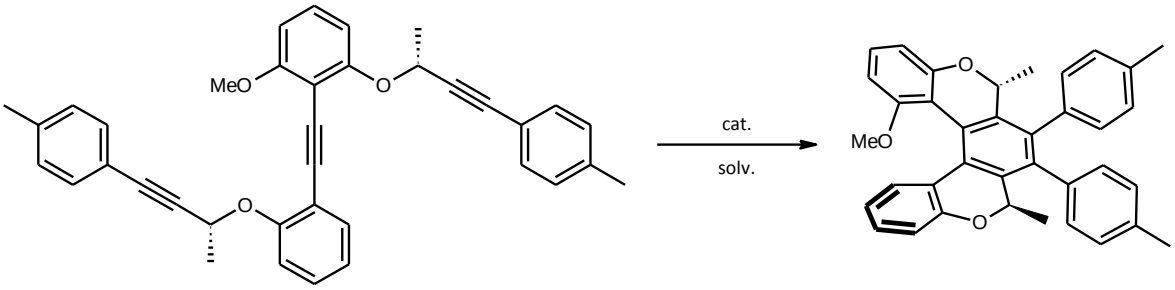

(*R*,*R*)-**283** (*M*,*R*,*R*)-**264**

Table 3.52

	cat.	%cat. [%]	solv.	temp. [°C]	time [min]	other conditions	yield[a] [%]
1	$CpCo(CO)_2$ **81**/ PPh_3	20 / 40	$C_{10}H_{22}$	140	180	hν	57
2	$Ni(cod)_2$ **254**/ PPh_3	20 / 40	THF	rt	120	-	78
3	CpCo(CO)(fum) **255**	100	THF	180	20	MW, ion. liq.[b]	96
4	CpCo(CO)(fum) **255**	20	THF	180	20	MW, ion. liq.[b]	63

[a]) isolated yield

[b]) ion. liq. = 1-butyl-2,3-dimethylimidazolium tetrafluoroborate

It is obvious that the reaction mediated by an equimolar amount of CpCo(CO)(fum) **255** proceeded with the highest yield of 96%. When a catalytic amount of a Ni(0) or Co(I) complex was used, the best candidate seemed to be $Ni(cod)_2$ **254** giving (*M*,*R*,*R*)-**264** in 78% yield. On the other hand, $CpCo(CO)_2$ **81** needed the longest reaction period along with high temperature (140 °C) and the yield was only 57%.

It was shown that the diastereoselective [2+2+2] cyclotrimerization mediated by transition metal complexes is a versatile methodology for preparation of [5]helicene analogues. The major advantages of this methodology was found to be 1) excellent diastereoselectivity (uniformly 100 : 0 *de* except one case of (*M*,*R*,*R*)-**256**); 2) high tolerance of the stereochemical outcome of cyclization to the structural diversity of the products; 3) configurational stability of 2*H*-pyran hetero[5]helicenes at higher temperature (in contrast to the parent [5]helicene that racemizes at room temperature); 4) easy computational prediction of helicity of the products; and 5) potential synthetic accessibility of both (*M*,*R*,*R*) and (*P*,*S*,*S*) stereoisomers as both enantiomers of but-3-yn-2-ol **217** (a key chiral building block) are commercially available.

3.1.2.2 [6]helicene-like compounds

In order to further extend the variability of the synthetic approach to the optically pure helicene-like compounds, the attention has been paid to the [6]helicene derivative (*M*,*R*,*R*)-**299** bearing amino group (Scheme 3.61)

Using the same synthetic strategy as discussed before, the key chiral triyne suitable for cyclization can be prepared form two basic building blocks. It was necessary to introduce the TIPS group into the chiral alcohol before it is connected with the aromatic unit. The synthesis of this substituted chiral alcohol was proposed to minimize the number of synthetic steps and necessary purifications. Starting from the commercially available (*S*)-but-3-yn-2-ol (*S*)-**217** (Scheme 3.53), the free alcohol group has to be protected first. It was found that the microwave assisted, solvent-free reaction with HMDS provides the protected alcohol (*S*)-**284** in excellent purity (as shown by GC). Such a protected alcohol can undergo the subsequent lithiation and silylation with no necessity to purify the product. The reaction with **248** followed by quenching with 3 N HCl provided the desired product (*S*)-**285** in high yield and purity (over 95%) as was proved by NMR (Scheme 3.53).

Scheme 3.53

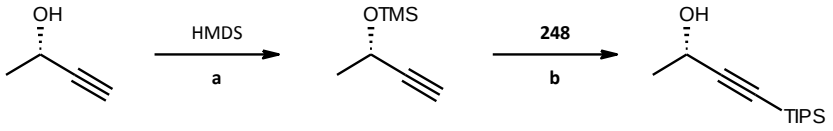

(*S*)-**217** (*S*)-**284** (*S*)-**285**

(a) HMDS (0.5 eq), MW, 15 min, **95%**

(b) *n*BuLi (1.15 eq), **248** (1.10 eq), THF, -78 °C, 60 min, rt, 45 min, HCl (3 M), rt, 60 min, **97%**

The chiral alcohol (*S*)-**285** was then used in a next step. The amino group in the commercially available 4-amino-2-iodophenol **286** (Scheme 3.54) was protected with the Boc group offering **287** (analogously to the protection of 4-aminophenol[125]) and consequently treated with (*S*)-**285** under Mitsunobu reaction conditions to provide (*R*)-**288** as a key intermediate (Scheme 3.54).

Scheme 3.54

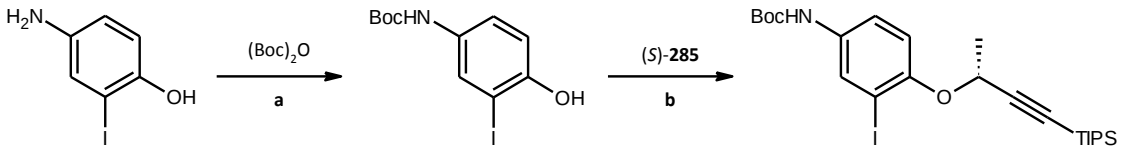

286 **287** (*R*)-**288**

(a) $(Boc)_2O$ (1.2 eq), NEt_3 (1.2 eq), DMF, °C to rt, overnight, **92%**

(b) (*S*)-**285** (1.0 eq), PPh_3 (1.0 eq), DIAD (1.0 eq), C_6H_6, rt, 48 h, **84%**

To build up the [6]helicene derivative with six rings in its helical scaffold, an extra benzene ring has to be annulated. To fulfil this requirement, a naphthalene building block instead of benzene one has to be incorporated into the skeleton. The commercially available 1-iodo-2-naphthol **289** (Scheme 3.55) can be easily converted into (*R*)-**290** using (*S*)-**285** under Mitsunobu conditions (Scheme 3.55).

Scheme 3.55

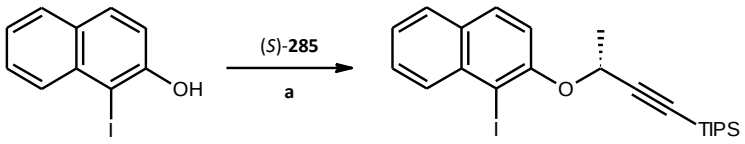

289 (*R*)-**290**

(a) (*S*)-**285** (1.1 eq), PPh_3 (1.05 eq), DIAD (1.05 eq), C_6H_6, rt, 48 h, **77%**

Then, (*R*)-**288** was turned into diyne (*R*)-**291** using the Sonogashira coupling protocol. After its deprotection to the terminal alkyne (*R*)-**292** it was reacted with (*R*)-**290** under Pd catalysis to give (*R*,*R*)-**293** that can be desilylated to (*R*,*R*)-**294**, for a further functionalization (Scheme 3.56).

Scheme 3.56

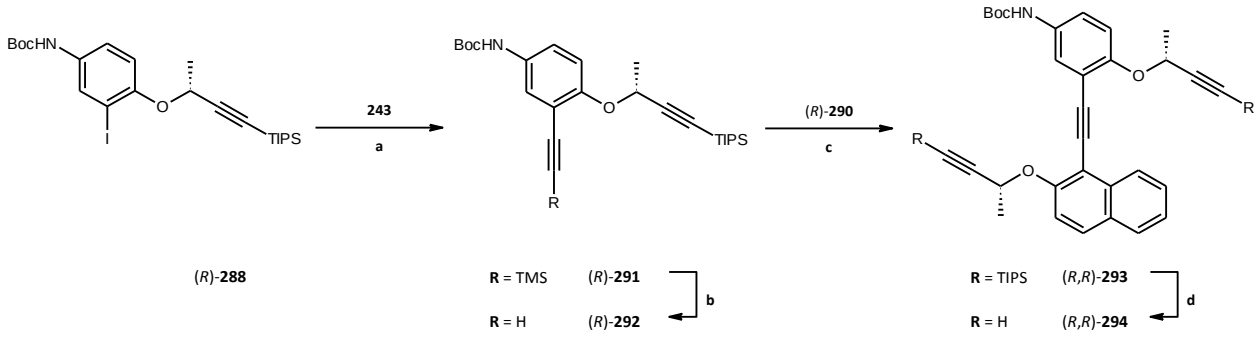

(a) **243** (2.0 eq), $Pd(PPh_3)_4$ (5 mol%), CuI (9 mol%), *i*Pr_2NH, rt, overnight, **94%**

(b) K_2CO_3 (5.0 eq), MeOH, rt, 2 h, **90%**

(c) (*R*)-**290** (1.0 eq), $Pd(PPh_3)_4$ (5 mol%), CuI (9 mol%), *i*Pr_2NH, rt, overnight, **28%**

(d) NBu_4F (2.5), THF, rt, 2 h, **68%**

Having in mind the proposed use of the compound **210** (Figure 2.4) in the field of heterogeneous catalysis, 4-(methylsulfanyl)phenyl substituents were connected to (*R*,*R*)-**294** via Sonogashira coupling. To pursue the coupling reaction smoothly, the commercially available 4-bromothioanisole **295** (Scheme 3.57) was firstly converted into 4-iodothioanisole **296** using the microwave assisted Finkelstein-type reaction (Scheme 3.57).

Scheme 3.57

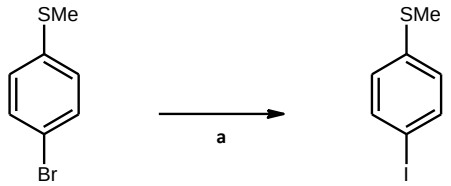

295 **296**

(a) NaI (2.0 eq), CuI (19 mol%), *trans*-N,N´-dimethyl-1,2-cyclohexandiamine (38 mol%), MW, 200 °C, 9 h, **98%**

The coupling reaction between **296** and (*R*,*R*)-**294** gave the triyne (*R*,*R*)-**297** suitable for following cyclization (Scheme 3.58).

Scheme 3.58

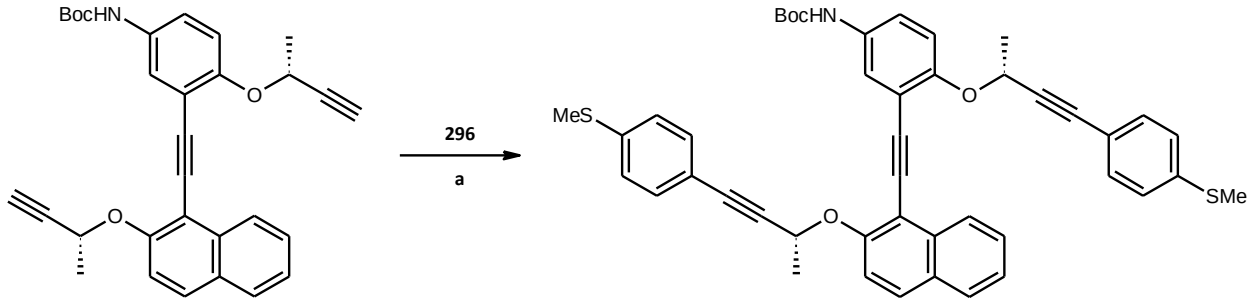

(*R*,*R*)-**294** (*R*,*R*)-**297**

(a) **296** (2.1 eq), $Pd(PPh_3)_4$ (10 mol%), CuI (18 mol%), *i*Pr_2NH, rt, overnight, **81%**

[2+2+2] cyclotrimerization (Scheme 3.59) afforded the desired product (*M*,*R*,*R*)-**298** as a sole diastereomer. The (*M*) helicity was assigned to the product analogously as it was done in the previous study. Cyclization experiments are summarized in the following table (Table 3.60).

Scheme 3.59

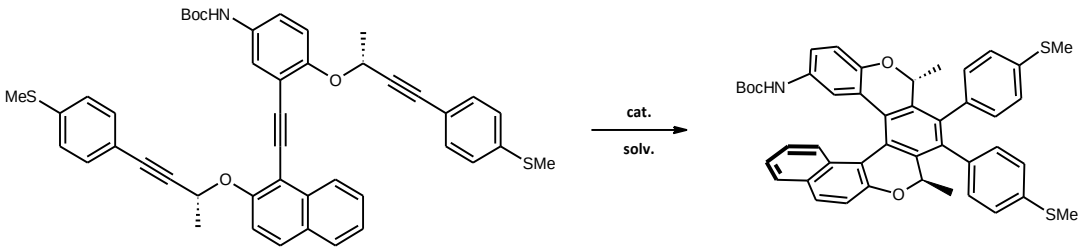

(*R*,*R*)-**297** (*M*,*R*,*R*)-**298**

Table 3.60

	cat.	%cat. [%]	solv.	temp. [°C]	time [min]	other conditions	yield[a] [%]
1	$CpCo(CO)_2$ **81**/ PPh_3	20 / 40	$C_{10}H_{22}$	140	120	hν	61
2	$Ni(cod)_2$ **254**/ PPh_3	20 / 40	THF	rt	120	-	47
3	CpCo(CO)(fum) **255**	100	THF	180	20	MW, ion. liq.[b]	14
4	CpCo(CO)(fum) **255**	20	THF	180	20	MW, ion. liq.[b]	83

[a]) isolated yield

[b]) ion. liq. = 1-butyl-2,3-dimethylimidazolium tetrafluoroborate

The reaction under Ni(0) or Co (I) catalysis delivered the cyclized product in fair to very good yields except for the cyclization mediated by an equimolar amount of CpCo(CO)(fum) **255** when a poor 14% yield was achieved.

The aminohelicene (*M*,*R*,*R*)-**299** was received after the Boc deprotection (Scheme 3.61).

Scheme 3.61

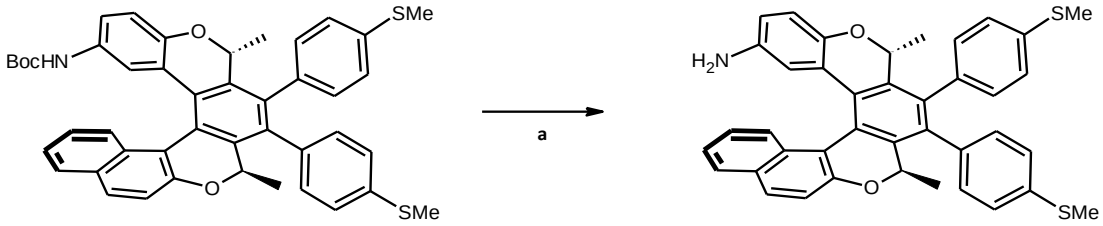

(*M*,*R*,*R*)-**298** (*M*,*R*,*R*)-**299**

(a) TFA : DCM = 1 : 4 (vol.), rt, overnight, **86%**

The product (*M*,*R*,*R*)-**299** was then turned into the urea derivative (*M*,*R*,*R*)-**210** upon treatment with 3,5-bis(trifluoromethyl)phenyl isocyanate **300** (Scheme 3.62).

Scheme 3.62

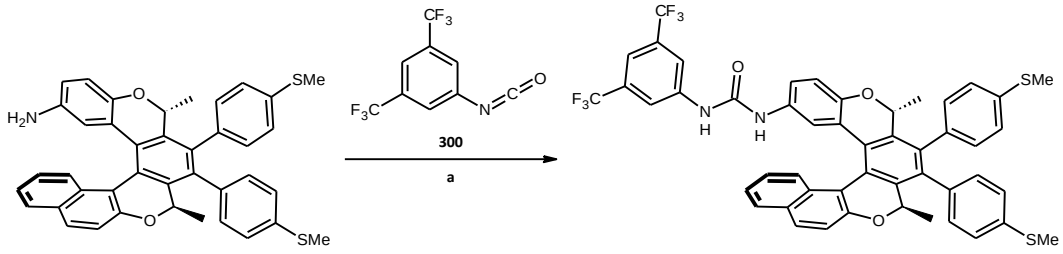

(*M*,*R*,*R*)-**299** (*M*,*R*,*R*)-**210**

(a) **300** (1.5 eq), THF, 50 °C, overnight, **57%**

The product (*M*,*R*,*R*)-**210** was obtained in a fair yield of 57%. The whole synthesis of this compound were aimed towards its use as a chiral modifier in heterogeneous hydrogenation of ethyl pyruvate (see Chapter *3.2.3.2*).

It was proved that the stereochemical outcome of diastereoselective [2+2+2] cyclotrimerization of chiral triynes is independent on a structural diversity of educts/products and can be utilized in the asymmetric synthesis of optically pure both [5]helicene-like and [6]helicene-like compounds.

3.2 The use of helicene-like compounds in asymmetric catalysis

3.2.1 The use of dihydrooxepine derivatives in asymmetric allylic amination

The ligand (*P*,*S*,*S*)-**234** (see Figure 3.12) with a cyclic phospholane moiety has been proposed to extend the family of chiral ligands represented by (*P*,*S*)-**65** that was successfully employed in asymmetric allylic amination receiving the substitution products in good yields with up to 94% *ee* (see Scheme 1.33)[33]. Although the detailed mechanism of the action of the ligand is not fully understood, it was suggested that C–H activation of its methyl group at the phospholane ring takes place to give a five-membered Ir(I) metallacycle as an intermediate in the catalytic cycle (see part *1.2.1.5*). The ligand (*P*,*S*,*S*)-**235** containing diethylphosphite moiety has been proposed to behave in a similar way. Moving to the ligand (*P*,*S*,*S*)-**236** comprising a six-membered phospholane moiety, the formation of an Ir(I) metallacycle might also be proposed, which would be in this case six-membered.

Based on the previously published results,[33] all ligands ((*P*,*S*,*S*)-**234**, (*P*,*S*,*S*)-**235**, (*P*,*S*,*S*)-**236**) were employed in asymmetric allylic substitution using the substrate **102**,[126] which was prepared from commercially available cinnamyl alcohol **301** (Scheme 3.63).

Scheme 3.63

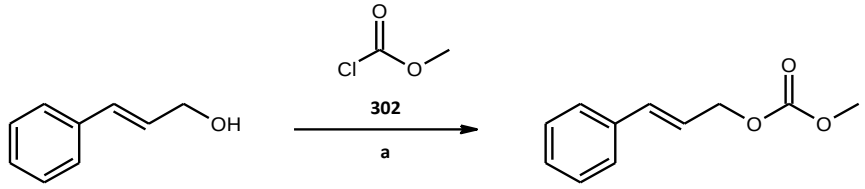

301 **102**

(a) **302** (1.1 eq), py (1.2 eq), DCM, 0 °C to rt, **59%**

Phosphite (*P*,*S*,*S*)-**234** was studied firstly, because of its structural similarity to (*P*,*S*)-**65**. Cyclic secondary amines **99** – **101** (see Figure 1.29) were employed in asymmetric allylic amination of **102**. The results are summarized below (Figure 3.64).

Figure 3.64

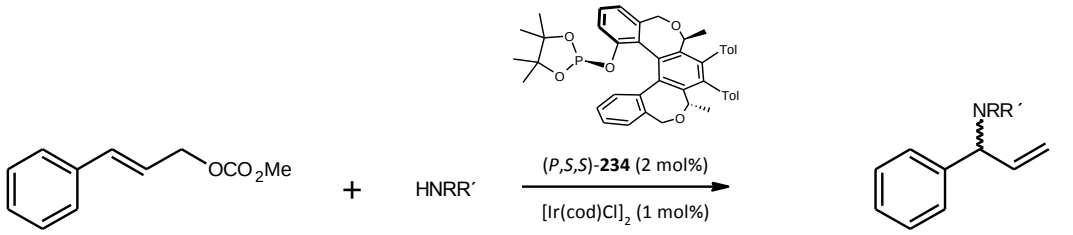

102

99: R = R´ = -$(CH_2)_4$-

100: R = R´ = -$(CH_2)_2O(CH_2)_2$-

101: R = R´ = -$(CH_2)_5$-

(+)-**105:** R = R´ = -$(CH_2)_4$-

(+)-**106:** R = R´ = -$(CH_2)_2O(CH_2)_2$-

(+)-**209:** R = R´ = -$(CH_2)_5$-

entry	amine	time [h]	temperature [°C]	solvent	yield [%][a]	*ee* [%][b]
1	**99**	16	30	DCM	23	(+)-82
2	**100**	16	30	DCM	34	(+)-81
3	**101**	16	30	DCM	60	(+)-80

[a]) isolated yield

[b]) determined by chiral HPLC using UV/polarimetric detector; (+) or (-) correspond to (+) or (-) enantiomer

In all cases the branched products (+)-**105**, (+)-**106** and (+)-**209** were formed exclusively according to ^{1}H NMR spectra as no signals of linear products were observed. The enantiomeric excess was determined by separation of enantiomerically enriched mixtures by chiral HPLC (for details see Experimental Part) employing the UV detection at 254 nm (in red) in combination with polarimetric one (in blue, Figure 3.65). The consistent *ee* values were obtained from chromatograms using either UV or polarimetric detection.

Figure 3.65

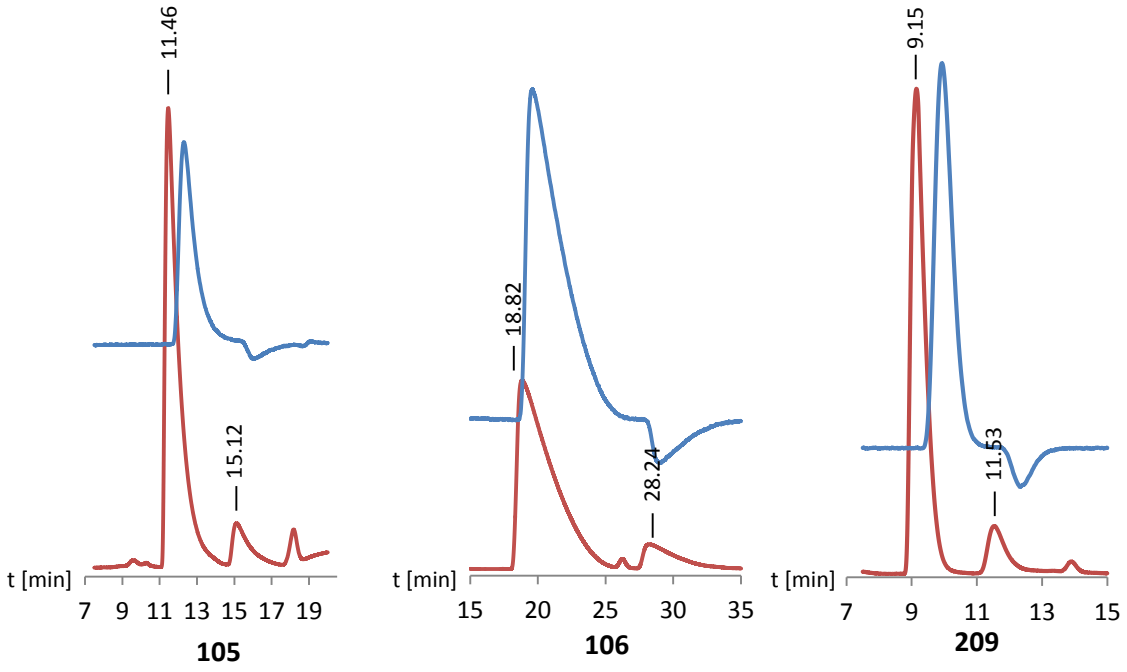

Being encouraged by the results obtained with the ligand (*P*,*S*,*S*)-**234**, the phosphites (*P*,*S*,*S*)-**235** and (*P*,*S*,*S*)-**236** were employed in the same reaction. Although we observed in both cases a dominant formation of branched products, the stereochemical outcome was different. Using the ligand (*P*,*S*,*S*)-**235** containing a diethoxyphosphanyl moiety, the laevorotatory products (-)-**105**, (-)-**106** and (-)-**209** were received with moderate *ee*'s (Figure 3.66). Such results were in contrast to the use of (*P*,*S*,*S*)-**234** possessing the same helicity but delivering dextrorotatory product with good *ee*'s. The application of the ligand (*P*,*S*,*S*)-**236** comprising a 5,5-dimethyl-1,3,2-dioxaphosphinan-2-yl unit resulted again in dextrorotatory products but the *ee* values dropped down even more significantly (Figure 3.67).

Figure 3.66

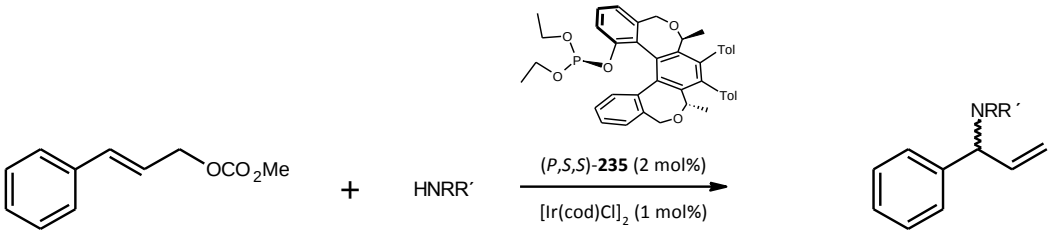

102

99: R = R´ = -$(CH_2)_4$-

100: R = R´ = -$(CH_2)_2O(CH_2)_2$-

101: R = R´ = -$(CH_2)_5$-

(-)-**105:** R = R´ = -$(CH_2)_4$-

(-)-**106:** R = R´ = -$(CH_2)_2O(CH_2)_2$-

(-)-**209:** R = R´ = -$(CH_2)_5$-

Entry	Amine	Time [h]	Temperature [°C]	Solvent	Yield [%][a]	*ee* [%][b]
1	**99**	overnight	30	DCM	62	(-)-45
2	**100**	overnight	30	DCM	61	(-)-62
3	**101**	overnight	30	DCM	60	(-)-64

[a]) isolated yield

[b]) determined by chiral HPLC using UV/polarimetric detector; (+) or (-) correspond to (+) or (-) enantiomer

Figure 3.67

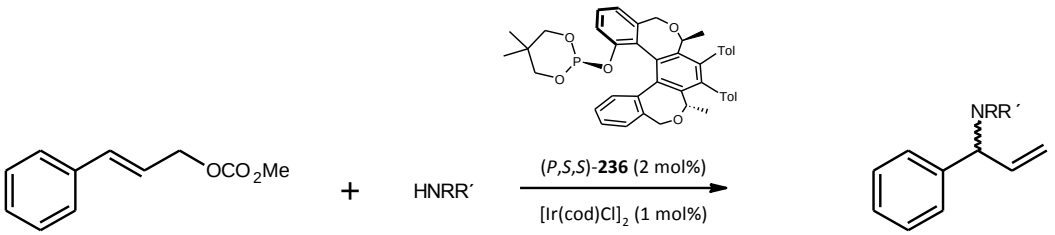

102

99: R = R´ = -$(CH_2)_4$-

100: R = R´ = -$(CH_2)_2O(CH_2)_2$-

101: R = R´ = -$(CH_2)_5$-

(+)-**105:** R = R´ = -$(CH_2)_4$-

(+)-**106:** R = R´ = -$(CH_2)_2O(CH_2)_2$-

(+)-**209:** R = R´ = -$(CH_2)_5$-

Entry	Amine	Time [h]	Temperature [°C]	solvent	Yield [%][a]	ee [%][b]
1	**99**	overnight	30	DCM	25	(+)-10
2	**100**	overnight	30	DCM	36	(+)-27
3	**101**	overnight	30	DCM	61	(+)-36

[a]) isolated yield

[b]) determined by chiral HPLC using UV/polarimetric detector; (+) or (-) correspond to (+) or (-) enantiomer

From the results achieved with the ligands (*P*,*S*,*S*)-**234**, (*P*,*S*,*S*)-**235** and (*P*,*S*,*S*)-**236** it might be inferred that ligands enabling the formation of a five-membered metallacycle through C–H activation (probably in (*P*,*S*,*S*)-**234** and (*P*,*S*,*S*)-**235**) provide higher *ee* of the substitution products (in contrast to the ligand (*P*,*S*,*S*)-**236**, which might form a six-membered metallacycle). This study demonstrated the ability of optically pure helicene-derived phosphites to control absolute stereochemistry as well as regioselectivity in asymmetric allylic amination (achieving up to 82% *ee* at exclusively formed branched products). Naturally, there is a significant room for further structural variations of a helicene backbone as well as phosphorus moiety to possibly increase both *ee*'s and stability of the respective ligands towards oxidation but such studies go beyond the horizon of this Thesis. Nevertheless, this is the second successful use of helicene-like ligands in asymmetric allylic amination (*cf*. lit.[33]) indicating the potential of helicene ligands as chiral inductors in transition metal catalyzed reactions.

3.2.2 The use of 2*H*-pyran derivatives in asymmetric organocatalysis

As described in chapter 1.2.2, helically chiral compounds have recently been put under spotlight as efficient organocatalysts in several reactions. In particular, chiral catalysts containing a DMAP moiety can successfully be employed in asymmetric acyl transfer reactions as demonstrated by Carbery *et al*[69]. In cooperation with the Justus-Liebig University in Giessen, Germany, the catalysts (*M*,*R*,*R*)-**211** was applied to kinetic resolution of racemic sulfoximines **303** – **305** using acetic anhydride as an acyl donor reagent (Figure 3.68).

Figure 3.68

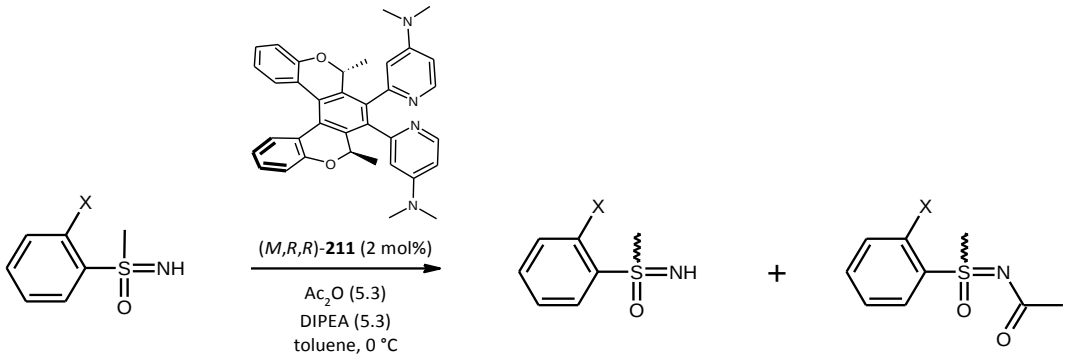

substrate	catalyst (*M*,*R*,*R*)-**211**	reaction time [h]	acylated product [% *ee*]	reactant [% *ee*]	conversion [%]	*s*-value
303	2 mol%	1	24.5	0.0	0.1	1.6
303	2 mol%	3	0.8	0.1	9.1	1.0
303	2 mol%	24	7.2	0.2	2.6	1.2
303	-	1	1.8	0.2	8.2	1.0
303	-	3	0.1	0.1	50.0	1.0
303	-	24	7.8	0.1	1.5	1.2
304	2.3 mol%	1	6.9	0.3	4.2	1.2
304	2.3 mol%	3	4.4	0.3	6.4	1.1
304	2.3 mol%	24	7.2	0.1	1.4	1.2
304	-	1	nd	nd	nd	nd
304	-	3	nd	nd	nd	nd
304	-	24	nd	nd	nd	nd
305	1.9 mol%	1	10.7	3.0	21.9	1.3
305	1.9 mol%	3	0.3	3.1	91.2	1.0
305	1.9 mol%	24	3.2	2.9	47.5	1.1
305	-	1	2.9	1.4	32.6	1.1
305	-	3	1.2	2.0	62.5	1.0
305	-	24	1.6	1.2	42.9	1.0

The conversion and selectivity (see table in Figure 3.68) were calculated according to the method of Kagan[127]. The resulting low *s*-values were in the range of only 1.0 to 1.6. Since a slow uncatalyzed background acylation reaction proceeded as well, the observed *s*-values indicated negligible asymmetric induction by (*M*,*R*,*R*)-**211**. The same organocatalyst was employed also in asymmetric kinetic resolution of racemic 1-phenylethanol **133** (see Scheme 1.36). In contrast to the results by Starý[66] and Carbery[69], no

conversion was observed. This unreactivity apparently reflected the presence of a substituent in the position 2 of the DMAP moiety, which is known to diminished reactivity the DMAP organocatalyst owing to steric reasons.

Evidently, it was shown that the organocatalyst (*M*,*R*,*R*)-**211** exhibits only a marginal catalytic activity in asymmetric acyl transfer reactions. Further representative studies on asymmetric phosphorylation and Morita-Baylis-Hillman reaction done at the Justus-Liebig University in Giessen, Germany were not available to the date of submitting this Thesis.

3.2.3 The use of helicene-like compounds in asymmetric heterogeneous catalysis

An amazing level of performance in terms of enantioselectivity was achieved by using chiral transition-metal complexes as homogeneous catalysts. On the other hand, controlling enantioselectivity is still a major problem in asymmetric heterogeneous catalysis. As mentioned in Chapter 1.3, many important homogenous catalysts are used in industry having been immobilized on solid supports. The bridge between these two approaches is now being built through the use of metal nanoparticles (NPs) whose activity is very high under mild conditions because of their very large surface area. This frontier is sometimes called "semi-heterogeneous" because the NPs are synthetized by bottom-up approach contrary to classical heterogeneous catalysts. The combination of a catalytic activity with absolute stereocontrol of the reaction led to various strategies in designing solid enantioselective catalysts. Among these approaches, the modification of a catalytic (supported) metal surface by strongly adsorbing chiral compounds, termed *modifiers*, has a significant synthetic potential[128]. From the practical catalysis point of view, the most promising solid enantioselective catalysts are metals modified by adsorbed chiral compounds that are otherwise soluble.

The concept of chiral modification has been applied primarily to the Pt group metals and Ni but there are only a few catalytic systems that afford high enantioselectivity. Commonly used modifiers are the naturally occurring cinchona alkaloids such as **309** – **312** or tartaric acid **313**. The only synthetic modifier that offers better than 90% *ee* is pantoylnaphtylethylamine (PNEA)[129] **314** (Figure 3.69).

Figure 3.69

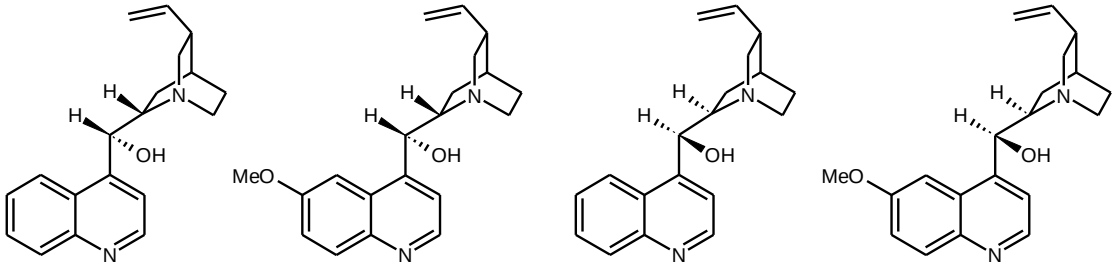

Cinchonidine (CD) **309**

Quinine (QN) **310**

Cinchonine (CN) **311**

Quinidine (QD) **312**

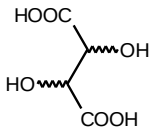

Tartaric acid (TA) **313**

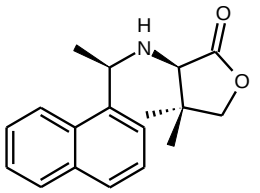

Pantoylnaphtylethylamine (PNEA) **314**

One of the most studied asymmetric reactions employing chiral heterogeneous catalysts is asymmetric hydrogenation. Platinum catalysts modified by chinona alkaloids are known to provide the best results in asymmetric hydrogenation of activated ketones such as pyruvate esters that was discovered by Orito and coworkers (Scheme 3.70).[130] Accordingly, this process has attracted significant attention and become a benchmark reaction in asymmetric heterogeneous catalysis.[131]

Scheme 3.70

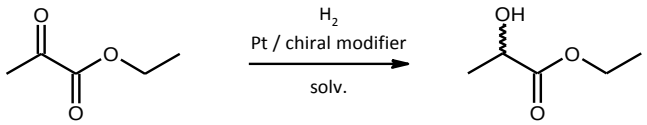

315 **316**

There are two views on the origin of enantiodifferentiation using a Pt-cinchona alkaloid catalyst system. It is proposed the formation of a 1 : 1 complex between cinchona alkaloid and a substrate molecule at the Pt surface, where the enantioselection step takes place[128a,132]. Alternatively, a “shielding effect model” is

suggested that encompasses the formation of a “substrate-chiral template” complex in the liquid phase and such a supramolecule undergoes hydrogenation over Pt sites[133].

The absence of a wider portfolio of synthetic chiral modifiers applicable to Orito's reaction prompted us to propose the helicene-like compound (*M*,*R*,*R*)-**210** reflecting the requirements of both enantiodifferentiation models. Such a chiral modifier comprising the urea moiety might complex a ketone substrate through hydrogen bonding as well as activate its carbonyl group towards reduction to comply with the “substrate-chiral template” model. In addition, the thiomethyl anchors might ensure adsorption of the helicene modifier onto the Pt surface to comply with the "chiral surface model".

As was shown by Baiker and coll.,[75] Orito’s reaction is Pt nanoparticle shape-sensitive. Accordingly, hydrogenation of ethyl pyruvate was investigated first under screening the Pt sources.

3.2.3.1 The synthesis of heterogeneous Pt catalysts

Detailed studies on metal surfaces modified by chiral molecules led to a closer insight into the interaction between the substrate, chiral modifier and metal surface[134]. Numerous factors are proposed to play an important role in stereocontrol of the reaction to significantly influence its enantioselectivity. A catalyst pretreatment (in reductive atmosphere[130b], by heating[135] or by ultrasonication[136]) or varying the size of metallic NPs might be crucial. Although there are plenty reports on size effect,[74,128e,137] the results are rather contradictory. The influence of surface morphology on the reaction rate and chemoselectivity was also reported[75,138].

Accordingly, the tetrahedral Pt NPs exposing (111) crystallographic planes were synthetized using El-Sayed protocol[139] or an improved procedure of Zaera *et al*[140]. The original El-Sayed methodology[139] is based on a growth of Pt nanocrystals controlling their shapes and sizes by concentrations of the capping polymer material and Pt(II) cations used in the reductive synthesis of colloidal particles in solution at room temperature. Zaera[140] contributed to optimizing parameters determining the shape of Pt NPs. The chemical nature of the tetrahedral (T_d) Pt NPs is presented in the next scheme (Scheme 3.71).

Scheme 3.71

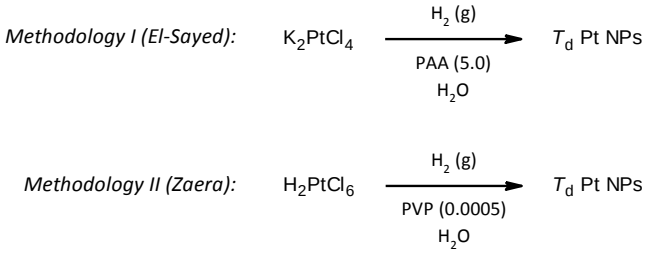

In both cases an aqueous solutions of platinum cations (Pt (II) or Pt(IV)) are reduced by gaseous hydrogen of high purity in the presence of a capping polymer (PAA_{2000} = polyacrylic acid or $PVP_{363\,000}$ = poly(*N*-vinyl-2-pyrolidone); subscripts correspond to average molecular mass) preventing aggregation. The most critical factor in controlling both the particle shape and size is a ratio between the transition metal precursor and capping agent. The use of low concentrations leads to narrower size distributions, but not necessarily to well-defined particle shapes. Generally, the lighter the capping polymer, the higher the concentration needed. Despite an effort to prepare well-defined Pt NPs, the methodology I gave inconsistent results regarding shape-defined NPs but their size distribution was satisfactory. For the TEM image of Pt NPs prepared by the methodology I, see the next picture (Figure 3.72).

Figure 3.72

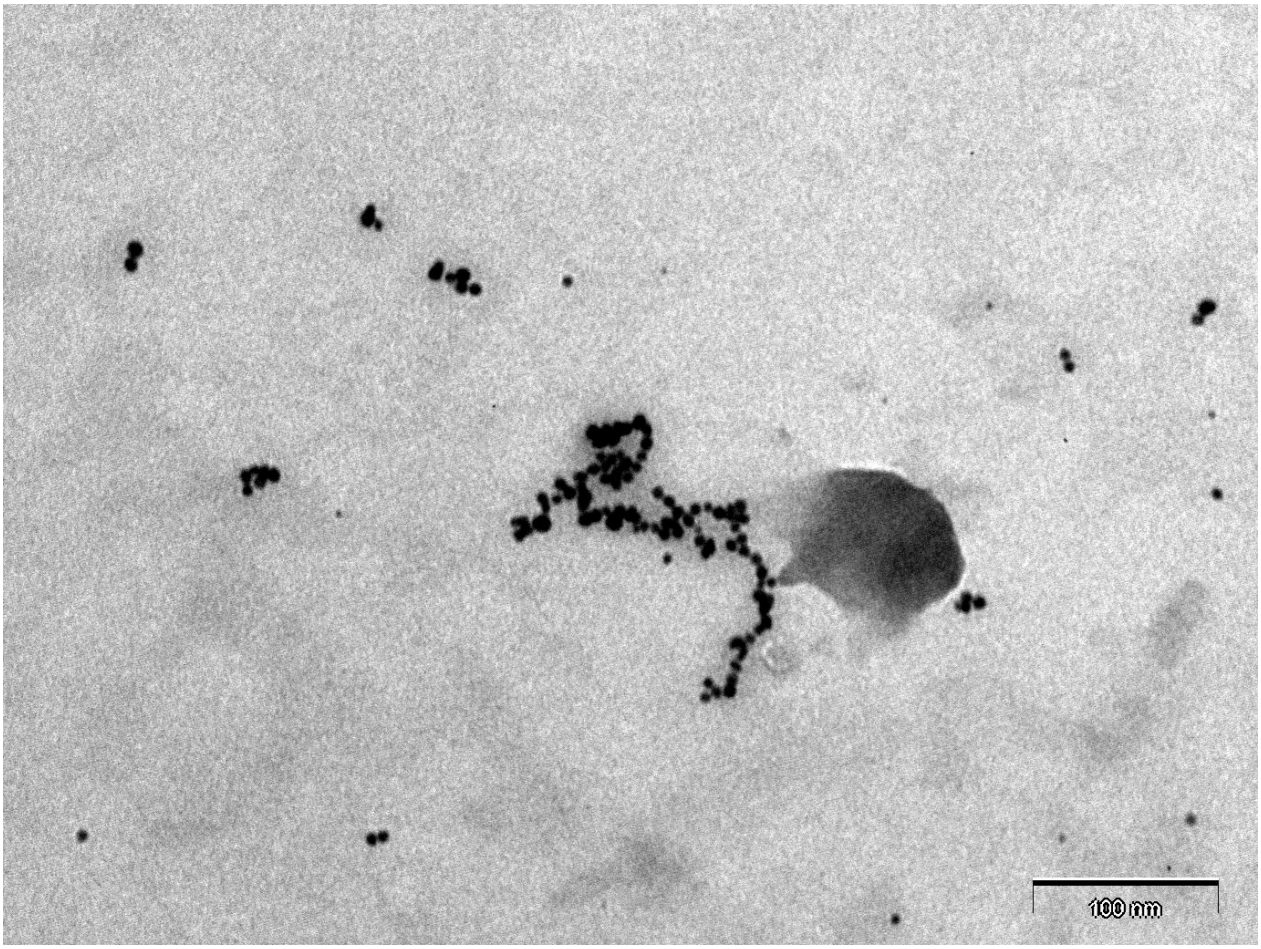

The methodology II gave more satisfactory results as far as shape-defined Pt NPs and their size distribution are concerned. Morphology of high-quality tetrahedral particles with preferential exposed (111) facets is indicated by the following TEM image (Figure 3.73).

Figure 3.73

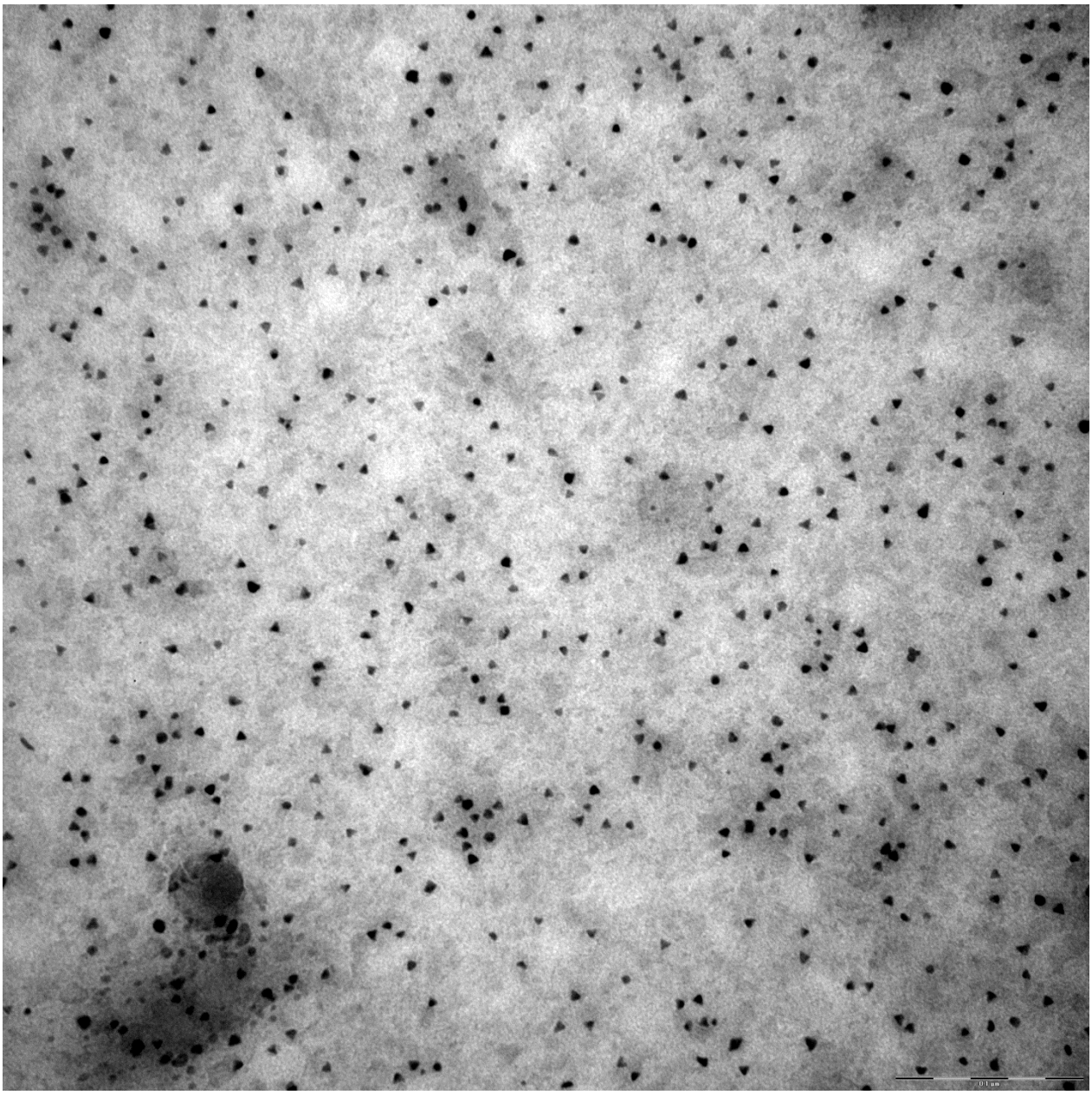

The deposition of Pt NPs on a high-surface-area support is the most critical aspect of the preparation of a heterogeneous Pt catalyst because the capping polymer has to be removed with no significant loss of the particle size and shape. The impregnation process was preferred rather than i*n-situ* approaches (*e.g.*, the formation of NPs in the presence of a support or the use on the sol-gel synthesis) for its simplicity. Evonik Aerosil 200® was chosen as a high-surface-area support according to the literature.[75] The published way of impregnation was followed. It was shown that washing the supported Pt/SiO_2 catalyst **317** (5 wt% Pt on

SiO_2) with water was insufficient regarding the removal of the capping polymer ($PVP_{360\,000}$) from its surface and, accordingly, its activation. A sequential wash with water, ethanol and diethyl ether had to be applied. It was shown that the treatment of the supported catalyst by a UV light/ozone cleaner was insufficient in removing the capping agent from the catalyst's surface. The activity of the home-made supported catalyst was compared to that one of the commercially available 5 wt% Pt/Al_2O_3 **318** (Strem, Escat^{TM} 2941) in asymmetric reduction of ethyl pyruvate **315** using cinchonidine (CD) **309** as a chiral modifier and the results are summarized in the next figure (Figure 3.74)

Figure 3.74

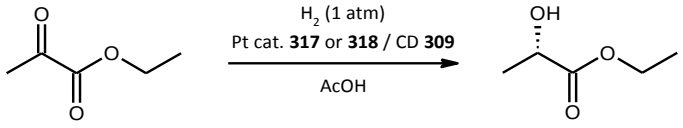

315 (*S*)-**316**

Pt cat.	$m_{Pt\ cat.}$ [mg]	m_{CD} [mg]	conversion [%][a]	ee [%][a]
317	10	0,5	84	45
318	10	0,5	100	71

[a]) determined by chiral GC after 16 h

It was found that the commercially available catalyst **318** provided better results regardless to its unknown morphology. With respect to the difficult preparation and activation of the home-made well-defined Pt catalyst (such as **317**), all other hydrogenation experiments were performed with the commercially available catalyst **318**.

3.2.3.2 The attempts at asymmetric hydrogenation of ethyl pyruvate

All hydrogenation experiments were performed with ethyl pyruvate **315** and the commercial Pt/Al_2O_3 catalyst **318**. Both the background reaction with no chiral modifier and reaction in the presence of cinchonidine (CD) **309** were carried out as reference reactions, which were juxtaposed to the reactions employing the helicene-derived chiral modifiers (*M*)-**2**, (*M*,*R*,*R*)-**210**, (*P*,*S*,*S*)-**213**, *rac*-**319**, *rac*-**320**, (*M*,*R*,*R*)-**321** and (*M*,*R*,*R*)-**322** (Figure 3.75). The results are summarized in the next table (Table 3.76).

Figure 3.75

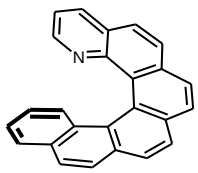

(*M*)-**2**

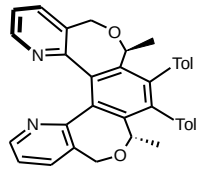

(*P*,*S*,*S*)-**213**

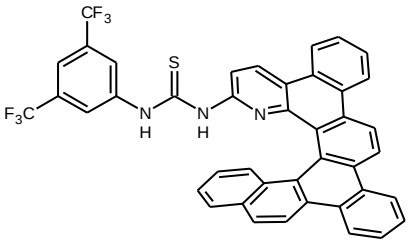

319

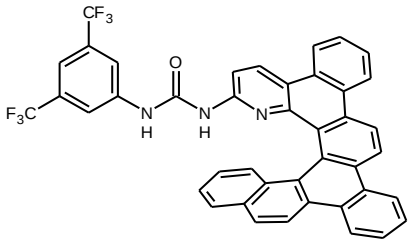

320

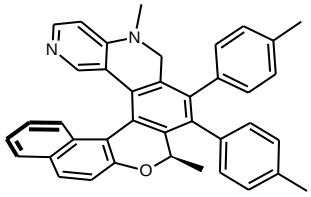

(*M*,*R*,*R*)-**321**

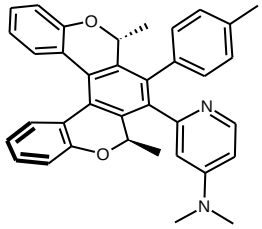

(*M*,*R*,*R*)-**322**

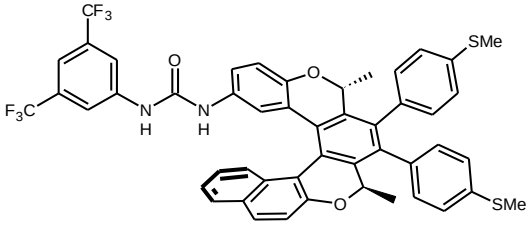

(*M*,*R*,*R*)-**210**

Table 3.76

entry	chiral modifier	conversion [%][a]	ee [%][b]
1	-	30	-
2	**309**	100[c]	71 (L)
3	(*M*)-**2**	65	0
4	(*P*,*S*,*S*)-**213**	96	0
5	(*M*,*R*,*R*)-**321**	100	4 (D)
6	(*M*,*R*,*R*)-**322**	98	2 (L)
7	*rac*-**319**	65	-
8	*rac*-**319**[d]	60[e]	-
9	(-)-**319**[d]	95[e]	0
10	*rac*-**320**	98	-
11	(*M*,*R*,*R*)-**210**	14[e]	0

[a]) conversion determined by chiral GC after 20 hours (standard $C_{11}H_{24}$)

[b]) enantiomeric excess determined by chiral GC; (L) or (D) corresponds to (L) or (D)-**316**

[c]) conversion after 16 hours

[d]) reaction performed in THF

[e]) conversion after 24 hours

Except for (*M*,*R*,*R*)-**210**, all chiral modifiers accelerated reduction of the carbonyl group of ethyl pyruvate **315** using the Pt/Al_2O_3 catalyst **318** in comparison with the background reaction in the absence of any modifier (Table 3.76, entries 1 – 11). As far as the enantiomeric excess is concerned, the highest *ee* was achieved with alkaloid cinchonidine **309** yielding (L)-**316** in 71% *ee*. However, all other examined chiral modifiers provided low or no enantiomeric excess in ethyl lactate **316**. Interestingly, the presence of the thiourea moiety in the modifier *rac*-**319** lowered conversion of the starting ethyl pyruvate **315** in acetic acid in comparison with the use of its urea analogue *rac*-**320** (Table 3.76, entries 7 and 10). In THF, *rac*-**319** promoted incomplete reduction of ethyl pyruvate **315** as well (Table 3.84, entry 8). Surprisingly, the use of enantiopure (-)-**319** in THF resulted in the complete conversion but no enantiomeric excess of the product was recorded (Table 3.76, entry 9). Unfortunately, a rational design of the chiral modifier (*M*,*R*,*R*)-**210** comprising both the activating group (3,5-bis(trifluoromethyl)phenylureido moiety) and anchoring ones (methylsulfanyl moieties, Chapter *3.2.1.2*) resulted in a poor conversion and no enantiomeric excess of ethyl lactate **316** (Table 3.76, entry 11).

.

3.3 Preparation of transition metal complexes with helical ligands and their X-ray analysis

Whit respect to the presence of nitrogen atom(s) in the pyridohelicene-like compounds (*P*,*S*,*S*)-**212**, (*P*,*S*,*S*)-**213** and (*P*,*S*,*S*)-**214** (see Figure 2.5, 3.77), coordination chemistry of such *N*-donating ligands was studied with the aim of their possible application to asymmetric catalysis. As mentioned in Chapter 1.3.2, coordination chemistry of ligands exhibiting helical chirality is so far rather unexplored. The structure of catalytically active complexes with chiral helicene-derived ligands has not been systematically studied as most *in situ* formed complexes were not subjected to a detailed structural analysis (part 1.2). Therefore, no relevant mechanistic study on the action of such ligands in chirality transfer processes is known. Ligands (*P*,*S*,*S*)-**212**, (*P*,*S*,*S*)-**213** and (*P*,*S*,*S*)-**214** were chosen as model compounds for several reasons: (i) They are optically pure, (ii) the nitrogen atom electron pair is pointing to the "bay" of the helical backbone thus maximizing the chiral environment around the possibly coordinated metal and (iii) depending on their close structure and heteroatom variations they might serve as monodentate ((*P*,*S*,*S*)-**212**) or bidentate ((*P*,*S*,*S*)-**213**, (*P*,*S*,*S*)-**214**) ligands.

The attempts at the formations of the corresponding transition metal complexes were performed on a milligram scale by simply mixing helicene-derived ligands with metal salts in an appropriate solvent at room temperature. A special attention was paid to the crystallization techniques which might lead to single crystals suitable for the X-ray diffraction analysis. The experiments are summarized below (Figure 3.77).

Figure 3.77

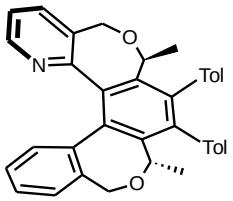

(*P*,*S*,*S*)-**212**

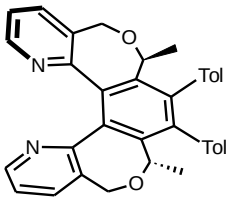

(*P*,*S*,*S*)-**213**

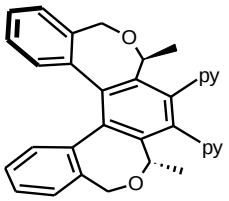

(*P*,*S*,*S*)-**214**

	helicene	metal precursor	solvent/ conditions	single crystal
1	(*P*,*S*,*S*)-**213**	$AgPF_6$ (0.6 eq)	THF/rt	No
2	(*P*,*S*,*S*)-**213**	AgOTf (0.6 eq)	THF/rt	**Yes**[a]
3	(*P*,*S*,*S*)-**213**	$AgSbF_6$ (0.6 eq)	THF/rt	No
4	(*P*,*S*,*S*)-**213**	$PdCl_2(PPh_3)_2$ (0.37 eq)	DCM/rt	**Yes**[b]
5	(*P*,*S*,*S*)-**213**	$PdCl_2$(dppe) (0.37 eq)	DCM/rt	**Yes**[b]
6	(*P*,*S*,*S*)-**212**	$[Pd(allyl)Cl]_2$ (0.48 eq)	$CHCl_3$/rt	No
7	(*P*,*S*,*S*)-**213**	CuI (0.5 eq)	THF/rt	No
8	(*P*,*S*,*S*)-**213**	$[Cu(MeCN)_2(PPh_3)_2]BF_4$ (0.5 eq)	$CHCl_3$/rt	No
9	(*P*,*S*,*S*)-**212**	$[IrCl(cod)]_2$ (1/6 eq)	DCM/MW, 120°C, 20 min	No
10	(*P*,*S*,*S*)-**212**	AgOTf (0.6 eq)	THF/rt	No
11	(*P*,*S*,*S*)-**212**	AgOAc (0.6 eq)	THF/rt	**Yes**[b]
12	(*P*,*S*,*S*)-**212**	$IrCl(cod)(PCy_3)$ (1/6 eq) NH_4PF_6 (1/2 eq)	MeOH:DCM:EtOAc (4:1:1)/rt	No
13	(*P*,*S*,*S*)-**212**	$[IrCl(cod)]_2$ (1/20 eq)	EtOH/65 °C, 20 min	No
14	(*P*,*S*,*S*)-**214**	$Pd(dba)_2$ (0.5 eq)	DCM	No
15	(*P*,*S*,*S*)- **214**	$Ni(OAc)_4.4H_2O$ (0.5 eq)	DCM	No
16	(*P*,*S*,*S*)-**214**	$Ni(dppe)Cl_2$ (1.0 eq)	DCM	**Yes**[c]
17	(*P*,*S*,*S*)-**214**	$Ni(PPh_3)_2I_2$ (1.0 eq)	DCM	No
18	(*P*,*S*,*S*)-**214**	$Pd(dppe)Cl_2$ (1.0 eq)	DCM	**Yes**[c]
19	(*P*,*S*,*S*)-**214**	$[Ir(cod)Cl]_2$ (0.5 eq)	DCM	No
20	(*P*,*S*,*S*)-**214**	Cu(acac) (0.5 eq)	DCM	**Yes**[c]
21	(*P*,*S*,*S*)-**214**	$CoCl_2.6\ H_2O$ (1.0 eq)	DCM	No
22	(*P*,*S*,*S*)-**214**	$NiCl_2.6\ H_2O$ (1.0 eq)	DCM	No
23	(*P*,*S*,*S*)-**214**	$PdCl_2$ (1.0 eq)	DCM	No
24	(*P*,*S*,*S*)-**214**	$Na_2[PdCl_4]$ (1.0 eq)	DCM	No
25	(*P*,*S*,*S*)-**214**	$Pd(PhCN)_2Cl_2$ (1.0 eq)	DCM	No
26	(*P*,*S*,*S*)-**214**	$[Cu(MeCN)_2(PPh_3)_2]BF_4$ (1.0 eq)	DCM	No
27	(*P*,*S*,*S*)-**214**	$CpRu(PPh_3)_2Cl$ (0.5 eq) NH_4PF_6 (ex.)	MeOH/MW, 160 °C 30 min	No

[a]) an unsolved structure (incomplete charge compensation)

[b]) a single crystal of helicene (free ligand)

[c]) a single crystal of metal precursor

Single crystal metal complexes derived from (*P*,*S*,*S*)-**214** were not formed as starting transition metal salts crystalized preferably from the solutions (entries 16, 18, 20, Figure 3.77). Free ligand single crystals[141] were obtained for both (*P*,*S*,*S*)-**212** (entry 11, Figure 3.77) and (*P*,*S*,*S*)-**213** (entries 4, 5, Figure 3.77). The ligand (*P*,*S*,*S*)-**213** provided a metal complex with silver(I) triflate whose Ag(I) : (*P*,*S*,*S*)-**213** stoichiometry was 2 : 1 (Figure 3.78). However, its structure could not be fully resolved owing to an incomplete charge compensation.

Figure 3.78

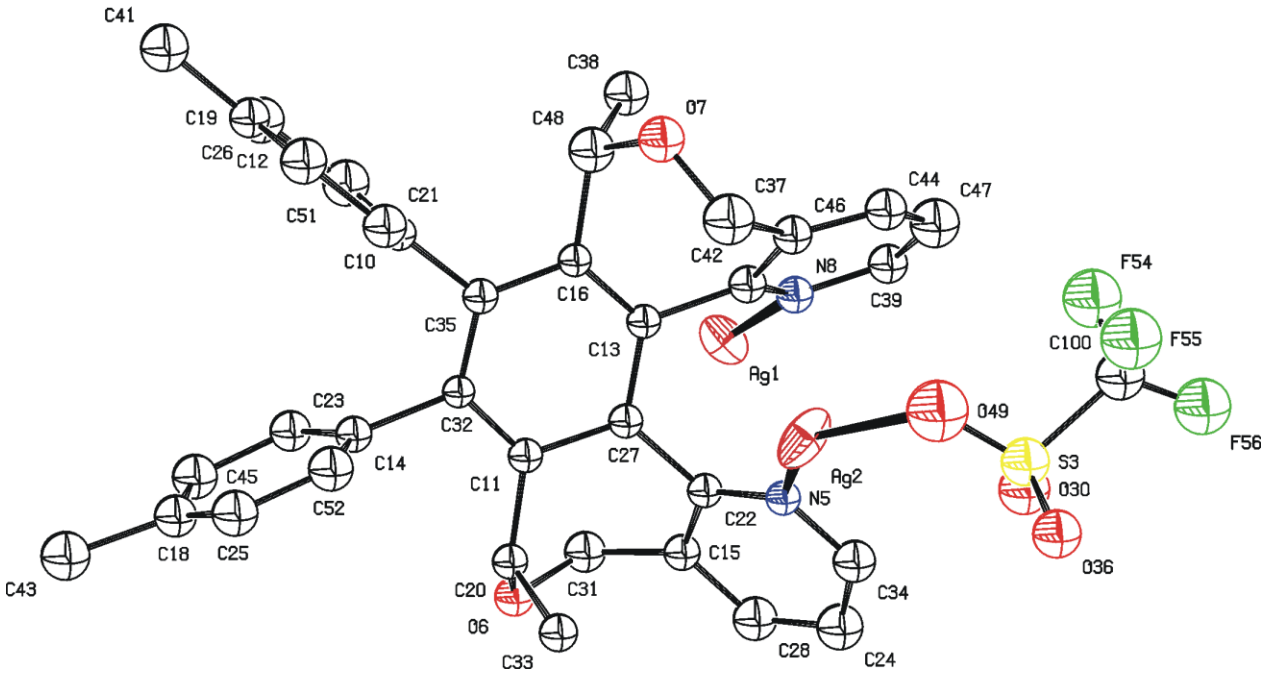

A half occupancy of the silver atom led to the higher *R* value. The structure demonstrates that the *N*-donating pyridohelicene ligand (*P*,*S*,*S*)-**213** is able to form complexes with Ag(I) similarly to **2** (see Figure 1.47)[67].

4. Conclusions

The attention has been paid to the development of asymmetric synthesis of functionalized helicene-like compounds in an optically pure form, their characterization and use in enantioselectice catalysis as chiral ligands, organocatalysts or chiral modifiers. The main achievements are as follows:

(1) I have contributed to the development of a general method for the preparation of optically pure [5]- and [6]heterohelicenes by asymmetric synthesis that has not been available before. It is based on diastereoselective [2+2+2] cycloisomerization of centrally chiral triynes in the presence of Co(I), Ni(0) or Rh(I) complexes, which play a key role in the formation of helical scaffolds comprising two 2*H*-pyran or 2,7-dihydrooxepine rings. The major advantages of this methodology are that (i) excellent diastereoselectivity is guaranteed (*d.r*. uniformly 100:0); (ii) the stereochemical outcome of the cyclization is highly tolerant to the structural diversity of the products; (iii) the synthesized 2*H*-pyran or 2,7-dihydrooxepine hetero[5]helicenes exist as single helices even at higher temperature (in contrast to the parent [5]helicene that racemizes at room temperature); (iv) the helicity of the products can be easily predicted computationally; and (v) helicene-like compounds having both (*M*) and (*P*) helicity are accessible as both enantiomers of but-3-yn-2-ol (a key chiral building block) are commercially available.

(2) Based both on experimental and computational approaches, I have shown that stereochemical outcome of the highly diastereoselective [2+2+2] cycloisomerization of centrally chiral triynes mediated/catalyzed by transition metal complexes is controlled by 1,3-allylic-type strain, which plays a key role under the thermodynamic control when the asymmetric transformation of the first order takes place.

(3) I have successfully applied the aforementioned principles of asymmetric synthesis of optically pure 2*H*-pyran or 2,7-dihydrooxepine helicene-like compounds to the preparation of their functionalized derivatives comprising the hydroxy, phosphite, pyridine, urea or sulfanyl moieties.

(4) In collaboration with other experts, I have contributed to the structural and physicochemical characterization of selected compounds including absolute stereochemistry determination (by ECD correlation), barrier to epimerization (computationally or by dynamic NMR), basicity (by capillary electrophoreses) or single-crystal structure (by X-ray analysis).

(5) I have explored optically pure 2,7-dihydrooxepine [5]helicene-like phosphite ligands, which I have prepared, in enantioselective allylic amination under catalysis by iridium(I) complexes to reach up to 82% *ee*. This is the second successful use of helicene-like ligands in asymmetric allylic amination indicating the

potential of helicene-based ligands as chiral inducers in enantioselective transition metal catalyzed reactions.

(6) I have synthesized optically pure 2*H*-pyran [5]helicene-like DMAP analogue, which has been studied as an organocatalysts in kinetic resolution of racemic sulfoximines in cooperation with the Justus-Liebig University in Giessen, Germany to find only a low reactivity of this helical DMAP derivative as well as low enantioselectivity of the acyl transfer reaction.

(7) I have searched for new chiral modifiers applicable to asymmetric heterogeneous catalysis. The screened pyrido, ureido and DMAP derivatives of helicenes and helicene-like compounds accelerated the benchmark reduction of ethyl pyruvate to ethyl lactate in the presence of the commercially available Pt/Al_2O_3 catalyst but no (or negligible) enantioselectivity of the carbonyl group reduction has been observed.

To conclude, the results have demonstrated that the diastereoselective synthesis of helically chiral compounds based on [2+2+2] cyclotrimerization of aromatic triynes under transition metal catalysis is a general, flexible and practical method, which provides an easy access to chiral ligands, organocatalysts or modifiers in a nonracemic form. We believe that the first promising results in the area of enantioselective catalysis employing helicene-like compounds as chiral inductors will stimulate the further endeavor to understand the role of helicity in catalysis and coordination chemistry.

5. Experimental part

General

The ^{1}H NMR spectra were measured at 400.13 MHz, 499.88 MHz, and 600.13 MHz, the ^{13}C NMR spectra at 100.61 MHz, 125.71 MHz, and 150.90 MHz in $CDCl_3$, acetone-d_6 or DMSO-d_6 as indicated in 5 mm PFG probe with indirect detection. For standardization of ^{1}H NMR spectra the internal signal of TMS (δ 0.0, $CDCl_3$) or residual signal of solvent (δ 7.26, chloroform-*d*) was used. In the case of ^{13}C spectra the residual signals of solvents (δ 77.0 for $CDCl_3$) were used. The chemical shifts are given in δ-scale, the coupling constants *J* are given in Hz. The HMBC experiments were set up for $J_{C\text{-}H}$ = 5 Hz. For the correct assignment of both the ^{1}H and ^{13}C NMR spectra of key compounds, COSY, HSQC, and HMBC experiments were performed. The IR spectra were measured in $CHCl_3$. The EI mass spectra were determined at an ionizing voltage of 70 eV, the *m*/*z* values are given along with their relative intensities (%). The standard 70 eV spectra were recorded in the positive ion mode. The sample was dissolved in chloroform, loaded into a quartz cup of the direct probe and inserted into the ion source. The source temperature was 220 °C. For exact mass measurement, the spectra were internally calibrated using perfluorotri-*n*-butylamine (Heptacosa). The ESI mass spectra were recorded using ZQ micromass mass spectrometer (Waters) equipped with an ESCi multi-mode ion source and controlled by MassLynx software. Methanol was used as solvent. Accurate mass measurements were obtained by the EI or ESI MS. Optical rotations were measured in CH_2Cl_2 or $CHCl_3$ using an Autopol IV (Rudolph Research Analytical) instrument. The CD spectra were acquired on a J-815 CD spectrometer (Jasco Analytical Instruments, Inc.) in acetonitrile using a 10 mm quartz sample cell. The *ee* values were determined by integration of UV traces (254 nm) of HPLC chromatograms or FID GC chromatograms. The HPLC analyses were performed on CHIRALCEL® OJ-H column (250 x 4.6 mm, 5 µm) or CHIRALCEL® OD-H column (250 x 4.6 mm, 5 µm) using *n*-heptane or *n*-heptane – 2-propanol as mobile phase at a flow rate of 0.5 or 0.6 mL/min. Peaks corresponding to (+)- and (-)-compounds were assigned by comparison of the UV trace with a trace from a downstream polarimetric detector. The GC analyses were performed on CP-Chirasil-Dex CB (L: 25 m x I.D.: 0.250 mm x T.P.: 0.25 µm; Agilent) capillary column or HP-CHIRAL-20B (L: 30 m x I.D.: 0.250 mm x T.P.: 0.25 µm; J&W –Scientific) capillary column using $C_{11}H_{24}$ as an internal standard. Peaks corresponding to (L)- and (D)-ethyl lactate were assigned by comparison with commercially available standard of (L)-ethyl lactate (Sigma-Aldrich). TEM analyses were performed on JEOL JEM-1200EX at 60 kV. Single-crystal X-ray diffraction data were obtained from Nonius KappaCCD diffractometer by monochromatized MoK_α radiation (λ = 0.71073 Å) at 150(2)K. The structures were solved by direct methods (SIR92)[142] and refined by full-matrix least squares based on F^2 (SHELXL97)[143]. The hydrogen atoms were found on difference Fourier map and recalculated

into idealized position and fixed into their positions (riding model) with assigned temperature factors either H_{iso} (H) = 1.2 U_{eq} (pivot atom) or H_{iso} (H) = 1.5 U_{eq} (pivot atom) for methyl moiety. Melting points were determined on a Kofler apparatus and are uncorrected. The high pressure experiments were performed in a high pressure multi-sample catalyst screening vessels CAT7 (HEL Inc.). An ozone cleaner ProCleaner™ model UV.PC.220 (Bioforce Nanosciences) and pH-meter CyberScan 6000 (Eutech Instruments) equipped with a glass electrode Hamilton POLILYTE PRO 120 were used in preparation of heterogeneous catalysts.

Reactions were performed under inert atmosphere (using standard Schlenk technique or glove box, MBraun). The commercially available HPLC grade methanol, ethanol, catalysts, and reagent grade materials were used as received. The anhydrous decane was degassed by three freeze-pump-thaw cycles before use; the dichloromethane, diisopropylamine, and *N*,*N*-diisopropyl-ethylamine were distilled from calcium hydride under argon; the THF, benzene, and toluene were freshly distilled from sodium/benzophenone under nitrogen; the DMF was dried over molecular sleves. TLC was performed on Silica gel 60 F_{254}-coated aluminium sheets (Merck) and spots were detected by the solution of $Ce(SO_4)_2.4\ H_2O$ (1%) and $H_3P(Mo_3O_{10})_4$ (2%) in sulfuric acid (10%). Preparative thin-layer chromatography was performed on activated glass plates 20 x 20 cm with (Silica gel 60 PF_{254} containing gypsum (Merck)) using UV detection. The flash chromatography was performed on Silica gel 60 (0.040-0.063 mm, Fluka) or on Biotage® KP-C18-HS SNAP or Biotage KP-Sil® Silica cartridges (0.040-0.063 mm) using the Sp1 or Isolera One HPFC system (Biotage, Inc.). Biotage Initiator EXP EU (300 W power) was used for reactions carried out in microwave oven. All other chemicals were used as received from the commercial sources.

{[2-(Bromomethyl)-6-methoxyphenyl]ethynyl}[tris(1-methylethyl)]silane (74)

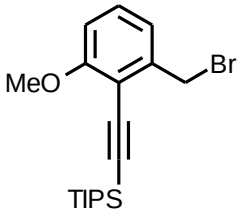

A Schlenk flask was charged with CBr_4 (6.4450 g, 19.43 mmol, 2.4 eq) under argon. Benzylic alcohol **222** (2.5788 g, 8.10 mmol) was added in acetonitrile (15 mL). Triphenylphosphine (5.0970 g, 19.43 mmol, 2.4 eq) was added in hot acetonitrile (40 mL) under argon and the volume of the solvent was refilled into 100 mL. The reaction was stirred for 3 h at room temperature. The solvent was removed at reduced pressure and the residue was purified by flash chromatography on silica gel (hexane – diethyl ether 95 : 5) to give **77** (2.7005 g, 88%) as a yellow oil.

^{1}H NMR was in agreement with the published data.[36]

^{1}H NMR (400 MHz, $CDCl_3$): 1.24 (s, 21 H), 3.86 (s, 3 H), 4.72 (s, 2 H), 6.79 (d, *J* = 8.3, 1H), 7.03 (dd, *J* = 7.7, 0.9, 1H), 7.23 (d, *J* = 8.0, 1H).

(-)-(*S*)-4-(4-Methylphenyl)but-3-yn-2-ol (75)

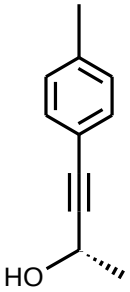

A Schlenk flask was charged with 4-iodotoluene **218** (1.3162 g, 6.04 mmol, 1.0 eq), triphenylphosphine (23.8 mg, 0.093 mmol, 1.5 mol%), copper iodide (17.7 mg, 0.093 mmol, 1.5 mol%), and bis(triphenylphosphine)palladium dichloride (12.2 mg, 0.017 mmol, 0.3 mol%). The content was dissolved in toluene (15 mL) under argon and cooled down to 0 °C. (*S*)-**217** (0.47 mL, 423.1 mg, 6.04 mmol) and diisopropylamine (0.85 mL, 610.8 mg, 6.04 mmol, 1.0 eq) were slowly added. Reaction mixture was allowed to warm up to room temperature and stirred overnight. The solvent was removed at reduced pressure and the residue was purified by flash chromatography on silica gel (hexane – acetone 80 : 20) to give **75** (931.5 mg, 96%) as a yellow solid.

^{1}H NMR was in agreement with the published data.[38]

^{1}H NMR (400 MHz, $CDCl_3$): 1.55 (d, *J* = 6.6, 3H), 2.34 (s, 3H), 4.75 (q, *J* = 6.6, 1H), 7.10 (m, 2H), 7.32 (m, 2H).

(-)-{[2-Methoxy-6-({[(1*S*)-1-methyl-3-(4-methylphenyl)prop-2-yn-1-yl]oxy}methyl)phenyl]ethynyl}[tris(1-methylethyl)]silane (76)

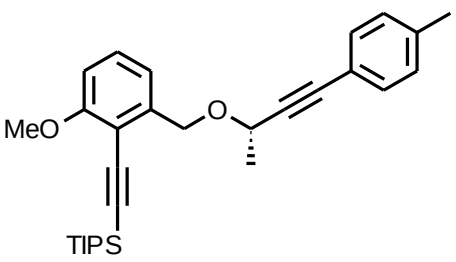

A Schlenk flask was charged with 30% potassium hydride suspension in mineral oil (1.9237 g, 14.39 mmol, 4.3 eq). Hexane (10 mL) was added and the mixture was stirred at room temperature for 2 min, the liquid was removed via syringe and the hydride was dried several min *in vacuo*. THF (20 mL) was added and the stirred suspension was cooled down to 0 °C. A solution of (*S*)-**75** (649.0 mg, 4.05 mmol, 1.2 eq) in THF (20 mL) was added dropwise. The reaction mixture was stirred at 0 °C for 1 h and solution of **74** (1.2835 g, 3.37 mmol) was added. The reaction was allowed to warm up to room temperature and stirred for 2 h. The solvent was removed at reduced pressure and the crude product was extracted with diethyl ether (4 x 50 mL) and washed with an aqueous solution of NH_4Cl. The combined organic fractions were dried over anhydrous magnesium sulfate. The solvent was removed in vacuo and the residue was purified by flash chromatography on silica gel (gradient elution hexane – diethyl ether 100 : 0 to 90 : 10) to provide (*S*)-**76** (1.3585 g, 88%) as an oil.

^{1}H NMR was in agreement with the published data.[36]

^{1}H NMR (500 MHz, $CDCl_3$): 1.07-1.16 (m, 21H), 1.58 (d, *J* = 6.6, 3H), 2.34 (s, 3H), 3.85 (s, 3H), 4.51 (q, *J* = 6.6, 1H), 4.82 (d, *J* = 13.3, 1H), 4.91 (d, *J* = 13.3, 1H), 6.78 (dd, *J* = 8.2, 0.9, 1H), 7.10 (m, 2H), 7.14 (dq, *J* = 7.9, 0.9, 0.9, 0.9, 1H), 7.27 (t, *J* = 8.1, 1H), 7.31 (m, 2H).

(-)-2-Ethynyl-1-methoxy-3-({[(1*S*)-1-methyl-3-(4-methylphenyl)-prop-2-yn-1-yl]oxy}methyl)benzene (77)

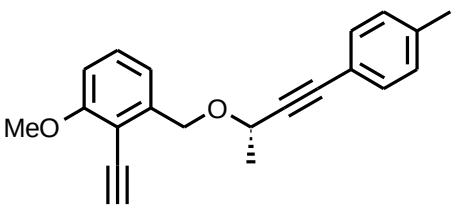

A Schlenk flask was charged with (*S*)-**76** (1.3103 g, 2.84 mmol) and the content was dissolved in THF (12 mL) under argon. A solution of tetrabutylammonium fluoride (7.5 mL, 0.914 M, 6.85 mmol, 2.4 eq) in THF was added. The reaction mixture was stirred for 1 h at room temperature. The solvent was removed *in vacuo* and the residue was purified by flash chromatography on silica gel (gradient elution hexane – diethyl ether 100 : 0 to 90 : 10) to provide (*S*)-**77** (813.8 mg, 94%) as amorphous yellowish solid.

^{1}H NMR was in agreement with the published data.[36]

^{1}H NMR (500 MHz, $CDCl_3$): 1.57 (d, *J* = 6.6, 3H), 2.34 (s, 3H), 3.53 (s, 1H), 3.90 (s, 3H), 4.50 (q, *J* = 6.6, 1H), 4.79 (d, *J* = 12.8, 1H), 4.97 (d, *J* = 12.8, 1H), 6.83 (dd, *J* = 8.3, 1.0, 1H), 7.11 (m, 2H), 7.16 (dq, *J* = 7.8, 0.9, 0.9, 0.9, 1H), 7.32 (t, *J* = 8.0, 1H), 7.33 (m, 2H).

Methyl (2*E*)-3-phenylprop-2-en-1-yl carbonate (102)

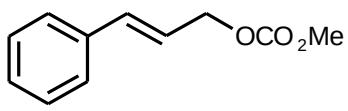

A round bottom flask was charged with cinnamyl alcohol **302** (4.9334 g, 36.77 mmol), 4-(dimethylamino)pyridine (24.7 mg, 0.202 mmol, 0.5 mol%), and pyridine (14.8 mL, 14.54 g, 138.8 mmol, 5.0 eq). The content was dissolved in DCM (45 mL) and methylchloroformate (14.2 mL, 17.37 g, 183.8 mmol, 5.0 eq) was slowly added at 0 °C. The reaction mixture was stirred at 0 °C for 30 min, allowed to warm up to room temperature and stirred for additional 5 h at the same temperature. The reaction was washed by hydrochloric acid (2 M, 3 x 30 mL) and the combined aqueous layers were extracted with DCM (3 x 30 mL). The combined organic layers were dried over anhydrous sodium sulfate and the solvents were removed in vacuo. The residue was purified by flash chromatography on silica gel (gradient elution hexane – diethyl ether 100 : 0 to 90 : 10) to provide **102** (6.7231 g, 95%) as a colorless to yellowish oil.

^{1}H NMR was in agreement with the published data.[144]

^{1}H NMR (400 MHz, $CDCl_3$): 3.81 (s, 3H), 4.79 (dd, *J* = 6.5, 1.3, 2H), 6.29 (dt, *J* = 15.9, 6.4, 6.4, 1H), 6.69 (d, *J* = 15.9, 1H), 7.22 – 7.31 (m, 1H), 7.30 – 7.35 (m, 2H), 7.37 – 7.41 (m, 2H).

General procedure for iridium catalyzed allylic amination

$[Ir(cod)Cl]_2$ **91** (1 mol%) and phosphite ligand ((*P*,*S*,*S*)-**234**, (*P*,*S*,*S*)-**235** or (*P*,*S*,*S*)-**236**) (2 mol%) were dissolved in dry DCM (0.5 mL) under argon and stirred at 30 °C for 30 min. The freshly distilled amine (**99**, **100** or **101**) (1.6 eq) and carbonate **102** (1.0 eq) were added via syringe and the reaction was stirred at 30 °C overnight. The solvent was removed and the ratio of regioisomers (branched to linear) was determined by ^{1}H-NMR of the crude reaction mixture (branched products were formed exclusively in all cases). The crude reaction mixture was purified by column chromatography on silica gel or filtration through a short column of alumina to give the desired product (**105**, **106** or **209**).

1-(1-Phenylprop-2-en-1-yl)pyrrolidine (105)

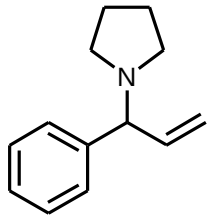

Procedure using ligand 234 (Table 3.65, entry 1)

The General procedure for allylic aminations was followed with $[Ir(cod)Cl]_2$ **91** (1.9 mg, 2.8 µmol, 1 mol%), ligand (*P*,*S*,*S*)-**234** (3.7 mg, 5.4 µmol, 2 mol%), cinnamyl methyl carbonate **102** (56.2 mg, 0.292 mmol), and pyrrolidine **99** (35.5 µl, 30.2 mg, 0.429 mmol, 1.6 eq). Chromatography on silica gel (hexane – ethyl acetate – triethylamine 90 : 10 : 10) gave the title compound **105** (12.4 mg, 23%) as a colourless oil. HPLC analysis indicated that the enantiomeric excess of the product was (+)-82% *ee*. [Diacel Chiralcel® OJ-H (0.46 cm x 25 cm, 5 µm); heptane/2-propanol = 100/0; flow rate = 0.6 mL min^{-1}; detection wavelength = 254 nm; TR = 11.5 (+), 15.1 (–) min].

^{1}H NMR was in agreement with the published data.[145]

^{1}H NMR (400 MHz, $CDCl_3$): 1.74-1.82 (m, 4H), 2.53-2.44 (m, 2H), 2.48-2.56 (m, 2H), 3.61 (d, *J* = 8.6, 1H), 5.02 (dd, *J* = 10.0, 1.7, 1H), 5.23 (ddd, *J* = 17.0, 1.7, 0.8, 1H), 6.06 (ddd, *J* = 17.0, 10.1, 8.6, 1H), 7.21-7.27 (m, 1H), 7.30-7.35 (m, 2H), 7.36-7.40 (m, 2H).

Procedure using ligand 235 (Table 3.71, entry 1)

The General procedure for allylic aminations was followed with $[Ir(cod)Cl]_2$ **91** (1.4 mg, 2.1 µmol, 1 mol%), ligand (*P*,*S*,*S*)-**235** (2.8 mg, 4.2 µmol, 2 mol%), cinnamyl methyl carbonate **102** (40.1 mg, 0.209 mmol), and pyrrolidine **99** (27.4 µl, 23.7 mg, 0.333 mmol, 1.6 eq). Chromatography on silica gel (hexane – ethyl acetate – triethylamine 95 : 5 : 10) gave the title compound **105** (24.1 mg, 62%) as a colourless oil. HPLC analysis indicated that the enantiomeric excess of the product was (–)-45% *ee*. [Diacel Chiralcel® OJ-H (0.46 cm x 25 cm, 5 µm); heptane/2-propanol = 100/0; flow rate = 0.6 mL min^{-1}; detection wavelength = 254 nm; TR = 12.4 (+), 14.7 (–) min].

Procedure using ligand 236 (Table 3.73, entry 1)

The General procedure for allylic aminations was followed with $[Ir(cod)Cl]_2$ **91** (1.7 mg, 2.5 µmol, 1 mol%), ligand (*P*,*S*,*S*)-**236** (3.4 mg, 5.1 µmol, 2 mol%), cinnamyl methyl carbonate **102** (48.6 mg, 0.253 mmol), and

pyrrolidine **99** (33.2 µl, 28.8 mg, 0.405 mmol, 1.6 eq). Chromatography on silica gel (hexane – ethyl acetate – triethylamine 95 : 5 : 10) gave the title compound **105** (11.8 mg, 25%) as a colourless oil. HPLC analysis indicated that the enantiomeric excess of the product was (+)-10% *ee*. [Diacel Chiralcel® OJ-H (0.46 cm x 25 cm, 5 µm); heptane/2-propanol = 100/0; flow rate = 0.6 mL min^{-1}; detection wavelength = 254 nm; TR = 12.2 (+), 14.7 (–) min].

4-(1-Phenylprop-2-en-1-yl)morpholine (106)

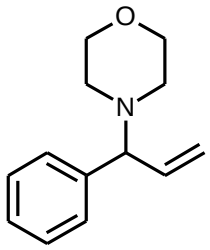

Procedure using ligand 234 (Table 3.65, entry 2)

The General procedure for allylic aminations was followed with $[Ir(cod)Cl]_2$ **91** (3.6 mg, 5.1 µmol, 1 mol%), ligand (*P*,*S*,*S*)-**234** (7.0 mg, 10.3 µmol, 2 mol%), cinnamyl methyl carbonate **102** (98.7 mg, 0.513 mmol), and morpholine **100** (71 µl, 71.6 mg, 0.822 mmol, 1.6 eq). Chromatography on silica gel (hexane – ethyl acetate – diethyl ether – triethylamine 80 : 10 : 10 : 3) gave the title compound **106** (35.3 mg, 34%) as a colourless oil. HPLC analysis indicated that the enantiomeric excess of the product was (+)-81% *ee*. [Diacel Chiralcel® OJ-H (0.46 cm x 25 cm, 5 µm); heptane/2-propanol = 99.8/0.2; flow rate = 0.7 mL min^{-1}; detection wavelength = 254 nm; TR = 18.6 (+), 28.1 (–) min].

^{1}H NMR was in agreement with the published data.[145]

^{1}H NMR (400 MHz, $CDCl_3$): 2.29-2.37 (m, 2H), 2.43-2.55 (m, 2H), 3.62 (d, *J* = 8.8, 1H), 3.69 (ddd, *J* = 5.2, 3.7, 1.1, 4H), 5.10 (dd, *J* = 10.1, 1.6, 1H), 5.23 (ddd, *J* = 17.1, 1.7, 0.7, 1H), 5.91 (ddd, *J* = 17.1, 10.1, 8.8, 1H), 7.19-7.28 (m, 1H), 7.29-7.37 (m, 4H).

Procedure using ligand 235 (Table 3.71, entry 2)

The General procedure for allylic aminations was followed with $[Ir(cod)Cl]_2$ **91** (1.3 mg, 1.9 µmol, 1 mol%), ligand (*P*,*S*,*S*)-**235** (2.6 mg, 3.9 µmol, 2 mol%), cinnamyl methyl carbonate **102** (37.2 mg, 0.194 mmol), and morpholine **100** (26.8 µl, 27.0 mg, 0.310 mmol, 1.6 eq). Chromatography on silica gel (hexane – ethyl acetate – triethylamine 95 : 5 : 10) gave the title compound **106** (24.1 mg, 62%) as a colourless oil. HPLC

analysis indicated that the enantiomeric excess of the product was (–)-62% *ee*. [Diacel Chiralcel® OJ-H (0.46 cm x 25 cm, 5 µm); heptane/2-propanol = 100/0; flow rate = 0.6 mL min^{-1}; detection wavelength = 254 nm; TR = 33.8 (+), 44.3 (–) min].

Procedure using ligand 236 (Table 3.73, entry 2)

The general procedure for allylic aminations was followed with $[Ir(cod)Cl]_2$ **91** (1.9 mg, 2.8 µmol, 1 mol%), ligand (*P*,*S*,*S*)-**236** (3.8 mg, 5.6 µmol, 2 mol%), cinnamyl methyl carbonate **102** (52.2 mg, 0.272 mmol), and morpholine **100** (39 µl, 39.4 mg, 0.452 mmol, 1.6 eq). Filtration through a short column of alumina (DCM) gave the title compound **106** (19.9 mg, 36%) as a colourless oil. HPLC analysis indicated that the enantiomeric excess of the product was (+)-27% *ee*. [Diacel Chiralcel® OJ-H (0.46 cm x 25 cm, 5 µm); heptane/2-propanol = 99.5/0.5; flow rate = 0.6 mL min^{-1}; detection wavelength = 254 nm; TR = 10.0 (+), 12.1 (–) min].

(-)-(*P*,3*R*,6*S*)-3,6-Dimethyl-4,5-bis(4-methylphenyl)-1,3,6,8-tetrahydrodibenzo[*e*,*e'*]benzo[1,2-*c*:4,3-*c'*]bisoxepin-12-ol (208)

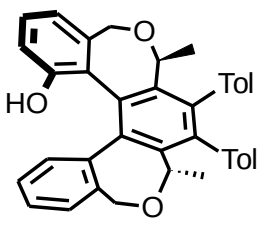

A Schlenk flask was charged with a 60% suspension of sodium hydride in mineral oil (65.5 mg, 1.64 mmol, 20 eq) under argon. The suspension was washed by hexane (2 mL) which was decanted off and the hydride was dried *in vacuo* for several min. It was suspended in DMF (2 mL). Ethylthiol (121 µl, 101.8 mg, 1.64 mmol, 20 eq) and a solution of (*P*,*S*,*S*)-**233** (45.3 mg, 0.082 mmol) in DMF (3 mL) were added dropwise at 0°C. The reaction mixture was stirred overnight at 130 °C. The reaction mixture was poured into water (20 mL) forming a white precipitate (which dissolved after acidifying to pH ~ 1 by 5% HCl) after cooling down to room temperature. The product was extracted with DCM (3 x 50 mL), the organic fractions were collected, and washed with water (3 x 50 mL) and dried over anhydrous sodium sulfate. The solvents were removed in vacuo and the residue was purified by flash chromatography on silica gel (gradient elution of hexane – diethyl ether 100 : 0 to 60 : 40) to provide (*P*,*S*,*S*)-**209** (38.8 mg, 88%) as a white to yellow to pale brown solid.

Optical rotation: $[\alpha]^{22}_D$ -71° (c 0.08, CH_2Cl_2).

Mp: 234-236 °C (hexane).

^{1}H NMR (500 MHz, $CDCl_3$): 0.61 (d, *J* = 7.1, 3H), 0.70 (d, *J* = 7.1, 3H), 2.24 (s, 6H), 4.56 (d, *J* = 11.6, 1H), 4.58 (d, *J* = 11.6, 1H), 4.66 (bs, 1H), 4.75 (d, *J* = 11.6, 1H), 4.80 (d, *J* = 11.6, 1H), 4.91 (q, *J* = 7.1, 1H), 4.93 (q, *J* =

7.1, 1H), 6.54 (dd, *J* = 8.1, 1.2, 1H), 6.69 (dd, *J* = 7.7, 1.3, 1H), 6.73 (m, 2H), 6.88 (m, 2H), 6.98 (dt, *J* = 7.6, 7.6, 1.4, 1H), 7.01 (m, 4H), 7.02 (dd, *J* = 7.3, 1.2, 1H), 7.18 (dd, *J* = 8.1, 7.3, 1H), 7.23 (dt, *J* = 7.5, 7.5, 1.3, 1H), 7.39 (dd, *J* = 7.5, 1.4, 1H).

^{13}C NMR (125 MHz, $CDCl_3$): 21.14 (q), 21.67 (q), 22.20 (2 x q), 67.40 (t), 67.51 (t), 72.44 (d), 72.67 (d), 116.01 (d), 121.02 (d), 126.66 (s), 127.10 (d), 128.07 (d), 128.14 (d), 128.19 (d), 128.32 (d), 128.43 (d), 128.71 (d), 129.29 (d), 129.46 (d), 129.64 (d), 129.70 (d), 129.75 (d), 130.22 (d), 131.72 (s), 135.76 (2 x s), 136.73 (s), 136.83 (s), 137.16 (s), 137.23 (s), 137.43 (s), 138.40 (s), 138.59 (s), 139.47 (s), 142.68 (s), 142.78 (s), 151.90 (s).

IR ($CHCl_3$): 3591 w, 3561 w, 3176 v, br, 1612 w, 1588 w, sh, 1583 w, 1515 m, 1487 w, 1460 m, sh, 1443 w, sh, 1404 w, 1371 m, 1293 m, 1280 m, sh, 1262 s, 1239 m, 1182 m, 1163 w, 1111 s, 1076 vs, 1046 m, 1022 s, 951 w, 818 m, 697 w, 563 w cm^{-1}.

EI MS: 538 ($M^{+\bullet}$, 40), 523 (25), 477 (30), 417 (11), 385 (5), 343 (5), 149 (14), 97 (21), 91 (40), 69 (39), 55 (58), 43 (100).

HR EI MS: calculated for $C_{38}H_{34}O_3$ 538.25080; found 538.2500.

1-(1-Phenylprop-2-en-1-yl)piperidine (209)

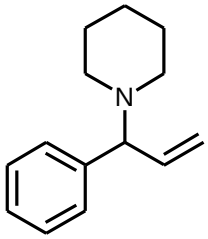

Procedure using ligand* 234 *(Table 3.65, entry 3)

The General procedure for allylic aminations was followed with $[Ir(cod)Cl]_2$ **91** (3.5 mg, 5.1 µmol, 1 mol%), ligand (*P*,*S*,*S*)-**234** (6.9 mg, 10.1 µmol, 2 mol%), cinnamyl methyl carbonate **102** (97.0 mg, 0.505 mmol), and piperidine **101** (80 µl, 69.0 mg, 0.810 mmol, 1.6 eq). Chromatography on silica gel (hexane – ethyl acetate – triethylamine 95 : 5 : 10) gave the title compound **209** (61.0 mg, 60%) as a colourless oil. HPLC analysis indicated that the enantiomeric excess of the product was (+)-80% *ee*. [Diacel Chiralcel® OJ-H (0.46 cm x 25 cm, 5 µm); heptane/2-propanol = 100/0; flow rate = 0.6 mL min^{-1}; detection wavelength = 254 nm; TR = 9.2 (+), 11.6 (–) min].

^{1}H NMR was in agreement with the published data.[146]

^{1}H NMR (400 MHz, $CDCl_3$): 1.38-1.50 (m, 2H), 1.51-1.66 (m, 4H), 2.31 (dt, *J* = 11.1, 5.4, 2H), 2.40-2.52 (m, 2H), 3.67 (d, *J* = 8.7, 1H), 5.10 (dd, *J* = 10.1, 1.7, 1H), 5.20 (ddd, *J* = 17.1, 1.8, 0.9, 1H), 5.99 (ddd, *J* = 17.1, 10.1, 8.7, 1H), 7.19-7.28 (m, 1H), 7.29-7.38 (m, 4H).

Procedure using ligand* 235 *(Table 3.71, entry 3)

The General procedure for allylic aminations was followed with $[Ir(cod)Cl]_2$ **91** (1.9 mg, 2.8 µmol, 1 mol%), ligand (*P*,*S*,*S*)-**235** (3.7 mg, 5.6 µmol, 2 mol%), cinnamyl methyl carbonate **102** (54.4 mg, 0.283 mmol), and piperidine **101** (44.7 µl, 38.5 mg, 0.452 mmol, 1.6 eq). Chromatography on silica gel (hexane – ethyl acetate – triethylamine 95 : 5 : 10) gave the title compound **209** (34.3 mg, 60%) as a colourless oil. HPLC analysis indicated that the enantiomeric excess of the product was (–)-64% *ee*. [Diacel Chiralcel® OJ-H (0.46 cm x 25 cm, 5 µm); heptane/2-propanol = 100/0; flow rate = 0.6 mL min^{-1}; detection wavelength = 254 nm; TR = 9.9 (+), 12.2 (–) min].

Procedure using ligand* 236 *(Table 3.73, entry 3)

The General procedure for allylic aminations was followed with $[Ir(cod)Cl]_2$ **91** (1.5 mg, 2.2 µmol, 1 mol%), ligand (*P*,*S*,*S*)-**236** (2.9 mg, 4.3 µmol, 2 mol%), cinnamyl methyl carbonate **102** (42.9 mg, 0.223 mmol), and piperidine **101** (35.2 µl, 30.3 mg, 0.356 mmol, 1.6 eq). Filtration through a short column of alumina (acetone) gave the title compound **209** (27.5 mg, 61%) as a colourless oil. HPLC analysis indicated that the enantiomeric excess of the product was (–)-64% *ee*. [Diacel Chiralcel® OJ-H (0.46 cm x 25 cm, 5 µm); heptane/2-propanol = 100/0; flow rate = 0.6 mL min^{-1}; detection wavelength = 254 nm; TR = 9.9 (+), 12.4 (–) min].

(-)-1-[3,5-Bis(trifluoromethyl)phenyl]-3-{(*M*,2*R*,5*R*)-2,5-dimethyl-3,4-bis[4-(methylsulfanyl)phenyl]-2,5-dihydrobenzo[*f*]benzo[1,2-*c*:4,3-*c'*]dichromen-14-yl}urea (210)

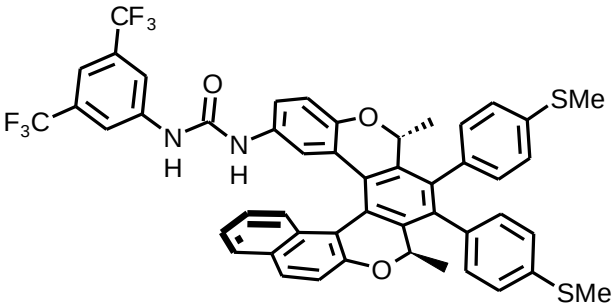

Amine (*M*,*R*,*R*)-**299** (15.3 mg, 0.025 mmol) was dissolved in THF (2 mL) under argon. 3,5-Bis(trifluoromethyl)phenyl isothiocyanate **300** (3.6 µL, 9.4 mg, 0.037 mmol, 1.5 eq) was added and the reaction mixture was stirred at 50 °C overnight. The solvent was removed in vacuo and the residue was purified by preparative TLC (petrol ether – ethyl acetate 80 : 10) to give (*M*,*R*,*R*)-**210** (12.4 mg, 57%) as a yellow amorphous solid.

Optical rotation: $[\alpha]^{22}_{D}$ -270° (c 0.20, $CHCl_3$).

^{1}H NMR (500 MHz, $CDCl_3$): 0.92 (d, *J* = 6.7, 3H), 1.03 (d, *J* = 6.6, 3H), 2.46 (s, 3H), 2.47 (s, 3H), 5.34 (q, *J* = 6.7, 1H), 5.39 (q, *J* = 6.6, 1H), 6.20 (bs, 1H), 6.51 (d, *J* = 2.5, 1H), 6.72 – 6.81 (m, 3H), 6.89 (dd, *J* = 8.5, 2.6, 1H), 6.94 – 7.02 (m, 3H), 7.10 (d, *J* = 8.4, 1H), 7.16 (d, *J* = 4.7, 1H), 7.18 – 7.24 (m, 4H), 7.29 (d, *J* = 8.8, 1H), 7.53 (d, *J* = 8.7, 1H), 7.53 (d, *J* = 8.4 Hz, 1H), 7.72 (bs, 2H), 7.79 (bs, 1H).

^{13}C NMR (126 MHz, $CDCl_3$): 15.36 (q), 15.37 (q), 17.68 (q), 18.88 (q), 73.33 (d), 73.56 (d), 117.28 (s), 119.78 (d), 120.64 (d), 120.75 (d), 123.03 (2x q, J_{CF} = 272.9), 123.19 (d), 124.38 (s), 124.96 (s), 125.16 (d), 125.30 (d), 125.59 (d), 1225.39 (d), 125.76 (d), 125.85 (d), 126.06 (d), 126.50 (2x d), 126.56 (s), 126.65 (d), 128.06 (s), 128.27 (d), 128.67 (s), 129.38 (d), 129.51 (d), 129.89 (s), 130.75 (d), 130.88 (d), 131.30 (d), 131.71 (2x s J_{CF} = 33.6), 133.86 (2x s), 136.20 (s), 137.30 (s), 137.41 (2x s), 138.48 (s), 139.97 (s), 140.49 (s), 152.97 (s), 153.41 (s), 180.36 (s).

^{19}F NMR (470 MHz): -62.82.

IR ($CHCl_3$): 3399 w, 3350 w, 3075 vw, 3059 vw, 2986 w, 2927 w, 1619 vw, 1601 w, 1592 w, 1519 w, br, 1511 w, 1500 w, 1488 w, 1473 w, 1435 w, 1398 vw, sh, 1383 m, 1370 w, 1321 vw, 1279 vs, 1246 w, 1239 w, 1182 m, 1142 m, 1107 vw, 1095 w, 1073 w, 1061 vw, 1032 vw, 1015 w, 905 vw, 891 vw, 867 vw, 846 w, 820 w, 682 w, 428 vw cm^{-1}.

ESI MS: 917 ($[M+K]^+$), 901 ($[M+Na]^+$), 896 ($[M+NH_4]^+$).

HR APCI MS: calculated for $C_{49}H_{37}F_6N_2O_3S_2$ 879.2144 found 879.2146.

(-)-2,2'-[(*M*,2*R*,5*R*)-2,5-Dimethyl-2,5-dihydrobenzo[1,2-*c*:4,3-*c'*]dichromene-3,4-diyl]bis(*N*,*N*-dimethylpyridin-4-amine) (211)

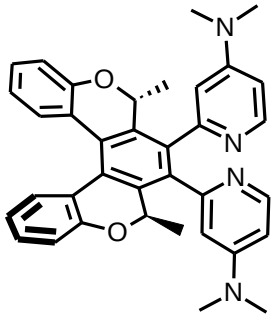

Procedure using CpCo(CO)(fum) (1.0 eq) and microwave irradiation at 180 °C in a small scale (Table 3.40, entry 1)

A microwave vial was charged with triyne (*R*,*R*)-**262** (49.5 mg, 0.089 mmol) and CpCo(CO)(fum) **255** (26.5 mg, 0.089 mmol, 1.0 eq) under argon. THF (4 mL) and 1-butyl-2,3-dimethylimidazolium tetrafluoroborate

(20 µL) were added. The reaction mixture was heated to 180 °C for 20 min. Then the solvent was removed *in vacuo* and the residue was purified by flash chromatography on silica gel (DCM – acetone – ethanol 70 : 30 : 10) to give (*M*,*R*,*R*)-**211** (30.3 mg, 61%) as a yellow amorphous solid.

Procedure using CpCo(CO)(fum) (20 mol%) and microwave irradiation at 180 °C in a small scale (Table 3.40, entry 2)

A microwave vial was charged with triyne (*R*,*R*)-**262** (20.5 mg, 0.037 mmol) and CpCo(CO)(fum) **255** (2.2 mg, 0.007 mmol, 20 mol%) under argon. THF (2 mL) and 1-butyl-2,3-dimethylimidazolium tetrafluoroborate (10 µL) were added. The reaction mixture was heated to 180 °C for 20 min. Then the solvent was removed *in vacuo* and the residue was purified by flash chromatography on silica gel (DCM – acetone – ethanol 70 : 30 : 10) to give (*M*,*R*,*R*)-**211** (10.4 mg, 51%) as a yellow amorphous solid.

Procedure using $Ni(cod)_2$/PPh_3 (20 mol%/40 mol%) at rt in a small scale (Table 3.40, entry 3)

A microwave vial was charged with triyne (*R*,*R*)-**262** (21.2 mg, 0.038 mmol), $Ni(cod)_2$ **254** (2.1 mg, 0.008 mmol, 20 mol%), and triphenylphosphine (4.0 mg, 0.015 mmol, 40 mol%) in glovebox. The content was dissolved in THF (2 mL) under argon. The reaction mixture was stirred at room temperature for 210 min. Then the solvent was removed *in vacuo* and the residue was purified by flash chromatography on silica gel (DCM – acetone – ethanol 70 : 30 : 10) to give (*M*,*R*,*R*)-**211** (10.7 mg, 50%) as a yellow amorphous solid.

Procedure using CpCo(CO)(fum) (1.0 eq) and microwave irradiation at 180 °C in a larger scale (Table 3.40, entry 4)

A microwave vial was charged with triyne (*R*,*R*)-**262** (98.0 mg, 0.177 mmol) and CpCo(CO)(fum) **255** (52.4 mg, 0.177 mmol, 1.0 eq) under argon. THF (10 mL) and 1-butyl-2,3-dimethylimidazolium tetrafluoroborate (50 µL) were added. The reaction mixture was heated to 180 °C for 20 min. Then the solvent was removed *in vacuo* and the residue was purified by flash chromatography on silica gel (DCM – acetone – ethanol 70 : 30 : 10) to give (*M*,*R*,*R*)-**211** (15.2 mg, 16%) as a yellow amorphous solid.

Procedure using CpCo(CO)(fum) (20 mol%) and a microwave irradiation at 180 °C in a larger scale (Table 3.40, entry 5)

A microwave vial was charged with triyne (*R*,*R*)-**262** (200.0 mg, 0.361 mmol) and CpCo(CO)(fum) **255** (21.4 mg, 0.072 mmol, 20 mol%) under argon. THF (20 mL) and 1-butyl-2,3-dimethylimidazolium tetrafluoroborate (50 µL) were added. The reaction mixture was heated to 180 °C for 20 min. Then the

solvent was removed *in vacuo* and the residue was purified by flash chromatography on silica gel (DCM – acetone – ethanol 70 : 30 : 10) to give (*M*,*R*,*R*)-**211** (54.2 mg, 27%) as a yellow amorphous solid.

Procedure using $Ni(cod)_2$/PPh_3 (1.0 eq/2.0 eq) at 50 °C in a larger scale (Table 3.40, entry 6)

A microwave vial was charged with triyne (*R*,*R*)-**262** (183.0 mg, 0.330 mmol), $Ni(cod)_2$ **254** (90.7 mg, 0.330 mmol, 1.0 eq), and triphenylphosphine (173.1 mg, 0.660 mmol, 2.0 eq) in glovebox. The content was dissolved in THF (20 mL) under argon. The reaction mixture was stirred at 50 °C overnight. Then the solvent was removed *in vacuo* and the residue was purified by flash chromatography on silica gel (acetone) to give (*M*,*R*,*R*)-**211** (161.5 mg, 88%) as a yellowish amorphous solid.

Procedure using $Ni(cod)_2$/PPh_3 (5 mol%/10 mol%) at 50 °C in a larger scale (Table 3.40, entry 7)

A microwave vial was charged with triyne (*R*,*R*)-**262** (83.7 mg, 0.151 mmol), $Ni(cod)_2$ **254** (2.1 mg, 0.008 mmol, 5 mol%), and triphenylphosphine (4.0 mg, 0.015 mmol, 10 mol%) in glovebox. The content was dissolved in THF (10 mL) under argon. The reaction mixture was stirred at 50 °C overnight. Then the solvent was removed *in vacuo* and the residue was purified by flash chromatography on silica gel (acetone – ethyl acetate 40 : 60) to give (*M*,*R*,*R*)-**211** (64.9 mg, 78%) as a yellowish amorphous solid.

Optical rotation: $[\alpha]^{22}_D$ -276° (c 0.23, $CHCl_3$).

^{1}H NMR (500 MHz, DMSO-d_6, t = 120 °C): 1.04 (d, *J* = 6.5, 6H), 2.95 (bs, 12H), 5.40 (q, *J* = 6.5, 2H), 6.60 (bd, *J* = 5.6, 2H), 6.63 (bs, 2H), 6.84 (ddd, *J* = 7.7, 7.4, 1.2, 2H), 7.06 (dd, *J* = 8.0, 1.2, 2H), 7.27 (ddd, *J* = 8.0, 7.4, 1.3, 2H), 7.34 (bdd, *J* = 7.7, 1.3, 2H), 8.08 (bd, *J* = 5.6, 2H).

^{13}C NMR (126 MHz, DMSO-d_6, t = 120 °C): 17.93 (q), 38.47 (2 x q), 71.18 (d), 105.34 (d), 108.87 (d), 118.87 (d), 120.73 (d), 122.21 (s), 125.63 (s), 128.08 (d), 129.47 (d), 133.14 (s), 138.64 (s), 144.77 (d), 152.75 (s), 154.73 (s). Quaternary carbon on DMAP moiety was not detected.

IR ($CHCl_3$): 3081 w, 3064 w, 3041 w, 2977 m, 2819 w, 1631 w, 1599 vs, 1585 s, sh, 1567 m, 1541 s, 1503 s, 1487 m, 1452 m, 1445 m, sh, 1436 s, 1419 m, 1374 s, 1363 m, sh, 1292 m, 1276 m, 1251 m, 1172 w, sh, 1154 m, 1128 w, sh, 1118 m, 1067 s, 1037 w, 993 s, 946 w, 813 m, 857 m, 691 w, 559 vw, 488 w cm^{-1}.

ESI MS: 555 (M^+, 100), 278 (18).

HR ESI MS: calculated for $C_{36}H_{35}N_4O_2$ 555.2755, found 555.2753.

2-Formyl-6-methoxyphenyl 1,1,2,2,3,3,4,4,4-nonafluorobutane-1-sulfonate (219)

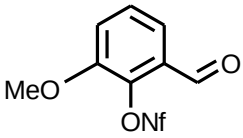

To a 60% suspension of sodium hydride in mineral oil (341.6 mg, 11.52 mmol, 1.3 eq) in DMF (5 mL) a solution of *o*-vanillin **73** (1.3484 g, 8.86 mmol) in DMF (10 mL) was added at 0 °C under argon. The reaction mixture was stirred 10 min at 0 °C and then allowed to warm up to room temperature and stirred an additional hour at this temperature. Nonaflate fluoride (1.9 mL, 3.2127 g, 10.58 mmol, 1.2 eq) was added and the reaction was stirred for 20 h at room temperature. The solvent was removed in vacuo and the crude reaction mixture was purified by flash chromatography on silica gel (hexane – diethyl ether – acetone – triethylamine 79 : 10 : 10 : 1) to provide **219** (2.4895 g, 65%) as a colourless to pale brown oil.

^{1}H NMR wax in agreement with the published data.[36]

^{1}H NMR (500 MHz, $CDCl_3$): 3.92 (s, 3H), 7.28 (dd, *J* = 8.2, 1.7, 1H), 7.42 (ddd, *J* = 8.2, 7.8, 0.8, 1H), 7.48 (dd, *J* = 7.8, 1.7, 1H), 10.22 (m, 1H).

3-Methoxy-2-{[tris(1-methylethyl)silyl]ethynyl}benzaldehyde (221)

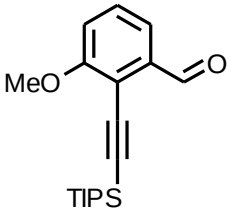

A Schlenk flask was charged with bis(triphenylphosphine)palladium chloride (273.7 mg, 0.39 mmol, 5 mol%). A solution of **219** (2.6777 g, 6.17 mmol) was added in DMF (40 mL) under argon. Then triethylamine (5.4 mL, 3.9204 g, 38.78 mmol, 6.0 eq) and (triisopropylsilyl)acetylene **220** (2.1 mL, 1.7241 g, 9.45 mmol, 1.5 eq) were added and the reaction mixture was stirred for 1.5 h at 90 °C. After cooling down to room temperature, the reaction mixture was diluted with diethyl ether and filtered through a kieselguhr layer. Solvents were evaporated at reduced pressure and the residue purified by flash chromatography (gradient elution hexane – diethyl ether 100 : 0 to 90 : 10) to provide **221** (1.6515 g, 85%) as a yellow oil.

^{1}H NMR was in agreement with the published data.[36]

^{1}H NMR (500 MHz, $CDCl_3$): 1.12-1.18 (m, 21H), 3.91 (s, 3H), 7.10 (dd, *J* = 8.2, 1.1, 1H), 7.37 (dt, *J* = 8.1, 8.1, 1.0, 1H), 7.51 (dd, *J* = 7.8, 1.1, 1H), 10.62 (d, *J* = 1.0, 1H).

(3-Methoxy-2-{[tris(1-methylethyl)silyl]ethynyl}phenyl)methanol (222)

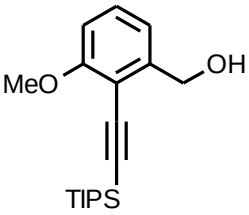

Aldehyde **221** (2.9283 g, 9.25 mmol) was dissolved in toluene (40 mL) under argon. Diisobutylaluminium hydride (1.5 M, 9.7 mL, 14.55 mmol, 1.6 eq) in toluene was added dropwise at -78 °C. The reaction mixture was stirred for 4 h at -78 °C. The reaction was quenched with aqueous NH_4Cl and extracted with DCM (3 x 200 mL). The organic fractions were combined and dried over anhydrous Na_2SO_4. The solvents were removed at reduced pressure and the residue was purified by flash chromatography on silica gel (hexane – acetone 95 : 5) to provide **222** (2.5792 g, 88%) as amorphous solid.

^{1}H NMR was in agreement with the published data.[36]

^{1}H NMR (500 MHz, $CDCl_3$): 1.12-1.17 (m, 21H), 2.33 (m, 1H), 3.87 (s, 3H), 4.82 (bd, *J* = 5.6, 2H), 6.82 (dd, *J* = 8.3, 0.6, 1H), 7.01 (ddt, *J* = 7.7, 1.0, 0.7, 0.7, 1H), 7.27 (dd, *J* = 8.3, 7.7, 1H).

(-)-1-Iodo-2-({[(1*S*)-1-methyl-3-(4-methylphenyl)prop-2-yn-1-yl]oxy}methyl)benzene (224)

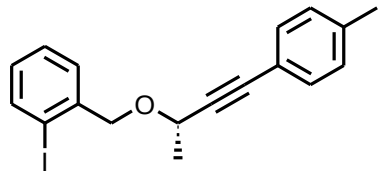

To a 30% suspension of potassium hydride in mineral oil (290.4 mg, 2.17 mmol, 1.2 eq) in THF (5 mL) a solution of (*S*)-**75** (319.0 mg, 1.81 mmol, 1.0 eq) in THF (4 mL) was added at 0 °C under argon. The reaction mixture was stirred for 1 h at 0 °C and then 2-iodobenzyl bromide **223** (537.4 mg, 1.81 mmol) was added in THF (4 mL). The reaction mixture was stirred and allowed to warm up to room temperature for 2 h. A saturated ammonium chloride solution (5 mL) was added to quench the excess of potassium hydride and the product was extracted with diethyl ether (3 x 30 mL). The combined organic layers were washed with water (3 x 30 mL) and dried over anhydrous sodium sulfate. The solvent was removed at reduced pressure and the residue was purified by flash chromatography on silica gel (hexane – diethyl ether 98 : 2) to give (*S*)-**224** (558.3 mg, 82%) as a yellow amorphous solid.

Optical rotation: $[\alpha]^{22}_D$ -95° (c 0.20, CH_2Cl_2).

^{1}H NMR (500 MHz, $CDCl_3$): 1.59 (d, *J* = 6.6, 3H), 2.34 (bs, 3H), 4.52 (q, *J* = 6.6, 1H), 4.57 (d, *J* = 12.5, 1H), 4.83 (d, *J* = 12.5, 1H), 6.98 (ddd, *J* = 7.9, 7.4, 1.8, 1H), 7.12 (m, 2H), 7.34 (ddd, *J* = 7.7, 7.4, 1.3, 1H), 7.35 (m, 2H), 7.49 (ddt, *J* = 7.7, 1.8, 0.8, 0.8, 1H), 7.82 (dd, *J* = 7.8, 1.3, 1H).

^{13}C NMR (125 MHz, $CDCl_3$): 21.45 (q), 22.21 (q), 65.75 (d), 74.44 (t), 85.60 (s), 88.05 (s), 98.13 (s), 119.61 (s), 128.17 (d), 129.01 (2 x d), 129.13 (d), 129.18 (d), 131.63 (2 x d), 138.42 (s), 139.18 (d), 140.44 (s).

IR ($CHCl_3$): 3058 w, 3033 w, 2226 w, 1609 w, 1588 w, 1566 m, 1510 vs, 1466 m, 1452 m, 1407 w, 1373 m, 1329 s, 1313 m, sh, 1273 w, 1259 m, 1181 w, 1160 w, 1114 s, 1095 vs, 1045 m, 1014 s, 819 vs, 649 w, 429 w cm^{-1}.

EI MS: 376 ($M^{+\bullet}$, 1), 361 (5), 346 (2), 256 (2), 249 (2), 217 (24), 205 (100), 143 (50), 129 (88), 115 (24), 102 (5), 90 (24), 71 (8), 57 (12), 43 (44).

HR EI MS: calculated for $C_{18}H_{17}IO$ 376.0324, found 376.0314.

(-)-1-Methoxy-3-({[(1*S*)-1-methyl-3-(4-methylphenyl)prop-2-yn-1-yl]oxy}methyl)-2-{[2-({[(1*S*)-1-methyl-3-(4-methylphenyl)prop-2-yn-1-yl]oxy}methyl)phenyl]ethynyl}benzene (225)

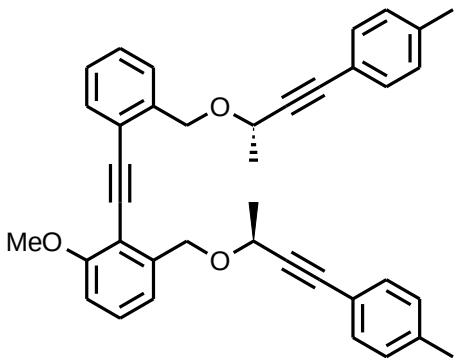

A Schlenk flask was charged with (*S*)-**224** (606.5 mg, 1.61 mmol), tetrakis(triphenylphosphine)palladium (93.9 mg, 0.081 mmol, 5 mol%), and copper iodide (27.8 mg, 0.146 mmol, 9 mol%). A solution of (*S*)-**77** (488.5 mg, 1.60 mmol) in diisopropylamine (15 mL) was added under argon. Reaction mixture was stirred at 80 °C for 3 h. The crude reaction mixture was filtered through a short pad of silica and eluted with hexane. The solvents were removed at reduced pressure and the residue was purified by flash chromatography on silica gel (hexane – diethyl ether 90 : 10) to give (*S*,*S*)-**225** (630.0 mg, 72%) as a pale yellow amorphous solid.

Optical rotation: $[\alpha]^{22}_D$ -251° (c 0.38, CH_2Cl_2).

^{1}H NMR (500 MHz, $CDCl_3$): 1.56 (d, *J* = 6.6, 3H), 1.57 (d, *J* = 6.6, 3H), 2.31 (bs, 3H), 2.32 (bs, 3H), 3.85 (s, 3H), 4.53 (q, *J* = 6.6, 1H), 4.55 (q, *J* = 6.6, 1H), 4.88 (d, *J* = 12.7, 1H), 4.96 (d, *J* = 13.0, 1H), 5.05 (d, *J* = 12.7, 1H), 5.07 (d, *J* = 13.0, 1H), 6.80 (dd, *J* = 8.4, 1.1, 1H), 7.02 (m, 2H), 7.04 (m, 2H), 7.16 (dt, *J* = 7.6, 7.6, 1.2, 1H), 7.18 (dd, *J* = 7.8, 1.1, 1H), 7.27 (m, 4H), 7.30 (dd, *J* = 8.4, 7.8, 1H), 7.32 (dt, *J* = 7.6, 7.6, 1.4, 1H), 7.51 (ddd, *J* = 7.6, 1.4, 0.4, 1H), 7.55 (ddq, *J* = 7.7, 1.2, 0.7, 0.7, 0.7, 1H).

^{13}C NMR (125 MHz, $CDCl_3$): 21.43 (q), 21.43 (q), 22.27 (2 x q), 55.83 (q), 65.63 (d), 65.72 (d), 68.77 (t), 68.85 (t), 85.22 (s), 85.38 (s), 87.84 (s), 88.39 (s), 88.57 (s), 96.13 (s), 109.41 (d), 111.15 (s), 119.61 (s), 119.66 (s), 119.81 (d), 121.98 (s), 126.98 (d), 127.24 (d), 128.26 (d), 128.88 (2 x d), 128.91 (2 x d), 129.20 (d), 131.56 (2 x d), 131.62 (2 x d), 131.90 (d), 138.17 (s), 138.23 (s), 140.08 (s), 141.70 (s), 160.19 (s).

IR ($CHCl_3$): 3069 w, 3032 m, 2990 s, 2840 m, 2226 w, 1607 w, 1596 m, 1577 s, 1510 vs, 1490 m, 1473 vs, 1460 s, 1448 s, sh, 1438 s, 1407 w, 1389 m, 1372 s, 1329 vs, 1313 m, sh, 1299 m, sh, 1272 vs, 1185 w, 1160

m, sh, 1132 s, sh, 1115 s, sh, 1106 vs, 1092 vs, 1079 s, sh, 1060 vs, 1040 m, sh, 1031 m, sh, 1022 s, 965 w, 947 w, 867 w, 819 vs, 647 w, 556 w, 542 m, 502 w cm^{-1}.

EI MS: 552 ($M^{+\bullet}$, 6), 538 (4), 524 (5), 409 (100), 379 (25), 337 (20), 305 (12), 265 (22), 245 (14), 165 (18), 143 (72), 128 (62), 115 (30), 55 (41), 41 (34).

HR EI MS: calculated for $C_{39}H_{36}O_3$ 552.2664, found 552.2686.

(η^4-Cycloocta-1,5-diene)(η^5-cyclopentadienyl)cobalt(I) (226)

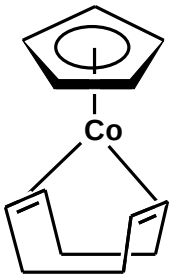

Bis(carbonyl)(η^5-cyclopentadienyl)cobalt(I) **81** (3.0 g, 2.2 mL, 16.7 mmol) was dissolved in decalin (250 mL) under argon. Cycloocta-1,5-diene (15.0 g, 17.0 mL, 138.7 mmol, 8.3 eq) was added and the reaction mixture was heated to 145 °C for 62 h under argon. The solvent was distilled out from the reaction mixture at reduced pressure (oil pump vacuum, ca 60 °C). The residue was diluted by pentane (20 mL), filtered through a short silica gel pad and crystalized at -78 °C overnight. The mother liqueur was filtered off at -78 °C and concentrated at reduced pressure for the next crystallization. The product was dried in vacuum. Two crystallizations from pentane provided **226** (295.7 mg, 8%) as a yellow-orange powder.

^{1}H NMR was in agreement with the published data.[147]

^{1}H NMR (400 MHz, C_6D_6): 1.68 (m, 4H), 2.44 (m, 4H), 3.43 (bs, 4H), 4.34 (s, 5H).

Bis(η^2-ethylene)(η^5-cyclopentadienyl)rhodium(I) (227)

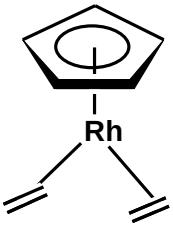

Two-necked Schlenk flask equipped by a rubber septa was loaded by di(η^2-ethylene)rhodium chloride dimer (997.5 mg, 2.5647 mmol) in a glovebox. The septum was changed for an air condenser under argon-flow. The content was dissolved in THF (35 mL) and a solution of sodium cyclopentadienide (2.0 M, 2.56 mL, 5.1295 mmol, 2.0 eq) in THF was added dropwise. The reaction mixture was heated to reflux for 1 h, then allowed to cool down to room temperature and stirred for additional 16 h at this temperature. The solvent was removed at the reduced pressure and the crude product was transferred into the sublimator in glovebox. The product was sublimated at 50 °C under an oil pump vacuum for 8 h to provide **227** (764.1 mg, 66%) as a yellow needle crystals.

^{1}H NMR was in agreement with the published data.[108]

^{1}H NMR (400 MHz, $CDCl_3$): 1.05 (bs, 4H), 2.89 (bs, 4H), 5.22 (s, 5H).

Bis(η^2-ethylene)(η^5-1,2,3,4,5-pentamethylcyclopentadienyl)rhodium(I) (228)

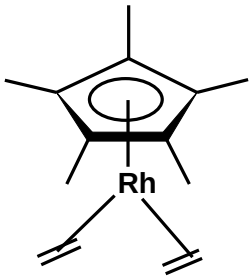

A Schlenk flask was charged with μ-dichlorobis(chloropentamethylcyclopentadienylrhodium) (192.0 mg, 0.31 mmol) and sodium carbonate (98.8 mg, 0.93 mmol, 3.0 eq). The content was suspended in ethanol (96%, 30 mL) under argon. Ethylene was bubbled through the reaction mixture at 65 °C for 3 h. After cooling down to room temperature the reaction mixture was filtered through a short silica gel pad (ca 1.5 cm) under argon. The solvent was removed at reduced pressure and the product was dried *in vacuo* for several min. The reaction provided **228** (172.8 mg, 95%) as a yellow to light brown powder.

^{1}H NMR was in agreement with the published data.[109]

^{1}H NMR (400 MHz, $CDCl_3$): 1.26 (m, 4H), 1.74 -1.76 (m, 19H).

(-)-(*P*,3*S*,6*S*)-11-Methoxy-3,6-dimethyl-4,5-bis(4-methylphenyl)-1,3,6,8-tetrahydro dibenzo[*e*,*e'*]benzo[1,2-*c*:4,3-*c'*]bisoxepine (231)

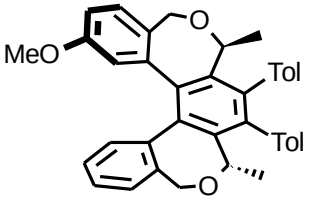

Procedure using CpCo(cod) (1.0 eq) at 50 °C (Table 3.8, entry 1):

A Schlenk flask was charged with triyne (*S*,*S*)-**229** (44.1 mg, 0.080 mmol) and CpCo(cod) **226** (18.5 mg, 0.080 mmol, 1.0 eq). The content was dissolved in THF (6 mL) under argon. The reaction mixture was heated to 50 °C for 45 min. No reaction proceeded according to the TLC analysis.

Procedure using CpCo(cod)/PPh_3 (1.0 eq/2.0 eq) and halogen lamp irradiation at 140 °C (Table 3.8, entry 2)

A two-necked Schlenk flask was charged with triyne (*S*,*S*)-**229** (43.6 mg, 0.079 mmol) and CpCo(cod) **226** (18.3 mg, 0.079 mmol, 1.0 eq) under argon. The content was dissolved in decane (18 mL) and the reaction mixture was heated by halogen lamp irradiation at 140 °C for 60 min. Then triphenylphosphine (41.4 mg, 0.158 mmol, 2.0 eq) was added and the reaction mixture was heated by halogen lamp irradiation at 140 °C for an additional h. No reaction proceeded according to the TLC analysis.

Procedure using CpCo(cod) (1.0 eq) and microwave irradiation at 140 °C (Table 3.8, entry 3)

A microwave vial was charged with triyne (*S*,*S*)-**229** (26.2 mg, 0.047 mmol) and CpCo(cod) **226** (11.0 mg, 0.047 mmol, 1.0 eq). The content was dissolved in THF (4 mL) under argon. The reaction mixture was heated in a microwave reactor at 140 °C for 20 min. No reaction proceeded according to the TLC analysis.

Procedure using CpRh(ethylene)$_2$ (1.0 eq) at 50 °C (Table 3.8, entry 4)

A Schlenk flask was charged with triyne (*S*,*S*)-**229** (32.7 mg, 0.059 mmol) and CpRh(=)$_2$ **227** (13.2 mg, 0.059 mmol, 1.0 eq). The content was dissolved in THF (7 mL) under argon. The reaction mixture was heated to 50 °C for 45 min. No reaction proceeded according to the TLC analysis.

Procedure using CpRh(ethylene)$_2$ (1.0 eq) at 110 °C (Table 3.8, entry 5)

A Schlenk flask was charged with triyne (*S*,*S*)-**229** (47.7 mg, 0.086 mmol) and CpRh(=)$_2$ **227** (19.6 mg, 0.087 mmol, 1.0 eq). The content was dissolved in toluene (5 mL) under argon and a condenser was connected. The reaction mixture was heated to reflux for 60 min. No reaction proceeded according to the TLC analysis.

Procedure using CpRh(ethylene)$_2$ (1.0 eq) and halogen lamp irradiation at 140 °C (Table 3.8, entry 6)

A two-necked Schlenk flask was charged with triyne (*S*,*S*)-**229** (25.3 mg, 0.046 mmol) and CpRh(=)$_2$ **227** (10.4 mg, 0.046 mmol, 1.0 eq) under argon. The content was dissolved in decane (5 mL) and the reaction mixture was heated by halogen lamp irradiation at 140 °C for 35 min. The solvent was removed at the reduced pressure and the residue was purified by flash chromatography on silica gel (gradient elution hexane – ethyl ether 100 : 0 to 80 : 20) to provide (*P*,*S*,*S*)-**231** (19.1 mg, 75%) as a yellow to brown amorphous solid.

Procedure using CpRh(ethylene)$_2$ (10 mol%) and halogen lamp irradiation at 140 °C (Table 3.8, entry 7)

A two-necked Schlenk flask was charged with triyne (*S*,*S*)-**229** (48.1 mg, 0.087 mmol) and CpRh(=)$_2$ **227** (2.0 mg, 0.009 mmol, 10 mol%) under argon. The content was dissolved in decane (5 mL) and the reaction mixture was heated by halogen lamp irradiation at 130 °C for 60 min (until a presence of the catalyst was detectable by TLC). The solvent was removed at the reduced pressure and the residue was purified by flash chromatography on silica gel (gradient elution hexane – ethyl ether 100 : 0 to 80 : 20) to provide (*P*,*S*,*S*)-**231** (12.0 mg, 25%) as a brown amorphous solid.

Procedure using CpRh(ethylene)$_2$ (5 mol%) and halogen lamp irradiation at 50 °C (Table 3.8, entry 8)

A two-necked Schlenk flask was charged with triyne (*S*,*S*)-**229** (54.1 mg, 0.098 mmol) and CpRh(=)$_2$ **227** (1.2 mg, 0.005 mmol, 5 mol%) under argon. The content was dissolved in THF (5 mL) and the reaction mixture was heated by halogen lamp irradiation at 50 °C for 40 min. No reaction proceeded according to the TLC analysis.

Procedure using Cp*Rh(ethylene)$_2$ (1.0 eq) and microwave irradiation at 140 °C (Table 3.8, entry 9)

A microwave vial was charged with triyne (*S*,*S*)-**229** (27.9 mg, 0.051 mmol) and Cp*Rh(=)$_2$ **228** (15.3 mg, 0.052 mmol, 1.0 eq). The content was dissolved in THF (4 mL) and the reaction mixture was heated in a microwave reactor at 140 °C for 20 min. The solvent was removed at reduced pressure and the residue was purified by flash chromatography on silica gel (gradient elution hexane – acetone 100 : 0 to 95 : 5) to provide (*P*,*S*,*S*)-**231** (16.9 mg, 61%) as brown amorphous solid.

^{1}H NMR was in agreement with the published data.[148]

^{1}H NMR (500 MHz, $CDCl_3$): 0.62 (d, *J* = 7.1, 3H), 0.65 (d, *J* = 7.1, 3H), 2.24 (s, 6H), 3.32 (s, 3H), 4.54 (d, *J* = 11.5, 1H), 4.58 (d, *J* = 11.4, 1H), 4.80 (d, *J* = 11.5, 1H), 4.87 (d, *J* = 11.4, 1H), 4.91 (q, *J* = 7.1, 1H), 4.93 (q, *J* = 7.1, 1H), 6.09 (d, *J* = 2.6, 1H), 6.62 (dd, *J* = 7.7, 1.3, 1H), 6.72 (m, 2H), 6.74 (dd, *J* = 8.3, 2.6, 1H), 6.86 (m, 2H), 7.01 (m, 2H), 7.01 (dt, *J* = 7.5, 7.5, 1.4, 1H), 7.05 (m, 2H), 7.21 (dt, *J* = 7.4, 7.4, 1.3, 1H), 7.28 (d, *J* = 8.3, 1H), 7.40 (dd, *J* = 7.5, 1.4, 1H).

(-)-(*P*,3*S*,6*S*)-11,14-Dimethoxy-3,6-dimethyl-4,5-bis(4-methylphenyl)-1,3,6,8-tetrahydrodibenzo[*e*,*e'*]benzo[1,2-*c*:4,3-*c'*]bisoxepine (232)

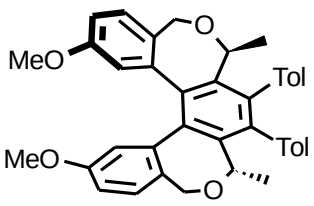

A two-necked Schlenk flask was charged with triyne (*S*,*S*)-**230** (28.6 mg, 0.049 mmol) and CpRh(=)$_2$ **227** (11.0 mg, 0.049 mmol, 1.0 eq) under argon. The content was dissolved in decane (5 mL) and the reaction mixture was heated by halogen lamp irradiation at 130 °C for 60 min. The solvent was removed at the reduced pressure and the residue was purified by flash chromatography on silica gel (gradient elution hexane – ethyl ether 100 : 0 to 40 : 60) to provide (*P*,*S*,*S*)-**232** (18.0 mg, 63%) as a yellow amorphous solid.

^{1}H NMR was in agreement with the published data.[145]

^{1}H NMR (500 MHz, $CDCl_3$): 0.67 (d, *J* = 7.1, 6H), 2.24 (s, 6H), 3.35 (s, 6H), 4.54 (d, *J* = 11.6, 2H), 4.80 (d, *J* = 11.6, 2H), 4.91 (q, *J* = 7.1, 2H), 6.14 (d, *J* = 2.6, 2H), 6.71 (dd, *J* = 7.7, 1.9, 2H), 6.76 (dd, *J* = 8.2, 2.6, 2H), 6.86 (ddq, *J* = 7.7, 1.9, 0.9, 0.9, 0.9, 2H), 7.01 (ddq, *J* = 7.8, 1.9, 0.8, 0.8, 0.8, 2H), 7.04 (dd, *J* = 7.8, 1.9, 2H), 7.29 (d, *J* = 8.2, 2H).

(-)-(*P*,3*S*,6*S*)-12-Methoxy-3,6-dimethyl-4,5-bis(4-methylphenyl)-1,3,6,8-tetrahydrodibenzo[*e*,*e'*]benzo[1,2-*c*:4,3-*c'*]bisoxepine (233)

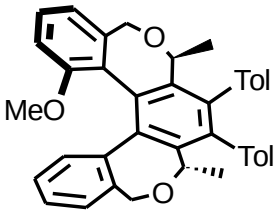

Procedure using CpRh(ethylene)$_2$ (0.5 eq) and microwave irradiation at 140 °C (Table 3.10, entry 2)

A microwave vial was charged with triyne (*S*,*S*)-**225** (39.8 mg, 0.072 mmol) and $CpRh(=)_2$ **227** (8.1 mg, 0.036 mmol, 0.5 eq). The mixture was dissolved in tetrahydrofuran (4 mL) under argon and 1-butyl-2,3-dimethylimidazolium tetrafluoroborate (20 µL) was added. The reaction mixture was heated to 140 °C for 30 min in a microwave reactor. Then the solvent was removed *in vacuo* and the residue was purified by flash chromatography on silica gel (hexane – diethyl ether 80 : 20) to give (*P*,*S*,*S*)-**233** (33.3 mg, 84%) as a yellow amorphous solid.

Procedure using CpCo(CO)$_2$/PPh$_3$ (1.0 eq/2.0 eq) and microwave irradiation at 200 °C (Table 3.10, entry 3)

A microwave vial was charged with triyne (*S*,*S*)-**225** (49.7 mg, 0.090 mmol) and triphenylphosphine (51.8 mg, 0.184 mmol, 2.0 eq). The mixture was dissolved in tetrahydrofuran (20 mL) under argon. 1-Butyl-2,3-dimethylimidazolium tetrafluoroborate (0.1 mL) and $CpCo(CO)_2$ **81** (16.2 mg, 0.090 mmol, 1.0 eq) were added. The reaction mixture was heated to 200 °C for 20 min in a microwave reactor. Then the solvent was removed *in vacuo* and the residue was purified by flash chromatography on silica gel (hexane – diethyl ether 80 : 20) to give (*P*,*S*,*S*)-**233** (41.9 mg, 84%) as a yellow amorphous solid.

Procedure using $CpCo(CO)_2$/PPh_3 (0.5 eq/1.0 eq) and microwave irradiation at 200 °C (Table 3.10, entry 4)

A microwave vial was charged with triyne (*S*,*S*)-**225** (120.1 mg, 0.217 mmol) and triphenylphosphine (57.0 mg, 0.217 mmol, 1.0 eq). The mixture was dissolved in tetrahydrofuran (20 mL) under argon. 1-Butyl-2,3-dimethylimidazolium tetrafluoroborate (0.1 mL) and $CpCo(CO)_2$ **81** (20.4 mg, 0.113 mmol, 0.5 eq) were added. The reaction mixture was heated to 200 °C for 20 min in a microwave reactor. Then the solvent was removed *in vacuo* and the residue was purified by flash chromatography on silica gel (hexane – diethyl ether 80 : 20) to give (*P*,*S*,*S*)-**233** (75.0 mg, 62%) as a yellow amorphous solid.

Procedure using $CpCo(CO)_2$ (1.0 eq) and microwave irradiation at 200 °C (Table 3.10, entry 5)

A microwave vial was charged with triyne (*S*,*S*)-**225** (90.8 mg, 0.164 mmol). The mixture was dissolved in tetrahydrofuran (20 mL) under argon. 1-butyl-2,3-dimethylimidazolium tetrafluoroborate (0.1 mL) and $CpCo(CO)_2$ **81** (29.6 mg, 0.164 mmol, 1.0 eq) were added. The reaction mixture was heated to 200 °C for 20 min in a microwave reactor. Then the solvent was removed *in vacuo* and the residue was purified by flash chromatography on silica gel (hexane – diethyl ether 80 : 20) to give (*P*,*S*,*S*)-**233** (45.3 mg, 50%) as a yellow amorphous solid.

Procedure using Cp*Rh(ethylene)$_2$ (1.0 eq) and microwave irradiation at 140 °C (Table 3.10, entry 6)

A microwave vial was charged with triyne (*S*,*S*)-**225** (61.2 mg, 0.111 mmol) and Cp*Rh(=)$_2$ **228** (32.5 mg, 0.111 mmol, 1.0 eq). The mixture was dissolved in tetrahydrofuran (4 mL) under argon and 1-butyl-2,3-dimethylimidazolium tetrafluoroborate (20 µL) was added. The reaction mixture was heated to 140 °C for 30 min in a microwave reactor. Then the solvent was removed *in vacuo* and the residue was purified by flash chromatography on silica gel (hexane – diethyl ether 80 : 20) to give (*P*,*S*,*S*)-**233** (33.4 mg, 55%) as a yellow amorphous solid.

Optical rotation: $[\alpha]^{22}_D$ -100° (c 0.42, CH_2Cl_2).

^{1}H NMR (500 MHz, $CDCl_3$): 0.62 (d, *J* = 7.1, 3H), 0.72 (d, *J* = 7.1, 3H), 2.23 (bs, 6H), 3.03 (s, 3H), 4.56 (d, *J* = 11.1, 1H), 4.56 (d, *J* = 11.5, 1H), 4.77 (d, *J* = 11.5, 1H), 4.84 (d, *J* = 11.1, 1H), 4.91 (q, *J* = 7.1, 2H), 6.51 (dd, *J* = 8.3, 1.1, 1H), 6.57 (dd, *J* = 7.7, 1.3, 1H), 6.75 (m, 2H), 6.88 (dt, *J* = 7.6, 7.6, 1.4, 1H), 6.88 (m, 2H), 7.00 (m, 2H), 7.04 (dd, *J* = 7.4, 1.1, 1H), 7.04 (m, 2H), 7.14 (dt, *J* = 7.3, 7.3, 1.3, 1H), 7.24 (dd, *J* = 8.3, 7.4, 1H), 7.38 (bdd, *J* = 7.4, 1.3, 1H).

^{13}C NMR (125 MHz, $CDCl_3$): 21.13 (2 x q), 21.91 (q), 22.35 (q), 54.49 (q), 67.16 (t), 67.39 (t), 72.55 (d), 72.65 (d), 110.53 (d), 120.70 (d), 126.41 (d), 127.22 (d), 127.85 (d), 127.97 (d), 128.01 (d), 128.27 (d), 128.32 (d), 128.68 (s), 128.98 (d), 129.28 (d), 129.50 (d), 129.60 (d), 129.88 (d), 129.90 (d), 132.81 (s), 135.49 (2 x s), 136.83 (s), 137.14 (s), 137.25 (s), 137.38 (s), 137.72 (s), 138.34 (s), 138.74 (s), 141.08 (s), 141.63 (s), 141.82 (s), 155.37 (s).

IR ($CHCl_3$): 3039 w, 2838 m, sh, 1600 w, 1585 m, 1575 w, sh, 1514 m, 1493 m, 1471 s, 1464 s, 1450 m, sh, 1439 m, 1398 m, 1367 s, 1306 m, 1290 m, sh, 1274 s, 1259 s, 1185 m, 1159 m, 1120 m, sh, 1111 m, 1095 m, sh, 1045 m, 1032 m, 1023 m, 947 w, 820 m, 697 w, 648 w, sh, 561 w cm^{-1}.

EI MS: 552 ($M^{+\bullet}$, 5), 538 (4), 531 (4), 492 (3), 466 (3), 191 (4), 149 (16), 97 (29), 83 (38), 69 (70), 54 (92), 41 (100).

HR EI MS: calculated for $C_{39}H_{36}O_3$ 552.2664; found 552.2656.

(*P*,3*R*,6*S*)-3,6-Dimethyl-4,5-bis(4-methylphenyl)-12-[(4,4,5,5-tetramethyl-1,3,2-dioxaphospholan-2-yl)oxy]-1,3,6,8-tetrahydrodibenzo[*e*,*e'*]benzo[1,2-*c*:4,3-*c'*]bisoxepine (234)

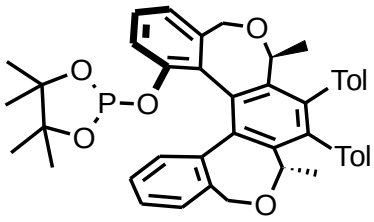

A Schlenk flask was charged with 60% suspension of NaH in mineral oil (14.0 mg, 0.350 mmol, 4.0 eq) under argon. The flask was cooled to 0 °C and the hydride was suspended in THF (1 mL). A solution of (*P*,*S*,*S*)-**208** (47.3 mg, 0.088 mmol) in THF (2 mL) was added dropwise at 0°C. The reaction mixture was stirred at 0 °C for 15 min and then allowed to warm up to room temperature and stirred for additional 45 min at the same temperature. 2-chloro-4,4,5,5-tetramethyl-1,3,2-dioxaphospholane **70** (16 µL, 18.5 mg, 0.101 mmol, 1.1 eq) was added dropwise. The reaction was stirred at room temperature for 2 h. The solvents were removed at reduced pressure and the residue was purified on a short silica gel column (hexane – ethyl ether – acetone 80 : 10 : 10) to give (*P*,*S*,*S*)-**234** (45.2 mg, 75%) as a white amorphous solid.

The product is easily oxidized on air therefore no further analysis than ^{1}H and ^{31}P NMR were done.

^{1}H NMR (400 MHz, $CDCl_3$): 0.95 (s, 3H), 0.98 (s, 3H), 1.03 (s, 3H), 1.08 (d, *J* = 7.1, 3H), 1.12 (s, 3H), 1.14 (d, *J* = 7.1, 3H), 1.98 (s, 6H), 4.69 (d, *J* = 11.4, 1H), 5.00 (d, *J* = 11.4, 1H), 5.02 (d, *J* = 11.5, 1H), 5.53 (q, *J* = 7.1, 1H), 5.58 (d, *J* = 11.5, 1H), 5.61 (q, *J* = 7.0, 1H), 6.80 (m, 2H), 6.84 (dd, *J* = 7.7, 1.7, 1H), 6.92 – 6.96 (m, 2H), 6.99 (dd, *J* = 7.8, 1.4, 2H), 7.02 (dd, *J* = 7.7, 1.8, 1H), 7.05 – 7.11 (m, 2H), 7.15 (dd, *J* = 7.3, 1.6, 1H), 7.19 (dd, *J* = 7.5, 1.9, 1H), 7.31 (dd, *J* = 7.7, 1.8, 1H), 7.42 (dd, *J* = 7.8, 1.7, 1H), 7.51 (dd, *J* = 7.5, 0.8, 1H).

^{31}P NMR (162 MHz, $CDCl_3$): 137.12 (s).

(*P*,3*R*,6*S*)-3,6-Dimethyl-4,5-bis(4-methylphenyl)-1,3,6,8-tetrahydrodibenzo[*e*,*e'*]benzo[1,2-*c*:4,3-*c'*]bisoxepin-12-yl diethyl phosphite (235)

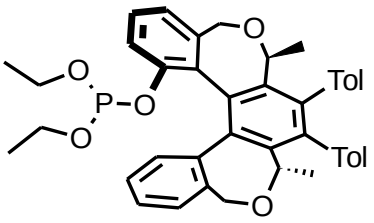

A Schlenk flask was charged with 60% suspension of NaH in mineral oil (12.0 mg, 0.300 mmol, 4.0 eq) under argon. The flask was cooled to 0 °C and hydride was suspended in THF (1 mL). A solution of (*P*,*S*,*S*)-**208** (40.4 mg, 0.075 mmol) in THF (2 mL) was added dropwise at 0°C. The reaction mixture was stirred at 0 °C for 15 min and then allowed to warm up to the room temperature and stirred for additional 45 min at the same temperature. Diethyl chlorophosphite **237** (25 µL, 25.8 mg, 0.165 mmol, 2.2 eq) was added dropwise. The reaction was stirred at room temperature for 2 h. The solvents were removed at reduced pressure and the residue was purified on a short silica gel column (hexane – ethyl acetate 80 : 20) to give (*P*,*S*,*S*)-**235** (14.5 mg, 29%) as a yellow amorphous solid.

The formation of product **235** was detected according to the TLC analysis and immediately used in a catalytical experiment due to its rapid decomposition on air. Product: R_f (**235**) = 0.62 (observed as sole spot); standard: R_f (**208**) = 0.10. Mobile phase: hexane – diethyl ether – acetone 80 : 10 : 10. No traces of **208** were observed.

(*P*,3*R*,6*S*)-12-[(5,5-Dimethyl-1,3,2-dioxaphosphinan-2-yl)oxy]-3,6-dimethyl-4,5-bis(4-methylphenyl)-1,3,6,8-tetrahydrodibenzo[*e*,*e'*]benzo[1,2-*c*:4,3-*c'*]bisoxepine (236)

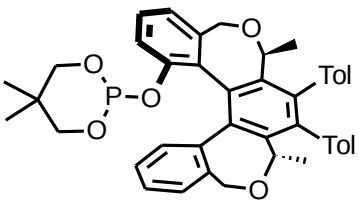

A Schlenk flask was charged with 60% suspension of NaH in mineral oil (18.7 mg, 0.468 mmol, 4.0 eq) under argon. The flask was cooled to 0 °C and hydride was suspended in THF (1 mL). A solution of (*P*,*S*,*S*)-**208** (62.9 mg, 0.117 mmol) in THF (0.6 mL) was added dropwise at 0°C. The reaction mixture was stirred at 0 °C for 15 min and then allowed to warm up to room temperature and stirred for additional 45 min at the same temperature. Chlorophosphite **238** (36 µL, 43.3 mg, 0.257 mmol, 2.2 eq) was added dropwise. The reaction was stirred at room temperature for 2 h. The solvents were removed at reduced pressure and the residue was purified on a short silica gel column (hexane – ethyl acetate 80 : 20) to give (*P*,*S*,*S*)-**236** (47.5 mg, 61%) as a yellowish amorphous solid.

The formation of product **236** was detected according to the TLC analysis and immediately used in a catalytical experiment due to its rapid decomposition on air. Product: R_f (**236**) = 0.70 (observed as sole

spot); Standard: R_f (**208**) = 0.16. Mobile phase: hexane – diethyl ether – ethyl acetate 80 : 10 : 10. No traces of **208** were observed.

(-)-(*M*,2*R*,5*R*)-2,5-Dimethyl-3,4-bis(4-methylphenyl)-2,5-dihydrobenzo[1,2-*c*:4,3-*c'*]-dichromene (239)

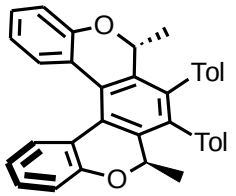

Procedure using $CpCo(CO)_2/PPh_3$ (20 mol%/40 mol%) and halogen lamp irradiation at 140 °C (Table 3.23, entry 1)

A two-necked Schlenk flask was charged with triyne (*R*,*R*)-**242** (44.5 mg, 0.090 mmol), $CpCo(CO)_2$ **81** (2.4 µL, 0.018 mmol, 20 mol%), and triphenylphosphine (9.4 mg, 0.036 mmol, 40 mol%) under argon. The content was dissolved in decane (3 mL) and the reaction mixture was heated by halogen lamp irradiation at 140 °C for 60 min. Then the solvent was removed *in vacuo* and the residue was purified by flash chromatography on silica gel (hexane – diethyl ether 90 : 10) to give (*M*,*R*,*R*)-**239** (36.0 mg, 81%) as a yellow amorphous solid.

Procedure using $Ni(cod)_2/PPh_3$ (20 mol%/40 mol%) at rt (Table 3.23, entry 2)

A microwave vial was charged with triyne (*R*,*R*)-**242** (30.5 mg, 0.062 mmol), $Ni(cod)_2$ **254** (3.4 mg, 0.012 mmol, 20 mol%), and triphenylphosphine (6.5 mg, 0.025 mmol, 40 mol%) in glovebox. The content was dissolved in THF (2 mL) under argon. The reaction mixture was stirred at room temperature for 30 min. Then the solvent was removed *in vacuo* and the residue was purified by flash chromatography on silica gel (hexane – diethyl ether 90 : 10) to obtain the desired cyclic product (*M*,*R*,*R*)-**239** (27.9 mg, 91%) as a yellow amorphous solid.

Procedure using CpCo(CO)(fum) (1.0 eq) and microwave irradiation at 200 °C (Table 3.23, entry 3)

A microwave vial was charged with triyne (*R*,*R*)-**242** (34.6 mg, 0.070 mmol) and CpCo(CO)(fum) **255** (20.8 mg, 0.070 mmol, 1.0 eq) under argon. THF (3 mL) and 1-butyl-2,3-dimethylimidazolium tetrafluoroborate (20 µL) were added. The reaction mixture was heated to 200 °C for 30 min. Then the solvent was removed *in vacuo* and the residue was purified by flash chromatography on silica gel (pentane – diethyl ether 95 : 5) to furnish the desired cyclic product (*M*,*R*,*R*)-**239** (24.3 mg, 70%) as a yellow amorphous solid.

Procedure using CpCo(CO)(fum) (20 mol%) and microwave irradiation at 180 °C (Table 3.23, entry 4)

A microwave vial was charged with triyne (*R*,*R*)-**242** (26.6 mg, 0.054 mmol) and CpCo(CO)(fum) **255** (3.2 mg, 0.011 mmol, 20 mol%) under argon. THF (3 mL) and 1-butyl-2,3-dimethylimidazolium tetrafluoroborate (20 µL) were added. The reaction mixture was heated to 180 °C for 20 min. Then the solvent was removed *in vacuo* and the residue was purified by flash chromatography on silica gel (pentane – diethyl ether 95 : 5) to furnish the desired cyclic product (*M*,*R*,*R*)-**239** (23.6 mg, 89%) as a yellow amorphous solid.

Procedure using $[Rh(cod)_2]BF_4$ (10 mol%) and microwave irradiation at 180 °C (Table 3.23, entry 5)

To $[Rh(cod)_2]BF_4$ **257** (3.6 mg, 0.009 mmol, 10 mol%), and triphenylphosphine (4.7 mg, 0.018 mmol, 20 mol%) in a argon-purged Schlenk flask was DCM (1 mL) added under argon. The solution was stirred for 5 min at room temperature. The solution was freezed by liquid nitrogen and the flask was charged with 1 atm of hydrogen. The reaction mixture was warmed up to room temperature and stirred for 1 h at the same temperature. Then the solvent was evaporated to a dryness and the residue was dissolved in DCM (1 mL) again. Then the solution of triyne (*R*,*R*)-**242** (44.1 mg, 0.089 mmol) in DCM (1 mL) was added. The reaction mixture was stirred at room temperature for 48 h (full conversion was not achieved according to TLC). The solvent was removed *in vacuo* and the residue was purified by flash chromatography on silica gel (hexane – diethyl ether 90 : 10) to furnish the desired cyclic product (*M*,*R*,*R*)-**239** (8.6 mg, 20%) as a yellow amorphous solid.

Optical rotation: $[\alpha]^{22}_D$ -591° (c 0.396, $CHCl_3$).

^{1}H NMR (400 MHz, $CDCl_3$): 0.93 (d, *J* = 6.6, 6H), 2.26 (s, 6H), 5.26 (q, *J* = 6.6, 2H), 6.66 (dd, *J* = 7.7, 1.5, 2H), 6.77 (m, 2H), 6.86 (d, *J* = 7.6, 2H), 7.00 (dd, *J* = 8.0, 0.9, 2H), 7.08 (d, *J* = 7.7, 2H), 7.12 – 7.18 (m, 4H), 7.45 (dd, *J* = 7.8, 1.2, 2H).

^{13}C NMR (101 MHz, $CDCl_3$): 18.33 (q), 21.16 (q), 72.93 (d), 119.15 (d), 120.87 (d), 123.57 (s), 125.34 (s), 128.38 (d), 128.57 (d), 128.97 (d), 129.06 (d), 129.32 (d), 130.73 (d), 134.87 (s), 136.04 (s), 137.12 (s), 139.12 (s), 153.43 (s).

IR ($CHCl_3$): 3081 w, 3064 w, 3044 w, 2985 m, 1603 m, 1584 m, 1564 vw, 1517 s, 1486 s, 1464 m, 1454 s, 1446 s, 1425 s, 1406 vw, 1368 s, 1332 m, 1283 w, 1275 s, 1244 m, 1233 m, 1145 m, 1110 m, 1064 vs, 1022 m, 1011 w, 945 w, 838 s, 692 w, 459 m cm^{-1}.

EI MS: 494 ($M^{+\bullet}$, 49), 479 (100), 464 (11), 435 (9), 419 (3), 224 (10), 209 (11), 183 (5), 111 (4), 97 (5), 81 (5), 69 (8), 57 (11), 44 (32), 32 (73).

HR EI MS: calculated for $C_{36}H_{30}O_2$ 494.2246, found 494.2256.

(+)-1-Iodo-2-{[(2*R*)-4-(4-methylphenyl)but-3-yn-2-yl]oxy}benzene (241)

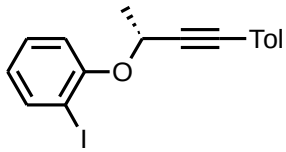

A Schlenk flask was charged with 2-iodophenol **240** (1.0595 g, 4.82 mmol) and triphenylphosphine (1.5958 g, 5.78 mmol, 1.2 eq). The content was dissolved in DCM (28 mL) and stirred for 20 min under argon. The alcohol (*S*)-**75** (771.5 mg, 4.82 mmol, 1.0 eq) and DIAD (1.04 mL, 1.0712 g, 5.30 mmol, 1.1 eq) were added. The reaction was stirred at room temperature for 3 h. The solvent was removed at reduced pressure and the residue was purified by flash chromatography on silica gel (hexane) to give (*R*)-**241** (1.2401 g, 71%) as a yellowish oil.

Optical rotation: $[\alpha]^{22}_D$ +20° (c 0.57, $CHCl_3$).

^{1}H NMR (400 MHz, $CDCl_3$): 1.84 (d, *J* = 6.6, 3H), 2.35 (s, 3H), 5.08 (q, *J* = 6.5, 1H), 6.76 (td, *J* = 7.6, 7.6, 1.4, 1H), 7.11 (m, 2H), 7.19 (dd, *J* = 8.3, 1.4, 1H), 7.29 – 7.35 (m, 3H), 7.81 (dd, *J* = 7.8, 1.6, 1H).

^{13}C NMR (101 MHz, $CDCl_3$): 21.42 (q), 22.43 (q), 66.33 (d), 86.37 (s), 87.10 (s), 87.81 (s), 115.25 (d), 119.19 (s), 123.28 (d), 128.95 (2 x d), 129.17 (d), 131.55 (2 x d), 138.63 (s), 139.38 (d), 156.63 (s).

IR ($CHCl_3$): 3083 m, 3063 m, 3032 m, 2236 m, 1607 m, 1570 s, 1510 s, 1470 s, 1452 m, 1439 m, 1373 m, 1239 m, 1164 m, 1125 s, 1036 s, 1019 s, 938 m, 818 s, 709 m, 651 m, 431 m cm^{-1}.

EI MS: 362 ($M^{+\bullet}$, 20), 347 (100), 271 (5), 220 (13), 205 (6), 189 (9), 165 (5), 143 (36), 128 (10), 115 (7).

HR APCI MS: calculated for $C_{17}H_{16}IO$ 363.0240, found 363.0240.

(-)-1,1'-Ethyne-1,2-diylbis(2-{[(1*R*)-1-methyl-3-(4-methylphenyl)prop-2-yn-1-yl]oxy}benzene) (242)

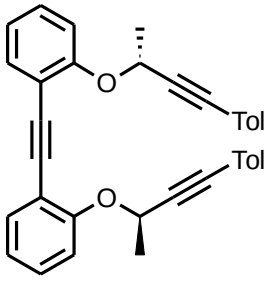

***Procedure using reaction between* (*R*)-241 *and* (*R*)-246**

A Schlenk flask was charged with iodide (*R*)-**241** (66.6 mg, 0.184 mmol), tetrakis(triphenylphosphine)-palladium (10.6 mg, 0.009 mmol, 5 mol%), and copper iodide (16.6 mg, 0.017 mmol, 9 mol%). Diyne (*R*)-**246** (47.9 mg, 0.184 mmol, 1.0 eq) was added in freshly degassed diisopropylamine (3 mL) under argon.

The reaction mixture was stirred overnight at room temperature. Then the reaction was diluted with diethyl ether (20 mL) and filtered through a pad of silica gel (diethyl ether). The solvents were evaporated under reduced pressure and the residue was purified by flash chromatography on silica gel (gradient elution hexane – diethyl ether 100 : 0 to 95 : 5) to give (*R*,*R*)-**242** (80.8 mg, 89%) as an amorphous yellow solid.

***Procedure using functionalization of* (*R*,*R*)-252**

A Schlenk flask was charged with triyne (*R*,*R*)-**252** (109.0 mg, 0.347 mmol), 4-iodotoluene **218** (158.8 mg, 0.728 mmol, 2.1 eq), tetrakis(triphenylphosphine)palladium (40.0 mg, 0.035 mmol, 10 mol%), and copper iodide (11.9 mg, 0.062 mmol, 18 mol%). Then freshly degassed diisopropylamine (5 mL) was added under argon. The reaction mixture was stirred at room temperature for 2 h. Then the reaction was diluted with diethyl ether (20 mL) and filtered through a pad of silica gel (diethyl ether). The solvents were evaporated under reduced pressure and the residue was purified by flash chromatography on silica gel (hexane – diethyl ether 95 : 5) to give (*R*,*R*)-**242** (158.8 mg, 93%) as an amorphous yellow solid.

Optical rotation: $[\alpha]^{22}_{D}$ -235° (c 0.60, $CHCl_3$).

^{1}H NMR (400 MHz, $CDCl_3$): 1.82 (d, *J* = 6.5, 6H), 2.29 (s, 6H), 5.20 (q, *J* = 6.5, 2H), 6.97 (t, *J* = 7.4, 2H), 7.05 (d, *J* = 8.0, 4H), 7.20 (d, *J* = 8.0, 2H), 7.25 – 7.29 (m, 6H), 7.53 (d, *J* = 7.5, 2H).

^{13}C NMR (101 MHz, $CDCl_3$): 21.42 (q), 22.50 (q), 66.23 (d), 86.10 (s), 87.73 (s), 90.11 (s), 114.92 (s), 116.27 (d), 119.49 (s), 121.68 (d), 128.93 (2 x d), 129.20 (d), 131.59 (2 x d), 133.51 (d), 138.47 (s), 158.20 (s).

IR ($CHCl_3$): 3077 w, 3058 w, 2236 w, 1610 w, 1600 w, 1593 m, 1574 m, 1510 vs, 1496 vs, 1481 s, 1450 s, 1408 w, 1375 m, 1331 s, 1289 s, 1236 vs, 1181 vw, 1164 m, 1122 s, 1109 m, 1086 vs, 1036 s, 1020 m, 946 s, 819 vs cm^{-1}.

EI MS: 494 ($M^{+\bullet}$, 32), 479 (100), 464 (22), 435 (6), 352 (19), 337 (52), 321 (8), 292 (6), 250 (8), 210 (11), 181 (13), 143 (79), 128 (47), 91 (5).

HR EI MS: calculated for $C_{36}H_{30}O_2$ 494.2246, found 494.2237.

(-)-Trimethyl[(2-{[(1*R*)-1-methyl-3-(4-methylphenyl)prop-2-yn-1-yl]oxy}phenyl)ethynyl]silane (244)

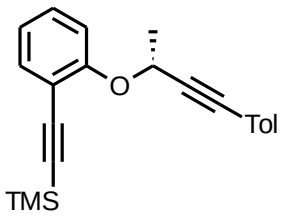

A Schlenk flask was charged with iodide (*R*)-**241** (93.0 mg, 0.257 mmol), tetrakis(triphenylphosphine)palladium (14.8 mg, 0.013 mmol, 5 mol%), and copper iodide (4.9 mg, 0.026 mmol, 10 mol%). Diisopropylamine (3 mL) and ethynyltrimethylsilane **243** (145 µL, 100.9 mg, 1.027 mmol, 4.0 eq) were added

under argon. The reaction mixture was stirred overnight at room temperature. The crude reaction mixture was diluted with diethyl ether and filtered through a kieselguhr layer. The solvent was evaporated at reduced pressure and the residue was purified by flash chromatography on silica gel (hexane) to give (*R*)-**244** (50.7 mg, 59%) as a yellowish oil.

^{1}H NMR and ^{13}C NMR were in agreement with the published data.[110]

^{1}H NMR (400 MHz, $CDCl_3$): 0.28 (s, 9H), 1.79 (d, *J* = 6.6, 3H), 2.34 (s, 3H), 5.13 (q, *J* = 6.5, 1H), 6.95 (td, *J* = 7.5, 7.5, 1.2, 1H), 7.10 (m, 2H), 7.19 (dd, *J* = 8.3, 1.2, 1H), 7.29 (m, 3H), 7.45 (dd, *J* = 7.6, 1.7, 1H).

^{13}C NMR (101 MHz, $CDCl_3$): 0.02 (3 x q), 21.43 (q), 22.34 (q), 66.23 (d), 86.16 (s), 87.57 (s), 98.68 (s), 101.33 (s), 114.30 (s), 116.24 (d), 119.43 (s), 121.58 (d), 128.96 (2 x d), 129.61 (d), 131.56 (2 x d), 133.56 (d), 138.53 (s), 158.94 (s).

(+)-1-Ethynyl-2-{[(2*R*)-4-(4-methylphenyl)but-3-yn-2-yl]oxy}benzene (246)

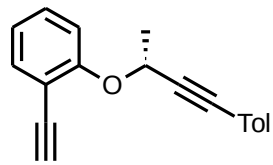

Diyne (*R*)-**244** (185.2 mg, 0.557 mmol) was dissolved in methanol (2 mL). Potassium carbonate (384.9 mg, 2.785 mmol, 5.0 eq) was added and the reaction was stirred for 3 h at room temperature. The reaction mixture was diluted with diethyl ether (30 mL) and washed with water (3 x 30 mL). The organic layer was dried over anhydrous sodium sulfate. The sulfate was filtered off and the solvent was removed *in vacuo*. The residue was purified by flash chromatography on silica gel (hexane) to give (*R*)-**246** (123.3 mg, 85%) as a yellow oil.

^{1}H NMR and ^{13}C NMR were in agreement with the published data.[110]

^{1}H NMR (400 MHz, $CDCl_3$): 1.80 (d, *J* = 6.6, 3H), 2.33 (s, 3H), 3.29 (s, 1H), 5.13 (q, *J* = 6.6, 1H), 6.96 (td, *J* = 7.5, 7.5, 1.1, 1H), 7.09 (m, 2H), 7.21 (dd, *J* = 8.4, 1.1, 1H), 7.35 – 7.27 (m, 3H), 7.48 (dd, *J* = 7.6, 1.7, 1H).

^{13}C NMR (101 MHz, $CDCl_3$): 21.38 (q), 22.31 (q), 65.74 (d), 80.01 (s), 81.18 (d), 86.20 (s), 87.30 (s), 112.75 (s), 115.09 (d), 119.28 (s), 121.26 (d), 128.93 (2 x d), 129.85 (d), 131.53 (2 x d), 134.01 (d), 138.55 (s), 158.87 (s).

(+)-1-Iodo-2-{[(1*R*)-1-methylprop-2-yn-1-yl]oxy}benzene (247)

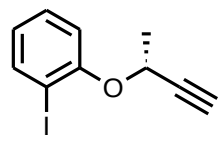

A Schlenk flask with stirring bar was charged with 2-iodophenol **240** (5.0579 g, 22.99 mmol) and triphenylphosphine (6.0301 g, 22.99 mmol, 1.0 eq). The content was dissolved in benzene (8 mL, 3 M solution) under argon and cooled to 0°C. (*S*)-Butyn-

2-ol **217** (1.90 mL, 1.6919 g, 24.14 mmol, 1.05 eq) was added while an orange solution was formed. Then diisopropyl azodicarboxylate (4.53 mL, 4.6487 g, 22.99 mmol, 1.0 eq) was added dropwise. The reaction mixture was allowed to warm up to room temperature and stirred overnight. The solvent was evaporated at reduced pressure and the residue was purified by flash chromatography on silica gel (hexane – diethyl ether 97 : 3) to provide (*R*)-**247** (5.1512 g, 82%) as white crystals melting at room temperature.

Optical rotation: $[\alpha]^{22}_{D}$ +56.6° (c 0.196, $CHCl_3$).

^{1}H NMR (400 MHz, $CDCl_3$): 1.75 (d, *J* = 6.6, 3H), 2.50 (d, *J* = 2.0, 1H), 4.86 (dq, *J* = 6.6, 6.6, 6.6, 2.0, 1H), 6.75 (dt, *J* = 7.6, 7.6, 1.4, 1H), 7.07 (dd, *J* = 8.2, 1.3, 1H), 7.30 (ddd, *J* = 8.2, 7.3, 1.6, 1H), 7.78 (dd, *J* = 7.8, 1.6, 1H).

^{13}C NMR (101 MHz, CDCl3): 22.21 (q), 65.34 (d), 74.41 (d), 82.48 (s), 87.64 (s), 114.92 (d), 123.48 (d), 129.20 (d), 139.55 (d), 156.37 (s).

IR ($CHCl_3$): 3307 vs, 3086 vw, 3067 w, 2119 w, 1582 s, 1571 s, 1470 vs, 1453 m, 1439 vs, 1377 s, 1328 s, 1286 s, 1277 vs, 1259 m, 1241 vs, 1164 m, 1129 s, 1091 vs, 1047 s, 1036 s, 1019 vs, 944 s, 923 m, 836 w, 707 w, 652 s, 643 s, 586 w, 434 w cm^{-1}.

EI MS: 272 ($M^{+\bullet}$, 47), 221 (9), 220 (100), 190 (10), 145 (10), 115 (12), 91 (14), 92 (14), 65 (16), 64 (16), 63 (16), 53 (5).

HR EI MS: calculated for $C_{10}H_9OI$ 271.9698, found 271.9694.

(+)-[(3*R*)-3-(2-Iodophenoxy)but-1-yn-1-yl][tris(1-methylethyl)]silane (249)

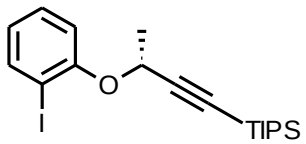

Lithium diisopropylamide was freshly prepared before the reaction: A Schlenk flask was filled with THF (10 mL) and diisopropylamine (2.81 mL, 19.88 mmol, 1.05 eq), and cooled to 0 °C under argon. A solution of *n*-butyllithium (1.6 M in hexanes, 11.8 mL, 18.93 mmol, 1.0 eq) was added dropwise. The solution was stirred at 0 °C for 40 min. The reaction was then cooled to -78 °C and a solution of (*R*)-**247** (5.151 g, 18.93 mmol) in THF (15 mL) was added dropwise, and the reaction mixture was stirred at the same temperature for 1.5 h while the yellow-brown solution was formed. Triisopropylsilyl chloride **248** (4.015 g, 20.83 mmol, 1.1 eq) was added dropwise. The resulted reaction mixture was allowed to warm up slowly to room temperature within 1 h and then stirred for additional 2 h at the same temperature. Then the reaction was carefully quenched by adding ethanol (1 mL). The solvents were evaporated under reduced pressure and the residue was purified by flash chromatography on silica gel (hexane) to give (*R*)-**249** (7.202 g, 89%) as a colorless oil.

Optical rotation: $[\alpha]^{22}_{D}$ +43° (c 0.79, $CHCl_3$).

^{1}H NMR (400 MHz, $CDCl_3$): 1.01 (s, 21H), 1.74 (d, *J* = 6.6, 3H), 4.88 (q, *J* = 6.6, 1H), 6.72 (dt, *J* = 7.7, 7.7, 1.4, 1H), 7.14 (dd, *J* = 8.3, 1.5, 1H), 7.25 (ddd, *J* = 8.2, 7.3, 1.5, 1H), 7.76 (dd, *J* = 7.8, 1.6, 1H).

^{13}C NMR (101 MHz, $CDCl_3$): 11.11 (3 x d), 18.49 (6 x q), 22.46 (q), 66.23 (d), 87.69 (s), 87.94 (s), 106.09 (s), 115.75 (d), 123.32 (d), 129.00 (d), 139.31 (d), 156.62 (s).

IR ($CHCl_3$): 3066 w, 2959 s, 2945 vs, 2892 s, 2867 vs, 2169 w, 1582 m, 1571 m, 1470 vs, 1462 s, 1439 s, 1384 w, 1375 m, 1327 m, 1285 m, 1277 m, 1258 w, 1241 s, 1163 w, 1132 s, 1091 s, 1075 m, 1046 s, 1019 s, 997 m, 950 s, 921 m, 884 s, 842 vw, 679 s, 659 s, 583 m, 433 w cm^{-1}.

EI MS: 428 ($M^{+\bullet}$, 10), 385 (23), 333 (20), 329 (10), 305 (10), 277 (15), 263 (12), 220 (14), 216 (30), 208 (55), 187 (15), 167 (25), 165 (100), 125 (30), 111 (30), 109 (25), 83 (20), 59 (20).

HR EI MS: calculated for $C_{19}H_{29}IOSi$ 428.1032, found 428.1042.

(+)-Trimethyl{[2-({(1*R*)-1-methyl-3-[tris(1-methylethyl)silyl]prop-2-yn-1-yl}oxy)phenyl]ethynyl}silane (250)

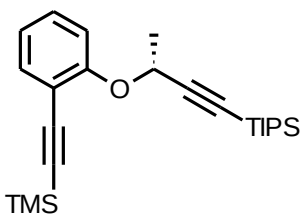

A Schlenk flask was charged with (*R*)-**249** (147.9 mg, 0.345 mmol), tetrakis(triphenylphosphine)palladium (19.9 mg, 0.017 mmol, 5 mol%) and copper iodide (5.9 mg, 0.031 mmol, 9 mol%). Freshly degassed diisopropylamine (3 mL) and ethynyltrimethylsilane **243** (98 µL, 67.8 mg, 0.690 mmol, 2.0 eq) were added under argon. The reaction mixture was stirred under argon at room temperature for 1 h. The crude reaction mixture was diluted with diethyl ether (20 mL) and filtered through a kieselguhr layer. The solvent was evaporated at reduced pressure and the residue purified by flash chromatography (hexane – diethyl ether 97 : 3) to give (*R*)-**250** (122.1 mg, 89%) as a yellowish oil.

Optical rotation: $[\alpha]^{22}_D$ +57° (c 0.334, $CHCl_3$).

^{1}H NMR (400 MHz, $CDCl_3$): 0.25 (s, 9H), 1.01 (s, 21H), 1.70 (d, *J* = 6.6, 3H), 4.94 (q, *J* = 6.6, 1H), 6.92 (td, *J* = 7.5, 7.5, 1.2, 1H), 7.16 (dd, *J* = 8.3, 1.0, 1H), 7.23 (m, 1H), 7.41 (dd, *J* = 7.6, 1.6, 1H).

^{13}C NMR (101 MHz, $CDCl_3$): 0.01 (3 x q), 11.13 (3 x d), 18.50 (6 x q), 22.41 (q), 66.17 (d), 87.21 (s), 98.49 (s), 101.42 (s), 106.57 (s), 114.39 (s), 116.75 (d), 121.60 (d), 129.44 (d), 133.50 (d), 158.89 (s).

IR ($CHCl_3$): 3076 vw, 2961 s, 2945 s, 2867 s, 2157 m, 2110 vw, 2067 w, 1596 w, 1573 w, 1463 m, 1446 m, 1409 vw, 1384 w, 1374 w, 1328 w, 1289 w, 1261 m, 1250 s, 1163 w, 1131 m, 1075 w, 1042 m, 1018 w, 997 w, 951 m, 935 w, 884 s, 862 vs, 846 vs, 700 w, 679 m, 661 m, 594 w, 455 w cm^{-1}.

EI MS: 398 ($M^{+\bullet}$, 6), 355 (8), 313 (8), 271 (9), 190 (60), 175 (100), 159 (32), 125 (18), 111 (16), 109 (13), 95 (10), 83 (15), 73 (38), 59 (21).

HR ESI MS: calculated for $C_{24}H_{39}OSi_2$ 399.2534, found 399.2533.

(+)-[(3*R*)-3-(2-Ethynylphenoxy)but-1-yn-1-yl][tris(1-methylethyl)]silane (251)

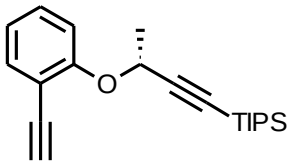

Silane (*R*)-**250** (122.1 mg, 0.306 mmol) was dissolved in methanol (3 mL) and anhydrous potassium carbonate (211.6 mg, 1.53 mmol, 5.0 eq) was added. The solution was stirred at room temperature for 2 h. The crude reaction mixture was diluted with diethyl ether (4 mL) and washed with water (3 x 10 mL). The combined organic portions were dried over anhydrous $MgSO_4$. The solvents were removed under reduced pressure and the residue was purified by flash chromatography on silica gel (hexane) to give (*R*)-**251** (92.6 mg, 93%) as a yellowish oil.

Optical rotation: $[\alpha]^{22}_D$ +41° (c 0.23, $CHCl_3$).

^{1}H NMR (400 MHz, $CDCl_3$): 1.01 (s, 21H), 1.72 (d, *J* = 6.6, 3H), 3.25 (s, 1H), 4.93 (q, *J* = 6.6, 1H), 6.92 (dt, *J* = 7.5, 7.5, 1.1, 1H), 7.18 (dd, *J* = 8.4, 1.1, 1H), 7.23 – 7.29 (m, 1H), 7.44 (dd, *J* = 7.6, 1.7, 1H).

^{13}C NMR (101 MHz, $CDCl_3$): 11.10 (3 x d), 18.47 (6 x q), 22.37 (q), 65.76 (d), 80.08 (s), 81.00 (d), 87.45 (s), 106.31 (s), 112.85 (d), 115.66 (s), 121.29 (d), 129.67 (d), 133.94 (d), 158.89 (s).

IR ($CHCl_3$): 3307 s, 3078 w, 3062 vw, 2959 s, 2945 vs, 2892 s, 2867 vs, 2169 w, 2108 w, 1596 m, 1575 w, 1487 vs, 1463 s, 1446 s, 1384 w, 1375 w, 1326 m, 1288 m, 1268 w, 1246 vs, 1164 w, 1131 s, 1109 m, 1091 s, 1074 m, 1043 s, 1018 w, 997 m, 951 s, 937 m, 884 s, 650 s, 679 s, 660 s, 614 m, 592 m, 452 w cm^{-1}.

EI MS: 326 ($M^{+\bullet}$, 3), 311 (18), 283 (18), 241 (42), 225 (16), 213 (26), 199 (30), 165 (100), 137 (14), 125 (17), 109 (16), 95 (13), 83 (11), 59 (8).

HR EI MS: calculated for $C_{21}H_{30}OSi$ 326.2066, found 326.2061.

(-)-{Ethyne-1,2-diylbis[benzene-2,1-diyloxy(3*R*)but-1-yne-3,1-diyl]}bis[tris(1-methylethyl)silane] (252)

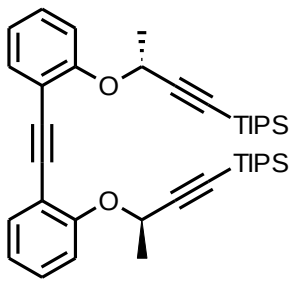

A Schlenk flask was charged with aryl iodide (*R*)-**249** (542.0 mg, 1.27 mmol), tetrakis(triphenylphosphine)palladium (73.1 mg, 0.063 mmol, 5 mol%), and copper iodide (21.7 mg, 0.114 mmol, 9 mol%). A solution of diyne (*R*)-**251** (413.1 mg, 1.27 mmol) in diisopropylamine (6 mL) was added under argon. The reaction mixture was stirred under argon at room temperature overnight. Then the crude product was filtered through a pad of silica gel (diethyl ether).

The solvents was evaporated under reduced pressure and the residue was purified by flash chromatography on silica gel (hexane – diethyl ether 95 : 5) to give (*R*,*R*)-**252** (763.2 mg, 96%) as a yellowish oil.

Optical rotation: $[\alpha]^{22}_D$ -22° (c 0.26, $CHCl_3$).

^{1}H NMR (400 MHz, $CDCl_3$): 1.01 (s, 42H), 1.74 (d, *J* = 6.6, 6H), 5.02 (q, *J* = 6.6, 2H), 6.96 (dt, *J* = 7.3, 7.3, 1.1, 2H), 7.18 (dd, *J* = 8.2, 1.1, 2H), 7.21 – 7.26 (m, 2H), 7.49 (dd, *J* = 7.3, 1.1, 2H).

^{13}C NMR (101 MHz, $CDCl_3$): 11.13 (3 x d), 18.49 (6 x q), 22.58 (q), 66.02 (d), 87.15 (s), 90.02 (s), 106.66 (s), 114.85 (s), 116.56 (d), 121.59 (d), 128.99 (d), 133.34 (d), 158.14 (s).

IR ($CHCl_3$): 3075 vw, 3062 vw, 2959 s, 2945 vs, 2892 s, 2866 vs, 2220 vw, 2168 w, 1600 w, 1593 w, 1574 w, 1496 s, 1481 m, 1463 s, 1450 s, 1384 w, 1374 w, 1327 m, 1278 m, 1260 w, 1238 s, 1164 w, 1131 s, 1114 m, 1075 w, 1091 s, 1042 m, 1018 w, 997 m, 951 s, 935 m, 884 s, 679 s, 663 s, 593 w, 454 w cm^{-1}.

EI MS: 626 ($M^{+\bullet}$, 2), 611 (5), 583 (15), 417 (100), 375 (36), 333 (28), 289 (11), 279 (13), 251 (24), 210 (83), 181 (22), 157 (17), 139 (5), 125 (30), 115 (36), 111 (33), 87 (14), 83 (16), 73 (33), 59 (30).

HR EI MS: calculated for $C_{40}H_{58}O_2Si_2$ 626.3975, found 626.3977.

(+)-1,1'-Ethyne-1,2-diylbis(2-{[(1*R*)-1-methylprop-2-yn-1-yl]oxy}benzene) (253)

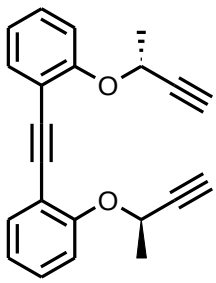

The silylated triyne (*R*,*R*)-**252** (340.6 mg, 0.862 mmol) was dissolved in THF (10 mL). A solution of *n*-tetrabutylammonium fluoride (1 M in THF, 4.1 mL, 4.14 mmol, 4.8 eq) was added under argon. The reaction was stirred at room temperature for 2 h. Then the solvent was evaporated under reduced pressure and the residue was purified by flash chromatography on a reverse phase column (methanol – water 70 : 30 to 100 : 0) to afford triyne (*R*,*R*)-**253** (258.5 mg, 95%) as a white amorphous solid.

Optical rotation: $[\alpha]^{22}_D$ +19° (c 0.40, $CHCl_3$).

^{1}H NMR (400 MHz, $CDCl_3$): 1.73 (d, J = 6.6, 6H), 2.48 (d, J = 2.0, 2H), 4.99 (dq, J = 6.6, 6.6, 6.6, 2.0, 2H), 6.99 (dt, J = 7.5, 7.5, 1.0, 2H), 7.12 (dd, J = 8.3, 0.7, 2H), 7.28 (ddd, J = 8.3, 7.5, 0.7, 2H), 7.51 (dd, J = 7.6, 1.7, 2H).

^{13}C NMR (101 MHz, $CDCl_3$): 22.26 (q), 65.16 (d), 74.07 (d), 82.91 (s), 89.94 (s), 114.71 (s), 115.88 (d), 121.82 (d), 129.23 (d), 133.51 (d), 157.81 (s).

IR ($CHCl_3$): 3307 vs, 3076 w, 3063 w, 2218 vw, 2118 w, 1600 w, 1593 m, 1575 m, 1497 vs, 1481 s, 1450 s, 1376 m, 1328 m, 1285 s, 1261 m, 1237 vs, 1164 m, 1129 s, 1112 m, 1091 vs, 1039 s, 1025 m, 945 s, 640 s cm^{-1}.

EI MS: 314 ($M^{+\bullet}$, 39), 299 (100), 284 (43), 261 (41), 255 (27), 247 (18), 231 (13), 218 (34), 215 (24), 202 (16), 189 (21), 181 (56), 165 (10), 152 (59), 126 (9), 53 (8).

HR EI MS: calculated for $C_{22}H_{18}O_2$ 314.1307, found 314.1309.

μ^1-Carbonyl-η^5-cyclopentadienyl-η^2-dimethylfumaratecobalt(I) (255)

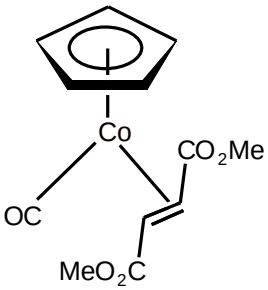

Dicarbonylcyclopentadienyl cobalt(I) **81** (1.5 mL, 2.04 g, 11.31 mmol) was added to a solution of dimethyl fumarate (1.6909 g, 11.73 mmol, 1.04 eq) in toluene (15 mL) under argon. The reaction was heated by halogen lamp irradiation to reflux for 5 h. After cooling to room temperature the volatile compounds were removed *in vacuo* and the residue was purified by flash chromatography on silica gel (hexane – ethyl acetate 70 : 30) to provide crude product **255**. The analytically pure product **255** (2.5678 g, 77%) was obtained after recrystallization from DCM/hexane (1 : 9) mixture as red-orange crystals.

^{1}H NMR was in agreement with the published data.[149]

^{1}H NMR (400 MHz, $CDCl_3$): 3.28 (d, *J* = 10.3, 1H), 3.61 (s, 3H), 3.71 (s, 3H), 3.86 (d, *J* = 10.3, 1H), 4.99 (s, 5H).

(*M*,2*R*,5*R*)/(*P*,2*R*,5*R*)-2,5-Dimethyl-2,5-dihydrobenzo[1,2-*c*:4,3-*c'*]dichromene (256)

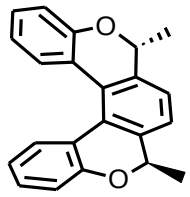

Procedure using $CpCo(CO)_2$/PPh_3 (20 mol%/40 mol%) and halogen lamp irradiation at 140 °C (Table 3.28, entry 1)

A two-necked Schlenk flask was charged with triyne (*R*,*R*)-**253** (36.4 mg, 0.116 mmol), $CpCo(CO)_2$ **81** (4.2 mg, 0.023 mmol, 20 mol%), and triphenylphosphine (12.1 mg, 0.046 mmol, 40 mol%) under argon. The content was dissolved in decane (3 mL) and the reaction mixture was heated by halogen lamp irradiation at 140 °C for 60 min. Then the solvent was removed *in vacuo* and the residue was purified by flash chromatography on silica gel (pentane – diethyl ether 95 : 5) to give a 34 : 66 mixture of products (*M*,*R*,*R*)-**256** and (*P*,*R*,*R*)-**256** (28.0 mg, 77%) as a white crystalline solid.

Procedure using $Ni(cod)_2/PPh_3$ (20 mol%/40 mol%) at rt (Table 3.28, entry 2)

A microwave vial was charged with triyne (*R*,*R*)-**253** (30.0 mg, 0.095 mmol), $Ni(cod)_2$ **254** (5.2 mg, 0.019 mmol, 20 mol%), and triphenylphosphine (10.0 mg, 0.038 mmol, 40 mol%) in glovebox. The content was dissolved in THF (2 mL) under argon. The reaction mixture was stirred at room temperature for 30 min. Then the solvent was removed *in vacuo* and the residue was purified by flash chromatography on silica gel (hexane – diethyl ether 95 : 5) to give a 34 : 66 mixture of products (*M*,*R*,*R*)-**256** and (*P*,*R*,*R*)-**256** (23.1 mg, 71%) as a white crystalline solid.

Procedure using CpCo(CO)(fum) (1.0 eq) and microwave irradiation at 200 °C (Table 3.28, entry 3)

A microwave vial was charged with triyne (*R*,*R*)-**253** (20.7 mg, 0.066 mmol) and CpCo(CO)(fum) **255** (19.5 mg, 0.066 mmol, 1.0 eq) under argon. THF (3 mL) and 1-butyl-2,3-dimethylimidazolium tetrafluoroborate (20 µL) were added. The reaction mixture was heated to 200 °C for 30 min. Then the solvent was removed *in vacuo* and the residue was purified by flash chromatography on silica gel (gradient elution hexane – ethyl acetate 100 : 0 to 95 : 5) to give a mixture of products (*M*,*R*,*R*)-**256** and (*P*,*R*,*R*)-**256** (15.4 mg, 74%) as a white crystalline solid.

Procedure using CpCo(CO)(fum) (20 mol%) and microwave irradiation at 180 °C (Table 3.28, entry 4)

A microwave vial was charged with triyne (*R*,*R*)-**253** (33.9 mg, 0.108 mmol) and CpCo(CO)(fum) **255** (6.4 mg, 0.021 mmol, 20 mol%) under argon. THF (3 mL) and 1-butyl-2,3-dimethylimidazolium tetrafluoroborate (20 µL) were added. The reaction mixture was heated to 180 °C for 20 min. Then the solvent was removed *in vacuo* and the residue was purified by flash chromatography on silica gel (hexane – diethyl ether 95 : 5) to give a mixture of products (*M*,*R*,*R*)-**256** and (*P*,*R*,*R*)-**256** (32.4 mg, 96%) as a white crystalline solid.

Mp: 183-184 °C (ethyl acetate)

Optical rotation: $[\alpha]^{22}_D$ -17° (c 0.28, $CHCl_3$).

^{1}H NMR (500 MHz, $CDCl_3$, t = 60°C): 1.58 (bs, 6H), 5.05 (bs, 2H), 6.75 (ddd, *J* = 7.8, 7.2, 1.3, 2H), 7.05 (dd, *J* = 8.1, 1.3, 2H), 7.07 (bs, 2H), 7.15 (ddd, *J* = 8.1, 7.2, 1.6, 2H), 7.41 (dd, *J* = 7.8, 1.6, 2H).

^{13}C NMR (126 MHz, $CDCl_3$, t = 60 °C): 19.36 (q), 74.70 (d), 118.41 (d), 121.11 (d), 122.60 (d), 123.76 (s), 126.87 (s), 129.09 (d), 141.39 (s), 155.10 (s).

IR ($CHCl_3$): 3044 w, 3032 w, 2984 m, 1604 m, 1584 w, 1572 w, 1488 s, 1455 s, 1442 m, 1437 m, 1420 s, 1378 m, 1370 m, 1335 m, 1326 m, 1289 w, 1279 w, 1244 vs, 1138 w, 1114 m, 1069 s, 1010 m, 946 w, 856 w, 824 m, 468 w cm^{-1}.

EI MS: 314 ($M^{+\bullet}$, 46), 299 (100), 284 (22), 269 (4), 255 (27), 239 (5), 226 (9).

HR EI MS: calculated for $C_{22}H_{18}O_2$ 314.1307, found 314.1313.

(-)-2,2'-{Ethyne-1,2-diylbis[benzene-2,1-diyloxy(3*R*)but-1-yne-3,1-diyl]}dipyridine (259)

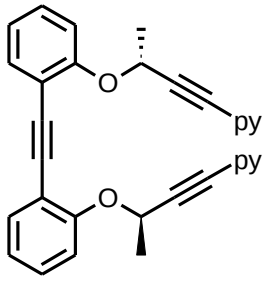

A Schlenk flask was charged with tetrakis(triphenylphosphine)palladium (31.1 mg, 0.027 mmol, 10 mol%) and copper iodide (9.2 mg, 0.048 mmol, 18 mol%). A solution of (*R*,*R*)-**253** (84.5 mg, 0.269 mmol) in diisopropyl amine (3 mL) was added under argon. 2-Bromopyridine **258** (55 µL, 89.2 mg, 0.564 mmol, 2.1 eq) was added dropwise. The reaction was stirred at room temperature overnight. The solvent was removed *in vacuo* and the residue was purified by flash chromatography on reverse phase column (methanol – water 70 : 30 to 100 : 0) to give (*R*,*R*)-**259** (104.5 mg, 83%) as a yellow amorphous solid.

Optical rotation: $[\alpha]^{22}_D$ -253° (c 0.52, $CHCl_3$).

^{1}H NMR (400 MHz, $CDCl_3$): 1.86 (d, *J* = 6.6, 6H), 5.25 (q, *J* = 6.6, 2H), 7.00 (dt, *J* = 7.5, 7.5, 1.2, 2H), 7.19 – 7.24 (m, 4H), 7.27 – 7.32 (m, 2H), 7.36 (td, *J* = 7.9, 1.1, 1.1, 2H), 7.54 (dd, *J* = 7.6, 1.6, 2H), 7.61 (dt, *J* = 7.7, 7.7, 1.8, 2H), 8.56 (ddd, *J* = 4.9, 1.7, 0.9, 2H).

^{13}C NMR (101 MHz, $CDCl_3$): 22.19 (q), 65.82 (d), 85.10 (s), 88.42 (s), 90.04 (s), 114.77 (s), 115.96 (d), 121.85 (d), 123.01 (d), 127.34 (d), 129.37 (d), 133.56 (d), 136.14 (d), 142.64 (s), 149.81 (d), 157.98 (s).

IR ($CHCl_3$): 3082 w, sh, 3060 w, 2242 w, 2220 vw, 1600 m, sh, 1585 vs, 1575 m, sh, 1564 m, 1496 s, 1481 s, 1466 vs, 1449 s, 1429 s, 1375 m, 1331 s, 1287 s, sh, 1259 s, sh, 1236 vs, 1126 s, 1151 m, 1113 m, 1094 s, sh, 1088 s, 1047 s, 1037 s, 993 m, 951 s, 631 w, 472 w, 400 w cm^{-1}.

EI MS: 468 ($M^{+\bullet}$, 100), 454 (7), 390 (4), 340 (9).

HR ESI MS: calculated for $C_{32}H_{25}O_2N_2$ 469.1911, found 469.1911.

(-)-2,2'-[(*M*,2*R*,5*R*)-2,5-dimethyl-2,5-dihydrobenzo[1,2-*c*:4,3-*c'*]dichromene-3,4-diyl]dipyridine (260)

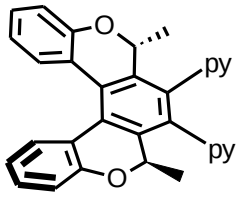

Procedure using $CpCo(CO)_2/PPh_3$ (20 mol%/40 mol%) and halogen lamp irradiation at 140 °C (Table 3.36, entry 1)

A two-necked Schlenk flask was charged with triyne (*R*,*R*)-**259** (23.4 mg, 0.050 mmol), $CpCo(CO)_2$ **81** (1.8 mg, 0.010 mmol, 20 mol%), and triphenylphosphine (5.2 mg, 0.020 mmol, 40 mol%) under argon. The content was dissolved in decane (3 mL) and the reaction mixture was heated by halogen lamp irradiation at 140 °C for 60 min. Then the solvent was removed *in vacuo* and the residue was purified by flash chromatography on silica gel (gradient elution pentane – ethyl acetate 70 : 30 to 50 : 50) to give (*R*,*R*)-**260** (11.5 mg, 49%) as a yellow amorphous solid.

Procedure using $Ni(cod)_2/PPh_3$ (20 mol%/40 mol%) at rt (Table 3.36, entry 2)

A microwave vial was charged with triyne (*R*,*R*)-**259** (26.9 mg, 0.057 mmol) $Ni(cod)_2$ **254** (3.2 mg, 0.012 mmol, 20 mol%), and triphenylphosphine (6.0 mg, 0.023 mmol, 40 mol%) in glovebox. The content was dissolved in THF (2 mL) under argon. The reaction mixture was stirred at room temperature for 6 h. Full conversion was not achieved according to TLC. Then the solvent was removed *in vacuo* and the residue was purified by flash chromatography on silica gel (gradient elution pentane – ethyl acetate 70 : 30 to 50 : 50) to give (*R*,*R*)-**260** (11.2 mg, 42%) as a yellow amorphous solid.

Procedure using CpCo(CO)(fum) (1.0 eq) and microwave irradiation at 180 °C (Table 3.36, entry 3)

A microwave vial was charged with triyne (*R*,*R*)-**259** (20.0 mg, 0.043 mmol) and CpCo(CO)(fum) **255** (12.7 mg, 0.043 mmol, 1.0 eq) under argon. THF (2 mL) and 1-butyl-2,3-dimethylimidazolium tetrafluoroborate (10 µL) were added. The reaction mixture was heated to 180 °C for 20 min. Then the solvent was removed *in vacuo* and the residue was purified by flash chromatography on silica gel (gradient elution pentane – ethyl acetate 70 : 30 to 50 : 50) to give (*R*,*R*)-**260** (14.4 mg, 72%) as a yellow amorphous solid.

Procedure using CpCo(CO)(fum) (20 mol%) and microwave irradiation at 180 °C (Table 3.36, entry 4)

A microwave vial was charged with triyne (*R*,*R*)-**259** (25.7 mg, 0.055 mmol) and CpCo(CO)(fum) **255** (3.3 mg, 0.011 mmol, 20 mol%) under argon. THF (2 mL) and 1-butyl-2,3-dimethylimidazolium tetrafluoroborate (10 µL) were added. The reaction mixture was heated to 180 °C for 20 min. Then the solvent was removed *in vacuo* and the residue was purified by flash chromatography on silica gel (gradient elution pentane – ethyl acetate 70 : 30 to 50 : 50) to give (*R*,*R*)-**260** (20.4 mg, 79%) as a yellow amorphous solid.

Optical rotation: $[\alpha]^{22}_{D}$ -381° (c 0.11, $CHCl_3$).

^{1}H NMR (500 MHz, $CDCl_3$, t = -40 °C): 0.82 (d, *J* = 6.7, 6H), 5.57 (q, *J* = 6.7, 2H), 6.72 – 6.85 (m, 4H), 7.03 (t, *J* = 8.2, 2H), 7.13 (m, 2H), 7.18 (m, 2H), 7.38 (m, 2H), 7.44 (t, *J* = 8.2, 2H), 8.66 (d, *J* = 4.4, 2H).

^{13}C NMR (126 MHz, $CDCl_3$, t = -40 °C): 18.00 (q), 71.36 (d), 119.01 (d), 120.95 (d), 121.90 (d), 122.86 (s), 125.87 (d), 126.63 (s), 129.04 (d), 129.08 (d), 134.16 (s), 136.03 (d), 138.54 (s), 149.07 (d), 152.71 (s), 156.40 (s).

IR ($CHCl_3$): 3079 w, 3065 w, 2979 m, 2865 w, 1603 m, 1589 vs, 1566 m, 1546 vw, sh, 1492 s, 1473 s, 1454 m, 1449 m, 1430 m, 1418 s, 1369 m, 1250 m, 1240 m, 1169 m, 1162 m, 1153 m, 1119 w, 1089 m, 1095 m, 1048 w, 1037 m, 1028 w, 1015 m, 995 m, 946 m, 628 w, 403 w cm^{-1}.

EI MS: 468 ($M^{+\bullet}$, 75), 453 (100), 437 (10), 409 (8), 390 (38), 374 (8), 360 (13), 331 (6), 281 (7), 234 (27), 226 (20), 219 (15), 207 (39), 204 (20), 190 (17), 188 (10), 183 (7), 179 (9), 166 (5).

HR ESI MS: calculated for $C_{32}H_{25}O_2N_2$ 469.1911, found 469.1933.

(-)-2,2'-{Ethyne-1,2-diylbis[benzene-2,1-diyloxy(3*R*)but-1-yne-3,1-diyl]}bis(*N*,*N*-dimethylpyridin-4-amine) (262)

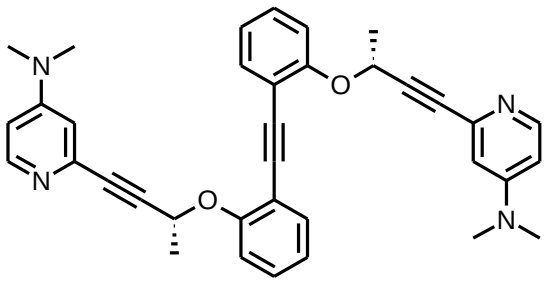

A Schlenk flask was charged with (*R*,*R*)-**253** (20.9 mg, 0.067 mmol), 2-iodo-4-(*N*,*N*-dimethylamino)pyridine **261** (34.6 mg, 0.140 mmol, 2.1 eq), tetrakis(triphenylphosphine)palladium (7.7 mg, 0.007, 10 mol%), and copper iodide (2.3 mg, 0.012 mmol, 18 mol%). The content was dissolved in degassed DMF (5 mL) and then freshly degassed diisopropylamine (47 mL, 33.6 mg, 0.332 mmol, 5.0 eq) was added under argon. The reaction mixture was stirred at 90 °C overnight. Then the reaction was diluted with diethyl ether (20 mL) and filtered through a pad of silica gel (diethyl ether). The solvents were

evaporated under reduced pressure and the residue was purified by flash chromatography on silica gel (acetone) to give (*R*,*R*)-**262** (22.6 mg, 61%) as an amorphous white solid.

Optical rotation: $[\alpha]^{22}_{D}$ -169° (c 0.18, $CHCl_3$ – MeOH 13 : 3 vol.).

^{1}H NMR (400 MHz, $CDCl_3$): 1.85 (d, *J* = 6.6, 6H), 2.94 (s, 12H), 5.20 (q, *J* = 6.6, 2H), 6.39 (dd, *J* = 6.0, 2.7, 2H), 6.60 (d, *J* = 2.7, 2H), 6.97 (dt, *J* = 7.4, 7.4, 1.4, 2H), 7.22 – 7.30 (m, 4H), 7.53 (dd, *J* = 7.6, 1.6, 2H), 8.14 (d, *J* = 6.1, 2H).

^{13}C NMR (101 MHz, $CDCl_3$): 22.31 (q), 39.05 (2 x q), 65.91 (d), 86.17 (s), 86.43 (s), 90.07 (s), 106.06 (d), 110.25 (d), 115.89 (d), 121.65 (d), 129.36 (d), 133.51 (d), 149.69 (d). Other quaternary carbons were not detected.

IR ($CHCl_3$): 3020 w, 3000 w, 2994 w, 2956 w, 2937 w, 2821 vw, 1595 vs, 1576 w, sh, 1540 w, 1508 w, sh, 1497 m, 1481 w, 1449 m, 1416 vw, 1376 w, 1329 w, 1295 w, 1233 m, 1165 vw, 1130 w, 1117 w, 1088 w, 1042 w, 997 w, 947 w, 905 vw, 812 w cm^{-1}.

EI MS: 554 ($M^{+\bullet}$, 11), 539 (8), 433 (7), 382 (40), 337 (72), 322 (100), 294 (25), 237 (16), 210 (29), 187 (9), 173 (32), 157 (11), 128 (16), 64 (8), 44 (29).

HR EI MS: calculated for $C_{36}H_{34}N_4O_2$ 554.2682, found 554.2693.

(-)-(*M*,2*R*,5*R*)-8-Methoxy-2,5-dimethyl-3,4-bis(4-methylphenyl)-2,5-dihydrobenzo[1,2-*c*:4,3-*c'*]dichromene (263)

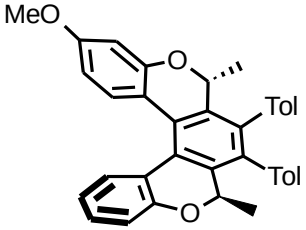

Procedure using $CpCo(CO)_2$/PPh_3 (20 mol%/40 mol%) and halogen lamp irradiation at 140 °C (Table 3.46, entry 1)

A two-necked Schlenk flask was charged with triyne (*R*,*R*)-**271** (23.6 mg, 0.045 mmol), $CpCo(CO)_2$ **81** (1.6 mg, 0.009 mmol, 20 mol%), and triphenylphosphine (4.7 mg, 0.018 mmol, 40 mol%) under argon. The content was dissolved in decane (3 mL) and the reaction mixture was heated by halogen lamp irradiation at 140 °C for 60 min. Then the solvent was removed *in vacuo* and the residue was purified by flash chromatography on silica gel (gradient elution hexane – diethyl ether 100 : 0 to 90 : 10) to give (*M*,*R*,*R*)-**263** (20.8 mg, 88%) as a yellow amorphous solid.

Procedure using $Ni(cod)_2/PPh_3$ (20 mol%/40 mol%) at rt (Table 3.46, entry 2)

A microwave vial was charged with triyne (*R*,*R*)-**271** (19.7 mg, 0.038 mmol), $Ni(cod)_2$ **254** (2.1 mg, 0.008 mmol, 20 mol%), and triphenylphosphine (3.9 mg, 0.015 mmol, 40 mol%) in glovebox. The content was dissolved in THF (2 mL) under argon. The reaction mixture was stirred at room temperature for 2 h. Then the solvent was removed *in vacuo* and the residue was purified by flash chromatography on silica gel (gradient elution hexane – diethyl ether 100 : 0 to 90 : 10) to give (*M*,*R*,*R*)-**263** (15.4 mg, 78%) as a yellow amorphous solid.

Procedure using CpCo(CO)(fum) (1.0 eq) and microwave irradiation at 180 °C (Table 3.46, entry 3)

A microwave vial was charged with triyne (*R*,*R*)-**271** (21.0 mg, 0.040 mmol) and CpCo(CO)(fum) **255** (11.9 mg, 0.040 mmol, 1.0 eq) under argon. THF (2 mL) and 1-butyl-2,3-dimethylimidazolium tetrafluoroborate (10 µL) were added. The reaction mixture was heated to 180 °C for 20 min. Then the solvent was removed *in vacuo* and the residue was purified by flash chromatography on silica gel (gradient elution hexane – diethyl ether 100 : 0 to 90 : 10) to give (*M*,*R*,*R*)-**263** (17.5 mg, 83%) as a yellow amorphous solid.

Procedure using CpCo(CO)(fum) (20 mol%) and microwave irradiation at 180 °C (Table 3.46, entry 4)

A microwave vial was charged with triyne (*R*,*R*)-**271** (20.3 mg, 0.039 mmol) and CpCo(CO)(fum) **255** (2.3 mg, 0.008 mmol, 20 mol%) under argon. THF (2 mL) and 1-butyl-2,3-dimethylimidazolium tetrafluoroborate (10 µL) were added. The reaction mixture was heated to 180 °C for 20 min. Then the solvent was removed *in vacuo* and the residue was purified by flash chromatography on silica gel (hexane – diethyl ether 90 : 10) to give (*M*,*R*,*R*)-**263** (11.6 mg, 57%) as a yellow amorphous solid.

Optical rotation: $[\alpha]^{22}_D$ -520° (c 0.14, $CHCl_3$).

^{1}H NMR (400 MHz, $CDCl_3$): 0.92 (d, *J* = 6.7, 3H), 0.95 (d, *J* = 6.7, 3H), 2.26 (s, 6H), 3.81 (s, 3H), 5.24 (q, *J* = 6.6, 1H), 5.25 (q, *J* = 6.6, 1H), 6.37 (dd, *J* = 8.7, 2.4, 1H), 6.56 (d, *J* = 2.6, 1H), 6.64 (t, *J* = 1.9, 1H), 6.66 (t, *J* = 1.9, 1H), 6.79 (m, 1H), 6.86 (d, *J* = 7.8, 2H), 6.99 (dd, *J* = 8.0, 1.0, 1H), 7.08 (d, *J* = 7.8, 2H), 7.12 – 7.17 (m, 3H), 7.36 (d, *J* = 8.7, 1H), 7.50 (dd, *J* = 7.9, 1.4, 1H).

^{13}C NMR (101 MHz, $CDCl_3$): 18.32 (q), 18.37 (q), 21.16 (q), 55.27 (q), 73.00 (d), 73.18 (d), 103.91 (d), 107.63 (d), 116.34 (s), 119.14 (d), 120.89 (d), 123.80 (s), 124.55 (s), 125.43 (s), 128.36 (2 x d), 128.55 (2 x d), 128.79 (d), 129.07 (2 x d), 129.11 (d), 130.06 (d), 130.75 (d), 130.82 (d), 134.97 (s), 134.99 (s), 135.97 (s), 135.98 (s), 136.34 (s), 137.10 (s), 137.86 (s), 139.08 (s), 153.41 (s), 154.81 (s), 160.55 (s).

IR ($CHCl_3$): 3080 w, 3046 w, 2985 m, 2840 w, 1615 s, 1605 m, 1583 m, 1565 w, 1517 m, 1503 s, 1486 m, 1461 m, 1444 m, 1425 s, 1405 vw, 1368 m, 1298 m, 1251 s, 1244 m, 1183 w, 1111 m, 1106 m, 1093 m, 1063 s, 1037 s, 1023 m, 1011 w, 947 vw, 836 m, 461 w cm^{-1}.

EI MS: 524 ($M^{+\bullet}$, 57), 509 (100), 494 (13), 479 (3), 465 (4), 451 (3), 435 (3), 262 (2), 247 (4).

HR EI MS: calculated for $C_{37}H_{32}O_3$ 524.2351, found 524.2350.

(-)-(*M*,2*R*,5*R*)-10-Methoxy-2,5-dimethyl-3,4-bis(4-methylphenyl)-2,5-dihydrobenzo[1,2-c:4,3-c']dichromenedichromene (264)

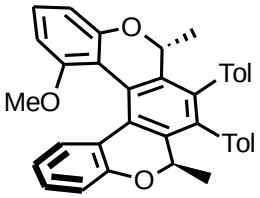

Procedure using $CpCo(CO)_2/PPh_3$ (20 mol%/40 mol%) and halogen lamp irradiation at 140 °C (Table 3.51, entry 1)

A two-necked Schlenk flask was charged with triyne (*R*,*R*)-**283** (21.0 mg, 0.040 mmol), $CpCo(CO)_2$ **81** (1.4 mg, 0.008 mmol, 20 mol%), and triphenylphosphine (4.2 mg, 0.016 mmol, 40 mol%) under argon. The content was dissolved in decane (3 mL) and the reaction mixture was heated by halogen lamp irradiation at 140 °C for 180 min. Then the solvent was removed *in vacuo* and the residue was purified by flash chromatography on silica gel (gradient elution hexane – diethyl ether 100 : 0 to 95 : 5) to give (*M*,*R*,*R*)-**264** (12.0 mg, 57%) as a yellow amorphous solid.

Procedure using $Ni(cod)_2/PPh_3$ (20 mol%/40 mol%) at rt (Table 3.51, entry 2)

A microwave vial was charged with triyne (*R*,*R*)-**283** (17.2 mg, 0.038 mmol) $Ni(cod)_2$ **254** (1.8 mg, 0.007 mmol, 20 mol%), and triphenylphosphine (3.4 mg, 0.013 mmol, 40 mol%) in glovebox. The content was dissolved in THF (2 mL) under argon. The reaction mixture was stirred at room temperature for 2 h. Then the solvent was removed *in vacuo* and the residue was purified by flash chromatography on silica gel (gradient elution hexane – diethyl ether 100 : 0 to 95 : 5) to give (*M*,*R*,*R*)-**264** (13.5 mg, 78%) as a yellow amorphous solid.

Procedure using CpCo(CO)(fum) (1.0 eq) and microwave irradiation at 180 °C (Table 3.51, entry 3)

A microwave vial was charged with triyne (*R*,*R*)-**283** (21.2 mg, 0.040 mmol) and CpCo(CO)(fum) **255** (12.0 mg, 0.040 mmol, 1.0 eq) under argon. THF (2 mL) and 1-butyl-2,3-dimethylimidazolium tetrafluoroborate (10 µL) were added. The reaction mixture was heated to 180 °C for 20 min. Then the solvent was removed *in vacuo* and the residue was purified by flash chromatography on silica gel (gradient elution hexane – diethyl ether 100 : 0 to 95 : 5) to give (*M*,*R*,*R*)-**264** (20.4 mg, 96%) as a yellow amorphous solid.

Procedure using CpCo(CO)(fum) (20 mol%) and microwave irradiation at 180 °C (Table 3.51, entry 4)

A microwave vial was charged with triyne (*R*,*R*)-**283** (21.1 mg, 0.040 mmol) and CpCo(CO)(fum) **255** (2.4 mg, 0.008 mmol, 20 mol%), under argon. THF (2 mL) and 1-butyl-2,3-dimethylimidazolium tetrafluoroborate (10 µL) were added. The reaction mixture was heated to 180 °C for 20 min. Then the solvent was removed *in vacuo* and the residue was purified by flash chromatography on silica gel (gradient elution hexane – diethyl ether 100 : 0 to 95 : 5) to give (*M*,*R*,*R*)-**264** (13.3 mg, 63%) as a yellow amorphous solid.

Optical rotation: $[\alpha]^{22}_{D}$ -402° (c 0.54, $CHCl_3$).

^{1}H NMR (400 MHz, $CDCl_3$): 0.97 (d, *J* = 6.7, 3H), 0.98 (d, *J* = 6.7, 3H), 2.24 (s, 6H), 3.12 (s, 3H), 5.24 (m, 2H), 6.39 (d, *J* = 7.7, 1H), 6.65 (dd, *J* = 7.7, 1.7, 1H), 6.70 – 6.75 (m, 3H), 6.86 (d, *J* = 7.8, 2H), 7.00 (dd, *J* = 8.0, 1.1, 1H), 7.04 – 7.07 (m, 2H), 7.10 – 7.14 (m, 3H), 7.16 – 7.20 (m, 2H).

^{13}C NMR (101 MHz, $CDCl_3$): 17.79 (q), 18.54 (q), 21.15 (q), 54.19 (q), 72.75 (d), 73.29 (d), 104.70 (d), 111.35 (d), 113.80 (s), 118.46 (d), 120.99 (d), 122.16 (s), 125.07 (d), 126.49 (s), 126.81 (s), 128.25 (d), 128.27 (d), 128.32 (d), 128.39 (d), 128.52 (d), 129.03 (d), 129.11 (d), 129.19 (d), 130.61 (d), 130.86 (d), 135.00 (s), 135.02 (s), 135.87 (s), 135.92 (2 x s), 136.49 (s), 138.00 (s), 139.14 (s), 151.82 (s), 155.21 (s), 155.92 (s).

IR ($CHCl_3$): 3082 w, 3048 w, 2984 m, 2963 m, 2840 w, 1600 s, 1582 s, 1517 m, 1481 s, 1469 s, 1458 m, 1446 m, 1437 m, 1423 s, 1405 vw, 1368 m, 1333 m, 1294 w, 1248 s, 1239 m, 1183 w, 1151 m, 1104 vs, 1063 s, 1032 m, 1023 m, 1012 w, 949 vw, 943 w, 838 m, 488 w, 459 w cm^{-1}.

EI MS: 524 ($M^{+\bullet}$, 41), 509 (100), 494 (8).

HR EI MS: calculated for $C_{37}H_{32}O_3$ 524.2351, found 524.2343.

2-Iodo-5-methoxyphenol (266)

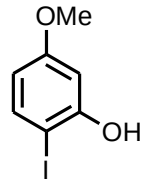

A flask was charged with iodine (2.331 g, 9.184 mmol, 1.05 eq). Water (10 mL) was added and the reaction mixture was cooled down to 0 °C. 3-Methoxyphenol **265** (1 mL, 1.0858 g, 8.747 mmol) was added and the reaction mixture was vigorously stirred while sodium bicarbonate (808.3 mg, 9.621 mmol, 1.1 eq) was added in five portions. The reaction mixture was stirred at the same temperature for 15 min and then allowed to warm up to the reaction mixture. The reaction mixture was diluted by ethyl acetate (50 mL) and washed with an 1 M solution of sodium thiosulfate (2 x 50 mL) and water (50 mL). The organic layer was dried over anhydrous sodium sulfate and the crude product was purified by flash chromatography on silica gel (hexane – ethyl acetate 90 : 10) to give **266** (1.0865 g, 50%) as a yellowish crystalline solid.

^{1}H NMR was in agreement with the published data.[119]

^{1}H NMR (400 MHz, $CDCl_3$): 3.77 (s, 3H), 5.28 (bs, 1H), 6.34 (dd, *J* = 8.8, 2.8, 1H), 6.60 (d, *J* = 2.8, 1H), 7.49 (d, *J* = 8.8, 1H).

(+)-1-Iodo-4-methoxy-2-{[(1*R*)-1-methylprop-2-yn-1-yl]oxy}benzene (267)

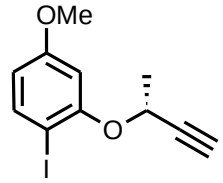

A Schlenk flask was charged with 2-iodo-5-methoxyphenol **266** (302.0 mg, 2.01 mmol) and triphenylphosphine (526.6 mg, 2.01 mmol, 1.0 eq) under argon. Then benzene (0.7 mL) and alcohol (*S*)-**217** (165 µL, 2.11 mmol, 1.05 eq) were added. The reaction was cooled to 0 °C and diisopropyl azodicarboxylate (395 µL, 2.01 mmol, 1.0 eq) was added dropwise. The reaction mixture was allowed to warm up to room temperature and stirred overnight. The solvent was evaporated under reduced pressure and the residue was purified by flash chromatography on silica gel (hexane – diethyl ether 95 : 5) to give (*R*)-**267** (466.5 mg, 77%) as a white amorphous solid.

Optical rotation: $[\alpha]^{22}_{D}$ +97° (c 0.48, $CHCl_3$).

^{1}H NMR (400 MHz, $CDCl_3$): 1.74 (d, *J* = 6.6, 3H), 2.51 (d, *J* = 2.0, 1H), 3.79 (s, 3H), 4.82 (dq, *J* = 6.6, 6.6, 6.6, 2.0, 1H), 6.37 (dd, *J* = 8.6, 2.7, 1H), 6.70 (d, *J* = 2.7, 1H), 7.62 (d, *J* = 8.6, 1H).

^{13}C NMR (101 MHz, $CDCl_3$): 22.17 (q), 55.50 (q), 65.33 (d), 74.54 (d), 76.23 (s), 82.37 (s), 102.60 (d), 108.60 (d), 139.16 (d), 157.09 (s), 161.00 (s).

IR ($CHCl_3$): 3307 s, 3088 w, 2839 w, 2118 vw, 1588 s, 1579 vs, 1481 s, 1468 s, 1443 m, 1419 m, 1406 m, 1377 m, 1327 m, 1287 s, 1255 s, 1240 m, 1170 vs, 1134 m, 1121 m, 1090 s, 1040 s, 1015 s, 982 m, 971 m, 837 m, 641 m, 586 w, 453 w cm^{-1}.

EI MS: 302 ($M^{+\bullet}$, 42), 287 (12), 250 (100), 235 (14), 221 (7), 207 (7), 175 (48), 160 (6), 132 (7), 122 (8), 107 (7), 79 (11), 63 (6), 51 (9).

HR EI MS: calculated for $C_{11}H_{11}IO_2$ 301.9804, found 301.9798.

(+)-[(3*R*)-3-(2-Iodo-5-methoxyphenoxy)but-1-yn-1-yl][tris(1-methylethyl)]silane (268)

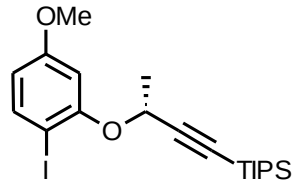

Lithium diisopropylamide was freshly prepared before the reaction: A Schlenk flask was filled with tetrahydrofuran (2 mL) and diisopropylamine (190 µL, 1.33 mmol, 1.05 eq) under argon, and cooled to 0 °C. A solution of *n*-butyllithium (1.6 M in hexanes, 0.8 mL, 1.27 mmol, 1.0 eq) was added dropwise. The solution was stirred at 0 °C for 40 min. Then the reaction was cooled to -78 °C and a solution of (*R*)-**267** (383.8 mg, 1.27 mmol) in tetrahydrofuran (3 mL) was added dropwise and stirred for 2 h at the same temperature while the yellow solution was formed. Triisopropylsilyl chloride **248** (0.31 mL, 1.40 mmol, 1.1 eq) was then added dropwise. The reaction mixture was allowed to warm up slowly to room temperature within 1 h and then stirred for additional 1 h at the same temperature. The solvents were evaporated under reduced pressure and the residue was purified by flash chromatography on silica gel (hexane) to give (*R*)-**268** (483.6 mg, 83%) as a colorless oil.

Optical rotation: $[\alpha]^{22}_D$ +94° (c 0.52, $CHCl_3$).

^{1}H NMR (400 MHz, $CDCl_3$): 1.01 (s, 21H), 1.73 (d, *J* = 6.6, 3H), 3.76 (s, 3H), 4.85 (q, *J* = 6.6, 1H), 6.35 (dd, *J* = 8.7, 2.7, 1H), 6.76 (d, *J* = 2.7, 1H), 7.59 (d, *J* = 8.7, 2H).

^{13}C NMR (101 MHz, $CDCl_3$): 11.09 (3 x d), 18.48 (6 x q), 22.48 (q), 55.42 (q), 66.22 (d), 76.47 (s), 87.73 (s), 102.97 (d), 106.05 (s), 108.93 (d), 138.91 (d), 157.40 (s), 161.01 (s).

IR ($CHCl_3$): 3088 vw, 2960 s, 2945 vs, 2893 s, 2867 vs, 2840 m, 2169 w, 1590 s, sh, 1580 s, 1480 s, 1466 s, 1443 m, 1419 m, 1405 m, 1384 w, 1375 w, 1324 m, 1278 m, 1254 m, 1239 w, 1170 s, 1133 m, 1126 m, 1090 s, 1075 w, 1045 s, 1015 s, 997 m, 983 m, 973 m, 883 s, 837 w, 679 s, 661 m, 587 w, 454 w cm^{-1}.

EI MS: 458 ($M^{+\bullet}$, 11), 363 (5), 331 (22), 289 (11), 250 (100), 245 (8), 217 (5), 205 (5), 165 (5), 122 (7), 109 (6), 95 (6), 83 (5), 59 (4).

HR EI MS: calculated for $C_{20}H_{31}IO_2Si$ 458.1138, found 458.1132.

(+)-[(3*R*)-3-(2-{[4-Methoxy-2-({(1*R*)-1-methyl-3-[tris(1-methylethyl)silyl]prop-2-yn-1-yl}oxy)phenyl]ethynyl}phenoxy)but-1-yn-1-yl][tris(1-methylethyl)]silane (269)

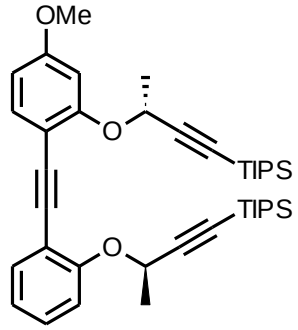

A Schlenk flask was charged with aryl iodide (*R*)-**268** (138.4 mg, 0.424 mmol), tetrakis(triphenylphosphine)palladium (24.5 mg, 0.021 mmol, 5 mol%), and copper iodide (7.3 mg, 0.038 mmol, 9 mol%). A solution of diyne (*R*)-**251** (194.3 mg, 0.424 mmol, 1.0 eq) in diisopropylamine (3 mL) was added under argon. The reaction mixture was stirred under argon at room temperature overnight. The crude product was filtered through a pad of silica gel (diethyl ether). The solvent was evaporated under reduced pressure and the residue was purified by flash chromatography on silica gel (hexane – diethyl ether 95 : 5) to give (*R*,*R*)-**269** (261.6 mg, 94%) as a yellowish oil.

Optical rotation: $[\alpha]^{22}_{D}$ +9° (c 0.48, $CHCl_3$).

^{1}H NMR (400 MHz, $CDCl_3$): 1.01 (s, 21H), 1.02 (s, 21H), 1.74 (d, *J* = 6.6, 6H), 3.78 (s, 3H), 5.01 (q, *J* = 6.4, 1H), 5.02 (q, *J* = 6.4, 1H), 6.52 (dd, *J* = 8.5, 2.4, 1H), 6.76 (d, *J* = 2.4, 1H), 6.92 – 6.96 (m, 1H), 7.16 – 7.23 (m, 2H), 7.39 (d, *J* = 8.5, 1H), 7.46 (dd, *J* = 7.6, 1.5, 1H).

^{13}C NMR (101 MHz, $CDCl_3$): 11.10 (3 x d), 18.47 (6 x q), 22.57 (q), 22.58 (q), 55.26 (q), 66.00 (d), 66.06 (d), 87.02 (s), 87.19 (s), 88.60 (s), 90.11 (s), 103.19 (d), 106.59 (s), 106.74 (s), 107.13 (s), 107.31 (d), 115.20 (s), 116.64 (d), 121.60 (d), 128.59 (d), 133.11 (d), 133.95 (d), 157.94 (s), 159.38 (s), 160.63 (s).

IR ($CHCl_3$): 3075 vw, 3060 vw, 2960 s, 2945 vs, 2892 s, 2867 vs, 2840 m, 2215 w, 2168 w, 1609 s, 1595 m, 1572 m, 1507 s, 1485 m, 1465 s, 1446 s, 1429 w, 1418 w, 1384 w, 1374 w, 1324 m, 1283 m, 1253 s, 1235 s, 1170 m, 1130 s, 1121 s, 1091 s, 1075 m, 1041 s, 1018 w, 997 m, 984 m, 973 w, 951 m, 884 s, 840 w, 824 w, 679 s, 660 m, 470 w cm^{-1}.

EI MS: 656 ($M^{+\bullet}$, 17), 613 (18), 531 (8), 499 (7), 447 (100), 405 (30), 363 (16), 319 (5), 281 (8), 240 (68), 225 (22), 211 (28), 196 (11), 125 (19), 115 (21), 83 (12), 73 (18), 59 (18).

HR EI MS: calculated for $C_{41}H_{60}O_3Si_2$ 656.4081, found 656.4083.

(+)-4-Methoxy-2-{[(1*R*)-1-methylprop-2-yn-1-yl]oxy}-1-[(2-{[(1*R*)-1-methylprop-2-yn-1-yl]oxy}phenyl)ethynyl]benzene (270)

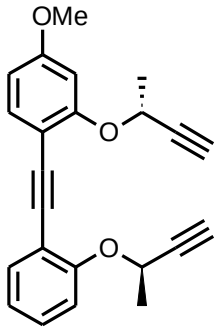

Silane (*R*,*R*)-**269** (268.0 mg, 0.408 mmol) was dissolved in tetrahydrofuran (5 mL) under argon. A solution of *n*-tetrabutylammonium fluoride (1 M, 2.0 mL, 2.04 mmol, 5.0 eq) in tetrahydrofuran was added. The reaction was stirred at room temperature for 2 h. The solvent was evaporated under reduced pressure and the residue was purified by flash chromatography on the reverse phase column (methanol – water 70 : 30 to 100 : 0) providing triyne (*R*,*R*)-**270** (110.0 mg, 78%) as a pale yellow amorphous solid.

Optical rotation: $[\alpha]^{22}_{D}$ +46° (c 0.44, $CHCl_3$).

^{1}H NMR (400 MHz, $CDCl_3$): 1.73 (d, *J* = 6.6, 6H), 2.47 (d, *J* = 2.0, 1H), 2.50 (d, *J* = 2.0, 1H), 3.80 (s, 3H), 4.99 (m, 2H), 6.54 (dd, *J* = 8.5, 2.4, 1H), 6.70 (d, *J* = 2.4, 1H), 6.98 (dt, *J* = 7.5, 7.5, 1.1, 1H), 7.11 (dd, *J* = 8.3, 0.9, 1H), 7.25 (ddd, J = 8.3, 7.5, 1.7, 1H), 7.42 (d, J = 8.5, 1H), 7.48 (ddd, *J* = 8.3, 7.6, 1.7, 1H).

^{13}C NMR (101 MHz, $CDCl_3$): 22.22 (q), 22.26 (q), 55.39 (q), 65.19 (d), 65.21 (d), 74.00 (d), 74.22 (d), 82.79 (s), 82.99 (s), 88.49 (s), 90.04 (s), 102.91 (d), 107.02 (d), 115.10 (s), 116.03 (d), 121.85 (d), 128.84 (d), 133.31 (d), 134.17 (d), 157.64 (s), 159.00 (s), 160.65 (s).

IR ($CHCl_3$): 3307 vs, 3074 vw, 3061 vw, 2840 w, 2215 w, 2118 vw, 1610 vs, 1595 m, 1573 m, 1507 vs, 1485 s, 1466 m, 1446 s, 1429 m, 1419 w, 1376 m, 1326 m, 1284 s, 1253 s, 1234 s, 1169 s, 1122 s, 1091 vs, 1037 vs, 983 w, 972 w, 944 m, 839 w, 824 m, 680 m, 640 s, 471 w cm^{-1}.

ESI MS: 383 ($[M+K]^+$), 367 ($[M+Na]^+$), 345 ($[M+H]^+$).

HR ESI MS: calculated for $C_{23}H_{21}O_3$ 345.1485, found 345.1486.

(-)-4-Methoxy-2-{[(1*R*)-1-methyl-3-(4-methylphenyl)prop-2-yn-1-yl]oxy}-1-[(2-{[(1*R*)-1-methyl-3-(4-methylphenyl)prop-2-yn-1-yl]oxy}phenyl)ethynyl]benzene (271)

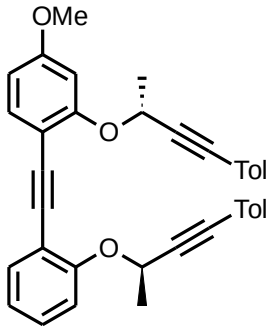

A Schlenk flask was charged with triyne (*R*,*R*)-**270** (81.0 mg, 0.235 mmol), 4-iodotoluene **218** (107.7 mg, 0.494 mmol, 2.1 eq), tetrakis(triphenylphosphine)palladium (27.2 mg, 0.024 mmol, 10 mol%), and copper iodide (8.1 mg, 0.042 mmol, 18 mol%). Then freshly degassed diisopropylamine (4 mL) was added under argon. The reaction mixture was stirred at room temperature for 1.5 h. The reaction was diluted with diethyl ether (20 mL) and filtered through a pad of silica gel (diethyl ether). The solvent

was evaporated under reduced pressure and the residue was purified by flash chromatography on silica gel (hexane – diethyl ether 90 : 10) to give (*R*,*R*)-**271** (113.1 mg, 92%) as a pale brown amorphous solid.

Optical rotation: $[\alpha]^{22}_{D}$ -174° (c 0.15, $CHCl_3$).

^{1}H NMR (400 MHz, $CDCl_3$): 1.81 (d, *J* = 6.6, 6H), 2.31 (s, 6H), 3.79 (s, 3H), 5.19 (q, *J* = 6.5, 1H), 5.21 (q, *J* = 6.3, 1H), 6.53 (dd, *J* = 8.5, 2.4, 1H), 6.80 (d, *J* = 2.4, 1H), 6.97 (dt, *J* = 7.4, 7.4, 1.1, 1H), 7.06 (m, 4H), 7.19 (dd, *J* = 8.3, 0.9, 1H), 7.23 – 7.28 (m, 5H), 7.44 (d, *J* = 8.5, 1H), 7.51 (dd, *J* = 7.6, 1.6, 1H).

^{13}C NMR (101 MHz, $CDCl_3$): 21.39 (q), 22.46 (q), 22.48 (q), 55.38 (q), 66.20 (d), 66.24 (d), 86.02 (s), 86.23 (s), 87.58 (s), 87.79 (s), 88.67 (s), 90.19 (s), 102.97 (d), 107.17 (d), 107.20 (s), 115.26 (s), 116.33 (d), 119.43 (s), 119.49 (s), 121.69 (d), 128.81 (d), 128.91 (2 x d), 128.94 (2 x d), 131.56 (2 x d), 131.57 (2 x d), 133.29 (d), 134.12 (d), 138.42 (s), 138.49 (s), 157.98 (s), 159.37 (s), 160.67 (s).

IR ($CHCl_3$): 3074 vw, 3055 vw, 2840 w, 2233 w, 2218 w, 1609 s, 1595 m, 1572 m, 1509 vs, 1485 m, 1466 m, 1446 s, 1428 m, 1418 w, 1407 w, 1375 w, 1329 m, 1298 s, 1283 m, 1252 s, 1234 s, 1168 s, 1121 m, 1086 s, 1035 s, 1021 m, 982 w, 946 w, 837 w, 819 s, 710 vw, 471 w cm^{-1}.

ESI MS: 563 ($[M+K]^+$), 547 ($[M+Na]^+$), 525 ($[M+H]^+$).

HR ESI MS: calculated for $C_{37}H_{33}O_3$ 525.2424, found 525.2425.

2-Iodo-3-methoxyphenol (272)

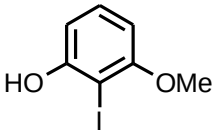

Carbamate **278** (2.0181 g, 9.64 mmol) was dissolved in diethyl ether (90 mL) under argon and cooled to 0 °C. *N*,*N*,*N*′,*N*′-Tetramethylethylenediamine (1.58 mL, 1.2332 g, 10.61 mmol, 1.1 eq) and trimethylsilyl trifluoromethanesulfonate (1.92 mL, 2.358 g, 10.61 mmol, 1.1 eq) were added dropwise. The reaction mixture was allowed to warm up to room temperature and stirred for 30 min at the same temperature. Then the reaction mixture was cooled down to -78 °C and *N*,*N*,*N*′,*N*′-tetramethylethylenediamine (2.87 mL, 2.2422 g, 19.29 mmol, 2.0 eq) and a solution of *t*-butyllithium (1.7 M in hexanes, 14.2 mL, 24.11 mmol, 2.5 eq) were added dropwise. The reaction mixture was stirred at this temperature for 1 h before a solution of iodine (2.4480 g, 9.64 mmol, 1.0 eq) in THF (9 mL) was added dropwise. The reaction was stirred for 2 h at -78 °C and then allowed to warm up slowly to room temperature and stirred at this temperature for additional 30 min. The reaction was quenched by an addition of aqueous ethanol (96%, 1 mL) and evaporated to dryness. The residue was dissolved in ethanol (90 mL) and an aqueous solution of NaOH (2 N, 19.3 mL, 38.58 mmol, 4.0 eq) was added. The reaction mixture was stirred at room temperature for 2 h. The crude product was extracted by diethyl ether (3 x 80 mL) and washed with solution of sodium thiosulfate (1 M, 3 x 80 mL). The organic

layer was dried over anhydrous magnesium sulfate. The product was purified by flash chromatography on silica gel (gradient elution hexane – diethyl ether 100 : 0 to 80 : 20) to give **272** (1.3497 g, 56%) as a colorless oil.

^{1}H NMR was in agreement with the published data.[124]

^{1}H NMR (400 MHz, $CDCl_3$): 3.87 (s, 3H), 5.72 (bs, 1H), 6.38 (dd, *J* = 8.2, 1.2, 1H), 6.66 (dd, *J* = 8.2, 1.2, 1H), 7.17 (t, *J* = 8.2, 1H).

3-Methoxyphenyl propan-2-ylcarbamate (278)

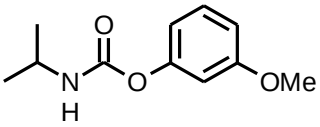

3-Methoxyphenol **276** (5 mL, 5.4288 g, 43.73 mmol) and 4-(dimethylamino)pyridine (534.3 mg, 4.373 mmol, 0.1 eq) were dissolved in THF (30 mL) under argon and the reaction mixture was cooled down to 0 °C. Prop-2-yl isocyanate **277** (4.8 mL, 4.0937 g, 48.10 mmol, 1.1 eq) was added dropwise. The reaction mixture was stirred at 0 °C for 10 min and then warmed up to 60 °C and stirred at the same temperature for 48 h. The reaction mixture was diluted by diethyl ether (70 mL) and washed with 2 M hydrochloric acid (3 x 100 mL). The organic layer was washed with an aqueous solution of sodium bicarbonate (3 x 50 mL) and dried over anhydrous sodium sulfate. The solvent was removed *in vacuo* and the residue was purified by flash chromatography on silica gel (gradient elution hexane – ethyl acetate 100 : 0 to 70 : 30) to give **278** (8.7146 g, 95%) as a white crystalline solid.

^{1}H NMR was in agreement with the published data.[124]

^{1}H NMR (400 MHz, $CDCl_3$): 1.23 (d, *J* = 6.5, 6H), 3.79 (s, 3H), 3.89 (m, 1H), 4.87 (bs, 1H), 6.69 (t, *J* = 2.3, 1H), 6.71 – 6.77 (m, 2H), 7.23 (d, *J* = 8.2, 1H).

(+)-2-Iodo-1-methoxy-3-{[(1*R*)-1-methylprop-2-yn-1-yl]oxy}benzene (279)

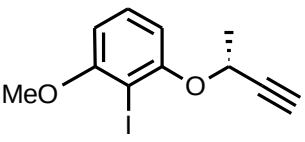

A Schlenk flask was charged with 2-iodo-3-methoxyphenol **272** (498.4 mg, 1.79 mmol) and triphenylphosphine (470.4 mg, 1.790 mmol, 1.0 eq) under argon. Then benzene (1 mL) and alcohol (*S*)-**217** (148 µL, 1.88 mmol, 1.05 eq) were added. The reaction was cooled to 0 °C and diisopropyl azodicarboxylate (353 µL, 1.79 mmol, 1.0 eq) was added dropwise. The reaction mixture was allowed to warm up to room temperature and stirred overnight. The solvent was evaporated under reduced pressure and the residue was purified by flash

chromatography on silica gel (hexane – diethyl ether 95 : 5) to give (*R*)-**279** (440.4 mg, 81%) as a colorless oil.

Optical rotation: $[\alpha]^{22}_D$ +42° (c 0.42, $CHCl_3$).

^{1}H NMR (400 MHz, $CDCl_3$): 1.75 (d, *J* = 6.6, 3H), 2.49 (d, *J* = 2.0, 1H), 3.88 (s, 3H), 4.88 (dq, *J* = 6.6, 6.6, 6.6, 2.0, 1H), 6.53 (dd, *J* = 8.3, 1.0, 1H), 6.72 (dd, *J* = 8.3, 1.0, 1H), 7.25 (t, *J* = 8.3, 1H).

^{13}C NMR (101 MHz, $CDCl_3$): 22.22 (q), 56.56 (q), 65.43 (d), 74.24 (d), 79.62 (s), 82.63 (s), 104.89 (d), 107.78 (d), 129.50 (d), 157.79 (s), 159.63 (s).

IR ($CHCl_3$): 3307 s, 3077 vw, 2968 w, 2941 m, 2841 w, 2118 vw, 1584 s, 1571 m, 1467 vs, 1446 m, 1435 s, 1377 m, 1328 m, 1290 m, 1252 vs, 1235 m, 1151 w, 1127 s, 1096 s, 1035 m, 975 w, 961 w, 883 w, 704 m, 643 m, 570 vw, 522 vw cm^{-1}.

EI MS: 302 ($M^{+\bullet}$, 47), 287 (100), 272 (12), 250 (36), 244 (5), 235 (5), 207 (6), 175 (11), 161 (11), 131 (5), 128 (16), 107 (7).

HR EI MS: calculated for $C_{11}H_{11}IO_2$ 301.9804, found 301.9812.

(+)-[(3*R*)-3-(2-Iodo-3-methoxyphenoxy)but-1-yn-1-yl][tris(1-methylethyl)]silane (280)

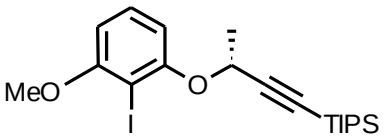

Lithium diisopropylamide was freshly prepared before the reaction: A Schlenk flask was filled with tetrahydrofuran (1 mL) and diisopropylamine (100 µL, 0.71 mmol, 1.05 eq) under argon, and cooled to 0 °C. A solution of *n*-butyllithium (1.6 M in hexanes, 0.42 mL, 0.680 mmol, 1.0 eq) was added dropwise. The solution was stirred at 0 °C for 30 min. Then the reaction was cooled to -78 °C and a solution of (*R*)-**279** (204.6 mg, 0.680 mmol) in tetrahydrofuran (3 mL) was added dropwise and stirred for 2 h at the same temperature while the yellow solution was formed. Triisopropylsilyl chloride **248** (158 µL, 0.740 mmol, 1.1 eq) was then added dropwise. The reaction mixture was stirred at -78 °C for 30 min and then it was allowed to warm up slowly to room temperature within 1 h, and stirred for additional 30 min at the same temperature. The solvents were evaporated under reduced pressure and the residue was purified by flash chromatography on silica gel (hexane) to give (*R*)-**280** (282.1 mg, 91%) a yellowish oil.

Optical rotation: $[\alpha]^{22}_D$ +26° (c 0.53, $CHCl_3$).

^{1}H NMR (400 MHz, $CDCl_3$): 1.01 (s, 21H), 1.74 (d, *J* = 6.6, 3H), 3.88 (s, 3H), 4.88 (q, *J* = 6.6, 1H), 6.51 (dd, *J* = 8.3, 1.0, 1H), 6.81 (dd, *J* = 8.3, 1.0, 1H), 7.21 (t, *J* = 8.3, 1H).

^{13}C NMR (101 MHz, $CDCl_3$): 11.09 (3 x d), 18.48 (6 x q), 22.48 (q), 56.54 (q), 66.37 (d), 79.92 (s), 87.44 (s), 104.73 (d), 106.26 (s), 108.67 (d), 129.27 (d), 158.08 (s), 159.50 (s).

IR ($CHCl_3$): 3087 vw, 2960 s, 2944 vs, 2867 vs, 2842 m, 2170 w, 1586 s, 1571 m, 1467 vs, 1445 m, 1435 s, 1375 m, 1384 w, 1368 w, 1327 m, 1290 m, 1251 vs, 1240 m, 1151 w, 1130 s, 1094 vs, 1041 m, 1021 m, 997 m, 978 m, 965 w, 884 s, 704 w, 679 s, 661 m, 575 w, 522 vw cm^{-1}.

EI MS: 458 ($M^{+\bullet}$, 3), 415 (14), 363 (10), 331 (16), 273 (9), 250 (100), 245 (19), 217 (8), 203 (11), 165 (44), 137 (11), 125 (15), 111 (15), 95 (13), 83 (12), 59 (11).

HR EI MS: calculated for $C_{20}H_{31}IO_2Si$ 458.1138, found 458.1131.

(-)-[(3*R*)-3-(2-{[2-Methoxy-6-({(1*R*)-1-methyl-3-[tris(1-methylethyl)silyl]prop-2-yn-1-yl}oxy)phenyl]ethynyl}phenoxy)but-1-yn-1-yl][tris(1-methylethyl)]silane (281)

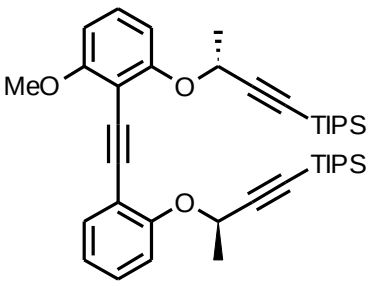

A Schlenk flask was charged with diyne (*R*,*R*)-**251** (147.8 mg, 0.453 mmol), tetrakis(triphenylphosphine)palladium (26.2 mg, 0.023 mmol, 5 mol%), and copper iodide (7.8 mg, 0.041 mmol, 9 mol%). A solution of iodide (+)-(*R*)-**31** (207.5 mg, 0.453 mmol, 1.0 eq) in diisopropylamine (3 mL) was added under argon. The reaction mixture was stirred at room temperature overnight. The crude product was filtered through a pad of silica gel (diethyl ether). The solvent was evaporated under reduced pressure and the residue was purified by flash chromatography on silica gel (hexane – diethyl ether 95 : 5) to give triyne (*R*,*R*)-**281** (141.6 mg, 48%) as a yellowish oil.

Optical rotation: $[\alpha]^{22}_D$ -50° (c 0.29, $CHCl_3$).

^{1}H NMR (400 MHz, $CDCl_3$): 1.01 (bs, 42H), 1.74 (d, *J* = 6.7, 3H), 1.76 (d, *J* = 6.7, 3H) 3.89 (s, 3H), 5.00 (q, *J* = 6.6, 1H), 5.08 (q, *J* = 6.6, 1H), 6.56 (d, *J* = 8.4, 1H), 6.84 (d, *J* = 8.3, 1H), 6.93 – 6.99 (m, 1H), 7.15 – 7.24 (m, 3H), 7.51 (m, 1H).

^{13}C NMR (101 MHz, $CDCl_3$): 11.11 (6 x d), 18.48 (12 x q), 22.55 (q), 22.58 (q), 56.07 (q), 66.04 (d), 66.22 (d), 86.21 (s), 86.97 (s), 87.0 (s), 94.37 (s), 104.20 (s), 104.52 (d), 106.72 (s), 106.85 (s), 109.09 (d), 115.45 (s), 117.26 (d), 121.70 (d), 128.75 (d), 128.94 (d), 133.38 (d), 158.01 (s), 159.53 (s), 161.18 (s).

IR ($CHCl_3$): 3062 vw, 2960 s, 2945 vs, 2866 vs, 2858 w, 2216 vw, 2168 w, 1600 w, sh, 1591 m, 1582 m, 1572 m, 1495 m, 1470 vs, 1438 m, 1444 m, 1384 w, 1374 w, 1327 m, 1294 w, 1254 s, 1240 m, 1163 w, 1131 s, 1102 vs, 1092 s, 1073 m, 1042 m, 1018 w, 997 m, 951 m, 934 w, 918 m, 884 s, 679 s, 661 m, 582 w, 511 w, 454 w cm^{-1}.

EI MS: 656 ($M^{+\bullet}$, 6), 641 (7), 613 (8), 555 (7), 499 (8), 447 (69), 433 (7), 405 (54), 363 (28), 319 (8), 309 (8), 281 (11), 275 (8), 240 (100), 225 (43), 211 (6), 196 (12), 167 (33), 157 (16), 125 (39), 111 (43), 109 (29), 83 (26), 73 (34), 59 (35), 55 (6).

HR EI MS: calculated for $C_{41}H_{60}O_3Si_2$ 656.4081, found 656.4083.

(+)-1-Methoxy-3-{[(1*R*)-1-methylprop-2-yn-1-yl]oxy}-2-[(2-{[(1*R*)-1-methylprop-2-yn-1-yl]oxy}phenyl)ethynyl]benzene (282)

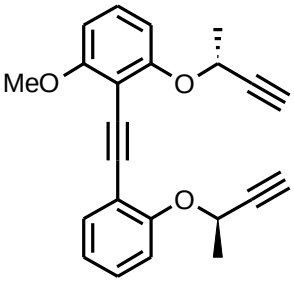

Silane (*R*,*R*)-**281** (141.6 mg, 0.215 mmol) was dissolved in tetrahydrofuran (5 mL). A solution of *n*-tetrabutylammonium fluoride (1 M in THF, 1.0 mL, 1.03 mmol, 4.8 eq) was added under argon. The reaction was stirred at room temperature for 2 h. The solvent was evaporated under reduced pressure and the residue was purified by flash chromatography (hexane – diethyl ether 90 : 10) to provide (*R*,*R*)-**282** (73.4 mg, 99%) as a pale yellow amorphous solid.

Optical rotation: $[\alpha]^{22}_D$ +34° (c 0.42, $CHCl_3$).

^{1}H NMR (400 MHz, $CDCl_3$): 1.73 (d, *J* = 6.6, 3H), 1.75 (d, *J* = 6.6, 3H), 2.46 (d, *J* = 2.0, 1H), 2.47 (d, *J* = 2.0, 1H), 3.90 (s, 3H), 4.99 (dq, *J* = 6.6, 6.6, 6.6, 2.0, 1H), 5.10 (dq, *J* = 6.6, 6.6, 6.6, 2.0, 1H), 6.59 (dd, *J* = 8.4, 0.5, 1H), 6.77 (dd, *J* = 8.4, 0.6, 1H), 7.00 (dt, *J* = 7.5, 7.5, 1.1, 1H), 7.12 (dd, *J* = 8.3, 0.9, 1H), 7.21 (t, *J* = 8.4, 1H), 7.26 (ddd, *J* = 8.3, 7.4, 1.7, 1H), 7.53 (dd, *J* = 7.6, 1.7, 1H).

^{13}C NMR (101 MHz, $CDCl_3$): 22.27 (q), 22.28 (q), 56.11 (q), 65.28 (d), 65.40 (d), 73.91 (d), 73.96 (d), 83.01 (s), 83.16 (s), 86.21 (s), 94.27 (s), 104.18 (s), 104.80 (d), 108.48 (d), 115.46 (s), 116.79 (d), 121.99 (d), 128.98 (d), 129.21 (d), 133.59 (d), 157.68 (s), 159.25 (s), 161.34 (s).

IR ($CHCl_3$): 3307 s, 3063 w, 2840 w, 2216 w, 2118 w, 1599 m, 1590 m, 1580 s, 1573 s, 1495 s, 1471 vs, 1445 s, 1438 s, 1376 m, 1328 m, 1295 m, 1254 s, 1237 s, 1164 w, 1129 s, 1103 vs, 1090 vs, 1038 s, 944 m, 640 s, 576 w cm^{-1}.

EI MS: 344 ($M^{+\bullet}$, 14), 329 (60), 314 (33), 291 (35), 276 (22), 259 (14), 248 (14), 231 (8), 205 (13), 196 (21), 181 (12), 168 (14), 149 (100), 139 (30), 113 (8), 86 (8), 69 (10), 57 (13), 53 (16).

HR EI MS: calculated for $C_{23}H_{20}O_3$ 344.1412, found 344.1406.

(-)-1-Methoxy-3-{[(1*R*)-1-methyl-3-(4-methylphenyl)prop-2-yn-1-yl]oxy}-2-[(2-{[(1*R*)-1-methyl-3-(4-methylphenyl)prop-2-yn-1-yl]oxy}phenyl)ethynyl]benzene (283)

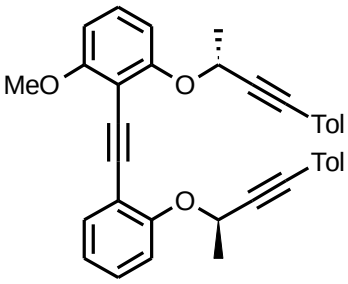

A Schlenk flask was charged with (*R*,*R*)-**282** (40.7 mg, 0.118 mmol), 4-iodotoluene **218** (54.1 mg, 0.248 mmol, 2.1 eq), tetrakis(triphenylphosphine)palladium (13.7 mg, 0.012 mmol, 10 mol%), and copper iodide (4.1 mg, 0.021 mmol, 18 mol%). Then freshly degassed diisopropylamine (4 mL) was added under argon. The reaction mixture was stirred at room temperature for 2 h. The reaction was diluted with diethyl ether (20 mL) and filtered through a pad of silica gel (diethyl ether). The solvent was evaporated under reduced pressure and the residue was purified by flash chromatography on silica gel (hexane – diethyl ether 90 : 10) to give (*R*,*R*)-**283** (53.6 mg, 86%) as a pale brown amorphous solid.

Optical rotation: $[\alpha]^{22}_{D}$ -182° (c 0.17, $CHCl_3$).

^{1}H NMR (400 MHz, $CDCl_3$): 1.82 (t, *J* = 6.3, 6H), 2.31 (s, 6H), 3.90 (s, 3H), 5.20 (q, *J* = 6.5, 1H), 5.29 (q, *J* = 6.5, 1H), 6.58 (d, *J* = 8.3, 1H), 6.85 (d, *J* = 8.1, 1H), 6.98 (dt, *J* = 7.5, 7.5, 1.2, 1H), 7.07 (d, *J* = 8.0, 4H), 7.19 – 7.28 (m, 7H), 7.56 (dd, *J* = 7.6, 1.6, 1H).

^{13}C NMR (101 MHz, $CDCl_3$): 21.42 (2 x q), 22.43 (q), 22.46 (q), 56.11 (q), 66.19 (d), 85.92 (s), 85.93 (s), 86.28 (s), 87.77 (s), 87.89 (s), 94.41 (s), 104.16 (s), 104.52 (d), 108.70 (d), 115.42 (s), 116.75 (d), 119.45 (s), 119.52 (s), 121.73 (d), 128.90 (d), 128.96 (d), 129.17 (d), 131.53 (d), 131.56 (d), 133.53 (d), 138.37 (s), 138.42 (s), 157.96 (s), 159.54 (s), 161.27 (s).

IR ($CHCl_3$): 3057 vw, 2842 w, 2236 w, 2226 w, 1599 w, 1590 m, 1581 m, 1574 m, 1510 s, 1495 m, 1470 vs, 1445 m, 1438 m, 1408 vw, 1375 w, 1331 m, 1295 w, 1252 s, 1239 m, 1164 w, 1121 m, 1101 vs, 1088 s, 1036 m, 1020 w, 819 s, 724 w cm^{-1}.

EI MS: 524 ($M^{+\bullet}$, 28), 509 (64), 494 (9), 382 (42), 367 (83), 351 (17), 337 (7), 291 (7), 240 (34), 225 (27), 143 (100), 128 (83), 115 (72), 91 (13), 63 (11), 51 (6).

HR EI MS: calculated for $C_{37}H_{32}O_3$ 524.2351, found 524.2353.

Trimethyl{[(1*S*)-1-methylprop-2-yn-1-yl]oxy}silane (284)

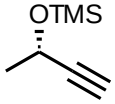

A microwave vial was charged with alcohol (*S*)-**217** (1 mL, 894 mg, 12.755 mmol), hexamethyldisilazane (1.33 mL, 1.029 g, 6.378 mmol, 0.5 eq), and the vial was capped. The reaction mixture was reacted in a microwave reactor at 300 W (using a pressure-air cooling

system keeping reaction temperature up to 100 °C) for 15 min. The reaction provides (*S*)-**284** (1.724 g, 95%) as a colourless liquid in a satisfactory purity as checked by ^{1}H NMR and GC analysis.

^{1}H NMR was in agreement with the published data.[150]

^{1}H NMR (400 MHz, $CDCl_3$): 0.17 (s, 9H), 1.43 (d, *J* = 7.1, 3H), 2.38 (d, *J* = 1.6, 1H), 4.50 (qd, *J* = 7.1, 1.6, 1H).

(-)-(2*S*)-4-[tris(1-methylethyl)silyl]but-3-yn-2-ol (285)

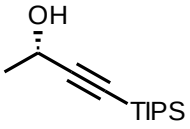

Silane (*S*)-**284** (300 µL, 244.6 mg, 1.719 mmol) was dissolved in THF (1 mL) under argon and the solution was cooled down to -78 °C. A solution of *n*-butyllithium (1.6 M in hexanes, 1.24 mL, 1.977 mmol, 1.15 eq) was added dropwise and the reaction mixture was stirred at the same temperature for an additional h. Triisopropylsilyl chloride **248** (417 µL, 364.6 mg, 1.891, 1.1 eq) was added dropwise and the reaction was stirred at -78 °C for 60 min. Then it was allowed to warm up to room temperature and stirred at the same temperature for 45 min. The reaction was quenched by an addition of water (1 mL) and the crude intermediate was extracted by diethyl ether (3 x 30 mL), dried over anhydrous sodium sulfate and evaporated to dryness. The residue was dissolved in THF (15 mL) and hydrochloric acid (3 N, 15 mL) was added. The reaction was stirred at room temperature for 1 h and then diluted by diethyl ether (50 mL) addition, washed with aqueous sodium bicarbonate (50 mL), and brine (50 mL) and dried over anhydrous sodium sulfate. The solvents were removed at reduced pressure to give (*S*)-**285** (375.8 mg, 97%) as a yellow oil in a satisfactory purity as checked by ^{1}H NMR.

^{1}H NMR was in agreement with the published data.[151]

^{1}H NMR (400 MHz, $CDCl_3$): 1.05-1.06 (m, 21H), 1.45 (d, *J* = 6.6, 3H), 2.14 (bs, 1H), 4.52 (d, *J* = 6.6, 1H).

***Tert*-butyl(4-hydroxy-3-iodophenyl)carbamate (287)**

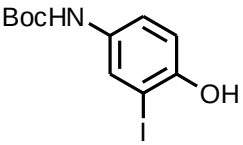

4-Amino-2-iodophenol **286** (862.7 mg, 3.671 mmol) was dissolved in DMF (10 mL) along with triethylamine (614 µL, 445.7 mg, 4.405 mmol, 1.2 eq) and cooled to 0 °C. A solution of di-*tert*-butyl dicarbonate (961.4 mg, 4.405 mmol, 1.2 eq) in DMF (10 mL) was added to the solution and left to stir and warm to room temperature overnight. The solvent was removed at reduced pressure and the residue was dissolved in DCM (15 mL). The organic layer was washed with aqueous solution of ammonium chloride (15%, 2 x 15 mL), water (2 x 15 mL), brine (15 mL), and dried over anhydrous sodium sulfate. The solvent was removed *in vacuo* and the residue was purified by flash

chromatography on silica gel (hexane – acetone 80 : 20) to give **287** (1.1026 g, 92%) as a yellow to brown amorphous solid.

^{1}H NMR (400 MHz, $CDCl_3$): 1.50 (s, 9H), 5.46 (s, 1H), 6.39 (bs, 1H), 6.87 (d, *J* = 8.7, 1H), 7.11 (dd, *J* = 8.7, 2.4, 1H), 7.79 (bs, 1H).

^{13}C NMR (125 MHz, $CDCl_3$): 28.46 (q), 80.90 (s), 85.37 (s), 114.88 (d), 121.55 (d), 128.90 (d), 132.24 (s), 151.28 (s), 153.16 (s).

IR ($CHCl_3$): 3586 w, 3504 m, 3439 m, 3354 w, br, 3091 vw, 2982 m, 2872 w, 2029 w, 1723 s, 1713 s, 1606 w, 1588 m, 1511 vs, 1491 s, 1455 m, 1402 s, 1394 s, 1369 s, 1272 m, 1243 s, sh, 1229 s, 1180 s, sh, 1158 vs, 1124 w, sh, 1056 m, 943 vw, 916 w, 875 w, 815 w, 697 w, 684 w, sh, 567 w, 531 w, 490 w, 461 vw, 446 w cm^{-1}.

ESI MS: 693 ($[2M+Na]^+$), 358 ($[M+Na]^+$).

HR ESI MS: calculated for $C_{11}H_{14}O_3NINa$ 357.9911, found 357.9910.

(+)-*Tert*-butyl [3-iodo-4-({(1*R*)-1-methyl-3-[tris(1-methylethyl)silyl]prop-2-yn-1-yl}oxy)phenyl]-carbamate (288)

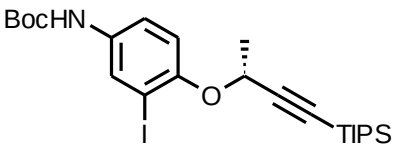

A Schlenk flask was charged with alcohol (*S*)-**285** (147.8 mg, 0.653 mmol, 1.10 eq) and triphenylphosphine (163.4 mg, 0.623 mmol, 1.05 eq). A solution of t*ert*-butyl (4-hydroxy-3-iodophenyl)carbamate **287** (192.9 mg, 0.593 mmol) in benzene (3 mL) was added under argon and the reaction mixture was cooled to 0 °C. Diisopropyl azodicarboxylate (123 µL, 0.623 mmol, 1.05 eq) was added dropwise. The reaction mixture was allowed to warm up to room temperature and stirred for 48 h. The solvent was removed under reduced pressure and the residue was purified by flash chromatography on silica gel (hexane – acetone 90 : 10) to give (*S*)-**288** (270.2 mg, 84%) as a yellow oil.

Optical rotation: $[\alpha]^{22}_D$ +77° (c 0.36, $CHCl_3$).

^{1}H NMR (400 MHz, $CDCl_3$): 1.01 (s, 21H), 1.50 (s, 9H), 1.71 (d, *J* = 6.6, 3H), 4.78 (q, *J* = 6.6, 1H), 6.33 (bs, 1H), 7.08 (d, *J* = 8.8, 1H), 7.22 (dd, *J* = 8.8, 1.6, 1H), 7.83 (bs, 1H).

^{13}C NMR (101 MHz, $CDCl_3$): 11.05 (3 x d), 18.47 (6 x q), 22.50 (q), 28.29 (3 x q), 66.95 (d), 80.53 (s), 87.49 (s), 88.25 (s), 106.22 (s), 116.40 (d), 119.49 (d), 129.43 (d), 133.67 (s), 152.68 (s), 152.77 (s).

IR ($CHCl_3$): 3439 m, 3091 vw, 3030 w, 2980 m, 2960 s, 2944 s, 2892 m, 2866 s, 2168 w, 1725 s, 1712, s, sh, 1600 w, 1581 m, 1508 s, 1489 s, 1472 m, sh, 1463 m, 1392 s, 1369 s, 1327 m, 1265 m, sh, 1248 s, 1233 m,

sh, 1157 vs, 1132 m, 1090 m, 1071 w, 1058 m, sh, 1046 m, 997 w, 951 m, 920 w, 884 m, 811 w, 679 m, 563 w, 532 vw, 457 vw cm^{-1}.

ESI MS: 582 ($[M+K]^+$), 566 ($[M+Na]^+$).

HR ESI MS: calculated for $C_{24}H_{38}O_3NINaSi$ 566.1558, found 566.1556.

(+)-{(3*R*)-3-[(1-Iodonaphthalen-2-yl)oxy]but-1-yn-1-yl}[tris(1-methylethyl)]silane (290)

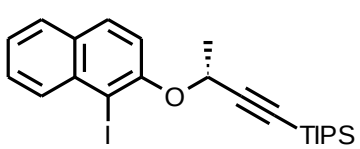

A Schlenk flask was charged with 1-iodo-2-naphthol **289** (167.0 mg, 0.618 mmol), alcohol (*S*)-**285** (154.0 mg, 0.680 mmol, 1.10 eq), and triphenylphosphine (170.3 mg, 0.649 mmol, 1.05 eq). Benzene (3 mL) was added under argon and the reaction mixture was cooled to 0 °C. Diisopropyl azodicarboxylate (128 µL, 0.649 mmol, 1.05 eq) was added dropwise. The reaction mixture was allowed to warm up to room temperature and stirred for overnight. The solvent was removed under reduced pressure and the residue was purified by flash chromatography on silica gel (hexane – diethyl ether 95 : 15) to give (*R*)-**290** (226.7 mg, 77%) as an orange oil.

Optical rotation: $[\alpha]^{22}_D$ +31° (c 0.31, $CHCl_3$).

^{1}H NMR (400 MHz, $CDCl_3$): 0.98 (s, 21H), 1.82 (d, *J* = 6.6, 3H), 5.04 (q, *J* = 6.6, 1H), 7.40 (ddd, *J* = 8.0, 6.9, 1.1, 1H), 7.47 (d, *J* = 8.9 Hz, 1H), 7.53 (ddd, *J* = 8.4, 6.9, 1.3 Hz, 1H), 7.74 (m, 1H), 7.77 (d, *J* = 8.9, 1H), 8.15 (m, 1H).

^{13}C NMR (101 MHz, $CDCl_3$): 11.06 (3 x d), 18.46 (6 x q), 22.74 (q), 67.42 (d), 87.94 (s), 91.00 (s), 106.25 (s), 117.47 (d), 124.67 (d), 127.78 (d), 128.08 (d), 129.66 (d), 130.56 (s), 131.63 (d), 133.61 (s), 155.52 (s).

IR ($CHCl_3$): 3061 w, 2959 s, 2945 vs, 2892 m, 2866 vs, 2169 w, 1622 m, 1594 m, 1556 w, 1501 s, 1470 m, sh, 1461 s, 1427 m, 1388 w, sh, 1384 m, 1372 w, sh, 1367 m, 1352 m, 1323 m, 1255 s, sh, 1240 s, 1155 m, 1135 m, sh, 1090 s, 1075 m, 1050 m, 1037 m, sh, 1029 m, 997 s, 948 m, 883 s, 862 w, 680 s, 637 m, sh, 519 m, 412 w cm^{-1}.

ESI MS: 517 ($[M+K]^+$), 501 ($[M+Na]^+$).

HR ESI MS: calculated for $C_{23}H_{31}OINaSi$ 501.1081, found 501.1078.

(+)-*Tert*-butyl {4-({(1*R*)-1-methyl-3-[tris(1-methylethyl)silyl]prop-2-yn-1-yl}oxy)-3-[(trimethylsilyl)ethynyl]-phenyl}carbamate (291)

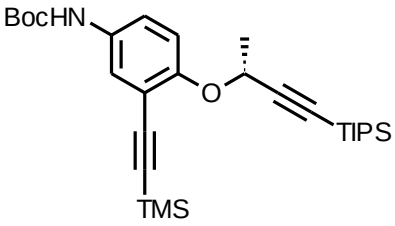

A Schlenk flask was charged with (*R*)-**288** (918.5 mg, 1.690 mmol), tetrakis(triphenylphosphine)palladium (97.6 mg, 0.085 mmol, 5 mol%), and copper iodide (29.0 mg, 0.152 mmol, 9 mol%). Freshly degassed diisopropylamine (20 mL) and ethynyltrimethylsilane **243** (478 µL, 331.9 mg, 3.380 mmol, 2.0 eq) were added under argon. The reaction mixture was stirred under argon at room temperature overnight. The crude reaction mixture was diluted with diethyl ether (50 mL) and filtered through a kieselguhr layer. The solvent was evaporated at reduced pressure and the residue purified by flash chromatography (hexane – acetone 95 : 5) to give (*R*)-**291** (817.3 mg, 94%) as a yellow amorphous solid.

Optical rotation: $[\alpha]^{22}_{D}$ +91° (c 0.49, $CHCl_3$).

^{1}H NMR (400 MHz, $CDCl_3$): 0.24 (s, 9H), 1.02 (s, 21H), 1.50 (s, 9H), 1.67 (d, 3H), 4.88 (q, *J* = 6.5, 1H), 6.33 (bs, 1H), 7.10 (d, *J* = 8.85 Hz, 1H), 7.17 (dd, *J* = 8.8, 2.4, 1H), 7.48 (bs, 1H).

^{13}C NMR (101 MHz, $CDCl_3$): -0.05 (3 x q), 11.12 (3 x d), 18.53 (6 x q), 22.48 (q), 28.34 (3 x q), 67.04 (d), 80.50 (s), 87.05 (s), 98.79 (s), 100.89 (s), 106.72 (s), 115.23 (s), 118.32 (d), 119.95 (d), 123.54 (d), 132.62 (s), 152.76 (s), 154.86 (s).

IR ($CHCl_3$): 3440 m, 3031 w, 2961 s, 2945 s, 2893 m, 2866 s, 2168 m, 2158 w, 1724 s, 1611 w, 1585 w, 1516 s, 1497 s, 1471 m, sh, 1463 m, 1455 m, sh, 1409 m, 1394 m, 1385 w, sh, 1369 s, 1328 m, 1308 w, 1269 s, 1251 s, 1158 vs, 1133 m, 1115 m, sh, 1090 m, 1072 w, 1040 m, 997 w, 950 m, 929 m, 855 s, 845 s, 883 s, 699 w, 679 m, 650 m, 516 w, 459 w cm^{-1}.

ESI MS: 1050 ($[2M+Na]^+$), 536 ($[M+Na]^+$), 514 ($[M+H]^+$).

HR ESI MS: calculated for $C_{29}H_{47}O_3NNaSi_2$ 536.2987, found 536.2986.

(+)-*Tert*-butyl [3-ethynyl-4-({(1*R*)-1-methyl-3-[tris(1-methylethyl)silyl]prop-2-yn-1-yl}oxy)phenyl]carbamate (292)

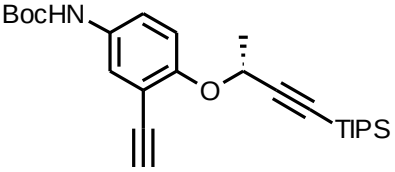

Silane (*R*)-**291** (48.0 mg, 0.093 mmol) was dissolved in methanol (5 mL) and anhydrous potassium carbonate (64.6 mg, 0.467 mmol, 5.0 eq) was added. The solution was stirred at room temperature for 2 h. The crude reaction mixture was diluted with diethyl ether (10 mL) and washed

with water (3 x 20 mL). The combined organic portions were dried over anhydrous Na_2SO_4. The reaction provided **292** (37.3 mg, 90%) as a yellow oil in a satisfactory purity as checked by ^{1}H NMR.

Optical rotation: $[\alpha]^{22}_D$ +89° (c 0.10, $CHCl_3$).

^{1}H NMR (400 MHz, $CDCl_3$): 1.01 (s, 21H), 1.51 (s, 9H), 1.69 (d, *J* = 6.6, 3H), 3.22 (s, 1H), 4.86 (q, *J* = 6.6, 1H), 6.34 (bs, 1H), 7.12 (d, *J* = 8.9, 1H), 7.19-7.31 (m, 1H), 7.45 (bs, 1H).

^{13}C NMR (101 MHz, $CDCl_3$): 11.08 (3 x d), 18.49 (6 xq), 22.45 (q), 28.33 (3 x q), 66.56 (d), 79.68 (s), 80.54 (s), 81.22 (d), 87.34 (s), 106.44 (s), 113.52 (s), 116.98 (d), 120.44 (d), 124.13 (d), 132.29 (s), 152.81 (s), 154.94 (s).

IR ($CHCl_3$): 3440 m, 3306 m, 3030 w, 2980 m, 2960 s, 2944 s, 2892 m, 2866 s, 2168 w, 2109 vw, 1724 s, 1711 s, sh, 1650 m, sh, 1611 w, 1586 w, 1517 s, 1499 vs, 1471 m, sh, 1463 m, 1456 m, 1408 m, 1394 m, 1385 m, sh, 1369 s, 1327 m, 1308 w, 1267 s, 1260 s, 1158 vs, 1132 m, 1119 m, 1091 m, 1072 w, 997 w, 950 m, 928 w, 884 m, 837 w, 830 w, 708 vw, 679 m, 620 m, 519 w, 459 w cm^{-1}.

ESI MS: 464 ($[M+Na]^+$).

HR ESI MS: calculated for $C_{26}H_{39}O_3NNaSi$ 464.2591, found 464.2591.

(+)-*Tert*-butyl [4-({(1*R*)-1-methyl-3-[tris(1-methylethyl)silyl]prop-2-yn-1-yl}oxy)-3-{[2-({(1*R*)-1-methyl-3-[tris(1-methylethyl)silyl]prop-2-yn-1-yl}oxy)naphthalen-1-yl]ethynyl}phenyl]carbamate (293)

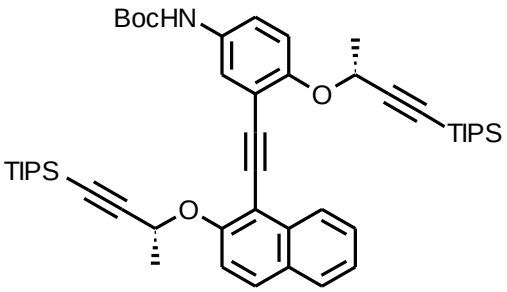

A Schlenk flask was charged with iodide (*R*)-**290** (40.4 mg, 0.085 mmol), tetrakis(triphenylphosphine)palladium (4.9 mg, 0.004 mmol, 5 mol%), and copper iodide (1.4 mg, 0.008 mmol, 9 mol%). A solution of diyne (*R*)-**292** (37.3 mg, 0.085 mmol, 1.0 eq) in diisopropylamine (3 mL) was added under argon. The reaction mixture was stirred at room temperature overnight. The crude product was filtered through a pad of silica gel (diethyl ether). The solvent was evaporated under reduced pressure and the residue was purified by flash chromatography on silica gel (hexane – acetone 96 : 4) to give triyne (*R*,*R*)-**293** (18.6 mg, 28%) as a yellow oil.

Optical rotation: $[\alpha]^{22}_D$ +22° (c 0.21, $CHCl_3$).

^{1}H NMR (400 MHz, $CDCl_3$): 0.99 (s, 21H), 1.01 (s, 21H), 1.53 (s, 9H), 1.80 (d, *J* = 6.5, 3H), 1.81 (d, *J* = 6.5, 3H), 5.01 (q, *J* = 6.5, 1H), 5.19 (q, *J* = 6.5, 1H), 6.37 (bs, 1H), 7.19 (d, *J* = 9.0, 1H), 7.38-7.45 (m, 3H), 7.49 (d, *J* = 9.0, 1H), 7.53 (ddd, *J* = 8.3, 6.9, 1.2, 1H), 7.76 (d, *J* = 9.0, 1H), 7.79 (bd, *J* = 8.0, 1H), 8.53 (d, *J* = 8.4, 1H).

^{13}C NMR (101 MHz, $CDCl_3$): 11.10 (6 x d), 18.49 (6 x q), 18.52 (6 x q), 22.80 (2 x q), 28.38 (3 x q), 66.11 (d), 67.22 (d), 87.34 (s), 87.38 (s), 88.37 (s), 95.30 (s), 106.63 (2 x s), 106.79 (2 x s), 109.72 (s), 115.08 (s), 116.39 (d), 118.38 (d), 124.54 (2 x d), 126.07 (d), 126.80 (2 x d), 127.86 (d), 129.29 (d), 129.41 (s), 132.18 (s), 134.55 (s), 154.33 (s), 157.23 (s).

IR ($CHCl_3$): 3441 w, 3060 w, 3033 w, 2990 m, sh, 2959 s, 2944 vs, 2930 vs, sh, 2892 s, 2866 vs, 2209 vw, 2168 w, 1724 s, 1709 m, sh, 1620 w, 1609 w, 1589 m, 1572 vw, sh, 1518 s, 1511 s, 1498 vs, 1463 s, 1434 w, 1407 m, 1393 m, 1382 m, 1369 s, 1324 m, 1311 m, sh, 1268 s, 1248 m, 1158 vs, 1130 s, 1090 s, 1045 m, 1037 m, sh, 997 m, 952 m, 918 m, 883 s, 869 w, sh, 854 w, 820 w, sh, 815 w, sh, 679 s, 559 w cm^{-1}.

ESI MS: 1606 ($[2M+Na]^+$), 830 ($[M+K]^+$), 814 ($[M+Na]^+$), 792 ($[M+H]^+$).

HR ESI MS: calculated for $C_{49}H_{69}O_4NNaSi_2$ 814.4657, found 814.4659.

(+)-*Tert*-butyl (4-{[(1*R*)-1-methylprop-2-yn-1-yl]oxy}-3-[(2-{[(1*R*)-1-methylprop-2-yn-1-yl]oxy}naphthalen-1-yl)ethynyl]phenyl)carbamate (294)

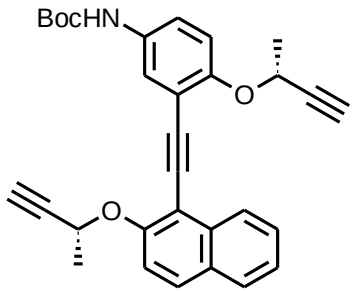

Silane (*R*,*R*)-**293** (109.1 mg, 0.138 mmol) was dissolved in tetrahydrofuran (2 mL). A solution of *n*-tetrabutylammonium fluoride (1 M in THF, 340 µL, 0.344 mmol, 2.5 eq) was added under argon. The reaction was stirred at room temperature for 2 h. The solvent was evaporated under reduced pressure and the residue was purified by flash chromatography (gradient elution hexane – acetone 95 : 5 to 90 : 10) to provide (*R*,*R*)-**294** (45.1 mg, 68%) as a pale yellow amorphous solid.

Optical rotation: $[\alpha]^{22}_D$ +42° (c 0.26, $CHCl_3$).

^{1}H NMR (400 MHz, $CDCl_3$): 1.53 (s, 9H), 1.80 (d, *J* = 6.5, 3H), 1.81 (d, *J* = 6.5, 3H), 2.49 (d, *J* = 2.0, 1H), 2.51 (d, *J* = 2.0, 1H), 5.03 (dq, *J* = 6.5, 6.5, 6.5, 1.9, 1H), 5.20 (dq, *J* = 6.5, 6.5, 6.5, 2.0, 1H), 6.40 (bs, 1H), 7.11 (d, *J* = 8.9, 1H), 7.40-7.49 (m, 4H), 7.55 (ddd, *J* = 8.2, 6.8, 1.1, 1H), 7.80 (d, *J* = 8.7, 2H), 8.54 (d, *J* = 8.4, 1H).

^{13}C NMR (101 MHz, $CDCl_3$): 22.37 (q), 22.47 (q), 28.35 (3 x q), 65.32 (d), 66.55 (d), 74.21 (d), 74.26 (d), 82.90 (s), 83.16 (s), 88.36 (s), 95.28 (s), 109.84 (s), 109.97 (s), 115.15 (s), 116.08 (d), 118.03 (d), 120.27 (d), 123.51 (d), 124.79 (d), 126.09 (d), 127.00 (d), 127.93 (d), 129.50 (s), 129.61 (d), 132.45 (s), 134.54 (s), 152.88 (s), 153.89 (s), 156.90 (s).

IR ($CHCl_3$): 3440 m, 3307 m, 3061 w, 3031 w, 2984 m, 2872 w, 2209 vw, 2118 vw, 1724 s, 1622 w, sh, 1610 w, 1588 m, 1518 s, 1513 w, sh, 1510 s, 1498 vs, 1467 m, 1434 w, 1407 m, 1393 m, 1376 m, 1369 m, 1326

m, 1311 w, sh, 1268 s, 1248 s, 1157 vs, 1128 s, 1090 s, 1041 m, 1032 m, sh, 958 vw, 943 w, 917 w, 870 w, sh, 852 w, 830 w, 815 w, sh, 641 m, 560 w cm^{-1}.

ESI MS: 981 ($[2M+Na]^+$), 518 ($[M+K]^+$), 502 ($[M+Na]^+$), 480 ($[M+H]^+$).

HR ESI MS: calculated for $C_{31}H_{29}O_4NNa$ 502.1989, found 502.1987.

4-Iodothioanisole (296)

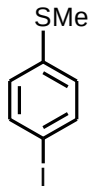

A microwave vial was charged with 4-bromothioanisole **295** (1.1219 g, 5.524 mmol), sodium iodide (1.6559 g, 11.048 mmol, 2.0 eq), copper iodide (84.2 mg, 0.442 mmol, 8 mol%), and (1*S*,2*S*)-*N*,*N´*-dimethyl-1,2-cyclohexanediamine (125.7 mg, 0.884 mmol, 16 mol%). 1,4-Dioxane (14 mL) was added and the reaction mixture was heated in a microwave reactor at 200 °C for 6 h. A GC/MS analysis did not shown a full conversion, therefore another portion of copper iodide (114.0 mg, 0.598 mmol, 11 mol%) and (1*S*,2*S*)-*N*,*N´*-dimethyl-1,2-cyclohexanediamine (170.0 mg, 1.195 mmol, 22 mol%) was added and the reaction mixture was heated in a microwave reactor at 200 °C for another 3 h. The reaction was diluted by addition of diethyl ether (50 mL) and washed by water (3 x 50 mL). The solvents were removed in vacuo to provide 4-iodoanisole **296** (1.3539 g, 98%) as a white to green solid in a satisfactory purity as checked by GC/MS analysis.

^{1}H NMR was in agreement with the published data.[152]

^{1}H NMR (400 MHz, $CDCl_3$): 2.45 (s, 3H), 6.98 (d, *J* = 8.6, 2H), 7.57 (d, *J* = 8.6, 2H).

(-)-*Tert*-butyl [4-({(1*R*)-1-methyl-3-[4-(methylsulfanyl)phenyl]prop-2-yn-1-yl}oxy)-3-{[2-({(1*R*)-1-methyl-3-[4-(methylsulfanyl)phenyl]prop-2-yn-1-yl}oxy)naphthalen-1-yl]ethynyl}phenyl]carbamate (297)

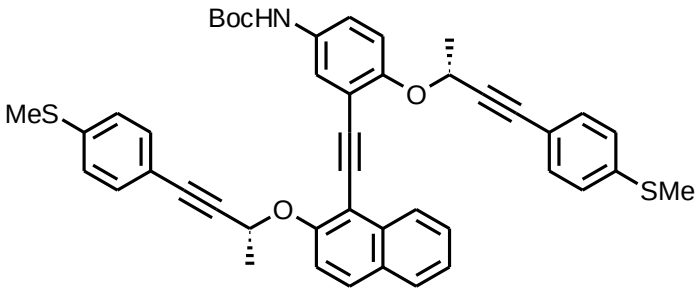

A Schlenk flask was charged with 4-iodothioanisole **296** (32.1 mg, 0.128 mmol, 2.1 eq), tetrakis(triphenylphosphine)palladium (7.1 mg, 0.006 mmol, 10 mol%), and copper iodide (2.1 mg, 0.011 mmol, 18 mol%). Then a solution of triyne (*R*,*R*)-**294** (29.3 mg, 0.061 mmol) in diisopropylamine (5 mL) was added under argon. The reaction mixture was stirred at room temperature overnight. The reaction was diluted with diethyl ether (20 mL) and filtered through a pad of silica gel (diethyl ether). The solvent was evaporated under reduced pressure and the residue was purified

by flash chromatography on silica gel (gradient elution hexane – acetone 90 : 10 to 80 : 20) to give (*R*,*R*)-**297** (36.0 mg, 81%) as a yellow amorphous solid.

Optical rotation: $[\alpha]^{22}_{D}$ -135° (c 0.25, $CHCl_3$).

^{1}H NMR (400 MHz, $CDCl_3$): 1.53 (s, 9H), 1.87 (d, *J* = 6.5, 3H), 1.88 (d, *J* = 6.5, 3H), 2.44 (s, 3H), 2.45 (s, 3H), 5.24 (q, *J* = 6.5, 1H), 5.41 (q, *J* = 6.5, 1H), 6.36 (bs, 1H), 7.11 (d, *J* = 8.2, 4H), 7.19 (d, *J* = 9.1, 1H), 7.28 (dd, *J* = 8.5, 1.1, 4H), 7.41 (ddd, *J* = 8.0, 7.0, 1.0, 1H), 7.45-7.50 (m, 2H), 7.54 (ddd, *J* = 8.1, 7.0, 1.0, 1H), 7.64-7.71 (m, 1H), 7.80 (d, *J* = 8.8, 2H), 8.58 (d, *J* = 8.4, 1H).

^{13}C NMR (101 MHz, $CDCl_3$): 15.38 (2 x q), 22.53 (q), 22.61 (q), 28.36 (3 x q), 66.31 (d), 67.48 (d), 85.83 (s), 85.86 (s), 88.40 (s), 88.47 (s), 88.69 (s), 93.87 (s), 95.39 (s), 115.27 (s), 116.35 (d), 116.39 (d), 118.30 (d), 124.73 (d), 125.77 (d), 126.11 (d), 127.00 (d), 127.91 (d), 128.42 (d), 128.54 (d), 129.46 (s), 129.55 (d), 181.88 (s), 131.89 (s), 131.96 (d), 132.00 (d), 132.05 (d), 132.15 (d), 132.37 (s), 134.59 (s), 154.18 (s), 157.15 (s). One quarternary carbon was not detected.

IR ($CHCl_3$): 3440 w, 3100 vw, sh, 3076 vw, 3061 w, 3032 vw, 2988 m, 2870 w, 2233 w, 1723 s, 1621 w, sh, 1609 w, 1589 m, 1572 vw, sh, 1517 s, 1512 s, 1499 vs, sh, 1493 vs, 1466 m, 1438 m, 1422 w, 1406 m, 1393 m, 1381 m, 1369 m, 1328 m, 1311 w, sh, 1268 m, 1247 m, 1158 vs, 1125m, 1121 m, sh, 1096 m, sh, 1083 s, 1038 m, 1030 m, 1015 m, 957 w, 947 w, 923 vw, 870 w, 855 w, 820 m, 705 vw, sh, 694 w, 559 w cm^{-1}.

ESI MS: 1470 ($[2M+Na]^+$), 762 ($[M+K]^+$), 746 ($[M+Na]^+$).

HR ESI MS: calculated for $C_{45}H_{41}O_4NNaS_2$ 746.2369, found 746.2371.

(-)-*Tert*-butyl {(*M*,2*R*,5*R*)-2,5-dimethyl-3,4-bis[4-(methylsulfanyl)phenyl]-2,5-dihydrobenzo[*f*]benzo[1,2-*c*:4,3-*c'*]dichromen-14-yl}carbamate (298)

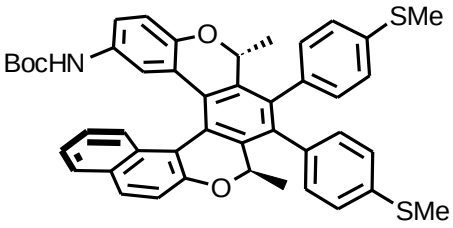

Procedure using $CpCo(CO)_2/PPh_3$ (20 mol%/40 mol%) and halogen lamp irradiation at 140 °C (Table 3.60, entry 1)

A two-necked Schlenk flask was charged with triyne (*R*,*R*)-**297** (20.2 mg, 0.028 mmol), $CpCo(CO)_2$ **81** (1.0 mg, 0.006 mmol, 20 mol%), and triphenylphosphine (2.9 mg, 0.011 mmol, 40 mol%) under argon. The content was dissolved in decane (3 mL) and the reaction mixture was heated by halogen lamp irradiation

at 140 °C for 120 min. Then the solvent was removed *in vacuo* and the residue was purified by flash chromatography on silica gel (hexane – acetone 80 : 20) to give (*M*,*R*,*R*)-**298** (12.4 mg, 61%) as a yellowish amorphous solid.

Procedure using $Ni(cod)_2/PPh_3$ (20 mol%/40 mol%) at rt (Table 3.60, entry 2)

A microwave vial was charged with triyne (*R*,*R*)-**297** (20.0 mg, 0.028 mmol), $Ni(cod)_2$ **254** (1.5 mg, 0.006 mmol, 20 mol%), and triphenylphosphine (2.9 mg, 0.011 mmol, 40 mol%) in glovebox. The content was dissolved in THF (2 mL) under argon. The reaction mixture was stirred at room temperature for 2 h. Then the solvent was removed *in vacuo* and the residue was purified by flash chromatography on silica gel (hexane – acetone 80 : 20) to give (*M*,*R*,*R*)-**298** (9.4 mg, 47%) as a yellowish amorphous solid.

Procedure using CpCo(CO)(fum) (1.0 eq) and microwave irradiation at 180 °C (Table 3.60, entry 3)

A microwave vial was charged with triyne (*R*,*R*)-**297** (22.2 mg, 0.031 mmol) and CpCo(CO)(fum) **255** (9.1 mg, 0.031 mmol, 1.0 eq) under argon. THF (2 mL) and 1-butyl-2,3-dimethylimidazolium tetrafluoroborate (10 µL) were added. The reaction mixture was heated to 180 °C for 20 min. Then the solvent was removed *in vacuo* and the residue was purified by flash chromatography on silica gel (hexane – acetone 80 : 20) to give (*M*,*R*,*R*)-**298** (3.0 mg, 14%) as a yellowish amorphous solid.

Procedure using CpCo(CO)(fum) (20 mol%) and microwave irradiation at 180 °C (Table 3.60, entry 4)

A microwave vial was charged with triyne (*R*,*R*)-**297** (20.3 mg, 0.028 mmol) and CpCo(CO)(fum) **255** (1.7 mg, 0.006 mmol, 20 mol%) under argon. THF (2 mL) and 1-butyl-2,3-dimethylimidazolium tetrafluoroborate (10 µL) were added. The reaction mixture was heated to 180 °C for 20 min. Then the solvent was removed *in vacuo* and the residue was purified by flash chromatography on silica gel (hexane – acetone 80 : 20) to give (*M*,*R*,*R*)-**298** (16.9 mg, 83%) as a yellowish amorphous solid.

Optical rotation: $[\alpha]^{22}_{D}$ -357° (c 0.25, $CHCl_3$).

^{1}H NMR (400 MHz, $CDCl_3$): 0.98 (d, *J* = 6.5, 3H), 1.00 (d, *J* = 6.5, 3H), 1.39 (s, 9H), 2.44 (s, 3H), 2.45 (s, 3H), 5.26 (q, *J* = 6.5, 1H), 5.30 (q, *J* = 6.5, 1H), 5.39 (bs, 1H), 6.16 (d, *J* = 2.5, 1H), 6.79 (m, 2H), 6.85-7.02 (m, 4H), 7.11-7.24 (m, 6H), 7.26 (d, *J* = 8.7, 1H), 7.46 (d, *J* = 8.5, 1H), 7.67 (d, *J* = 8.1, 1H), 7.75 (d, *J* = 8.7, 1H).

^{13}C NMR (101 MHz, $CDCl_3$): 15.41 (2 x q), 17.72 (q), 18.63 (q), 28.22 (3 x q), 72.83 (d), 73.20 (d), 117.63 (s), 118.51 (d), 119.65 (d), 123.61 (d), 124.02 (d), 124.13 (s), 125.28 (d), 125.40 (s), 125.53 (d), 125.61 (d), 125.65 (2 x d), 125.73 (d), 126.01 (s), 127.50 (s), 129.30 (s), 129.55 (d), 129.70 (d), 129.88 (d), 130.29 (s),

131.00 (d), 131.33 (d), 131.54 (s), 134.42 (d), 134.44 (d), 135.89 (s), 136.31 (s), 136.93 (s), 136.98 (s), 138.63 (s), 139.57 (s), 148.43 (s), 152.62 (s), 152.79 (s).

IR ($CHCl_3$): 3440 w, 3059 w, 2983 w, 2962 w, 2927 m, 2869 w, 2856 w, 1724 s, 1619 w, 1592 m, 1511 s, 1456 m, 1438 m, 1393 m, 1382 m, 1369 m, 1321 m, 1254 m, 1159 vs, 1123 m, 1030 m, 866 m, 462 w cm^{-1}.

ESI MS: 1470 ($[2M+Na]^+$), 762 ($[M+K]^+$), 746 ($[M+Na]^+$).

HR ESI MS: calculated for $C_{45}H_{41}O_4NNaS_2$ 746.2369, found 746.2365.

(-)-(*M*,2*R*,5*R*)-2,5-dimethyl-3,4-bis[4-(methylsulfanyl)phenyl]-2,5-dihydrobenzo[*f*]benzo[1,2-*c*:4,3-*c'*]dichromen-14-amine (299)

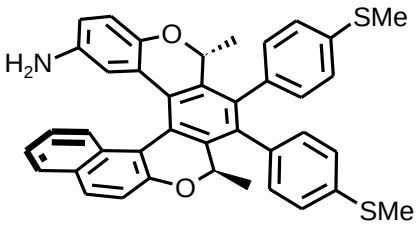

A Boc-protected aminohelicene (*M*,*R*,*R*)-**298** (21.0 mg, 0.290 mmol) was dissolved in DCM/TFA 4 : 1 solution (20 mL) and the reaction mixture was stirred at room temperature overnight. The reaction mixture was diluted by addition of an aqueous NaOH solution (2 M, 20 mL) and extracted by DCM (3 x 20 mL). The combined organic layers were dried over anhydrous sodium sulfate and then the solvent was removed at reduced pressure. The residue was purified by preparative TLC (petrol ether – acetone 80 : 20) extracted by DCM and the solvent was removed *in vacuo* to give (*M*,*R*,*R*)-**299** (15.6 mg, 86%) as a yellow amorphous solid.

Optical rotation: $[\alpha]^{22}_D$ -477° (c 0.31, $CHCl_3$).

^{1}H NMR (500 MHz, $CDCl_3$): 0.99 (d, *J* = 6.6, 6H), 2.45 (s, 3H), 2.45 (s, 3H), 5.22 (q, *J* = 6.6, 1H), 5.31 (q, *J* = 6.6, 1H), 5.79 (d, *J* = 2.7, 1H), 6.27 (dd, *J* = 8.4, 2.7, 1H), 6.74 (d, *J* = 8.4, 1H), 6.79 (dd, *J* = 7.7, 1.9, 1H), 6.80 (dd, *J* = 7.7, 1.9, 1H), 6.98 – 7.00 (m, 3H), 7.17 – 7.21 (m, 5H), 7.22 (dd, *J* = 8.1, 1.8, 1H), 7.28 (d, *J* = 8.7, 1H), 7.54 (d, *J* = 8.5, 1H), 7.69 (d, *J* = 8.1, 1H), 7.75 (d, *J* = 8.7, 1H).

^{13}C NMR (126 MHz, $CDCl_3$): 15.44 (q), 15.45 (q), 17.73 (q), 18.49 (q), 72.58 (d), 73.28 (d), 114.04 (s), 115.25 (d), 115.81 (d), 118.07 (s), 118.69 (d), 119.61 (d), 123.62 (d), 124.03 (s), 125.27 (d), 125.55 (d), 125.63 (d), 125.67 (d), 125.67 (d), 125.77 (d), 126.64 (s), 127.48 (d), 129.56 (s), 129.64 (d), 129.74 (d), 129.88 (s), 130.04 (d), 131.08 (d), 131.36 (d), 134.56 (s), 134.62 (s), 135.90 (s), 136.07 (s), 136.84 (s), 136.93 (s), 138.84 (s), 139.53 (s), 139.90 (s), 145.28 (s), 152.67 (s).

IR ($CHCl_3$): 3367 w, 3209 vw, 3076 w, sh, 3060 w, 3030 w, 2964 m, sh, 2927 s, 1620 m, 1602 m, sh, 1592 m, 1577 vw, sh, 1510 m, 1500 vs, 1494 s, 1465 m, sh, 1437 s, 1428 m, 1383 m, 1321 w, 1112 w, sh, 1095 m, 1073 s, 1060 m, 1051 m, 1032 vw, 1014 s, 867 m, 823 m, sh, 815 s, 693 vw, 557 vw cm^{-1}.

EI MS: 623 ($M^{+\bullet}$, 29), 608 (18), 312 (6), 281 (15), 226 (5), 207 (100), 191 (9), 133 (6), 96 (10).

HR ESI MS: calculated for $C_{40}H_{34}O_2NS_2$ 624.2025, found 624.2018.

General procedure for catalytic hydrogenation of ethyl pyruvate

Hydrogenation of ethyl pyruvate **315** was carried out in double-necked round bottom flasks at room temperature under hydrogen atmosphere at ambient pressure (of a water column), placed in a Stuart® Flask Shaker SF1. The dried catalyst **317** and **318** (10.0 mg, 5 wt% Pt) were shaken (720 rpm) in a freshly distilled neat acetic acid or THF (4.5 mL) for 5 min under flowing (bubbling through) argon followed by hydrogen flowing for 5 min. Chiral modifier **2**, **213**, **309**, **319** – **322** (0.2 or 0.5 mg) and *n*-undecane (25 µL) as internal standard were injected in the neat acetic acid or THF (0.5 mL), followed by further shaking for 5 min under hydrogen. For experiments in the absence of chiral modifier, the neat acetic acid (0.5 mL + internal standard) or THF (0.5 mL + internal standard) was used instead of the modifier solution. The reaction was started by injecting of ethyl pyruvate **315** (165 µL, 172.4 mg, 1.485 mmol). The reaction samples were collected each hour (for first 5 hours). If the full conversion was not achieved (typically after 10 h), the reaction was stopped after 16, 20 or 24 h. The *ee* values were determined at full conversion. The samples (containing the neat acetic acid) were treated as follows before GC analysis (CP-Chirasil-Dex Agilent or HP-CHIRAL-20B J&W–Scientific capillary column, FID detector).

Preparation of a sample for GC analysis: A GC vial (2 mL) was charged with a saturated aqueous potassium carbonate solution (20 µL) (the saturated stock solution was obtained by treating of potassium carbonate (750 mg) in deionized water (1 mL), followed by filtration through a paper). *n*-Hexane (1 mL) and crude reaction mixture from hydrogenation (10 µL) were added. The vial was capped and shaken on a shaker (SHAKER R5 - 1.5 x 1000) for 2 min. The aqueous layer was dried over anhydrous sodium sulfate.

Typical GC separation parameters: injected with split 20, inlet temperature of 230 °C, 1 µL injection volume, constant hydrogen column flow at 1.5 mL min^{-1}. Separation column parameters: HP-Chiral (30 m x 250 µm x 0.25 µm, Agilent). Temperature program: 60 °C (held for 5 min), increased at a rate of 5 °C/min to 70 °C, followed by a rate of 20 °C/min to 180 °C (held for 1 min). TR((L)-**316**): 8.83 min; TR((D)-**316**): 9.04 min; TR(**315**): 7.56 min; TR(standard): 10.14 min.

Ethyl lactate (316)

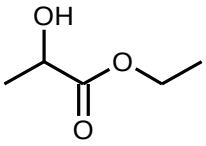

Procedure using catalyst* 317 *and* 309 *as a chiral modifier (Table 3.82, entry 1)

The General procedure for catalytic hydrogenation of ethyl pyruvate was followed with **317** as a catalyst and chiral modifier **309** (0.5 mg) in the neat acetic acid. The conversion and *ee* was determined by GC after 16 h (84%, (L)-45% *ee*).

The racemic mixture of ethyl lactate as standard was synthetized according to literatureprocedure[153]. ^{1}H NMR was in agreement with the published data[154].
^{1}H NMR (400 MHz, $CDCl_3$): 1.30 (t, *J* = 7.1, 3H), 1.42 (d, *J* = 6.9, 3H), 2.98 (bs, 1H), 4.24 (q, *J* = 7.1, 2H), 4.27 (q, *J* = 6.9, 1H).

Procedure using catalyst* 318 *and* 309 *as a chiral modifier (Table 3.82, entry 2, Table 3.84, entry 2)

The General procedure for catalytic hydrogenation of ethyl pyruvate was followed with **318** as a catalyst and chiral modifier **309** (0.5 mg) in the neat acetic acid. The conversion and *ee* was determined from GC by 16 h (100%, (L)-71% *ee*).

Procedure using catalyst* 318 *without any modifier (Table 3.84, entry 1)

The General procedure for catalytic hydrogenation of ethyl pyruvate was followed with **318** as a catalyst in neat acetic acid. The conversion was determined by GC after 20 h (30%).

Procedure using catalyst* 318 *and* (*M*)-2 *as a chiral modifier (Table 3.84, entry 3)

The General procedure for catalytic hydrogenation of ethyl pyruvate was followed with **318** as a catalyst and chiral modifier (-)-1-aza[6]helicene (*M*)-**2** (0.5 mg) in the neat acetic acid. The conversion and *ee* was determined by GC after 20 h (65%, 0% *ee*).

Procedure using catalyst* 318 *and* (*P*,*S*,*S*)-213 *as a chiral modifier (Table 3.84, entry 4)

The General procedure for catalytic hydrogenation of ethyl pyruvate was followed with **318** as a catalyst and chiral modifier (*P*,*S*,*S*)-**213** (0.5 mg) in the neat acetic acid. The conversion and *ee* was determined by GC after 20 h (65%, 0% *ee*).

Procedure using catalyst* 318 *and* (*M*,*R*,*R*)-321 *as a chiral modifier (Table 3.84, entry 5)

The General procedure for catalytic hydrogenation of ethyl pyruvate was followed with **318** as a catalyst and chiral modifier (*M*,*R*,*R*)-**321** (0.5 mg) in the neat acetic acid. The conversion and *ee* was determined by GC after 20 h (100%, (D)-4% *ee*).

Procedure using catalyst* 318 *and* (*M*,*R*,*R*)-322 *as a chiral modifier (Table 3.84, entry 6)

The General procedure for catalytic hydrogenation of ethyl pyruvate was followed with **318** as a catalyst and chiral modifier (*M*,*R*,*R*)-**322** (0.5 mg) in the neat acetic acid. The conversion and *ee* was determined by GC after 20 h (100%, (L)-2% *ee*).

Procedure using catalyst* 318 *and rac*-319 *as a modifier (Table 3.84, entry 7)

The General procedure for catalytic hydrogenation of ethyl pyruvate was followed with **318** as a catalyst and modifier *rac*-**319** (0.2 mg) in the neat acetic acid. The conversion was determined by GC after 20 h (65%).

Procedure using catalyst* 318 *and rac*-319 *as a modifier (Table 3.84, entry 8)

The General procedure for catalytic hydrogenation of ethyl pyruvate was followed with **318** as a catalyst and modifier *rac*-**319** (0.2 mg) in THF. The conversion was determined by GC after 24 h (60%).

Procedure using catalyst* 318 *and* (-)-319 *as a chiral modifier (Table 3.84, entry 9)

The General procedure for catalytic hydrogenation of ethyl pyruvate was followed with **318** as a catalyst and chiral modifier (-)-**319** (0.2 mg) in THF. The conversion and *ee* was determined by GC after 24 h (95%, 0% *ee*).

Procedure using catalyst* 318 *and rac*-320 *as a modifier (Table 3.84, entry 10)

The General procedure for catalytic hydrogenation of ethyl pyruvate was followed with **318** as a catalyst and modifier *rac*-**320** (0.2 mg) in the neat acetic acid. The conversion was determined by GC after 20 h (98%).

Procedure using catalyst* 318 *and* (*M*,*R*,*R*)-210 *as a chiral modifier (Table 3.84, entry 11)

The General procedure for catalytic hydrogenation of ethyl pyruvate was followed with **318** as a catalyst and chiral modifier (*M*,*R*,*R*)-**210** (0.2 mg) in the neat acetic acid. The conversion and *ee* was determined by GC after 24 h (14%, 0% *ee*).

Platinum nanoparticles (5 wt%) on silica gel (317)

Synthesis of T_d Pt NPs – methodology I[139]

To an aqueous solution of potassium tetrachloroplatinate(II) (200 mL, 1.0 10^{-4} M) sodium polyacrylate solution (1.0 mL, 0.1 M, 5.0 eq, MW ≈ 2000 g mol^{-1}) was added as a capping polymer. Argon was bubbled through the resulting solution for 20 min. Then hydrogen at a high flow rate was bubbled through the mixture for 5 min to reduce the Pt(II) ions, then the reaction vessel was sealed and left stirred at room temperature overnight (in the dark). Formation of Pt NPs reflected in the change of the solution color (golden to brown). The methodology I gives inconsistent results in NPs shape-definition (see Figure 3.79).

Synthesis of T_d Pt NPs – methodology II[140]

To an aqueous solution of chloroplatinic acid hexahydrate (250 mL, 1.0 10^{-4} M) polyvinylpyrrolidone (4.5 mg, 0.5 ‰, MW ≈ 360 000 g mol^{-1}) was added as a capping polymer. Argon was bubbled through the resulting solution for 20 min. Then hydrogen at a high flow rate was bubbled through the mixture for 5 min to reduce the Pt(IV) ions, then the reaction vessel was sealed and left stirred at room temperature overnight (in the dark). Formation of Pt NPs reflected in the change of the solution color (golden to brown). The methodology II gives consistent results in NPs shape- and size definition (see Figure 3.80).

Pt NPs dispersion on high-area support[75] ***and catalyst activation***

For the preparation of Pt/SiO_2, a suspension of SiO_2 (Evonik Aerosil 200®, 74.1 mg) in distilled water (2 mL) was prepared by sonification and added to the Pt colloidal solution (198.5 mL, 1.0 10^{-4} M, prepared by methodology II, above). After stirring for 1 h, the Pt NPs were deposited onto silica by dropwise acidification until pH = 2 (0.1 M HCl, checked by pH-meter). The samples containing 5 wt% Pt were filtered off, washed with distilled water (10 x 40 mL), and ethanol (1 x 50 mL), and dried at 100 °C for 2 h. Then the catalyst was homogenized in agate bowl and ozonized in a ozone cleaner for 70 min, washed with ethanol (3 x 40 mL), diethyl ether (1 x 40 mL), and dried at 100 °C for 1 h. Catalyst activated in such way was used in catalytic hydrogenation of ethyl pyruvate.

6. Appendixes

6.1 Appendix A: Computational details for (*M*,*R*,*R*)/(*P*,*R*,*R*)-239 and 256

Calculation of barriers to racemization of (*M*,*R*,*R*)/(*P*,*R*,*R*)-**239** and **256**:

Both minima (*M*,*R*,*R*)- and (*P*,*R*,*R*)-**239** as well as (*M*,*R*,*R*)- and (*P*,*R*,*R*)-**256** were initially optimized using B3LYP/cc-pVTZ method. Then the transition states were localized by the QST3 method as implemented in Gaussian09. Vibrational frequencies were calculated to confirm the saddle point order, evaluate free energies, and calculate the barriers to racemization.

The calculated structure and XYZ coordinates of (*M*,*R*,*R*)-**239**:

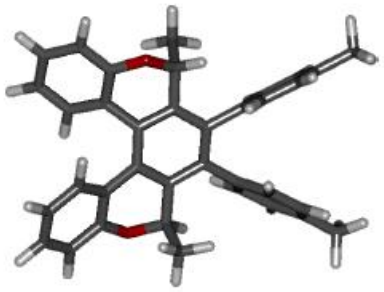

68

MRR-TOL 0.000000

H	3.9900	0.0990	1.4080
C	0.2660	-3.4970	-1.3050
H	1.0330	3.1160	1.9880
H	-0.7200	3.2060	1.6830
H	0.3280	4.5910	1.2650
H	-1.7850	2.0050	-2.2540
H	-3.9580	3.1750	-2.4720
C	-5.8990	3.5030	-0.5710
H	-4.8940	2.1830	1.6010
H	-2.7250	1.0100	1.8120
H	-0.3220	-3.2910	0.7590
H	-0.3220	3.2910	-0.7590
H	3.8690	-4.7400	0.3520
H	5.9280	-3.8870	-0.7910
C	0.4560	-2.9080	0.0980
O	1.6830	-3.4010	0.7040
C	0.4560	2.9080	-0.0980
H	-5.8150	-4.5300	0.1880
H	-6.2240	-3.5650	1.6160
H	-6.6840	-3.0020	-0.0090
H	-6.6830	3.0080	0.0150
H	-5.8130	4.5330	-0.1970
H	-6.2270	3.5580	-1.6150
H	0.3280	-4.5910	-1.2650
H	1.0330	-3.1160	-1.9870
H	-0.7200	-3.2060	-1.6820
H	-2.7250	-1.0100	-1.8120
H	-4.8930	-2.1830	-1.6010
C	-5.8990	-3.5030	0.5710
H	-3.9580	-3.1750	2.4720
H	-1.7850	-2.0050	2.2540
H	5.9400	-1.5780	-1.7390
H	3.9890	-0.0990	-1.4080
H	5.9400	1.5780	1.7390
C	-4.5830	2.7740	-0.4490
C	-4.2110	2.1550	0.7540
C	-2.9880	1.4980	0.8780
H	3.8690	4.7400	-0.3520
H	5.9280	3.8870	0.7900
C	3.9270	3.7200	0.0180

C	5.0640	3.2390	0.6660
C	-2.9870	-1.4990	-0.8780
C	-4.2110	-2.1550	-0.7540
C	-2.0930	1.4380	-0.2000
C	-4.5830	-2.7740	0.4490
C	0.2660	3.4970	1.3050
C	-3.6870	-2.7120	1.5250
C	5.0750	1.9400	1.1920
C	3.9730	1.1080	1.0110
C	-2.4610	-2.0560	1.4030
C	-2.0930	-1.4380	0.2000
O	1.6830	3.4010	-0.7040
C	2.8150	-2.8870	0.1280
C	3.9270	-3.7200	-0.0180
C	5.0640	-3.2390	-0.6660
C	5.0640	-3.2390	-0.6660
C	5.0750	-1.9400	-1.1920
C	3.9730	-1.1080	-1.0110
C	2.8400	-1.5410	-0.2990
C	0.4210	1.3900	-0.0810
C	-0.8020	0.7010	-0.0850
C	-0.8020	-0.7010	0.0850
C	0.4210	-1.3900	0.0810
C	1.6490	-0.7090	-0.0420
C	1.6490	0.7090	0.0420
C	2.8400	1.5410	0.2990
C	2.8150	2.8870	-0.1280
C	-2.4610	2.0560	-1.4030
C	-3.6870	2.7120	-1.5250
C	5.0750	-1.9400	-1.1920
C	3.9730	-1.1080	-1.0110
C	2.8400	-1.5410	-0.2990
C	0.4210	1.3900	-0.0810
C	-0.8020	0.7010	-0.0850
C	-0.8020	-0.7010	0.0850
C	0.4210	-1.3900	0.0810
C	1.6490	-0.7090	-0.0420
C	1.6490	0.7090	0.0420
C	2.8400	1.5410	0.2990
C	2.8150	2.8870	-0.1280
C	-2.4610	2.0560	-1.4030
C	-3.6870	2.7120	-1.5250

The calculated structure and XYZ coordinates of (*P*,*R*,*R*)-**239**:

68

PRR-TOL new 0.000000

C	5.8410	3.5500	-0.0280
C	-0.5510	-2.9240	0.3250
C	-0.5510	2.9240	-0.3260
C	5.8410	-3.5500	0.0280
C	4.5220	2.8240	-0.0470
C	3.6340	2.9030	1.0240
C	2.4260	2.2160	1.0070
C	-3.9900	3.6510	0.2960
C	-5.0390	3.1450	1.0490
C	2.4260	-2.2160	-1.0070
C	3.6340	-2.9030	-1.0240
C	2.0600	1.4260	-0.0820
C	4.5220	-2.8240	0.0470
C	4.1560	-2.0280	1.1360

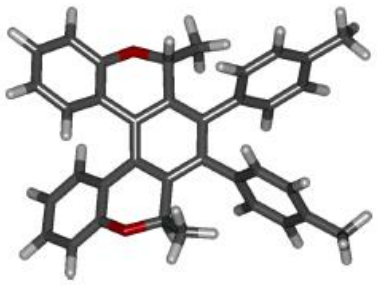

C	-4.9910	1.8340	1.5180
C	-3.9160	1.0190	1.1950
C	2.9540	-1.3380	1.1520
C	2.0600	-1.4260	0.0820
C	-2.9100	-2.8280	0.0030
C	-3.9900	-3.6500	-0.2960
C	-5.0390	-3.1450	-1.0490
C	-4.9910	-1.8340	-1.5180
C	-3.9160	-1.0190	-1.1950
C	-2.8720	-1.4890	-0.3900
C	-0.4640	1.4050	-0.1180
C	0.7510	0.7030	-0.0760
C	0.7510	-0.7030	0.0760
C	-0.4640	-1.4050	0.1180
C	-1.6730	-0.7050	-0.0370
C	-1.6730	0.7050	0.0370
C	-2.8720	1.4890	0.3900
C	-2.9100	2.8280	-0.0030
C	2.9540	1.3380	-1.1520
C	4.1560	2.0280	-1.1350
O	-1.8780	-3.3280	0.7330
O	-1.8780	3.3280	-0.7330
C	0.3250	3.5100	-1.4300
C	0.3250	-3.5100	1.4300
H	-0.3350	3.4370	0.6200
H	-0.3350	-3.4370	-0.6210
H	-3.8870	0.0060	1.5660
H	2.6980	0.7340	-2.0110
H	4.8240	1.9480	-1.9850
H	3.8890	3.5090	1.8840
H	1.7580	2.2940	1.8560
H	-3.9820	-4.6730	0.0560
H	-5.8810	-3.7790	-1.2910
H	6.0480	-4.0250	0.9880
H	6.6660	-2.8610	-0.1750
H	5.8600	-4.3210	-0.7410
H	5.8610	4.3190	0.7430
H	6.0470	4.0270	-0.9870
H	6.6660	2.8610	0.1720
H	1.7580	-2.2940	-1.8560
H	3.8890	-3.5090	-1.8840
H	4.8240	-1.9480	1.9850
H	2.6980	-0.7340	2.0110
H	-5.7890	-1.4480	-2.1350
H	-3.8870	-0.0060	-1.5660
H	-5.7890	1.4480	2.1360
H	-3.9820	4.6730	-0.0560
H	-5.8810	3.7790	1.2910
H	-0.0370	4.5170	-1.6350
H	0.2350	2.9210	-2.3430
H	1.3690	3.5690	-1.1500
H	-0.0370	-4.5170	1.6350
H	0.2350	-2.9220	2.3420
H	1.3690	-3.5690	1.1500

The structure and XYZ coordinates of the transition state for the (*M*,*R*,*R*)-**239** ↔ (*P*,*R*,*R*)-**239** process:

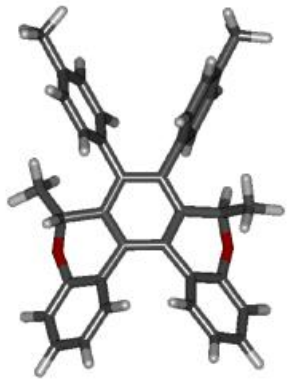

68

TS-TOL 0.000000

C	0.5430	3.6990	0.9740
C	0.5560	2.8340	-0.2950
C	0.5040	-2.9200	-0.4260
C	3.9290	-3.5040	-1.0840
C	5.1010	-3.3530	-0.3290
C	-0.6600	-3.5750	-1.1680
C	5.1080	-2.4740	0.7670
C	3.9910	-1.6670	1.0310
C	2.8830	2.6920	-0.4960
C	4.0260	3.4890	-0.6620
C	5.1740	3.2240	0.0980
C	5.1410	2.2040	1.0640
C	4.0080	1.3840	1.1780
C	2.8850	1.5300	0.3340
C	0.4010	-1.4450	-0.0100
C	-0.8180	-0.7270	0.0070
C	-0.7750	0.6880	-0.0500
C	0.4680	1.3430	-0.0170
C	1.6820	0.6500	0.2590
C	1.6510	-0.7910	0.2360
C	2.8430	-1.6920	0.2080
C	2.8030	-2.7280	-0.7690
O	1.7310	3.0920	-1.1210
O	1.6170	-3.0140	-1.3840
H	3.9960	-1.0560	1.9310
H	-1.5000	-3.8020	-0.4960
H	-1.0220	-2.9240	-1.9830
H	-0.2850	-4.5190	-1.6040
H	-0.2750	3.1390	-0.9460
H	0.7880	-3.5440	0.4520
H	3.9700	4.3400	-1.3490
H	6.0650	3.8540	-0.0170
H	1.3490	3.4000	1.6680
H	0.6700	4.7660	0.7090
H	-0.4310	3.5660	1.4810
H	5.9910	2.0470	1.7380
H	3.9740	0.6600	1.9880
H	5.9810	-2.4180	1.4280
H	3.8420	-4.2520	-1.8810
H	5.9810	-3.9670	-0.5560
C	-5.8130	3.6770	-0.2810
C	-5.9600	-3.4230	0.7760
C	-4.5160	2.8990	-0.2270
C	-4.0440	2.3560	0.9860
C	-2.8290	1.6570	1.0430
C	-3.1690	-1.3110	-0.7900
C	-4.3890	-1.9680	-0.5930
C	-2.0490	1.4740	-0.1150
C	-4.6270	-2.7370	0.5670
C	-3.5980	-2.8260	1.5240
C	-2.3700	-2.1740	1.3270
C	-2.1350	-1.4120	0.1640
C	-2.5170	2.0130	-1.3310
C	-3.7310	2.7150	-1.3840
H	-1.9270	1.8640	-2.2440
H	-4.0820	3.1200	-2.3420
H	-4.6430	2.4790	1.8980
H	-2.4860	1.2270	1.9920

H	-6.2760	-3.9710	-0.1330
H	-5.9170	-4.1400	1.6170
H	-6.7560	-2.6840	1.0020
H	-6.5260	3.3240	0.4880
H	-5.6350	4.7570	-0.0950
H	-6.2940	3.5900	-1.2730
H	-3.0040	-0.7230	-1.6980
H	-5.1760	-1.8870	-1.3550
H	-3.7610	-3.4170	2.4350
H	-1.5750	-2.2570	2.0780

The calculated structure and XYZ coordinates of (*M*,*R*,*R*)-**256**:

42

MRR-H 0.000000

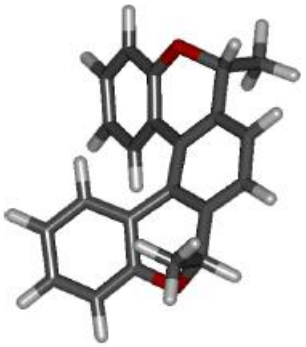

C	2.0330	2.5890	1.1090
C	1.5270	2.4430	-0.3320
C	3.3430	-2.4990	-2.7740
C	6.1830	-1.5160	-4.6860
C	6.5550	-0.4300	-5.4780
C	2.5790	-2.8120	-4.0680
C	5.8930	0.7970	-5.3400
C	4.9090	0.9500	-4.3660
C	3.2590	3.6230	-1.4130
C	3.9090	4.8590	-1.4160
C	5.2860	4.9120	-1.6270
C	6.0140	3.7280	-1.8020
C	5.3510	2.5030	-1.8310
C	3.9540	2.4250	-1.6950
C	2.8740	-1.2150	-2.1270
C	1.7600	-1.2230	-1.2890
C	1.2790	-0.0240	-0.7670
C	1.9910	1.1560	-0.9770
C	3.1800	1.1690	-1.7360
C	3.5480	-0.0150	-2.4360
C	4.5640	-0.1060	-3.5030
C	5.1710	-1.3620	-3.7350
O	1.9170	3.5960	-1.1290
O	4.7750	-2.4660	-3.0230
H	0.3700	-0.0060	-0.1680
H	1.2520	-2.1620	-1.0760
H	4.4050	1.9040	-4.2560
H	2.6940	-1.9920	-4.7850
H	1.5130	-2.9280	-3.8420
H	2.9570	-3.7380	-4.5160
H	0.4320	2.4780	-0.3440
H	3.2210	-3.3240	-2.0650
H	3.3270	5.7560	-1.2210
H	5.7960	5.8720	-1.6190
H	1.6920	3.5390	1.5360
H	3.1270	2.5560	1.1320
H	1.6480	1.7610	1.7150
H	7.0940	3.7600	-1.9170
H	5.9170	1.5890	-1.9760
H	6.1440	1.6310	-5.9880
H	6.6380	-2.4940	-4.8090
H	7.3340	-0.5510	-6.2250

The calculated structure and XYZ coordinates of (*P*,*R*,*R*)-**256**:

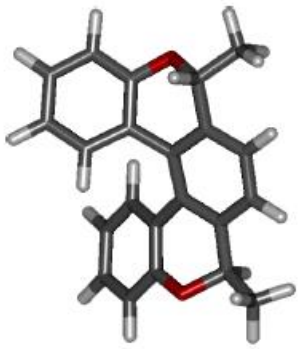

42

PRR-H 0.000000

C	3.7150	-1.7860	0.0040
C	3.2350	-2.9370	-0.6190
C	1.9410	-2.9590	-1.1550
C	2.8820	-0.6690	0.1150
C	1.5380	-0.7050	-0.3190
C	1.1070	-1.8530	-1.0060
C	2.9160	1.6740	-0.0210
C	1.3990	1.7220	0.0010
C	0.7070	0.4890	-0.0720
C	-0.7070	0.4890	0.0720
C	0.6970	2.9250	0.0330
C	-0.6970	2.9250	-0.0330
C	-1.3990	1.7220	-0.0010
C	-1.5380	-0.7050	0.3190
C	-2.9160	1.6740	0.0210
O	-3.3940	0.4800	-0.6620
C	-2.8820	-0.6690	-0.1150
C	-1.1070	-1.8530	1.0060
C	-1.9410	-2.9590	1.1550
C	-3.2350	-2.9370	0.6190
C	-3.7150	-1.7860	-0.0040
H	3.2560	1.5950	-1.0690
C	-3.6140	2.8500	-0.6480
H	4.7310	-1.7220	0.3820
H	3.8830	-3.8050	-0.7190
H	1.5820	-3.8370	-1.6830
H	0.1000	-1.8800	-1.4060
O	3.3940	0.4800	0.6620
H	-3.2560	1.5950	1.0690
H	-0.1000	-1.8800	1.4060
H	-1.5820	-3.8370	1.6830
H	-3.8830	-3.8050	0.7190
H	-4.7310	-1.7220	-0.3820
H	-3.2580	2.9720	-1.6770
H	-4.6940	2.6720	-0.6600
H	-3.4210	3.7740	-0.0940
C	3.6140	2.8500	0.6480
H	4.6940	2.6720	0.6600
H	3.2580	2.9720	1.6770
H	3.4210	3.7740	0.0940
H	1.2320	3.8680	0.0750
H	-1.2320	3.8680	-0.0750

The structure and XYZ coordinates of the transition state for the (*M*,*R*,*R*)-**256** ↔ (*P*,*R*,*R*)-**256** process:

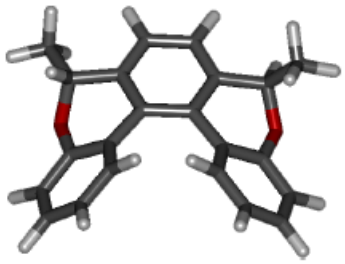

42

TS-H 0.000000

C	3.6680	-1.9480	-0.9540
C	2.7030	-1.9530	0.2310
C	-2.9930	-1.4890	-0.1520
C	-3.5020	1.8360	0.8130
C	-3.1810	3.0670	0.2620
C	-3.7640	-2.7270	0.2580
C	-2.1490	3.1460	-0.6650
C	-1.3760	2.0280	-0.9440
C	2.7830	0.3240	0.7110
C	3.6760	1.3270	1.0650
C	3.5800	2.5780	0.4760
C	2.6230	2.7910	-0.5070
C	1.7050	1.7950	-0.8100
C	1.6850	0.5630	-0.1460
C	-1.4980	-1.6340	-0.3080
C	-0.8980	-2.8800	-0.2700
C	0.4760	-2.9730	-0.1710
C	1.2440	-1.8240	-0.1260
C	0.6850	-0.5360	-0.2870
C	-0.7420	-0.4360	-0.3740
C	-1.5810	0.7980	-0.3080
C	-2.7540	0.7160	0.4770
O	3.0300	-0.9280	1.1910
O	-3.2170	-0.5010	0.8800
H	0.9510	-3.9400	-0.0630
H	-1.4990	-3.7760	-0.2500
H	-0.6330	2.1120	-1.7120
H	-3.7270	-3.4850	-0.5220
H	-3.3700	-3.1490	1.1820
H	-4.8070	-2.4580	0.4200
H	2.8400	-2.8780	0.7900
H	-3.4280	-1.0870	-1.0770
H	4.4650	1.0870	1.7640
H	4.2840	3.3560	0.7390
H	3.5620	-1.0500	-1.5590
H	4.6970	-2.0140	-0.5990
H	3.4650	-2.8110	-1.5890
H	2.5900	3.7280	-1.0460
H	1.0270	1.9690	-1.6200
H	-1.9450	4.0760	-1.1790
H	-4.3580	1.7080	1.4610
H	-3.7700	3.9400	0.5060

6.2 Appendix B: Calculation of the electronic circular dichroism (ECD) spectrum of (*M*,*R*,*R*)-239

The structure of (*M*,*R*,*R*)-**239** was first optimized using the DFT method with the B3LYP functional and cc-pVTZ basis set. The electronic CD spectra were calculated for this optimized structure sing TD-DFT with B2PLYP functional and cc-pVDZ or cc-pVTZ basis sets (both approaches provided similar outputs). The influence of solvent effects (acetonitrile) was also examined at the B2PLYP/cc-pVDZ/CPCM level of theory to see only negligible changes in the ECD spectra (see Figure 3.26).

Energy (cm-1)	Width (nm)	Abs	<--CD Spectrum	States-->	Wavelength (nm)	Energy (cm-1)	R(length)
25000.000000	400.000000	0.000000			312.049070	32046.241920	13.612600
25050.000000	399.201597	0.000000			281.639491	35506.384320	-27.391100
25100.000000	398.406375	0.000000			263.301344	37979.297280	-142.199300
25150.000000	397.614314	0.000000			257.563489	38825.378720	-55.842600
25200.000000	396.825397	0.000000			240.894025	41512.030080	62.331700
25250.000000	396.039604	0.000000			236.993858	42195.186400	-28.939900
25300.000000	395.256917	0.000000					
25350.000000	394.477318	0.000000					
25400.000000	393.700787	0.000000					
25450.000000	392.927308	0.000000					
25500.000000	392.156863	0.000000					
25550.000000	391.389432	0.000000					
25600.000000	390.625000	0.000000					
25650.000000	389.863548	0.000000					
25700.000000	389.105058	0.000000					
25750.000000	388.349515	0.000000					
25800.000000	387.596899	0.000000					
25850.000000	386.847195	0.000000					
25900.000000	386.100386	0.000000					
25950.000000	385.356455	0.000000					
26000.000000	384.615385	0.000000					
26050.000000	383.877159	0.000000					
26100.000000	383.141762	0.000000					
26150.000000	382.409178	0.000000					
26200.000000	381.679389	0.000000					
26250.000000	380.952381	0.000000					
26300.000000	380.228137	0.000000					
26350.000000	379.506641	0.000000					
26400.000000	378.787879	0.000000					
26450.000000	378.071834	0.000000					
26500.000000	377.358491	0.000000					
26550.000000	376.647834	0.000000					
26600.000000	375.939850	0.000000					
26650.000000	375.234522	0.000000					
26700.000000	374.531835	0.000000					
26750.000000	373.831776	0.000000					
26800.000000	373.134328	0.000000					
26850.000000	372.439479	0.000000					
26900.000000	371.747212	0.000000					
26950.000000	371.057514	0.000000					
27000.000000	370.370370	0.000000					
27050.000000	369.685767	0.000000					
27100.000000	369.003690	0.000000					
27150.000000	368.324125	0.000000					
27200.000000	367.647059	0.000000					
27250.000000	366.972477	0.000000					
27300.000000	366.300366	0.000000					
27350.000000	365.630713	0.000000					
27400.000000	364.963504	0.000000					
27450.000000	364.298725	0.000000					
27500.000000	363.636364	0.000000					
27550.000000	362.976407	0.000000					
27600.000000	362.318841	0.000000					
27650.000000	361.663653	0.000000					
27700.000000	361.010830	0.000000					
27750.000000	360.360360	0.000000					
27800.000000	359.712230	0.000000					
27850.000000	359.066427	0.000000					
27900.000000	358.422939	0.000000					
27950.000000	357.781753	0.000000					
28000.000000	357.142857	0.000000					
28050.000000	356.506239	0.000000					

28100.000000	355.871886	0.000000
28150.000000	355.239787	0.000000
28200.000000	354.609929	0.000000
28250.000000	353.982301	0.000000
28300.000000	353.356890	0.000000
28350.000000	352.733686	0.000000
28400.000000	352.112676	0.000000
28450.000000	351.493849	0.000000
28500.000000	350.877193	0.000000
28550.000000	350.262697	0.000000
28600.000000	349.650350	0.000000
28650.000000	349.040140	0.000000
28700.000000	348.432056	0.000000
28750.000000	347.826087	0.000001
28800.000000	347.222222	0.000001
28850.000000	346.620451	0.000002
28900.000000	346.020761	0.000004
28950.000000	345.423143	0.000006
29000.000000	344.827586	0.000009
29050.000000	344.234079	0.000015
29100.000000	343.642612	0.000023
29150.000000	343.053173	0.000036
29200.000000	342.465753	0.000056
29250.000000	341.880342	0.000086
29300.000000	341.296928	0.000132
29350.000000	340.715503	0.000200
29400.000000	340.136054	0.000302
29450.000000	339.558574	0.000451
29500.000000	338.983051	0.000670
29550.000000	338.409475	0.000986
29600.000000	337.837838	0.001441
29650.000000	337.268128	0.002089
29700.000000	336.700337	0.003006
29750.000000	336.134454	0.004292
29800.000000	335.570470	0.006080
29850.000000	335.008375	0.008548
29900.000000	334.448161	0.011924
29950.000000	333.889816	0.016507
30000.000000	333.333333	0.022675
30050.000000	332.778702	0.030909
30100.000000	332.225914	0.041809
30150.000000	331.674959	0.056118
30200.000000	331.125828	0.074745
30250.000000	330.578512	0.098789
30300.000000	330.033003	0.129565
30350.000000	329.489292	0.168621
30400.000000	328.947368	0.217764
30450.000000	328.407225	0.279068
30500.000000	327.868852	0.354880
30550.000000	327.332242	0.447818
30600.000000	326.797386	0.560751
30650.000000	326.264274	0.696767
30700.000000	325.732899	0.859120
30750.000000	325.203252	1.051159
30800.000000	324.675325	1.276238
30850.000000	324.149109	1.537601
30900.000000	323.624595	1.838248
30950.000000	323.101777	2.180788
31000.000000	322.580645	2.567268
31050.000000	322.061192	2.999009
31100.000000	321.543408	3.476425
31150.000000	321.027287	3.998864
31200.000000	320.512821	4.564456

31250.000000	320.000000	5.169994
31300.000000	319.488818	5.810851
31350.000000	318.979266	6.480941
31400.000000	318.471338	7.172739
31450.000000	317.965024	7.877358
31500.000000	317.460317	8.584694
31550.000000	316.957211	9.283626
31600.000000	316.455696	9.962289
31650.000000	315.955766	10.608385
31700.000000	315.457413	11.209546
31750.000000	314.960630	11.753722
31800.000000	314.465409	12.229577
31850.000000	313.971743	12.626881
31900.000000	313.479624	12.936875
31950.000000	312.989045	13.152591
32000.000000	312.500000	13.269113
32050.000000	312.012480	13.283762
32100.000000	311.526480	13.196201
32150.000000	311.041991	13.008445
32200.000000	310.559006	12.724786
32250.000000	310.077519	12.351628
32300.000000	309.597523	11.897248
32350.000000	309.119011	11.371491
32400.000000	308.641975	10.785415
32450.000000	308.166410	10.150906
32500.000000	307.692308	9.480280
32550.000000	307.219662	8.785889
32600.000000	306.748466	8.079754
32650.000000	306.278714	7.373235
32700.000000	305.810398	6.676741
32750.000000	305.343511	5.999514
32800.000000	304.878049	5.349463
32850.000000	304.414003	4.733068
32900.000000	303.951368	4.155339
32950.000000	303.490137	3.619836
33000.000000	303.030303	3.128738
33050.000000	302.571861	2.682943
33100.000000	302.114804	2.282205
33150.000000	301.659125	1.925280
33200.000000	301.204819	1.610093
33250.000000	300.751880	1.333883
33300.000000	300.300300	1.093361
33350.000000	299.850075	0.884834
33400.000000	299.401198	0.704315
33450.000000	298.953662	0.547611
33500.000000	298.507463	0.410377
33550.000000	298.062593	0.288153
33600.000000	297.619048	0.176367
33650.000000	297.176820	0.070328
33700.000000	296.735905	-0.034813
33750.000000	296.296296	-0.144105
33800.000000	295.857988	-0.262850
33850.000000	295.420975	-0.396655
33900.000000	294.985251	-0.551485
33950.000000	294.550810	-0.733693
34000.000000	294.117647	-0.950038
34050.000000	293.685756	-1.207671
34100.000000	293.255132	-1.514085
34150.000000	292.825769	-1.877027
34200.000000	292.397661	-2.304366
34250.000000	291.970803	-2.803901
34300.000000	291.545190	-3.383137
34350.000000	291.120815	-4.048999

34400.000000	290.697674	-4.807513
34450.000000	290.275762	-5.663448
34500.000000	289.855072	-6.619942
34550.000000	289.435601	-7.678124
34600.000000	289.017341	-8.836748
34650.000000	288.600289	-10.091860
34700.000000	288.184438	-11.436533
34750.000000	287.769784	-12.860676
34800.000000	287.356322	-14.350945
34850.000000	286.944046	-15.890777
34900.000000	286.532951	-17.460558
34950.000000	286.123033	-19.037933
35000.000000	285.714286	-20.598255
35050.000000	285.306705	-22.115172
35100.000000	284.900285	-23.561332
35150.000000	284.495021	-24.909186
35200.000000	284.090909	-26.131847
35250.000000	283.687943	-27.203992
35300.000000	283.286119	-28.102740
35350.000000	282.885431	-28.808488
35400.000000	282.485876	-29.305649
35450.000000	282.087447	-29.583267
35500.000000	281.690141	-29.635476
35550.000000	281.293952	-29.461784
35600.000000	280.898876	-29.067165
35650.000000	280.504909	-28.461968
35700.000000	280.112045	-27.661657
35750.000000	279.720280	-26.686380
35800.000000	279.329609	-25.560435
35850.000000	278.940028	-24.311634
35900.000000	278.551532	-22.970635
35950.000000	278.164117	-21.570259
36000.000000	277.777778	-20.144856
36050.000000	277.392510	-18.729743
36100.000000	277.008310	-17.360748
36150.000000	276.625173	-16.073872
36200.000000	276.243094	-14.905094
36250.000000	275.862069	-13.890291
36300.000000	275.482094	-13.065284
36350.000000	275.103164	-12.465958
36400.000000	274.725275	-12.128437
36450.000000	274.348422	-12.089255
36500.000000	273.972603	-12.385478
36550.000000	273.597811	-13.054725
36600.000000	273.224044	-14.135027
36650.000000	272.851296	-15.664488
36700.000000	272.479564	-17.680706
36750.000000	272.108844	-20.219930
36800.000000	271.739130	-23.315942
36850.000000	271.370421	-26.998692
36900.000000	271.002710	-31.292695
36950.000000	270.635995	-36.215274
37000.000000	270.270270	-41.774698
37050.000000	269.905533	-47.968337
37100.000000	269.541779	-54.780920
37150.000000	269.179004	-62.183039
37200.000000	268.817204	-70.129995
37250.000000	268.456376	-78.561126
37300.000000	268.096515	-87.399697
37350.000000	267.737617	-96.553444
37400.000000	267.379679	-105.915808
37450.000000	267.022697	-115.367868
37500.000000	266.666667	-124.780953

37550.000000	266.311585	-134.019832
37600.000000	265.957447	-142.946395
37650.000000	265.604250	-151.423639
37700.000000	265.251989	-159.319804
37750.000000	264.900662	-166.512443
37800.000000	264.550265	-172.892223
37850.000000	264.200793	-178.366267
37900.000000	263.852243	-182.860855
37950.000000	263.504611	-186.323350
38000.000000	263.157895	-188.723256
38050.000000	262.812089	-190.052361
38100.000000	262.467192	-190.323985
38150.000000	262.123198	-189.571393
38200.000000	261.780105	-187.845498
38250.000000	261.437908	-185.212005
38300.000000	261.096606	-181.748180
38350.000000	260.756193	-177.539442
38400.000000	260.416667	-172.675978
38450.000000	260.078023	-167.249560
38500.000000	259.740260	-161.350720
38550.000000	259.403372	-155.066396
38600.000000	259.067358	-148.478141
38650.000000	258.732212	-141.660898
38700.000000	258.397933	-134.682356
38750.000000	258.064516	-127.602807
38800.000000	257.731959	-120.475449
38850.000000	257.400257	-113.347000
38900.000000	257.069409	-106.258531
38950.000000	256.739409	-99.246391
39000.000000	256.410256	-92.343118
39050.000000	256.081946	-85.578249
39100.000000	255.754476	-78.978959
39150.000000	255.427842	-72.570487
39200.000000	255.102041	-66.376342
39250.000000	254.777070	-60.418272
39300.000000	254.452926	-54.716059
39350.000000	254.129606	-49.287151
39400.000000	253.807107	-44.146197
39450.000000	253.485425	-39.304539
39500.000000	253.164557	-34.769712
39550.000000	252.844501	-30.544998
39600.000000	252.525253	-26.629078
39650.000000	252.206810	-23.015800
39700.000000	251.889169	-19.694084
39750.000000	251.572327	-16.647974
39800.000000	251.256281	-13.856823
39850.000000	250.941029	-11.295612
39900.000000	250.626566	-8.935386
39950.000000	250.312891	-6.743791
40000.000000	250.000000	-4.685696
40050.000000	249.687890	-2.723899
40100.000000	249.376559	-0.819898
40150.000000	249.066002	1.065280
40200.000000	248.756219	2.970179
40250.000000	248.447205	4.931974
40300.000000	248.138958	6.985463
40350.000000	247.831475	9.162020
40400.000000	247.524752	11.488523
40450.000000	247.218789	13.986259
40500.000000	246.913580	16.669852
40550.000000	246.609125	19.546245
40600.000000	246.305419	22.613783
40650.000000	246.002460	25.861451

40700.000000	245.700246	29.268325
40750.000000	245.398773	32.803294
40800.000000	245.098039	36.425110
40850.000000	244.798042	40.082810
40900.000000	244.498778	43.716556
40950.000000	244.200244	47.258889
41000.000000	243.902439	50.636417
41050.000000	243.605359	53.771893
41100.000000	243.309002	56.586633
41150.000000	243.013366	59.003195
41200.000000	242.718447	60.948224
41250.000000	242.424242	62.355333
41300.000000	242.130751	63.167897
41350.000000	241.837969	63.341613
41400.000000	241.545894	62.846706
41450.000000	241.254524	61.669642
41500.000000	240.963855	59.814259
41550.000000	240.673887	57.302226
41600.000000	240.384615	54.172803
41650.000000	240.096038	50.481878
41700.000000	239.808153	46.300327
41750.000000	239.520958	41.711753
41800.000000	239.234450	36.809715
41850.000000	238.948626	31.694566
41900.000000	238.663484	26.470063
41950.000000	238.379023	21.239891
42000.000000	238.095238	16.104274
42050.000000	237.812128	11.156823
42100.000000	237.529691	6.481762
42150.000000	237.247924	2.151628
42200.000000	236.966825	-1.774450
42250.000000	236.686391	-5.251860
42300.000000	236.406619	-8.250983
42350.000000	236.127509	-10.757058
42400.000000	235.849057	-12.769477
42450.000000	235.571260	-14.300593
42500.000000	235.294118	-15.374133
42550.000000	235.017626	-16.023311
42600.000000	234.741784	-16.288769
42650.000000	234.466589	-16.216439
42700.000000	234.192037	-15.855447
42750.000000	233.918129	-15.256128
42800.000000	233.644860	-14.468237
42850.000000	233.372229	-13.539422
42900.000000	233.100233	-12.513965
42950.000000	232.828871	-11.431842
43000.000000	232.558140	-10.328073
43050.000000	232.288037	-9.232370
43100.000000	232.018561	-8.169037
43150.000000	231.749710	-7.157093
43200.000000	231.481481	-6.210581
43250.000000	231.213873	-5.339011
43300.000000	230.946882	-4.547895
43350.000000	230.680507	-3.839342
43400.000000	230.414747	-3.212664
43450.000000	230.149597	-2.664971
43500.000000	229.885057	-2.191732
43550.000000	229.621125	-1.787284
43600.000000	229.357798	-1.445267
43650.000000	229.095074	-1.159003
43700.000000	228.832952	-0.921790
43750.000000	228.571429	-0.727137
43800.000000	228.310502	-0.568931

43850.000000	228.050171	-0.441553
43900.000000	227.790433	-0.339941
43950.000000	227.531286	-0.259620
44000.000000	227.272727	-0.196698
44050.000000	227.014756	-0.147843
44100.000000	226.757370	-0.110244
44150.000000	226.500566	-0.081559
44200.000000	226.244344	-0.059863
44250.000000	225.988701	-0.043593
44300.000000	225.733634	-0.031497
44350.000000	225.479143	-0.022579
44400.000000	225.225225	-0.016060
44450.000000	224.971879	-0.011334
44500.000000	224.719101	-0.007937
44550.000000	224.466891	-0.005515
44600.000000	224.215247	-0.003802
44650.000000	223.964166	-0.002601
44700.000000	223.713647	-0.001765
44750.000000	223.463687	-0.001189
44800.000000	223.214286	-0.000795
44850.000000	222.965440	-0.000527
44900.000000	222.717149	-0.000347
44950.000000	222.469410	-0.000226
45000.000000	222.222222	-0.000147
45050.000000	221.975583	-0.000094
45100.000000	221.729490	-0.000060
45150.000000	221.483942	-0.000038
45200.000000	221.238938	-0.000024
45250.000000	220.994475	-0.000015
45300.000000	220.750552	-0.000009
45350.000000	220.507166	-0.000006
45400.000000	220.264317	-0.000003
45450.000000	220.022002	-0.000002
45500.000000	219.780220	-0.000001
45550.000000	219.538968	-0.000001
45600.000000	219.298246	-0.000000
45650.000000	219.058050	-0.000000
45700.000000	218.818381	-0.000000
45750.000000	218.579235	-0.000000
45800.000000	218.340611	-0.000000
45850.000000	218.102508	-0.000000
45900.000000	217.864924	-0.000000
45950.000000	217.627856	-0.000000
46000.000000	217.391304	-0.000000
46050.000000	217.155266	-0.000000
46100.000000	216.919740	-0.000000
46150.000000	216.684724	-0.000000
46200.000000	216.450216	-0.000000
46250.000000	216.216216	-0.000000
46300.000000	215.982721	-0.000000
46350.000000	215.749730	-0.000000
46400.000000	215.517241	-0.000000
46450.000000	215.285253	-0.000000
46500.000000	215.053763	-0.000000
46550.000000	214.822771	-0.000000
46600.000000	214.592275	-0.000000
46650.000000	214.362272	-0.000000
46700.000000	214.132762	-0.000000
46750.000000	213.903743	-0.000000
46800.000000	213.675214	-0.000000
46850.000000	213.447172	-0.000000
46900.000000	213.219616	-0.000000
46950.000000	212.992545	-0.000000

47000.000000	212.765957	-0.000000
47050.000000	212.539851	-0.000000
47100.000000	212.314225	-0.000000
47150.000000	212.089077	-0.000000
47200.000000	211.864407	-0.000000
47250.000000	211.640212	-0.000000
47300.000000	211.416490	-0.000000
47350.000000	211.193242	-0.000000
47400.000000	210.970464	-0.000000
47450.000000	210.748156	-0.000000
47500.000000	210.526316	-0.000000
47550.000000	210.304942	-0.000000
47600.000000	210.084034	-0.000000
47650.000000	209.863589	-0.000000
47700.000000	209.643606	-0.000000
47750.000000	209.424084	-0.000000
47800.000000	209.205021	-0.000000
47850.000000	208.986416	-0.000000
47900.000000	208.768267	-0.000000
47950.000000	208.550574	-0.000000
48000.000000	208.333333	-0.000000
48050.000000	208.116545	-0.000000
48100.000000	207.900208	-0.000000
48150.000000	207.684320	-0.000000
48200.000000	207.468880	-0.000000
48250.000000	207.253886	-0.000000
48300.000000	207.039337	-0.000000
48350.000000	206.825233	-0.000000
48400.000000	206.611570	-0.000000
48450.000000	206.398349	-0.000000
48500.000000	206.185567	-0.000000
48550.000000	205.973223	-0.000000
48600.000000	205.761317	-0.000000
48650.000000	205.549846	-0.000000
48700.000000	205.338809	-0.000000
48750.000000	205.128205	-0.000000
48800.000000	204.918033	-0.000000
48850.000000	204.708291	-0.000000
48900.000000	204.498978	-0.000000
48950.000000	204.290092	-0.000000
49000.000000	204.081633	-0.000000
49050.000000	203.873598	-0.000000
49100.000000	203.665988	-0.000000
49150.000000	203.458800	-0.000000
49200.000000	203.252033	-0.000000
49250.000000	203.045685	-0.000000
49300.000000	202.839757	-0.000000
49350.000000	202.634245	-0.000000
49400.000000	202.429150	-0.000000
49450.000000	202.224469	-0.000000
49500.000000	202.020202	-0.000000
49550.000000	201.816347	-0.000000
49600.000000	201.612903	-0.000000
49650.000000	201.409869	-0.000000
49700.000000	201.207243	-0.000000
49750.000000	201.005025	-0.000000
49800.000000	200.803213	-0.000000
49850.000000	200.601805	-0.000000
49900.000000	200.400802	-0.000000
49950.000000	200.200200	-0.000000

6.3 Appendix C: Crystal data for (*M*,*R*,*R*)-256

Crystal data for (*M*,*R*,*R*)-**256** (CCDC 851844), $C_{22}H_{18}O_2$, M_r = 314.36, Orthorhombic, *P* 2_1 2_1 2_1, (No 19), *a* = 7.13790 (10) Å, *b* = 13.9113 (3) Å, *c* = 16.4507 (4) Å, Z = 4, D_x = 1.278 Mg m^{-3}, colorless crystal of dimensions 0.4 × 0.4 × 0.25 mm, an absorption was neglected (μ = 0.08 mm^{-1}); 27671 diffraction collected (θ_{max}= 27.4˚), 3710 independent (R_{int} = 0.029) and 3370 observed ($I > 2\sigma(I)$). 219 parameters, goodness of fit 1.02, final R indices *R* [$F^2 > 2\sigma(F^2)$] = 0.032, $wR(F^2)$ = 0.084, maximal/minimal residual electron density ($\Delta\rho_{max}$ = 0.12, $\Delta\rho_{min}$ -0.17 e $Å^{-3}$).

7. References

[1] (a) Wynberg, H. *Acc. Chem. Res.* **1971**, *4*, 65. (b) Martin, R. H. *Angew. Chem., Int. Ed.* **1974**, *13*, 649. (c) Laarhoven, W. H.; Prinsen, W. J. C. *Top. Curr. Chem.* **1984**, *125*, 63. (d) Meurer, K. P.; Vögtle, F. *Top. Curr. Chem.* **1985**, *127*, 1. (e) Oremek, G.; Seiffert, U.; Janecka, A. *Chem.-Ztg.* **1987**, *111*, 69. (f) Vögtle, F. *Fascinating Molecules in Organic Chemistry*; Wiley: New York, **1992**; p 156. (g) Osuga, H.; Suzuki, H. *J. Syn. Org. Chem. Jpn*. **1994**, *52*, 1020. (h) Katz, T. J. *Angew. Chem., Int. Ed.* **2000**, *39*, 1921. (i) Urbano, A. *Angew. Chem., Int. Ed.* **2003**, *42*, 3986. (j) Collins, S. K.; Vachon, M. P. *Org. Biomol. Chem.* **2006**, *4*, 2518. (k) Grimme, S.; Harren, J.; Sobanski, A.; Vögtle, F. *Eur. J. Org. Chem*. **1998**, 1491. (l) Hopf, H. *Classics in Hydrocarbon Chemistry: Syntheses, Concepts, Perspectives*; Wiley-VCH: Weinheim, **2000**, p 323. (m) Sato, K.; Arai, S. In *Cyclophane Chemistry for the 21st Century*; Takemura, H., Ed.; Research Signpost: Trivandrum, **2002**, p 173. (n) Rajca, A.; Miyasaka, M. In *Functional Organic Materials: Syntheses, Strategies and Applications*; Müller, T. J. J., Bunz, U. H. F., Eds.; Wiley-VCH: Weinheim, **2007**, p 547. (o) Hoffmann, N. *Chem. Rev*. **2008**, *108*, 1052. (p) Wolf, C. *Dynamic Stereochemistry of Chiral Compounds: Principles and Applications*; Royal Society of Chemistry, Cambridge, U.K., **2008**, p 204. (q) Starý, I.; Stará, I. G. In *Strained Hydrocarbons: Beyond the van't Hoff and Le Bel Hypothesis*; Dodziuk, H., Ed.; Wiley-VCH: Weinheim, **2009**, p 166. (r) Dumitrascu, F.; Dumitrescu, D. G.; Aronb, I. *ARKIVOC* **2010**, *1*, 1. (s) Jørgensen, K. B. *Molecules* **2010**, *15*, 4334. (t) Stará, I. G.; Starý, I. In *Aromatic Ring Assemblies, Polycyclic Aromatic Hydrocarbons, and Conjugated Polyenes*; Siegel, J. S., Tobe, Y., Eds.; Thieme: Stuttgart, **2010**, Vol. 45b, p 885.

[2] Cahn, R. S.; Ingold, C.; Prelog, V. *Angew. Chem., Int. Ed*. **1966**, *5*, 385.

[3] Ben Hassine, B.; Gorsane, M.; Pecher, J.; Martin, R. H. *Bull. Soc. Chim. Belg.* **1985**, *94*, 597.

[4] Ben Hassine, B.; Gorsane, M.; Pecher, J.; Martin, R. H. *Bull. Soc. Chim. Belg.* **1987**, *96*, 801.

[5] Ben Hassine, B.; Gorsane, M.; Pecher, J.; Martin, R. H. *Bull. Soc. Chim. Belg.* **1985**, *94*, 759.

[6] Ben Hassine, B.; Gorsane, M.; Geerts-Evard, F.; Pecher, J.; Martin, R. H. Castelet, D. *Bull. Soc. Chim. Belg.* **1986**, *95*, 547.

[7] Ben Hassine, B.; Gorsane, M.; Pecher, J.; Martin, R. H. *Bull. Soc. Chim. Belg.* **1986**, *95*, 557.

[8] Ojima, I. In *Catalytic Asymmetric Synthesis*, VCH, New York, **1993**, p. 194.

[9] Reetz, M. T.; Beuttenmüller, E. W.; Goddard, R. *Tetrahedron Lett.* **1997**, *38*, 3211.

[10] Yamamoto, K.; Ikeda, T.; Kitsuki, T.; Okamoto, Y.; Chikamatsu, H.; Nakazaki, M. *J. Chem. Soc. Perkin Trans. I* **1990**, 271.

[11] Terfort, A.; Görls, H.; Brunner, H. *Synthesis* **1997**, 79.

[12] Nakano, D.; Yamaguchi, M. *Tetrahedron Lett.* **2003**, *44*, 4969.

[13] Nakano, D.; Hirano, R.; Yamaguchi, M.; Kabuto, C. *Tetrahedron Lett*. **2003**, *44*, 3683.

[14] Okubo, H.; Yamaguchi, M. *J. Org. Chem*. **2001**, *66*, 824.

[15] Reetz, M. T.; Sostmann, S. *J. Organomet. Chem.* **2000**, *603*, 105.

[16] Okubo, H.; Yamaguchi, M.; Kabuto, C. *J. Org. Chem.* **1998**, *63*, 9500.

[17] (a) Noyori, R.; Kitamura, M. *Angew. Chem., Int. Ed.* **1991**, *30*, 49. (b) Soai, K.; Niwa, S. *Chem. Rev*. **1992**, *92*, 833.

[18] (a) Newman, M. S.; Wolf, M. *J. Am. Chem. Soc*. **1952**, *74*, 3225. (b) Newman, M. S.; Wise, R. M. *J. Am. Chem. Soc*. **1956**, *78*, 450.

[19] Cheung, J.; Field, L. D.; Hambley, T. W.; Sternhell, S. *J. Org. Chem*. **1997**, *62*, 62.

[20] Oda, M.; Yamamuro, A.; Watabe, T. *Chem. Lett.* **1979**, 1427.

[21] Dreher, S. D.; Katz, T. J.; Lam, K. C.; Rheingold, A. L. *J. Org. Chem.* **2000**, *65*, 815.

[22] Russig, F. *J. Prakt. Chem*. **1900**, 33.

[23] Laatsch, H. *Liebigs Ann. Chem*. **1980**, 140.

[24] Sato, I.; Yamashima, R.; Kadowaki, K.; Yamamoto, J.; Shibata, T.; Soai, K. *Angew. Chem., Int. Ed.* **2001**, *40*, 1096.

[25] (a) Gingras, M. *Chem. Soc. Rev.* **2013**, *42*, 968. (b) Gingras, M.; Félix, G.; Peresutti, R. *Chem. Soc. Rev.* **2013**, *42*, 1007. (c) Gingras, M. *Chem. Soc. Rev.* **2013**, *42*, 1051.

[26] Shen, Y.; Chen, C.-F. *Chem. Rev.* **2012**, *112*, 1463.

[27] Kawasaki, T.; Suzuki, K.; Licandro, E.; Bossi, A.; Maiorana, S.; Soai, K. *Tetrahedron: Asymmetry* **2006**, *17*, 2050.

[28] Grohen, M. B.; Schadenberg, H.; Wynberg, H. *J. Org. Chem.* **1971**, *36*, 2797.

[29] Maiorana, S.; Papagni, A.; Licandro, E.; Annunziata, R.; Paravidino, P.; Perdicchia, D.; Giannini, C.; Bencini, M.; Clays, K.; Persoons, A *Tetrahedron* **2003**, *59*, 6481.

[30] Licandro, E.; Rigamonti, C.; Ticozzelli, M. T.; Monteforte, M.; Baldoli, C.; Giannini, C.; Maiorana, S. *Synthesis* **2006**, *21*, 3670.

[31] Wolberg, M.; Hummel, W.; Müller, M. *Chem. Eur. J.* **2001**, *8*, 4562.

[32] Monteforte, M.; Cauteruccio, S.; Maiorana, S.; Raimondi, L.; Licandro, E.; Benincori, T.; Forni, A.; Graiff, C.; Tiripicchio, A.; Stephenson, G. R. *Eur. J. Org. Chem.* **2011** , *28*, 5649.

[33] Krausová, Z.; Sehnal, P.; Bondzic, B. P.; Chercheja, S.; Eilbracht, P.; Stará, I. G.; Šaman, D.; Starý, I. *Eur. J. Org. Chem.* **2011**, 3849.

[34] Van Leeuwen, P. W. N. M.; Claver, C. *Rhodium-Catalysed Hydroformylation*, Kluwer Academic, Dordrecht, **2000**.

[35] (a) Gual, A.; Godard, C.; Castillón, S.; Claver, C. *Tetrahedron: Asymmetry* **2010**, *21*, 1135. (b) J. Klosin, J.; Landis, C. R. *Acc. Chem. Res.* **2007**, *40*, 1251. (c) Breit, B.; Seiche, W. *Synthesis* **2001**, 1.

[36] Sehnal, P.; Krausová, Z.; Teplý, F.; Stará, I. G.; Starý, I.; Rulíšek, L.; Šaman, D.; Císařová, I. *J. Org. Chem.* **2008**, *73*, 2074.

[37] Alexandrová, Z.; Stará, I. G.; Sehnal, P.; Teplý, F.; Starý, I.; Šaman, D.; Fiedler, P. *Collect. Czech. Chem. Commun.* **2004**, *69*, 2193.

[38] Stará, I. G.; Kollárovič, A.; Teplý, F.; Starý, I.; Šaman, D.; Fiedler, P. *Collect. Czech. Chem. Commun.* **2000**, *65*, 577.

[39] Stará, I. G.; Alexandrová, Z.; Teplý, F.; Sehnal, P.; Starý, I.; Šaman, D.; Buděšínský, M.; Cvačka, J. *Organic Lett*. **2005**, *13*, 2547.

[40] (a) Cammack, J. K.; Jalisatgi, S.; Matzger, A. J.; Negrón, A.; Vollhardt, K. P. C. *J. Org. Chem*. **1996**, *61*, 4798. (b) Jonas, K.; Deffense, E.; Habermann, D. *Angew. Chem., Int. Ed.* **1983**, *22*, 716; *Angew. Chem. Suppl.* **1983**, 1005.

[41] (a) Godleski, S. A. In *Comprehensive Organic Synthesis* (Eds.: B. M. Trost, I. Fleming), Pergamon, Amsterdam, **1991**, p 585. (b) Johannsen, M.; Jørgensen, K. A. *Chem. Rev.* **1998**, *98*, 1689. (c) Trost, B. M.; Van Vraken, D. L. *Chem. Rev.* **1996**, *96*, 395. (d) Trost, B. M.; Crawley, M. L. *Chem. Rev.* **2003**, *103*, 2921. (e) Lu, Z.; Ma, S. *Angew. Chem., Int. Ed.* **2008**, *47*, 258. (f) Helmchen, G.; Dahnz, A.; Dübon, P.; Schelwies, M.; Weihofen, R. *Chem. Commun.* **2007**, 675. (g) Hartwig, J. F.; Stanley, M. L. *Acc. Chem. Res.* **2010**, *43*, 1461.

[42] (a) Trost, B. M. *Chem. Pharm. Bull.* **2002**, *50*, 1. (b) Trost, B. M. *J. Org. Chem.* **2004**, *69*, 5813.

[43] You, S. L.; Zhu, X. Z.; Luo, Y. M.; Hou, X. L.; Dai, L. X. *J. Am. Chem. Soc.* **2001**, *123*, 7471.

[44] Torst, B. M.; Hachiya, I. *J. Am. Chem. Soc.* **1998**, *120*, 1104.

[45] Glorius, F.; Pfaltz, A. *Org. Lett.* **1999**, *1*, 141.

[46] Malkov, A. V.; Baxendale, I. R.; Dvořák, D.; Mansfield, D. J.; Kočovský, P. *J. Org. Chem.* **1999**, *64*, 2737.
[47] Evans, P. A.; Nelson, J. D. *J. Am. Chem. Soc.* **1998**, *120*, 5581.

[48] Takeuchi, R.; Ue, N.; Tanabe, K.; Yamashita, K.; Shiga, N. *J. Am. Chem. Soc.* **2001**, *123*, 9525.

[49] Janssen, J. P.; Helmchen, G. *Tetrahedron Lett.* **1997**, *38*, 8025.

[50] Ohmura, T.; Hartvig, J. F. *J. Am. Chem. Soc.* **2002**, *124*, 15164.

[51] Leither, A.; Shu, C. T.; Hartwig, J. F. *Org. Lett.* **2005**, *7*, 1093.

[52] (a) Raskatov, J. A.; Spiess, S.; Gnamm, C.; Brödner, K.; Rominger, F.; Helmchen, G. *Chem. Eur. J.* **2010**, *16*, 6601.(b) Marković, D.; Hartwig, J. F. *J. Am. Chem. Soc.* **2007**, *129*, 11680. (c) Leitner, A.; Shekhar, S.; Pouy, M. J.; Hartwig, J. F. *J. Am. Chem. Soc.* **2005**, *127*, 15506. (d) Kiener, C. A.; Shu, C.; Incarvito, C.; Hartwig, J. F. *J. Am. Chem. Soc.* **2003**, *125*, 14272.

[53] For example: (a) Berkessel, A., Groeger, H. In *Asymmetric Organocatalysis*, Weinheim: Wiley-VCH, **2005**. (b) List, B. *Chem. Rev.* **2007**, *107*, 5413. (c) Dalko, P. I.; Moisan, L. *Angew. Chem., Int. Ed.* **2004**, *43*, 5138. (d) Dalko; P. I.; Moisan, L. *Angew. Chem., Int. Ed.* **2001**, *40*, 3726.

[54] Takenaka, N.; Sarangthem, R. S.; Captain, B. *Angew. Chem., Int. Ed.* **2008**, *47*, 9708.

[55] Martin, R. H. *Chimia* **1975**, *29*, 137.

[56] Denmark, S. E.; Barsanti, P. A.; Wong, K.-T.; Stavenger, R. A. *J. Org. Chem.* **1998**, *63*, 2428.

[57] (a) Chelucci, G.; Baldino, S.; Pinna, G. A.; Benaglia, M.; Buffa, L.; Guizzetti, S. *Tetrahedron* **2008**, *64*, 7574. (b) Denmark, S. E.; Barsanti, P. A.; Beutner, G. L.; Wilson, T. W. *Adv. Synth. Catal.* **2007**, *349*, 567. (c) Tokuoka, E.; Kotani, E.; Matsunaga, H.; Ishizuka, T.; Hashimoto, S.; Nakajima, M. *Tetrahedron: Asymmetry* **2005**, *16*, 2391. (d) Paek, S. H.; Shim, S. C.; Cho, C. S.; Kim, T.-J. *Synlett* **2003**, 849. (e) Nakajima, M.; Saito, M.; Uemura, M.; Hashimoto, S. *Tetrahedron Lett.* **2002**, *43*, 8827. (f) Tao, B.; Lo, M. M.-C.; Fu, G. C. *J. Am. Chem. Soc.* **2001**, *123*, 353.

[58] Chow, H.-F.; Low, K.-H.; Wong, K. Y. *Synlett* **2005**, *14*, 2130.

[59] (a) Harrowven, D. C.; Guy, I. L.; Nanson, L. *Angew. Chem., Int. Ed.* **2006**, *45*, 2242. (b) Dunne, E. C.; Coyne, É. J.; Crowley, P. B.; Gilheany, D. G. *Tetrahedron Lett.* **2002**, *43*, 2449.

[60] (a) Staab, H. A.; Diehm, M.; Krieger, C. *Tetrahedron Lett.* **1994**, *35*, 8357. (b) Ross Kelly, T.; Li, Q.; Bhushan, V.; *Tetrahedron Lett.* **1990**, *31*, 161.

[61] Dick, A. R.; Hull, K. L.; Sanford, M. S. *J. Am. Chem. Soc.* **2004**, *126*, 2300.

[62] Chen, J. S.; Takenaka, N. *Chem.-Eur. J.* **2009**, *15*, 7268.

[63] Takenaka, N.; Chen, J. S.; Captain, B.; Sarangthem, R. S.; Chandrakumar, A. *J. Am. Chem. Soc.* **2010**, *132*, 4536.

[64] (a) Singh, A.; Johnston, J. N. *J. Am. Chem. Soc.* **2008**, *130*, 5866. (b) Shen, B.; Johnston, J. N. *Org. Lett.* **2008**, *10*, 4397. (c) Wilt, J. C.; Pink, M.; Johnston, J. N. *Chem. Commun.* **2008**, 4177. (d) Singh, A.; Yoder, R. A.; Shen, B.; Johnston, J. N. *J. Am. Chem. Soc.* **2007**, *129*, 3466. (e) Hess, A. S.; Yoder, R. A.; Johnston, J. N. *Synlett* **2006**, 147. (f) Nugent, B. M.; Yoder, R. A.; Johnston, J. N. *J. Am. Chem. Soc.* **2004**, *126*, 3418. (g) Ganesh, M.; Seidel, D. *J. Am. Chem. Soc.* **2008**, *130*, 16464. (h) Schuster, T.; Kurz, M.; Göbel, M. W. *J. Org. Chem.* **2000**, *65*, 1697.

[65] Yin, J.; Xiang, B.; Huffman, M. A.; Raab, C. E.; Davies, I. W. *J. Org. Chem.* **2007**, *72*, 4554.

[66] Šámal, M.; Míšek, J.; Stará, I. G.; Starý, I. *Collect. Czech. Chem. Commun.* **2009**, *74*, 1151.

[67] Míšek, J.; Teplý, F.; Stará, I. G.; Tichý, M.; Šaman, D.; Císařová, I.; Vojtíšek, P.; Starý, I. *Angew. Chem., Int. Ed.* **2008**, *47*, 3188.

[68] (a) Xu, S.; Held, I.; Kempf, B.; Mayr, H.; Steglich, W.; Zipse, H. *Chem. Eur. J.* **2005**, *11*, 4751. (b) Scriven, E. F. V. *Chem. Soc. Rev.* **1983**, *12*, 129. (c) Höfle, G.; Steglich, W.; Vorbrüggen, H. *Angew. Chem., Int. Ed.* **1978**, *17*, 569.

[69] Crittall, M. R.; Rzepa, H. S.; Carbery, D. R. *Org. Lett.* **2011**, *13*, 1250.

[70] Thomas, J. M.; Raja, R. *Acc. Chem. Res.* **2008**, *41*, 708.

[71] Simonneaux, G.; Le Maux, P.; Ferrand, Y.; Rault-Berthelot, J. *Coord. Chem. Rev.* **2006**, *250*, 2212.

[72] Gupta, K. C.; Alekha Kumar, S.; Chu-Chieh, L. *Coord. Chem. Rev.* **2009**, *253*, 1926.

[73] Barbaro, P.; Bianchini, C.; Giambastiani, G.; Parisel, S. L. *Coord.Chem. Rev.* **2004**, *248*, 2131.

[74] Mallat, T.; Orglmeister, E.; Baiker, A. *Chem.Rev*. **2007**, *107*, 4863.

[75] Schmidt, E.; Vargas, A.; Mallat, T.; Baiker, A. *J. Am. Chem. Soc.* **2009**, *131*, 12358.

[76] Niu, W.; Zhang, L.; Xu, G. *ASC Nano*, **2010**, *4*, 1987.

[77] Ahmadi, A.; Attard, G. A.; Feliu, J.; Rodes, A. *Langmuir* **1999**, *15*, 2420.

[78] Roy, S.; Pericas, M. A. *Org. Biomol. Chem*. **2009**, *7*, 2669.

[79] Aloui, F.; Jabli, M.; Ben Hassine, B. *Synth. Commun.* **2013**, *43*, 277.

[80] Aloui, F.; El Abed, R.; Marinetti, A.; Ben Hassine, B. *Tetrahedron Lett.* **2007**, *48*, 2017.

[81] (a) Taniguchi, M.; Nakagawa, H.; Yamagishi, A.; Yamada, K. *Surf. Sci.* **2000**, *454*, 1005. (b) Taniguchi, M.; Nakagawa, H.; Yamagishi, A.; Yamada, K. *J. Mol. Catal. A: Chem.* **2003**, *199*, 65.

[82] (a) Ernst, K. H.; Kuster, Y.; Fasel, R.; Muller, M.; Ellerbeck, U. *Chirality* **2001**, *13*, 675. (b) Fasel, R.; Parschau, M.; Ernst, K. H. *Angew. Chem., Int. Ed.* **2003**, *42*, 5178.

[83] (a) Ernst, K.-H.; Bohringer, M.; McFadden, C. F.; Hug, P.; Muller, U.; Ellerbeck, U. *Nanotechnology* **1999**, *10*, 355. (b) Ernst, K.-H.; Neuber, M.; Grunze, M.; Ellerbeck, U. *J. Am. Chem. Soc.* **2001**, *123*, 493. (c) Fasel, R.; Cossy, A.; Ernst, K.-H.; Baumberger, F.; Greber, T.; Osterwalder, J. *J. Chem. Phys.* **2001**, *115*, 1020. (d) Ernst, K.-H.; Kuster, Y.; Fasel, R.; McFadden, C. F.; Ellerbeck, U. *Surf. Sci.* **2003**, *530*, 195. (e) Fasel, R.; Parschau, M.; Ernst, K.-H. *Nature* **2006**, *439*, 449. (f) Ernst, K.-H. *Chimia* **2008**, *62*, 471. (g) Ernst, K.-H. *Z. Phys. Chem.* **2009**, *223*, 37.

[84] Goretta, S.; Tasciotti, C.; Mathieu, S, Smet, M.; Maes, W.; Chabre, Y. M.; Dehaen, W.; Giasson, R.; Raimundo, J.-M.; Henty, C. R.; Barth, C.; Gingras, M. *Org. Lett.* **2009**, *11*, 3846.

[85] Sehnal, P.; Stará, I. G.; Šaman, D.; Tichý, M.; Míšek, J.; Cvačka, J.; Rulíšek, L.; Chocholoušová, J.; Vacek, J.; Goryl, G.; Szymonski, M.; Císařová, I., Starý, I. *Proc. Natl. Acad. Sci. U.S.A.* **2009**, *106*, 13169.

[86] El Abed, R.; Aloui, F.; Genet, J.-P.; Ben Hassine, B.; Marinetti, A. J. Organomet. Chem. **2007**, *692*, 1156.

[87] (a) Otsuka, S.; Nakamura, A.; Kano, T.; Tani, K. *J. Am. Chem. Soc.* **1971**, *54*, 4301. (b) Wild, S. B. *Coord. Chem. Rev.* **1997**, *166* , 291. (c) Albert, J.; Granell, J.; Muller, G. *J. Organomet. Chem.* **2006**, *691*, 2101.

[88] (a) Albert, J.; Cadena, J.M.; Granell, J. *Tetrahedron: Asymmetry* **1997**, *8*, 991; (b) Durán, E.; Gordo, E.; Granell, J.; Font-Bardía, M.; Solans, X.; Velasco, D.; López-Calahorra, F. *Tetrahedron: Asymmetry* **2001**, *12*, 1987.

[89] Garcia, M. H.; Florindo, P.; Piedade, M. d. F. M.; Maiorana, S.; Licandro, E. *Polyhedron*. **2009**, *28*, 621.

[90] (a) Daul, C.A.; Ciofini, I.; Weber, V. *Int. J. Quantum Chem.* **2003**, *91*, 297. (b) Bossi, A.; Licandro, E.; Maiorana, S.; Rigamonti, C.; Righetto, S.; Stephenson, G. R.; Spassova, M.; Botek, E.; Champagne, B. *J. Phys. Chem. C* **2008**, *112*, 7900. (c) Campagne, B.; André, J.-M.; Botek, E.; Licandro, E.; Maiorana, S.; Bossi, A.; Clays, K.; Persoons, A. *ChemPhysChem* **2004**, *5*, 1438.

[91] (a) Graule, S.; Rudolph, M.; Vanthuyne, N.; Autschbach, J.; Roussel, C.; Crassous, J.; Réau, R. *J. Am. Chem. Soc.* **2009**, *131*, 3183. (b) Graule, S.; Rudolph, M.; Shen, W.; Lescop, C.; Williams, J. A. G.; Autschbach, J.; Crassous, J.; Réau, R. *Chem. Eur. J.* **2010**, *16*, 5976. (c) Shen, W.; Graule, S.; Crassous, J.; Lescop, C.; Gornitzka, H.; Réau, R. *Chem. Commun.* **2008**, 850.

[92] (a) Shen, W.; Graule, S.; Crassous, J.; Lescop, C.; Gornitzka, H.; Réau, R. *Chem. Commun.* **2008**, 850. (b) Fave, C.; Hissler, M.; Sénéchal, K.; Ledoux, I.; Zyss, J.; Réau, R. *Chem. Commun.* **2002**, 1674.

[93] (a) Katz, T. J.; Pesti, J. *J. Am. Chem. Soc.* **1982**, *104*, 346. (b) Sudhakar, A.; Katz, T. J. *J. Am. Chem. Soc.* **1986**, *108*, 179.

[94] (a) Katz, T. J.; Sudhakar, A.; Teasley, M. F.; Gilbert, A. M.; Geiger, W. E.; Robben, M. P.; Wuensch, M.; Ward, M. D. *J. Am. Chem. Soc.* **1993**, *115*, 3182. (b) Gilbert, A. M.; Katz, T. J.; Geiger, W. E.; Robben, M. P.; Rheingold, A. L. *J. Am. Chem. Soc.* **1993**, *115*, 3199.

[95] (a) Dai, Y.; Katz, T. J.; Nichols. D. A. *Angew. Chem., Int. Ed.* **1996**, *35*, 2109. (b) Dai, Y.; Katz, T. J. *J. Org. Chem.* **1997**, *62*, 1274.

[96] (a) Mandal B. K.; Sooksimuang, T. *J. Porphyrins Phthalocyanines* **2002**, *6*, 66. (b) Sooksimuang, T.; Behroozi, S. J.; Mandal, B. K. *J. Porphyrins Phthalocyanines* **2002**, *6*, 544. (c) Chen, L. X.; Shaw, G. B.; Tiede, D. M.; Zuo, X. B.; Zapol, P.; Redfern, P. C.; Curtiss, L. A.; Sooksimuang T.; Mandal, B. K. *J. Phys. Chem. B*, **2005**, *109*, 16598. (d) Lee, C. H.; Sooksimuang T.; Mandal, B. K. *J. Porphyrins Phthalocyanines*, **2006**, *10*, 135. (e) Sooksimuang, T.; Mandal, B. K. *J. Org. Chem.* **2003**, *68*, 652.

[97] Fox, J. M.; Katz, T. J.; Van Elshocht, S.; Verbiest, T.; Kauranen, M.; Persoons, A.; Thongpanchang, T.; Krauss, T. Brus, L. *J. Am. Chem. Soc.* **1999**, *121*, 3453.

[98] (a) Nuckolls, C.; Shao, R. F.; Jang, W. G.; Clark, N. A.; Walba, D. M.; Katz, T. J. *Chem. Mater.* **2002**, *14*, 773. (b) Lovinger, A. J.; Nuckolls, C.; Katz, T. J. *J. Am. Chem. Soc.* **1998**, *120*, 264.

[99] (a) Norel, L.; Rudolph, M.; Vanthuyne, N.; Williams, J. A. G.; Lescop, C.; Roussel, C.; Autschbach, J.; Crassous, J.; Réau, R. *Angew. Chem., Int. Ed.* **2010**, *49*, 99. (b) Anger, E.; Rudolph, M.; Shen, C.; Vanthuyne,

N.; Toupet, L.; Roussel, C.; Autschbach, J.; Crassous, J.; Réau, R. *J. Am. Chem. Soc.* **2011**, *133*, 3800. (c) Anger, E.; Rudolph, M.; Norel, L.; Zrig, S.; Shen, C.; Vanthuyne, N.; Toupet, L.; Williams, J. A. G.; Roussel, C.; Autschbach, J.; Crassous, J.; Réau, R. *Chem. Eur. J.* **2011**, *17*, 14178.

[100] Crespo, O.; Eguillor, B.; Esteruelas, M. A.; Fernández, I.; García-Raboso, J.; Gómez-Gallego, M.; Martín-Ortiz, M.; Oliván, M.; Sierra, M. A. *Chem. Commun.* **2012**, *48*, 5328.

[101] Vacek, J.; Vacek Chocholoušová, J. *unpublished results.*

[102] Wolf, C. In *Dynamic Stereochemistry of Chiral Compounds*, RSC Publishing: Cambridge, **2008**, p 334.

[103] (a) Evans, D. A.; Dinsmore, C. J. *Tetrahedron Lett.* **1993**, *34*, 6029. (b) Hoffmann, R. W. *Chem. Rev.* **1989**, *89*, 1841.

[104] Cha, J. K.; Kim, N.-S. *Chem. Rev.* **1995**, *95*, 1761.

[105] Broeker, J. L.; Hoffmann, R. W.; Houk, K. N. *J. Am. Chem. Soc.* **1991**, *113*, 5006.

[106] Krausová, Z.; Sehnal, P.; Teplý, F.; Stará, I. G.; Starý, I.; Šaman, D.; Cvačka, J.; Fidler, P. *Collect. Czech. Chem. Commun.* **2007**, *72*, 1499.

[107] Ondráček, J.; Schehlmann, V.; Maixner, J.; Kratochvíl, B. *Collect. Czech. Chem. Commun.* **1990**, *55*, 2447.

[108] King, R. B. *Inorg. Chem.* **1963**, *2*, 528.

[109] Moseley, K.; Kang, J. W.; Maitlis; P. M. *J. Chem. Soc. (A)* **1970**, 2875.

[110] Žádný, J.; Jančařík, A.; Andronova, A.; Šámal, M.; Vacek Chocholoušová, J.; Vacek, J.; Pohl, R.; Šaman, D.; Císařová, I.; Stará, I. G.; Starý, I. *Angew. Chem., Int. Ed.* **2012**, *51*, 5857.

[111] Pohl, R. *unpublished results.*

[112] Jančařík, A.; Pohl, R. *unpublished results.*

[113] Kašička, V.; Prusík, Z.; Sázelová, P.; Brynda, E.; Stejskal, J. *Electrophoresis* **1999**, *20*, 2484.

[114] Ehala, S.; Míšek, J.; Stará, I. G.; Starý, I.; Kašička, V. *J. Sep. Sci.* **2008**, *31*, 2686.

[115] Rived, F.; Roses, M.; Bosch, E. *Anal. Chim. Acta* **1998**, *374*, 309.

[116] Augustin-Nowacka, D.; Makowski, M.; Chmurzynski, L. *Anal. Chim. Acta* **2000**, *418*, 233.

[117] Napagoda, M.; Rulíšek, L.; Jančařík, A.; Klívar, J.; Šámal, M.; Stará, I. G.; Starý, I.; Šolínová, V.; Kašička, V.; Svatoš, A. *ChemPlusChem* **2013**, *78*, 937.

[118] Vedejs, E.; Chen, X. *J. Am. Chem. Soc*. **1996**, *118*, 1809.

[119] Carson, M. W.; Giese, M. W.; Coghlan, M. J. *Org. Lett.* **2008**, *10*, 2701.

[120] Dračínský, M.; Jansa, P.; Bouř, P. *Chem. Eur. J.* **2012**, *18*, 981.

[121] Dračínský, M. *unpublished results.*

[122] Sudo, Y.; Arai, S.; Nishida, A. *Eur. J. Org. Chem.* **2006**, 752.

[123] Kitamura, T.; Otsubo, K. *J. Org. Chem.* **2012**, *77*, 2978.

[124] Ganta, A.; Snowden, T. S. *Synlett* **2007**, *14*, 2227.

[125] Jones, M. W.; Strickland, R. A.; Schumacher, F. F.; Caddik, S.; Baker, J. R.; Gibson, M. I.; Haddleton, D. M. *J. Am. Chem. Soc.***2012**, *134*, 1847.

[126] Knight, D. W.; Redfern, A. L.; Gilmore, J. *J. Chem. Soc., Perkin Trans.* **2001**, *1,* 2874.

[127] Kagan, H. B.; Fiaud, J. C. *Top. Stereochem.* **1988**, *18*, 249.

[128] (a) Baiker, A.; Blaser, H. U. In *Handbook of Heterogeneous Catalysis*; Ertl, G., Knözinger, H., Weitkamp, J., Eds.; VCH: Weinheim, **1997**, Vol. 5, p 2422. (b) Mallat, T.; Baiker, A. In *Fine Chemicals through Heterogeneous Catalysis*; Sheldon, R. A., van Bekkum, H., Eds.; Wiley-VCH: Weinheim, **2001**, p 449. (c) Studer, M.; Blaser, H. U.; Exner, C. *Adv. Synth. Catal.* **2003**, *345*, 45. (d) Tungler, A.; Sipos, E.; Hadac, V. *ARKIVOC* **2004**, 223. (e) Murzin, D. Y.; Maki-Arvela, P.; Toukomiitty, E.; Salmi, T. *Catal. Rev. – Sci. Eng.* **2005**, *47*, 175.

[129] Diezi, S.; Hess, M.; Orglmeister, E.; Mallat, T.; Baiker, A. *Catal. Lett.* **2005**, *102*, 121.

[130] (a) Orito, Y.; Imai, S.; Niwa, S.; Hung, N. G. *J. Synth. Org. Chem.* **1997**, *37*, 173. (b) Orito, Y.; Imai, S.; Niwa, S. *J. Chem. Soc. Jpn.* **1979**, 1118. (c) Orito, Y.; Imai, S.; Niwa, S. *J. Chem. Soc. Jpn.* **1980**, 670.

[131] Tálas, E.; Margitfalvi, J. L. *Chirality* **2010**, *22*, 3.

[132] Blaser, H. U.; Jalett, H. P.; Garland, M.; Studer, M.; Thies, H.; Wirth-Tijani, A. *J. Catal.* **1998**, *173*, 282.

[133] (a) Margitflavi, J. L.; Hegedüs, M.; Tfirst, E. *Tetrahedron: Asymmetry* **1996**, 571. (b) Margitflavi, J. L.; Hegedüs, M.; Tfirst, E. *Stud. Surf. Sci. Catal.* **1996**, *101*, 241. (c) Margitflavi, J. L.; Tálas, E. *Appl. Catal. A* **1999**, *182*, 65. (d) Margitflavi, J. L.; Tfirst, E. *J. Mol. Catal. A: Chem* **1998**, *139*, 81.

[134] (a) Ferri, D.; Bürgi, T. *J. Am. Chem. Soc.* **2001**, *123*, 12074. (b) Zaera, F. *J. Phys. Chem. C* **2008**, *112*, 16196. (c) Laliberte, M. A.; Lavoie, S.; Hammer, B.; Mahieu, G.; McBreen, P. H. *J. Am. Chem. Soc.* **2008**, *130*, 5386. (d) Schmidt, E.; Ferri, D.; Vargas, A.; Baiker, A. *J. Phys. Chem. C* **2008**, *112*, 3866. (e) Baddeley, C. *J. Top. Catal.* **2003**, *25*, 17. (f) LeBlanc, R. J.; Chu, W.; Williams, C. T. *J. Mol. Catal. A: Chem.* **2004**, *212*, 277. (g) Bakos, I.; Szabó, S.; Bartók, M.; Kálmán, E. *J. Electroanal. Chem.* **2002**, *532*, 113. (h) Bonello, J. M.; Lindsay, R.; Santra, A. K.; Lambert, R. M. *J. Phys. Chem. B* **2002**, *106*, 2672. (i) Schmidt, E.; Ferri, D.; Baiker, A. *Langmuir* **2007**, *23*, 8087.

[135] Somorjai, G. A.; Park, J. Y. *Angew. Chem., Int. Ed.* **2008**, *47*, 9212.

[136] (a) Török, B.; Felföldi, K.; Szakonyi, G.; Balázsik, K.; Bartók, M. *Catal. Lett.* **1998**, *52*, 81. (b) Török, B.; Balázsik, K.; Felföldi, K.; Bartók, M. *Ultrason. Sonochem.* **2001**, *8*, 191.

[137] (a) Che, M.; Bennett, C. O. *Adv. Catal.* **1989**, *36*, 55. (b) Coq, B.; Figueras, F. *Coord. Chem. Rev.* **1998**, *180*, 1753. (c) Guczi, L.; Petö, G.; Beck, A.; Pászti, Z. *Top. Catal.* **2004**, *29*, 129. (d) VanSanten, R. A. *Acc. Chem. Res.* **2009**, *42*, 57. (e) VanHardeveld, R.; Hartog, F. *Surf. Sci.* **1969**, *15*, 189. (f) Bönnemann, H.; Braun, G. A. *Angew. Chem., Int. Ed.* **1996**, *35*, 1992. (g) Zuo, X.; Liu, H.; Guo, D.; Yang, X. *Tetrahedron* **1999**, *55*, 7787. (h) Nitta, Y.; Kubota, T.; Okamoto, Y. Bull. *Chem. Soc. Jpn.* **2000**, *73*, 2635. (i) Wehrli, J. T.; Baiker, A.; Monti, M.; Blaser, H. U. *J. Mol. Catal.* **1990**, *61*, 207. (j) Jackson, S. D.; Keegan, M. B. T.; McLellan, G. D. ; Meheux, P. A.; Moyes, R. B.; Webb, G.; Wells, P. B.; Whyman, R.; Willis, J. In Studies in Surface Science and Catalysis; Poncelet, G., Jacobs, P. A., Grange, G., Delmon, B., Eds.; Elsevier: Amsterdam, **1991**, p 135. (k) Hoxha, F.; Vegten, N. V.; Urakawa, A.; Krumeich, F.; Mallat, T.; Baiker, A. *J. Catal.* **2009**, *261*, 224. (l) Zuo, X.; Liu, H.; Liu, M. *Tetrahedron Lett.* **1998**, *39*, 1941.

[138] Burda, C.; Chen, X. B.; Narayanan, R.; El-Sayed, M. A. *Chem. Rev.* **2005**, *105*, 1025.

[139] Ahmadi, T. S.; Wang, Z. L.; Green, T. C.; Henglein, A.; El-Sayed, M. A. *Science* **1996**, *272*, 1924.

[140] Lee, I.; Morales, R.; Albiter, M. A.; Zaera, F. *PNAS* **2008**, *105*, 15241.

[141] Žádný, J.; Jančařík, A. *unpublished results.*

[142] Altomare, A.; Cascarano, G.; Giacovazzo, C.; Guagliardi, A.; Burla, M. C.; Polidori, G.; Camalli, M. *J. Appl. Cryst*. **1994**, *27*, 435.

[143] Sheldrick, G. M. *Acta Cryst*. **2008**, *A64*, 112.

[144] Lehmann, L.; Lloyd-Jones, G. C. *Tetrahedron* **1995**, *51*, 8863.

[145] Bondzić, B. P.; Farwick, A.; Liebich, J.; Eilbracht, P. *Org. Biomol. Chem.* **2008**, *6*, 3723.
[146] Kawatsura, M.; Uchida, K.; Terasaki, S.; Tsuji, H.; Minakawa, M.; Itoh, T. *Org. Lett.* **2014**, *16*, 1470.

[147] King, R. B.; Treichel, P. M.; Stone, F. G. A. *J. Am. Chem. Soc.* **1961**, *83*, 3593.

[148] Andronova, A. A. *PhD thesis*; Charles University in Prague, Faculty of Science, **2012**.

[149] Geny, A.; Agenet, N.; Iannazzo, L.; Malacria, M.; Aubert, C.; Gandon, V. *Angew. Chem., Int. Ed.* **2009**, *48*, 1810.

[150] Rajagopal, G.; Lee, H.; Kim, S. S. *Tetrahedron* **2009**, *65*, 4735.

[151] Arai, N.; Satoh, H.; Utsumi, N.; Murata, K.; Tsutsumi, K.; Ohkuma, T. *Org. Lett.* **2013**, *15*, 3030.

[152] Majek, M.; von Wangelin, A. J. *Chem. Commun.* **2013**, *49*, 5507.

[153] Watanabe, Y.; Ota, T.; Tsuji, Y. *Chem. Lett.* **1980**, *9*, 1585.

[154] Mahindaratne, M. P. D.; Wimalasena, K. *J. Org. Chem.* **1998**, *63*, 2858.